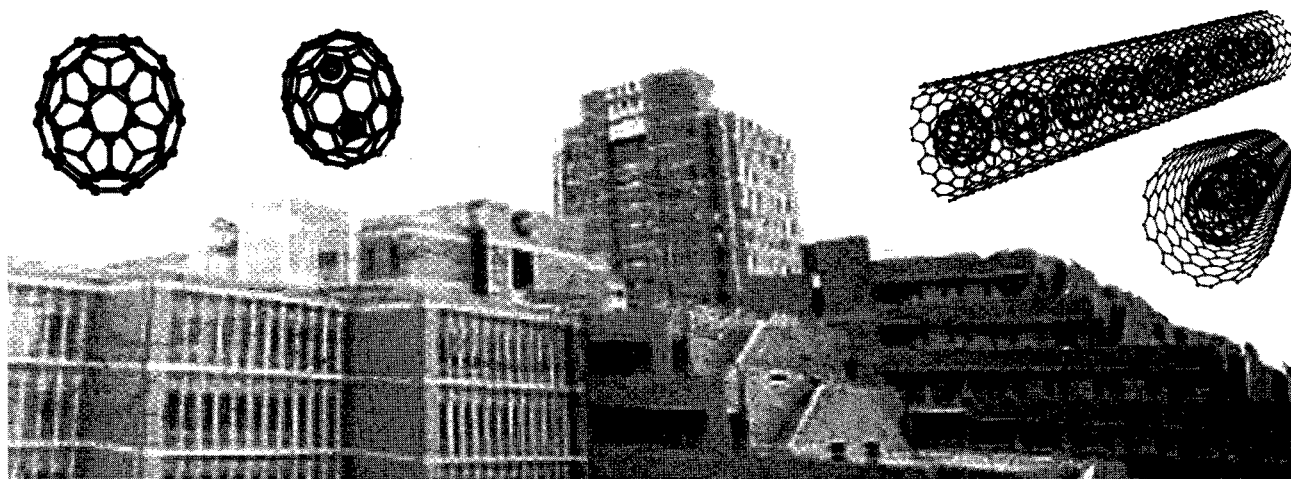


Abstract
The 32nd Fullerene-Nanotubes General Symposium

第 32 回 フラーレン・ナノチューブ
総合シンポジウム

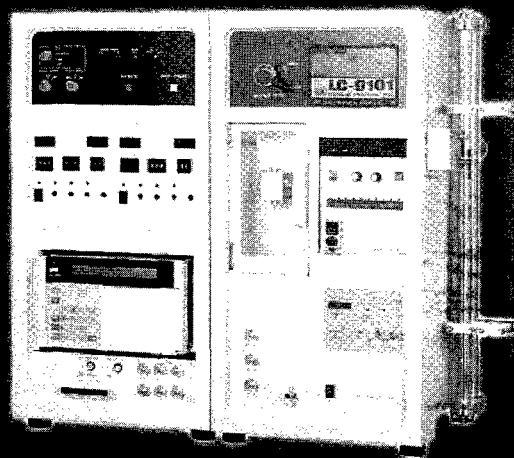
講演要旨集



February 13-15, 2007 Nagoya, Aichi
平成 19 年 2 月 13 日～15 日 名城大学

The Fullerenes and Nanotubes Research Society
フラーレン・ナノチューブ学会

装置販売実績1,000台超！！ 分取HPLCは JAIのLC-9000シリーズ！



LC-9101

リサイクル分取を最重視したLCです。分離困難とされていた試料を容易に分離することができます。分離効率の良い合成ポリマー充填剤を使用した高理論段数カラムを多数ラインアップしています。

リサイクル分析法では試料の溶解性のより良い溶媒や、単離分取後の溶媒除去が容易な溶媒を使用することで、短時間で効率良く、しかも試料に変化を与えずに分離精製することができます。さらにリサイクル中は、溶媒を全く消費せず、環境にも優しい装置です。



LC-9102

LC-9104

LC-9201/9204

◆LC-9101 標準モデル

専用のGPCカラム(20φ×600mm)を装着すれば、分離能を落とすことなく、常時300mgを注入することができます。NMR測定に充分な量を分取できる上、分子量分布測定など極微量試料の分析にも適しています。

◆LC-9102 グラジエントモデル

グラジエントとリサイクルがワンタッチで切替えられます。低圧4液混合グラジエントが標準装備されています。高圧グラジエント・流量グラジエントのコントローラーが内蔵されているので、応用範囲が広がります。

◆LC-9104 大量分取モデル

専用のGPCカラム(40φ×600mm)を装着すれば、試料処理量は、LC-9101型の約4倍。試料注入から分取まで自動化されています。また、ODS・シリカカラムなど、大量分取用カラムの性能を最大限に引き出す装置設計がなされています。

◆LC-9201/LC-9204 コンパクトモデル

分離分取に定評のあるLC-9101型の高い性能を受継ぎながら、サイズをコンパクトにし、省スペース化と低価格化を実現しました。LC-9204型は大口径カラムの接続も可能です。

——— 高分子分析の未来と取り組む！ ———



日本分析工業株式会社

URL: <http://www.jai.co.jp/> E-mail: sales-1@jai.co.jp

□本社・工場：〒190-1213 東京都西多摩郡瑞穂町武蔵208 TEL 042-557-2331 FAX 042-557-1892
□大阪営業所：〒532-0002 大阪市淀川区東三国5-13-8-303 TEL 06-6393-8511 FAX 06-6393-8525

Abstract
The 32nd Fullerene-Nanotubes General Symposium

第 32 回 フラーレン・ナノチューブ
総合シンポジウム

講演要旨集

The Fullerenes and Nanotubes Research Society

The Chemical Society of Japan

The Japan Society of Applied Physics

主催：フラーレン・ナノチューブ学会

共催：日本化学会

協賛：応用物理学会

Date: February 13th(Tue)~15th(Thu), 2007

Place: Meijo University
1-501 Shiogamaguchi, Tempaku-ku, Nagoya 468-8502
TEL: 052-832-1151

Presentation: Special Lecture (25 min presentation, 5min discussion)
General Lecture (10 min presentation, 5min discussion)
Poster Preview (1 min presentation, no discussion)

日時：平成 19 年 2 月 13 日(火)~15 日(木)

場所：名城大学
〒468-8502 愛知県名古屋市天白区塩釜口 1-501
TEL：052-832-1151

発表時間：特別講演	(発表 25 分・質疑応答 5 分)
一般講演	(発表 10 分・質疑応答 5 分)
ポスタープレビュー	(発表 1 分・質疑応答 なし)

展示団体御芳名(アイウエオ順、敬称略)

アプリオリ(株)
コスモ・バイオ(株)
サイバネットシステム(株)
 (株)島津製作所
ナカライテスク(株)
 (株)日本レーザー
(株)日立ハイテクノロジーズ
 (株)堀場製作所
(株)名城ナノカーボン
 (株)ATR

広告掲載団体御芳名(アイウエオ順、敬称略)

アプリオリ(株)
オザワ科学(株)
 (株)カーク
コスモ・バイオ(株)
産業タイムズ社(株)
三弘アルバック(株)
 (株)島津製作所
 住友商事(株)
(株)東京プログレスシステム
 東洋炭素(株)
 東レ(株)
ナカライテスク(株)
 日本電子(株)
 日本分光(株)
 日本分析工業(株)
フロンティアカーボン(株)
 (株)堀場製作所
 (株)マツボー
 (株)ATR

Contents

Time Table	i
Chairperson	iii
Program	Japanese	iv
	English	xiii
Abstract	Special lecture	1
	General lecture	7
	Poster preview	51
Author Index	169

目次

早見表	i
座長一覧	iii
プログラム	和文	iv
	英文	xiii
講演予稿	特別講演	1
	一般講演	7
	ポスター発表	51
発表索引	169

プログラム早見表

各項目敬称略

	2月13日(火)	2月14日(水)	2月15日(木)	
9:00	特別講演1(Stephan Irle) 9:00~9:30	特別講演3(永瀬 茂) 9:00~9:30	特別講演5(角田 裕三) 9:00~9:30	9:00
9:30	一般講演4件 (ナノチューブの物性) 9:30~10:30	一般講演4件 (金属内包フラーレン) 9:30~10:30	一般講演4件 (ナノチューブ:生成と精製) 9:30~10:30	9:30
10:30	休 憩 10:30~10:45			10:30
10:45	一般講演4件 (ナノチューブの物性) 10:45~11:45	一般講演4件 (フラーレン固体とフラーレンの化学) 10:45~11:45	一般講演4件 (ナノチューブ応用) 10:45~11:45	10:45
11:45	昼 食 (11:45~13:00)			11:45
13:00	特別講演2(中西 尚志) 13:00~13:30	授賞式 13:00~13:30	特別講演6(甲賀 研一郎) 13:00~13:30	13:00
13:30	一般講演5件 (ナノチューブの物性) 13:30~14:45	特別講演4(八名 純三) 13:30~14:00	一般講演2件 (ナノチューブ:生成と精製2件) 13:30~14:00	13:30
14:00		一般講演4件 (フラーレンの化学) 14:00~15:00	ポスタープレビュー 1分×38件 14:00~15:00	14:00
14:45	休 憩 14:45~15:00			
15:00	一般講演5件 (ナノチューブの物性と応用) 15:00~16:15	休 憩 15:00~15:15	ポスターセッション 15:00~16:20	15:00
15:15		一般講演3件 (ナノ炭素科学) 15:15~16:00		15:15
16:15	ポスタープレビュー 1分×40件 16:15~17:15	ポスタープレビュー 1分×39件 16:00~17:00		16:20
17:15	ポスターセッション 17:15~18:35	ポスターセッション 17:00~18:20		
18:35				

2月13日(火)
チュートリアル 103講義室
15:00~16:30
講師 中山 喜萬 先生
(大阪大学大学院工学研究
科 教授)

18:30~懇親会

特別講演 発表25分 質疑5分
一般講演 発表10分 質疑5分
ポスタープレビュー
発表1分 質疑なし

TIME TABLE

	Tue.Feb.13	Wed.Feb.14	Thu.Feb.15	
9:00	Special Lecture (S.Irle) 9:00~9:30	Special Lecture (S.Nagase) 9:00~9:30	Special Lecture (Y.Sumida) 9:00~9:30	9:00
9:30	General Lecture[4] (Properties of Nanotubes) 9:30~10:30	General Lecture[4] (Metallofullerenes) 9:30~10:30	General Lecture[4] (Formation and Purification of Nanotubes) 9:30~10:30	9:30
10:30	Break 10:30~10:45			10:30
10:45	General Lecture[4] (Properties of Nanotubes) 10:45~11:45	General Lecture[4] (Fullerene Solids and Chemistry of Fullerenes) 10:45~11:45	General Lecture[4] (Applications of Nanotubes) 10:45~11:45	10:45
11:45	Lunch (11:45~13:00)			11:45
13:00	Special Lecture (T.Nakanishi) 13:00~13:30	Awards Ceremony 13:00~13:30	Special Lecture (K.Koga) 13:00~13:30	13:00
13:30	General Lecture[5] (Properties of Nanotubes) 13:30~14:45	Special Lecture (J.Yana) 13:30~14:00	General Lecture[2] (Formation and Purification of Nanotubes) 13:30~14:00	13:30
14:00		General Lecture[4] (Chemistry of Fullerenes) 14:00~15:00	Poster Preview 1min × [38] 14:00~15:00	14:00
14:45	Break 14:45~15:00	Break 15:00~15:15	Poster Session 15:00~16:20	15:00
15:00	General Lecture[5] (Applications and Properties of Nanotubes) 15:00~16:15	General Lecture[3] (Science of Nanocarbons) 15:15~16:00		15:00
16:15	Poster Preview 1min × [40] 16:15~17:15	Poster Preview 1min × [39] 16:00~17:00		16:20
17:15	Poster Session 17:15~18:35	Poster Session 17:00~18:20		
18:35				

Tue.Feb.13
 Tutorial Room103
 15:00~16:30
 Prof.Yoshikazu Nakayama

18:30~ Banquet

Special Lectures 25min presentation, 5min discussion
 General Lectures 10min presentation, 5min discussion
 Poster Previews 1min presentation, No discussion

座長一覧

2月13日(火)

(敬称略)

	時 間	座 長
特 別 講 演(Stephan)	9:00 ~ 9:30	永瀬 茂
一 般 講 演	9:30 ~ 10:30	坂東 俊治
一 般 講 演	10:45 ~ 11:45	大野 雄高
特 別 講 演(中西)	13:00 ~ 13:30	村田 靖次郎
一 般 講 演	13:30 ~ 14:45	岡田 晋
一 般 講 演	15:00 ~ 16:15	菅井 俊樹
ポスタープレビュー	16:15 ~ 17:15	稲熊 正康
ポスターセッション	17:15 ~ 18:35	千足 昇平

2月14日(水)

	時 間	座 長
特 別 講 演(永瀬)	9:00 ~ 9:30	斎藤 晋
一 般 講 演	9:30 ~ 10:30	久保園 芳博
一 般 講 演	10:45 ~ 11:45	谷垣 勝己
特 別 講 演(八名)	13:30 ~ 14:00	斎藤 毅
一 般 講 演	14:00 ~ 15:00	松尾 豊
一 般 講 演	15:15 ~ 16:00	若原 孝次
ポスタープレビュー	16:00 ~ 17:00	小塩 明
ポスターセッション	17:00 ~ 18:20	兒玉 健

2月15日(木)

	時 間	座 長
特 別 講 演(角田)	9:00 ~ 9:30	片浦 弘道
一 般 講 演	9:30 ~ 10:30	北浦 良
一 般 講 演	10:45 ~ 11:45	岡崎 俊也
特 別 講 演(甲賀)	13:00 ~ 13:30	久保園 芳博
一 般 講 演	13:30 ~ 14:00	若林 知成
ポスタープレビュー	14:00 ~ 15:00	前田 優
ポスターセッション	15:00 ~ 16:20	平原 佳織

2月13日(火)

特別講演 発表25分・質疑応答5分
一般講演 発表10分・質疑応答5分
ポスタープレビュー 発表1分・質疑応答なし

特別講演(9:00-9:30)

- 1S-1 Quantum Chemical Molecular Dynamics Simulations of Fullerene and Carbon Nanotube Self-Assembly
Stephan Irle 1

一般講演(9:30-10:30)

ナノチューブの物性

- 1-1 スーパーグロース単層カーボンナノチューブフォレスト:1200 m²/g超の比表面積を有する理想的炭素表面材料
平岡樹、○山田健郎、畠賢治、二葉ドン、宮脇仁、湯田坂雅子、湯村守雄、飯島澄男 7
- 1-2 垂直配向単層カーボンナノチューブの内部構造
○Erik Einarsson、塩澤秀次、Christian Kramberger、Mark H. Ruemmeli、Alex Grueneis、Thomas Pichler、丸山茂夫 8
- 1-3 フラーレンを内包した単層ナノチューブの通電加熱による構造変化
○柚田博史、吉川雄也、長瀧篤子、秋田成司、中山喜萬 9
- 1-4 カーボンナノチューブの圧力誘起構造相転移により得られる新炭素結晶相
○斎藤晋、加藤幸一郎、櫻井誠大、山上雄一郎 10

☆☆☆☆☆☆ 休憩 (10:30-10:45) ☆☆☆☆☆☆

一般講演(10:45-11:45)

ナノチューブの物性

- 1-5 CNTs-FETsの電子物性に影響をおよぼす要因
○熊代良太郎、廣芝伸哉、大橋弘孝、畠山力三、谷垣勝己 11
- 1-6 C₆₀、C₇₀、C₈₄ 内包二層カーボンナノチューブにおける負性抵抗特性
○李永峰、金子俊郎、畠山力三 12
- 1-7 2本のカーボンナノチューブで構成した同軸円筒型キャパシタにおける量子効果
○内田和之、岡田晋、白石賢二、押山淳 13
- 1-8 アドアトム-欠陥ペアを持つナノチューブのエネルギー論と電子状態
○岡田晋 14

☆☆☆☆☆☆ 昼食 (11:45-13:00) ☆☆☆☆☆☆

特別講演(13:00-13:30)

- 1S-2 フラーレン超分子マテリアル化への新規アプローチ
中西 尚志 2

一般講演(13:30-14:45)

ナノチューブの物性

- 1-9 単層ナノチューブのラマン分光における励起子の効果
○齋藤理一郎、J. Jiang、佐藤健太郎、J. S. Park 15
- 1-10 二層カーボンナノチューブの吸収・発光・ラマン分光によるキャラクタリゼーション
○コンスタンチン・ヤクボフスキー、南 信次、上野太郎、サイ・カザウイ、宮田耕充、片浦弘道 16
- 1-11 化学修飾カーボンナノチューブの光誘起電荷分離挙動
○伊藤 攻、アツラ サンダナヤカ、荒木保幸、フランシス ドゾーサ 17
- 1-12 多層ナノチューブの振動エネルギー損失における直径依存性
○澤谷慎太郎、中山喜萬、秋田成司 18
- 1-13 気体分子の吸着による単層カーボンナノチューブの電子状態への影響
○アビジット チャテジー 19

☆☆☆☆☆☆ 休憩 (14:45-15:00) ☆☆☆☆☆☆

2月13日(火)

一般講演(15:00-16:15)

ナノチューブの物性と応用

- 1-14 酸素分子によるナノチューブ破壊に関する第一原理計算
○河合孝純、宮本良之 20
- 1-15 水素雰囲気中で加圧した多層カーボンナノチューブの構造変化
○中山敦子、沼尾茂悟、中野智志、坂東俊治、飯島澄男 21
- 1-16 ADF-STEMを用いたCNT/ポリマー複合材料中のCNTネットワーク可視化の検討
○松原徹、正田薫、伊藤幸助、國重敦弘、住山芳行 22
- 1-17 DNA / SWNTs コンポジットの光特性
○野口悠一、藤ヶ谷剛彦、新留康郎、中嶋直敏 23
- 1-18 超音波分散の改善法とカイラリティ依存性
齋藤浩、○佐野正人 24

ポスタープレビュー(16:15-17:15)

ポスターセッション(17:15-18:35)

ナノチューブの物性

- 1P-1 Origin of Linear Relationship Between $\text{CH}_2/\text{NH}/\text{O}(\text{n},\text{n})\text{SWCNT}$ Reaction Energies and Sidewall Curvature
Guishan Zheng, Zhi Wang, ○Stephan Irlle, Keiji Morokuma 51
- 1P-2 カーボンナノチューブの高速スクリーニング
○宮本良之 52
- 1P-3 単層カーボンナノチューブのラマン分光におけるG'バンドの強度のカイラリティ依存性
○朴珍成、齋藤理一郎、佐藤健太郎、Jie Jiang, Ki Kang Kim, Young Hee Lee, Gene Dresselhaus, Mildred S. Dresselhaus 53
- 1P-4 ミセル化単層カーボンナノチューブにおける発光の圧力依存性
○迫田哲、市田正夫、宮田耕充、片浦弘道、水野健一、安藤弘明 54
- 1P-5 グラフェンリボン端の電子状態と磁気モーメント
○坂下浩史、小田竜樹 55
- 1P-6 カーボンナノチューブ・グラフェンにおける超伝導理論
○佐々木健一、J. Jiang、齋藤理一郎、大成誠一郎、田仲由喜夫 56
- 1P-7 修飾された単層カーボンナノチューブの電子構造
○小林由和、笛野博之、田中一義、梅山有和、今堀 博 57
- 1P-8 低エネルギー照射によるSWNT単電子トランジスタのクーロンギャップの増大
○橋本惇一、鈴木哲、荻野俊郎、小林慶裕 58
- 1P-9 低エネルギー照射による金属的SWNTの室温FET特性の半導体化
○鈴木哲、橋本惇一、荻野俊郎、小林慶裕 59

ナノチューブ：生成と精製

- 1P-10 単層カーボンナノチューブにおける結合曲率に依存した酸化プロセス
○宮田耕充、河合孝純、宮本良之、柳和宏、真庭豊、片浦弘道 60
- 1P-11 Orientational control of carbon nanotube growth by plasma-enhanced hot filament chemical vapor deposition
○邱建超、吉村雅満、上田一之 61
- 1P-12 サファイア基板との相互作用によるカーボンナノチューブの配向成長
○山崎明、高木大輔、鈴木哲、Jeong Goo-Hwan、吉村英恭、本間芳和、小林慶裕 62
- 1P-13 パルスアークプラズマガンを用いたSi基板上カーボンナノチューブ成長の検討
○白岩倫行、加藤義明、谷奥健次、西村鈴香、丸山隆浩、成塚重弥 63
- 1P-14 単層カーボンナノチューブの誘電泳動分離
○丸山茂夫、塩見淳一郎、宮内雄平、林原、アンベリ グスタフ 64
- 1P-15 水素添加による単層カーボンナノチューブの直径増大効果
○早川雅博、坂東俊治、飯島澄男 65
- 1P-16 触媒化学気相成長法による多孔質物質からの単層カーボンナノチューブの成長
○小林慶太、北浦良、菅井俊樹、熊井葉子、後藤康友、稲垣伸二、篠原久典 66
- 1P-17 サファイア表面上における単層カーボンナノチューブの位置と方向の同時制御
○大堂良太、吾郷浩樹、品川直嗣、石神直樹、辻正治、生田竜也、高橋厚史 67

2月13日(火)

- 1P-18** Fe-Mo/MgO触媒上での単層・二層カーボンナノチューブのCVD成長における水蒸気酸化の化学
○吉原直記、吾郷浩樹、辻正治 68
- 1P-19** アルコール触媒化学気相成長法によるカーボンナノチューブの低温成長(II)
日浅健、鈴木祥吾、○佐藤英樹、畑浩一、梶原和夫、齋藤弥八 69
- 1P-20** 長尺カーボンナノチューブ合成のための先端放電型ラジカルCVD条件最適化とCO₂の効果
○岩崎孝之、真木翼、吉田剛、相川拓海、野末竜弘、近藤大雄、川端章夫、佐藤信太郎、二瓶瑞久、栗野祐二、川原田洋 70

ナノホーン

- 1P-21** カーボンナノホーンの毒性評価
○宮脇仁、湯田坂雅子、筋丈史、久保佳実、飯島澄男 71
- 1P-22** カーボンナノホーンの閉孔速度に及ぼす熱処理温度の影響
○范晶、湯田坂雅子、宮脇仁、弓削亮太、河合孝純、飯島澄男 72
- 1P-23** Streptavidin-modified Single Wall Carbon Nanohorns
○Xu Jianxun、湯田坂雅子、飯島澄男 73
- 1P-24** カーボンナノホーンとカーボンナノカプセルの複合構造の形成メカニズム
小林慶太、小塩明、高橋裕、○小海文夫 74
- 1P-25** シスプラチン水溶液を用いたシスプラチン内包カーボンナノホーンの作製とその評価
○安嶋久美子、湯田坂雅子、飯島澄男 75
- 1P-26** EuPt担持カーボンナノホーンを用いたメタン水蒸気改質による水素発生
○弓削亮太、村田克之、湯田坂雅子、久保佳実、吉武務、飯島澄男 76
- 1P-27** PEG-ペプチド複合体を用いた薬剤担持ナノホーン分散化
○松村幸子、湯田坂雅子、飯島澄男、芝清隆 77

フラーレンの化学

- 1P-28** 五つのフェロセニル基を持つフラーレン十重付加体の合成
○一木孝彦、松尾豊、中村栄一 78
- 1P-29** フラーレン-金属-アリアル連結分子の合成と電気化学
○七尾岳史、松尾豊、中村栄一 79
- 1P-30** 八重付加型[60]フラーレンの異種二核金属錯体の合成
○中江隆博、松尾豊、中村栄一 80
- 1P-31** ピリジンを鍵とした有機銅試薬のフラーレンに対する位置選択的八重および十重付加反応
○松尾 豊、田原一邦、森田耕平、松尾敬子、中村栄一 81
- 1P-32** 開口C₆₀誘導体内部へのヘリウム原子の導入とヘリウム内包C₆₀の合成
○田邊史行、森貞之、小松紘一、村田理尚、村田靖次郎 82

フラーレン固体

- 1P-33** フラロデンドロンのLB膜を用いた電界効果トランジスタの作製
○川崎菜穂子、長野高之、久保園芳博、酒向祐輝、高口豊、藤原明比古、日野照純、Chih-Chien Chu、今榮東洋子 83
- 1P-34** フラーレン誘導体ナノウイスキーとフラーレンナノチューブのTEMおよびラマン分光解析
○宮澤薫一、チェリー・リングル、増野匡彦、中村成夫 84
- 1P-35** C₆₀ナノチューブの成長に及ぼす紫外線照射の効果
○チェリー・リングル、宮澤薫一、栗根 徹 85
- 1P-36** 分子デバイスとしてのフラーレンの電気伝導特性の理論的解析
○白井信志、大島良久、廣瀬渉至、北島徹雄 86
- 1P-37** C₆₀ナノウイスキー FETの電気伝導特性
○小川健一、都司一、青木伸之、落合勇一 87
- 1P-38** 電子線重合C₆₀ポリマーの電気伝導特性
○都司一、小川健一、龍崎奏、青木伸之、尾上順、落合勇一 88
- 1P-39** 自由電子レーザーの成膜中照射によるC₆₀ポリマー膜の作製
○岩田展幸、野苺家亮、安藤慎悟、小柳津麗欧、山本寛 89
- 1P-40** 電荷移動型C₆₁H₂化合物の構造と物理的性質
○岩瀬崇行、本橋覚、相原康貴、瀬戸志穂里、緒方啓典 90

2月14日(水)

特別講演 発表25分・質疑応答5分
一般講演 発表10分・質疑応答5分
ポスターレビュー 発表1分・質疑応答なし

特別講演(9:00-9:30)

2S-3 金属内包フラーレンの構造
永瀬 茂 3

一般講演(9:30-10:30)

金属内包フラーレン

- 2-1 Non-IPR構造を有する金属内包フラーレン: La@C₇₂
○二川秀史、菊池 隆、若原孝次、仲程司、G. M. Aminur Rahman、土屋敬広、前田 優、赤阪 健、与座健治、Ernst Horn、山本和典、溝呂木直美、Zdenek Slanina、永瀬 茂 25
- 2-2 La₂@C₈₀誘導体における内包La原子の動的挙動
○山田道夫、仲程司、若原孝次、土屋敬広、前田優、赤阪健、与座健治、溝呂木直美、永瀬茂 26
- 2-3 Scカーバイド内包フラーレンの構造
○飯塚裕子、若原孝次、中嶋康二、土屋敬広、前田優、仲程司、赤阪健、与座健治、Michael T. H. Liu、溝呂木直美、永瀬茂 27
- 2-4 放射光を用いた金属内包フラーレンおよびナノピーボットのキャラクタリゼーション:磁気円二色性とX線回折
○北浦良、沖本治哉、加藤祐子、中村哲也、西堀英治、青柳忍、坂田誠、篠原久典 28

☆☆☆☆☆☆ 休憩 (10:30-10:45) ☆☆☆☆☆☆

一般講演(10:45-11:45)

フラーレン固体とフラーレンの化学

- 2-5 (NaH)_xC₆₀化合物の構造と電子状態(II)
○何木隆史、本橋覚、緒方啓典 29
- 2-6 1-アルカンチオールで修飾されたAu電極を用いたC₆₀FETデバイスのキャリア注入障壁の解析
○長野高之、太田洋平、川崎菜穂子、野内亮、久保園芳博、藤原明比古、日野照純 30
- 2-7 電極上におけるバッキーフェロセンの電気化学および光電気化学特性
○金井塚勝彦、松尾豊、中村栄一 31
- 2-8 フラーレン誘導体の抗酸化活性とプロオキシダント効果
○中村成夫、佐竹恵理子、畑中雅史、高橋恭子、松林賢司、増野匡彦 32

☆☆☆☆☆☆ 昼食 (11:45-13:00) ☆☆☆☆☆☆

☆☆☆☆☆☆ 授賞式 (13:00-13:30) ☆☆☆☆☆☆

特別講演(13:30-14:00)

2S-4 量産単層カーボンナノチューブの現状と課題
八名 純三 4

一般講演(14:00-15:00)

フラーレンの化学

- 2-9 水溶性水酸化フラーレンの新規合成法およびCMP研磨スラリーへの応用
○小久保研、白川翔吾、松林賢司、林照剛、三好隆志、大島巧 33
- 2-10 フェムト秒レーザーアブレーションによる固体C₆₀のフラグメントイオン化の研究
○小林徹、加藤俊幸、松尾由賀利、倉田(西村)美月、河合純、林崎良英 34
- 2-11 環状[5]パラフェニレンアセチレン:合成・物性およびその超分子化学的性質
○川瀬 毅、西山義隆、中村高光、衣斐隆浩、松本幸三、藏田浩之 35
- 2-12 タンパク質の吸着によるC₆₀ナノ粒子の分散安定化
○出口 茂、山崎智子、向井貞篤、津留美紀子、掘越弘毅 36

☆☆☆☆☆☆ 休憩 (15:00-15:15) ☆☆☆☆☆☆

2月14日(水)

一般講演(15:15-16:00)

ナノ炭素科学

- 2-13 ナノ炭素材料の一重項酸素除去能
○柳和宏、大窪清吾、岡崎俊也、宮田耕充、片浦弘道 37
- 2-14 光酸化によるカーボンナノホーンの開孔とその生物への応用可能性
○張民芳、湯田坂雅子、安嶋久美子、飯島澄男 38
- 2-15 カーボンナノチューブ内部での水の相変化に関する分子動力学
○塩見淳一郎、木村達人、丸山茂夫 39

ポスターレビュー(16:00-17:00)

ポスターセッション(17:00-18:20)

ナノチューブの物性

- 2P-1 単層カーボンナノチューブの遠赤外吸収ピークとチューブ長との相関
○鈴木宏貴、秋間新真、下谷秀和、岩佐義宏 91
- 2P-2 大きな直径を持つビーボッドから合成した2層カーボンナノチューブの発光
○岡崎俊也、Z. Shi、斎藤毅、若林秀明、末永和知、飯島澄男 92
- 2P-3 ラマン分光法による単層カーボンナノチューブCVD成長過程のカイラリティ識別その場観察
○田沢雅也、高木大輔、本間芳和、鈴木哲、小林慶裕 93
- 2P-4 単層カーボンナノチューブの π プラズモン領域におけるモル吸光係数決定
○桑原彰太、菅井俊樹、篠原久典 94
- 2P-5 カーボンナノチューブとフラーレン間の光誘起電子移動
○稲田浩司、荒木保幸、アツラ サンダナヤカ、伊藤 攻 95
- 2P-6 ホウ素をドーブした多層カーボンナノチューブのESR評価
○沼尾茂悟、坂東俊治、飯島澄男 96
- 2P-7 スーパーグローブ法単層カーボンナノチューブにおける水分子吸着のFT-IRによる研究
○横井裕之、秋丸博祐、兼武昭徳、黒田規敬、早水裕平、畠賢治 97
- 2P-8 C_{60} ビーボッドの ^{13}C NMR
○松田和之、真庭豊、片浦弘道、鈴木信三、阿知波洋次 98
- 2P-9 単層カーボンナノチューブの紫外-可視領域の発光励起スペクトルの偏光依存性
○宮内雄平、丸山茂夫 99

ナノチューブの応用

- 2P-10 ポリイミドを用いた単層カーボンナノチューブの可溶化
○重田真宏、平山康平、藤ヶ谷剛彦、中嶋直敏 100
- 2P-11 異なるpH条件における単層カーボンナノチューブ分散液の分光特性と物理特性の関係
○石井亨、高橋照央、Catalin Romeo Luclesc、内田勝美、石井忠浩、矢島博文 101
- 2P-12 多形態カーボンナノチューブの生体高分子水溶液中による分散挙動およびその分光特性評価
○前田範子、内田勝美、石井忠浩、矢島博文 102
- 2P-13 単層カーボンナノチューブシートを介したシトクロムcの還元速度解析
○松浦宏治、斎藤毅、大嶋哲、湯村守雄、飯島澄男 103
- 2P-14 SWNTs-有機ケイ素複合体の合成と電界放出特性
○前田優、長谷川正、佐藤義倫、田路和幸、加固昌寛、若原孝次、赤阪健、Jing Lu、永瀬茂 104
- 2P-15 カーボンナノチューブの組立てと蛍光観察
○新井史人、永井萌土、清水彬生、石島秋彦、福田敏男 105
- 2P-16 ハニカム構造をもつカーボンナノチューブフィルムの構築
○高森久義、藤ヶ谷剛彦、新留康郎、中嶋直敏 106

内包ナノチューブ

- 2P-17 サイズ制御したポリリン分子を内包した単層カーボンナノチューブのラマンスペクトル
○西出大亮、若林知成、菅井俊樹、北浦良、片浦弘道、阿知波洋次、篠原久典 107
- 2P-18 C_{60} と C_{70} 内包二層ナノビーボットの合成と同定
○ニン グォツイン、岸直希、沖本治哉、白石将浩、菅井俊樹、篠原久典 108
- 2P-19 準一次元系における水の構造と相挙動
○高岩大輔、甲賀研一郎、田中秀樹 109

2月14日(水)

2P-20	円筒およびスリット状細孔内流体の相挙動 ○濱田嘉信、甲賀研一郎、田中秀樹	110
2P-21	X線回折を用いたSingle-Wall Carbon Nanotubeとフラーレンピーポッドの構造評価 ○加藤祐子、北浦良、赤地孝夫、青柳忍、西堀英治、坂田誠、篠原久典	111
2P-22	C ₈₂ 構造異性体の高分解能電顕観察 ○若林秀明、大窪信吾、越野雅至、佐藤雄太、斉藤毅、岡崎俊也、末永和知	112
2P-23	空気酸化と電子線照射に対するC ₆₀ -Peapodの構造安定 ○白石将浩、桑原彰太、西出大亮、伊藤靖浩、北浦良、菅井俊樹、篠原久典	113
2P-24	金属錯体を内包したカーボンナノチューブの合成と評価 ○小川大輔、石田将史、西出大亮、北浦良、菅井俊樹、篠原久典	114
2P-25	カーボンナノチューブ内包空間におけるアイスナノチューブのエネルギ論 ○栗田貴宏、岡田晋、押山淳	115

フラーレンの化学

2P-26	効率的なDNA光切断活性を指向する水溶性カチオン性ポルフィリン-C ₆₀ ハイブリッド化合物の合成 ○吉田隆裕、廣田喬、奥田健介	116
2P-27	ニトロフラーレン中間体を用いたチオール化フラーレンの合成と金表面への薄膜形成への応用 ○関戸大、吹留博一、吉村雅満、上田一之、大野正富	117
2P-28	オリゴカルバゾール部位を有する[60]フラーレン付加体の合成と光物理的性質(2) ○今野高志、中村洋介、渡辺悟、鈴木正人、西村淳	118
2P-29	Two New Metalloporphyrin Dimers: Molecular Scaffold for C ₆₀ and C ₇₀ ○Sumanta Bhattacharya, Kazuyuki Tominaga, Takahide Kimura, Hidemitsu Uno, Naoki Komatsu	119
2P-30	フラーレンのメカノケミカル酸素酸化反応中におけるポリマリゼーション ○渡辺洋人、石山雄一、田島右副、仙名保	120
2P-31	アズレンのπ平面とフラーレンのπ曲面との相互作用に基づく錯形成 ○小松直樹、Sumanta Bhattacharya, A. F. M. Mustafizur Rahman, 木村隆英	121
2P-32	末端に[60]フラーレンを有するポリ(N-イソプロピルアクリルアミド)の相転移挙動の高分子鎖長依存性 ○田村篤志、内田勝美、矢島博文	122
2P-33	水溶性フラーレン-キトサン複合体の物理化学的特性 ○三島佳史、根本勝理、指輪仁之、内田勝美、矢島博文	123
2P-34	C ₆₀ の生成過程と反応性 ○上野裕亮、斎藤晋	124

金属内包フラーレン

2P-35	La ₂ @C ₈₀ カルベン誘導体の合成とキャラクタリゼーション ○染谷知香、山田道夫、若原孝次、土屋敬広、前田優、赤阪健、溝呂木直美、永瀬茂	125
2P-36	溶媒フリーの金属内包フラーレンM@C ₈₂ (I) (M = Y, La, Lu) 固体の磁気物性 ○赤地孝夫、伊藤靖浩、高橋仁美、梅本久、井上崇、坂東俊治、藤田渉、阿波賀邦夫、北浦良、菅井俊樹、篠原久典	126
2P-37	軟X線磁気円二色性を用いたErY金属内包フラーレンの元素選択磁化解析 ○沖本治哉、北浦良、北村豊、伊藤靖浩、小川大輔、赤地孝夫、今津直樹、菅井俊樹、松下智裕、室隆桂之、大沢仁志、中村哲也、篠原久典	127
2P-38	高分解能イオン移動能装置のためのパルスイオンバルブの開発 ○菅井俊樹、篠原久典	128
2P-39	水酸化による金属内包フラーレンGd@C ₈₂ の電子状態の変化 ○Jun Tang, Gengmei Xing, Yuliang Zhao, Long Jing, Xingfa Gao, 熊代良太郎、谷垣勝己	129

2月15日(木)

特別講演 発表25分・質疑応答5分
一般講演 発表10分・質疑応答5分
ポスタープレビュー 発表1分・質疑応答なし

特別講演(9:00-9:30)

- 3S-5 カーボンナノチューブの分散と透明導電塗料の開発
角田裕三 5

一般講演(9:30-10:30)

ナノチューブ：生成と精製

- 3-1 サファイア上でのSWNTの水平配向における表面原子配列とステップとの競合成長
○今本健太、吾郷浩樹、石神直樹、大堂良太、上原直保、辻正治 40
- 3-2 Optical Enrichment of SWNTs through Preferential Extraction with Pyridine-based Chiral Diporphyrin Nano-tweezers
○Xiaobin Peng, Naoki Komatsu, Takahide Kimura, Atsuhiko Osuka 41
- 3-3 Co触媒微粒子を用いた先端放電型ラジカルCVDによるCNT低温合成-LSI配線応用に向けて-
○横山大輔、岩崎孝之、吉田剛、佐藤信太郎、二瓶瑞久、栗野祐二、川原田洋 42
- 3-4 Electrochemical growth of Pd nanostructures for the synthesis of multiwalled carbon nanotubes
○Rakesh K. Joshi, Masamishi Yoshimura, Kazuyuki Ueda 43

☆☆☆☆☆☆ 休憩 (10:30-10:45) ☆☆☆☆☆☆

一般講演(10:45-11:45)

ナノチューブ応用

- 3-5 ビア配線応用のためのリモートプラズマCVDによるカーボンナノチューブ成長
○佐久間尚志、片桐雅之、酒井忠司、鈴木真理子、二瓶瑞久、佐藤慎太郎、百島孝、栗野祐二 44
- 3-6 光デバイス作製のための光ピンセットによる位置選択的カーボンナノチューブ堆積
○柏木謙、山下真司、セット・ジ・イオン 45
- 3-7 化学ドーピングによるカーボンナノチューブFETのコンタクト抵抗の減少
○能生陽介、大野雄高、岸本茂、水谷孝 46
- 3-8 簡便な手法で作製した単層カーボンナノチューブネットワークによる室温・超高感度NO₂検出
○アンナマライ・カルティゲヤン、南 信次、コンスタンチン・ヤクボフスキー 47

☆☆☆☆☆☆ 昼食 (11:45-13:00) ☆☆☆☆☆☆

特別講演(13:00-13:30)

- 3S-6 カーボンナノチューブ内の水および単純液体の相転移
甲賀研一郎 6

一般講演(13:30-14:00)

ナノチューブ：生成と精製

- 3-9 金銀銅からの単層カーボンナノチューブ成長
○高木大輔、本間芳和、日比野浩樹、鈴木哲、小林慶裕 48
- 3-10 遠心分級したナノ粒子触媒を用いた直径制御カーボンナノチューブの成長
○井上崇、郡司島造、岡本篤人 49

ポスタープレビュー(14:00-15:00)

ポスターセッション(15:00-16:20)

ナノチューブ：生成と精製

- 3P-1 アルコールガスを用いた高真空下でのSi基板上カーボンナノチューブ成長
○谷奥健次、白岩倫行、丸山隆浩、成塚重弥 130
- 3P-2 カーボンナノチューブ生成のための炭素原料ガス分離の検討
○日方 威、林和彦、佐藤謙一、水越朋之、桜井芳昭、石神逸男、青木学聡、瀬木利夫、松尾二郎 131

2月15日(木)

3P-3	Effect of metallicity on the diameter distribution of single walled carbon nanotubes synthesized by catalytic ACCVD ○Krishnendu Bhattacharyya, 須田善行, 酒井洋輔, 菅原広剛, 沖田篤士, 齊藤武, 尾関充史, 前川将之, 高山純一	132
3P-4	水素-アルゴン-メタン混合ガス中で交流アーク放電による単層カーボンナノチューブの作製 ○柴田匡文, 趙新洛, 井上栄, 安藤義則	133
3P-5	SWNT成長におけるSiO ₂ 膜厚の影響 ○村上俊也, 徳田孝弘, 長谷部祐樹, 東憲吾, 木曾田賢治, 西尾弘司, 一色俊之, 播磨弘	134
3P-6	両親媒性オリゴペプチドによって水中に分散されたカーボンナノチューブの回収 ○山本淳, 増原真也, 古川善啓, 川端亮作, 日高貴志夫, 釜堀政男, 小野慎	135
3P-7	電界による金属性と半導体性単層カーボンナノチューブの分離 ○脇坂嘉一, 中山健一, 田中聡, 櫻井芳昭, 兼松泰男, 横山正明	136
3P-8	メタン・水素ガスをもちいたマイクロ波プラズマ化学気相成長法による垂直配向したカーボンナノチューブの成長 ○内藤綱彦, 渡邊啓, 林靖彦, 徳永智春, 金子賢治	137
3P-9	カーボンナノチューブ径制御に向けた熱処理による触媒微粒子のサイズ制御 ○山崎明, Jeong Goo-Hwan, 鈴木哲, 吉村英恭, 小林慶裕	138
3P-10	水素アーク放電による二層カーボンナノチューブの生成, 精製と評価 ○今津直樹, 白石将浩, 岸直希, 北浦良, 菅井俊樹, 橋本剛, 趙新洛, 安藤義則, 篠原久典	139

ナノチューブの応用

3P-11	カーボンナノチューブ粒子の細胞培養法による毒性評価 ~in vitroテストの標準化に向けて~ 森岡幸, 斎藤隆雄, 楠美智子, 山本元弘, ○加藤且也	140
3P-12	カーボンナノチューブからの電界放出その場観察:電界増強因子の電極間距離依存性 ○奥村健介, 世古和幸, 安坂幸師, 齋藤弥八	141
3P-13	アルミ蒸着によるMWNTの電界放出特性への影響 ○山下徹也, 松川知弘, 世古和幸, 安坂幸師, 中原仁, 齋藤弥八	142
3P-14	反応性カーボンナノチューブ可溶化剤-孤立可溶化とパルスレーザー照射 ○成松香織, 藤ヶ谷剛彦, 新留康郎, 中嶋直敏	143
3P-15	長鎖ベンゼンジアゾニウム塩を用いた半導体性カーボンナノチューブの分離 ○豊田昇平, 山口芳文, 樋渡真敬, 友成安彦, 村上裕人, 中嶋直敏	144
3P-16	光グラフト反応を利用したポリマーフィルムへのカーボンナノチューブコーティング ○原口辰介, 山口芳文, 藤ヶ谷剛彦, 新留康郎, 中嶋直敏	145
3P-17	カーボンナノチューブ直流電着法におけるファンデルワールス相互作用の役割 ○松本貴紀 佐野正人	146

ナノホーン

3P-18	触媒担持アークスートをを用いたDMFCスタックセルの開発 ○篠原賢司, 東敬亮, 和泉勇毅, 山本真伸, 桶真一郎, 滝川浩史, 青柳伸宜, 大川隆, 榊原敏洋, 中村宗太郎, 菅原秀一, 吉川和男, 三浦光治, 伊藤茂生, 山浦辰雄	147
3P-19	化学修飾カーボンナノホーンの光誘起電荷分離 ○伊藤 攻, アツラ サンダナヤカ, 荒木保幸, 湯田坂雅子, 飯島澄男, ニコス タグマタチス	148
3P-20	高純度カーボンナノホーンの生成 ○蒔丈史, 弓削亮太, 糟屋大介, 吉武務, 久保佳実, 湯田坂雅子, 飯島澄男	149
3P-21	電気化学キャパシタのためのRuO ₂ 高分散アークスート電極 ○山本真伸, 東敬亮, 篠原賢司, 桶真一郎, 滝川浩史, 伊藤茂生, 山浦辰雄, 三浦光治, 吉川和男	150
3P-22	吸着酸素の磁性変化によるナノホーン内部空間の評価 ○高橋仁美, 坂東俊治, 飯島澄男	151
3P-23	アーク放電で作製されるボロン担持ナノホーン ○稲垣貴之, 坂東俊治, 飯島澄男	152
3P-24	直流アーク放電による小さな直径のカーボンナノホーンの高収率作製と評価 ○稲垣貴之, 原田学, 坂東俊治, 飯島澄男	153

金属内包フラーレン

3P-25	多極磁場ミラー型ECR放電プラズマを利用した窒素内包フラーレンの形成 ○阿部重幸, 石田裕康, 西垣昭平, 金子俊郎, 畠山力三	154
-------	---	-----

2月15日(木)

- 3P-26** RF放電を利用した窒素原子内包フラーレン合成におけるプラズマ特性の効果
○西垣昭平、阿部重幸、金子俊郎、畠山力三 155
- 3P-27** $\text{Lu}_2\text{@C}_{82}$ (II)の光電子分光スペクトル
○宮崎隆文、加藤真之、古川浩之介、隅井良平、梅本久、沖本治哉、菅井俊樹、篠原久典、日野照純 156
- 3P-28** $\text{Pr}_2\text{@C}_{80}$ の ^{13}C NMRの研究
○伊藤学、長岡志保、兒玉健、三宅洋子、鈴木信三、菊地耕一、阿知波洋次 157
- 3P-29** エルビウム金属内包フラーレン(Er_2C_2)@ C_{2n} の蛍光特性
○赤地祐彦、伊藤靖浩、北浦良、菅井俊樹、篠原久典 158

炭素ナノ粒子

- 3P-30** Electronic and magnetic properties of acid-adsorbed nanoporous activated carbon fibers
○Hao Sijia、高井和之、榎敏明 159
- 3P-31** ナノダイヤモンド表面の化学制御による分散性の制御
○瀧本竜哉、門田直樹、森田陽一、青沼秀児、木村隆英、小松直樹 160
- 3P-32** アーク放電法によるランタン内包カーボンオニオン構造の生成
○山本和典、若原孝次、赤阪健 161

その他

- 3P-33** Effect of annealed temperature on the capacitance of electrochemical capacitors
○X.J. He, M. Yamamoto, K. Higashi, K. Shinohara, S. Oke, H. Takikawa, S. Itoh, T. Yamaura, K. Miura, K. Yoshikawa 162
- 3P-34** スーパーグロース単層カーボンナノチューブのグラムスケール生産に向けた全自動CVDシステム
-工業量産へのステップ-
○二葉ドン、生井竜紀、平岡樹、畠賢治、山田健郎、湯村守雄、飯島澄男 163
- 3P-35** カーボンナノツイストの大量合成とそのエミッション特性
○細川雄治、杉浦遼平、志岐肇、滝川浩史、伊奈孝、伊藤茂生、山浦辰雄 164
- 3P-36** フラーレンLB膜の作製法
○三浦康弘、山下敦史、松岡一誠、漆畑光貴、杉道夫 165
- 3P-37** CNTの溶媒処理方法の違いによる発生ガスの比較
○福本真治、和田豊仁、鈴木康志 166
- 3P-38** X線回折による多層カーボンナノチューブの直径評価
○國重敦弘、川元亨、加瀬庄一、住山芳行 167

February 13th, Tuesday

Special lectures : 25 min (Presentation) + 5 min (discussion)

General lecture : 10 min (Presentation) + 5 min (discussion)

Poster previews : 1 min (Presentation), no discussion

Special lecture (9 : 00-9 : 30)

- 1S-1 Quantum Chemical Molecular Dynamics Simulations of Fullerene and Carbon Nanotube Self-Assembly
Stephan Irle 1

General lecture (9 : 30-10 : 30)

Properties of Nanotubes

- 1-1 Super-Growth Single-Walled Carbon Nanotube Forest: An Ideal Graphene Surface Material with a Surface Area Over 1200 m²/g
Tatsuki Hiraoka, Takeo Yamada, Kenji Hata, Don N. Futaba, Jin Miyawaki, Masako Yudasaka, Motoo Yumura, Sumio Iijima 7
- 1-2 Internal structure of vertically aligned single-walled carbon nanotubes
Erik Einarsson, Hidetsugu Shiozawa, Christian Kramberger, Mark H. Ruemmel, Alex Grueneis, Thomas Pichler, Shigeo Maruyama 8
- 1-3 Current-Induced Structural Change of Fullerene-Encapsulated Single Wall Carbon Nanotubes
Hiroshi Somada, Yuya Yoshikawa, Atsuko Nagataki, Seiji Akita, Yoshikazu Nakayama 9
- 1-4 New Crystalline Phases of Carbon Transformed from Carbon Nanotubes under Pressure
Susumu Saito, Koichiro Kato, Masahiro Sakurai, Yuichiro Yamagami 10

☆☆☆☆☆☆ Coffee Break (10 : 30-10 : 45) ☆☆☆☆☆☆

General lecture (10 : 45-11 : 45)

Properties of Nanotubes

- 1-5 Factors Affecting on Electronic Properties of CNTs-FETs
Ryotaro Kumashiro, Nobuya Hiroshiba, Hirotaka Ohashi, Rikizo Hatakeyama, Katsumi Tanigaki 11
- 1-6 Negative differential resistance transport through C₆₀, C₇₀, and C₈₄ encapsulated double-walled carbon nanotubes
Y. F. Li, T. Kaneko, R. Hatakeyama 12
- 1-7 Electric Polarization of Cylindrical Carbon-Nanotube Capacitor
Kazuyuki Uchida, Susumu Okada, Kenji Shiraishi, Atsushi Oshiyama 13
- 1-8 Energetics and Electronic Structure of Carbon Nanotubes with Adatom-vacancy Pairs
Susumu Okada 14

☆☆☆☆☆☆ Lunch Time (11 : 45-13 : 00) ☆☆☆☆☆☆

Special lecture (13 : 00-13 : 30)

- 1S-2 Novel Approaches for Materialization of Supramolecular Fullerenes
Takashi Nakanishi 2

General lecture (13 : 30-14 : 45)

Properties of Nanotubes

- 1-9 Exciton effect on Raman spectra on single wall carbon nanotubes
R. Saito, J. Jiang, K. Sato, J. S. Park 15
- 1-10 Characterization of double-wall carbon nanotubes by absorption, photoluminescence, and Raman spectroscopies
Konstantin Iakoubovskii, Nobutsugu Minami, Taro Ueno, Said Kazaoui, Yasumitsu Miyata, Hiromichi Kataura 16
- 1-11 Photoinduced Charge Separation of Chemically Modified Carbon Nanotubes
Osamu Ito, Atula Sandanayaka, Yasuyuki Araki, Francis D' Souza 17
- 1-12 Diameter-Dependent Dissipation of Vibration Energy of Cantilevered Multiwall Carbon Nanotubes
Shintaro Sawaya, Yoshikazu Nakayama, Seiji Akita 18
- 1-13 Effect of Adsorption of various gas molecules on the electronic structure of single walled CNT
Abhijit Chatterjee 19

☆☆☆☆☆☆ Coffee Break (14 : 45-15 : 00) ☆☆☆☆☆☆

February 13th, Tuesday

General lecture (15 : 00-16 : 15)

Applications and Properties of Nanotubes

1-14	First principles calculations for nanotube disruption by oxygen molecule ○Takazumi Kawai, Yoshiyuki Miyamoto	20
1-15	Structural change in MWCNTs pressurized under H ₂ gas atmosphere ○Atsuko Nakayama, Shigenori Numao, Satoshi Nakano, Shyunji Bandow, Sumio Iijima	21
1-16	Visualization of CNT networks in CNT/polymer nanocomposites by ADF-STEM ○Tohoru Matsubara, Kaoru Shoda, Kousuke Itou, Atsuhiko Kunishige, Yoshiyuki Sumiyama	22
1-17	Unique Optical Properties of DNA-dissolved Carbon Nanotubes ○Yuichi Noguchi, Tsuyohiko Fujigaya, Yasuro Niidome, Naotoshi Nakashima	23
1-18	Improved Ultrasonic Dispersion of Carbon Nanotubes Hiroshi Saito, ○Masahito Sano	24

Poster preview (16 : 15-17 : 15)

Poster session (17 : 15-18 : 35)

Properties of Nanotubes

1P-1	Origin of Linear Relationship Between CH ₂ /NH/O-(n, n)SWCNT Reaction Energies and Sidewall Curvature Guishan Zheng, Zhi Wang, ○Stephan Irle, Keiji Morokuma	51
1P-2	High-Speed Screening of Carbon Nanotube ○Yoshiyuki Miyamoto	52
1P-3	Chirality Dependence of G'-band Intensity on Raman Spectra of Single Wall Carbon Nanotubes ○Jin Sung Park, Riichiro Saito, Kentaro Sato, Jie Jiang, Ki Kang Kim, Young Hee Lee, Gene Dresselhaus, Mildred S. Dresselhaus	53
1P-4	Pressure dependence of photoluminescence spectra in single-walled carbon nanotubes dispersed in D ₂ O with deoxycholic acid ○Satoru Sakoda, Masao Ichida, Yasumitsu Miyata, Hiromichi Kataura, Kenichi Mizuno, Hiroaki Ando	54
1P-5	Electronic structures and magnetic moments at edges of graphene ribbon ○Hirofumi Sakashita, Tatsuki Oda	55
1P-6	Theory of superconductivity of carbon nanotubes and graphene ○K. Sasaki, J. Jiang, R. Saito, S. Onari, Y. Tanaka	56
1P-7	Electronic Structures of Functionalized Single-Walled Carbon Nanotubes ○Yoshikazu Kobayashi, Hiroyuki Fueno, Kazuyoshi Tanaka, Tomokazu Umeyama, Hiroshi Imahori	57
1P-8	Coulomb gap increase in SWNT single-electron transistors induced by low-energy irradiation ○Junichi Hashimoto, Satoru Suzuki, Toshio Ogino, Yoshihiro Kobayashi	58
1P-9	Conversion of metallic SWNT-FETs to semiconducting at room temperature by low-energy irradiation ○Satoru Suzuki, Junichi Hashimoto, Toshio Ogino, Yoshihiro Kobayashi	59

Formation and Purification of Nanotubes

1P-10	Bond Curvature Dependent Oxidation Process in Single-Wall Carbon Nanotubes ○Yasumitsu Miyata, Takazumi Kawai, Yoshiyuki Miyamoto, Kazuhiro Yanagi, Yutaka Maniwa, Hiromichi Kataura	60
1P-11	Orientalional control of carbon nanotube growth by plasma-enhanced hot filament chemical vapor deposition ○Chien-Chao Chiu, Masamichi Yoshimura, Kazuyuki Ueda	61
1P-12	Aligned growth of single-walled carbon nanotubes due to interaction with sapphire substrates ○Akira Yamazaki, Daisuke Takagi, Satoru Suzuki, Goo-Hwan Jeong, Hideyuki Yoshimura, Yoshikazu Homma, Yoshihiro Kobayashi	62
1P-13	Growth of carbon nanotube on Si substrate using pulse arc plasma as carbon source ○Tomoyuki Shiraiwa, Yoshiaki Kato, Kenji Tanioku, Suzuka Nishimura, Takahiro Maruyama, Shigeya Naritsuka	63
1P-14	Dielectrophoresis separation of single-walled carbon nanotubes ○Shigeo Maruyama, Junichiro Shiomi, Yuhei Miyauchi, Yuan Lin, Gustav Amberg	64
1P-15	Effect of hydrogen on increasing of the diameters of single-wall carbon nanotubes ○Masahiro Hayakawa, Shunji Bandow, Sumio Iijima	65
1P-16	Growth and Synthesis of Single-Wall Carbon Nanotubes within Mesoporous Materials by Catalyst-supported Chemical Vapor Deposition ○Keita Kobayashi, Ryo Kitaura, Toshiki Sugai, Youko Kumai, Yasutomo Goto, Shinji Inagaki, Hisanori Shinohara	66

February 13th, Tuesday

- 1P-17** Control of Location and Orientation of Single-Walled Carbon Nanotubes on Sapphire Surface
○*Ryota Ohdo, Hiroki Ago, Masashi Shinagawa, Naoki Ishigami, Masaharu Tsuji, Tatsuya Ikuta, Koji Takahashi* 67
- 1P-18** Chemistry of Water-Oxidation during CVD Growth of Single- and Double-Walled Carbon Nanotubes over Fe-Mo/MgO Catalyst
○*Naoki Yoshihara, Hiroki Ago, Masaharu Tsuji* 68
- 1P-19** Low-temperature growth of carbon nanotubes by alcohol CCVD (II)
Ken Hiasa, Shogo Suzuki, Hideki Sato, Koichi Hata, Kazuo Kajiwara, Yahachi Saito 69
- 1P-20** Half-centimeter long vertically aligned carbon nanotubes using optimized radical CVD conditions and study of CO₂ effects
○*Takayuki Iwasaki, Tasuku Maki, Tsuyoshi Yoshida, Takumi Aikawa, Tatsuhiro Nozue, Daiyu Kondo, Akio Kawabata, Shintaro Sato, Mizuhisa Nihei, Yuji Awano, Hiroshi Kawarada* 70

Nanohorns

- 1P-21** Toxicological study of single-wall carbon nanohorns
○*Jin Miyawaki, Masako Yudasaka, Takeshi Azami, Yoshimi Kubo, Sumio Iijima* 71
- 1P-22** Closing Rates of Holes in Single-Wall Carbon Nanohorns at Various Heating Temperature
○*Jing Fan, Masako Yudasaka, Jin Miyawaki, Ryota Yuge, Takazumi Kawai, Sumio Iijima* 72
- 1P-23** Streptavidin-modified Single Wall Carbon Nanohorns
○*Xu Jianxun, Masako Yudasaka, Sumio Iijima* 73
- 1P-24** Formation mechanism of single-wall carbon nanohorn aggregates hybridized with carbon nanocapsules
Keita Kobayashi, Akira Koshio, Yutaka Takahashi, Fumio Kokai 74
- 1P-25** Effect of solvents on CDDP incorporation into SWNHs
○*Kumiko Ajima, Masako Yudasaka, Sumio Iijima* 75
- 1P-26** Hydrogen production by steam reforming of methane at low temperature using EuPt catalyst supported on single-wall carbon nanohorns
○*Ryota Yuge, Katsuyuki Murata, Masako Yudasaka, Yoshimi Kubo, Tsutomu Yoshitake, Sumio Iijima* 76
- 1P-27** Drug-loaded single-wall carbon nanohorns dispersed with a polyethylene glycol-peptide conjugate
○*Sachiko Matsumura, Masako Yudasaka, Sumio Iijima, Kiyotaka Shiba* 77

Chemistry of Fullerenes

- 1P-28** Synthesis and Characterization of Deca(organo)[60]fullerenes Containing Five Ferrocenyl Groups
○*Takahiko Ichiki, Yutaka Matsuo, Eiichi Nakamura* 78
- 1P-29** Synthesis and Electrochemistry of Fullerene-Metal-Arene Conjugated System
○*Takeshi Nanao, Yutaka Matsuo, Eiichi Nakamura* 79
- 1P-30** Synthesis of Heterodinuclear Metal Complexes of Octa(organo)[60]fullerenes
○*Takahiro Nakae, Yutaka Matsuo, Eiichi Nakamura* 80
- 1P-31** Regioselective Octa- and Deca-additions of Pyridine-modified Organocopper Reagent to [60]Fullerene
○*Yutaka Matsuo, Kazukuni Tahara, Kouhei Morita, Keiko Matsuo, Eiichi Nakamura* 81
- 1P-32** Encapsulation of Helium Atom inside an Open-Cage C₆₀ Derivative and Synthesis of He@C₆₀
○*Fumiyuki Tanabe, Sadayuki Mori, Koichi Komatsu, Michihisa Murata, Yasujiro Murata* 82

Fullerene Solids

- 1P-33** Fabrication of field-effect transistor devices with Langmuir-Blodgett films of fullerodendron
○*Naoko Kawasaki, Takayuki Nagano, Yoshihiro Kubozono, Yuki Sako, Yutaka Takaguchi, Akihiko Fujiwara, Shojun Hino, Chih-Chien Chu, Toyoko Imae* 83
- 1P-34** TEM and Raman Spectroscopy Analyses of Fullerene Derivative Nanowhiskers and Fullerene Nanotubes
○*Kun-ichi Miyazawa, Cherry Ringor, Tadahiko Mashino, Shigeo Nakamura* 84
- 1P-35** Enhanced Growth of C₆₀ Nanotubes by Illumination with UV Light
○*Cherry Ringor, Kun'ichi Miyazawa, Tohru Awane* 85
- 1P-36** Theoretical Study of Electronic and Transport Properties of Fullerene as a Molecular Device
○*Shinji Usui, Yoshihisa Ohshima, Shoji Hirose, Tetsuo Kitajima* 86
- 1P-37** Electrical Properties of FET devices with C₆₀ Nano-Whiskers
○*Kenichi Ogawa, Hajime Tsuji, Nobuyuki Aoki, Yuichi Ochiai* 87
- 1P-38** Electronic transport properties of electron-beam-irradiated C₆₀ polymers
○*H.Tsuji, K.Ogawa, K.Ryuzaki, N.Aoki, J.Onoe, Y.Ochiai* 88

February 13th, Tuesday

- 1P-39** Synthesis of polymerized C_{60} films by irradiation of a free electron laser during a deposition
○*Nobuyuki Iwata, RyoNokariya, Shingo Ando, Reo Koyaizu, Hiroshi Yamamoto* 89
- 1P-40** Structure and Physical Properties of Charge transfer $C_{61}H_2$ (dihydrofulleroid) Compounds
○*Takayuki Iwase, Satoru Motohashi, Yasutaka Aihara, Shihori Seto, Hironori Ogata* 90

February 14th, Wednesday

Special lectures: 25 min (Presentation) + 5 min (discussion)

General lecture: 10 min (Presentation) + 5 min (discussion)

Poster previews: 1 min (Presentation), no discussion

Special lecture (9 : 00-9 : 30)

- 2S-3 Structures of Endohedral Metallofullerenes
Shigeru Nagase 3

General lecture (9 : 30-10 : 30)

Metallofullerenes

- 2-1 La@C₇₂ Having a Non-IPR Carbon Cage
○*Hidefumi Nikawa, Takashi Kikuchi, Takatsugu Wakahara, Tsukasa Nakahodo, G. M. Aminur Rahman, Takahiro Tsuchiya, Yutaka Maeda, Takeshi Akasaka, Kenji Yoza, Ernst Horn, Kazunori Yamamoto, Naomi Mizorogi, Zdenek Slanina, Shigeru Nagase* 25
- 2-2 Motion of the La Atoms in La₂@C₈₀ Derivatives
○*Michio Yamada, Tsukasa Nakahodo, Takatsugu Wakahara, Takahiro Tsuchiya, Yutaka Maeda, Takeshi Akasaka, Kenji Yoza, Naomi Mizorogi, Shigeru Nagase* 26
- 2-3 Structure of Scandium Carbide-encapsulated Metallofullerene
○*Yuko Iiduka, Takatsugu Wakahara, Koji Nakajima, Takahiro Tsuchiya, Yutaka Maeda, Tsukasa Nakahodo, Takeshi Akasaka, Kenji Yoza, Michael T. H. Liu, Naomi Mizorogi, Shigeru Nagase* 27
- 2-4 Characterization of Metallofullerenes and Fullerene Nano-peapods by Synchrotron Radiation: Soft X-ray Magnetic Circular Dichroism Spectroscopy and X-ray Diffraction.
○*Ryo Kitaura, Haruya Okimoto, Yuko Kato, Tetsuya Nakamura, Eiji Nishibori, Shinobu Aoyagi, Makoto Sakata, Hisanori Shinohara* 28

☆☆☆☆☆☆ Coffee Break (10 : 30-10 : 45) ☆☆☆☆☆☆

General lecture (10 : 45-11 : 45)

Fullerene solids and Chemistry of Fullerenes

- 2-5 Structure and Electronic Properties of (NaH)_xC₆₀ Compounds(II)
○*Takashi Naniki, Satoru Motohashi, Hironori Ogata* 29
- 2-6 Analyses of the carrier injection barrier of C₆₀ FET devices with Au source/drain electrodes modified by 1-alkanethiol
○*Takayuki Nagano, Yohei Ohta, Naoko Kawasaki, Ryo Nouchi, Yoshihiro Kubozono, Akihiko Fujiwara, Shojun Hino* 30
- 2-7 Electrochemical and Photoelectrochemical Properties of Buckyferrocenes on Electrodes
○*Katsuhiko Kanaizuka, Yutaka Matsuo, Eiichi Nakamura* 31
- 2-8 Fullerene derivatives have antioxidant activity but no metal-dependent prooxidant activity
○*Shigeo Nakamura, Eriko Satake, Masashi Hatanaka, Kyoko Takahashi, Kenji Matsubayashi, Tadahiko Mashino* 32

☆☆☆☆☆☆ Lunch Time (11 : 45-13 : 00) ☆☆☆☆☆☆

☆☆☆☆☆☆ Awards Ceremony (13 : 00-13 : 30) ☆☆☆☆☆☆

Special lecture (13 : 30-14 : 00)

- 2S-4 Present status of SWCNT mass production & future problems
Junzo Yana 4

General lecture (14 : 00-15 : 00)

Chemistry of Fullerenes

- 2-9 A New Route to Water-Soluble Fullerenol and its Application to CMP Slurry
○*Ken Kokubo, Syogo Shirakawa, Kenji Matsubayashi, Terutake Hayashi, Takashi Miyoshi, Takumi Oshima* 33
- 2-10 Ionization and fragmentation of solid C₆₀ by femtosecond laser ablation
○*Tohru Kobayashi, Toshiyuki Kato, Yukari Matsuo, Mizuki Kurata-Nishimura, Jun Kawai, Yoshihide Hayashizaki* 34
- 2-11 Cyclic [5]Paraphenyleneacetylene: Synthesis, properties and its supramolecular properties
○*Takeshi Kawase, Yoshitaka Nishiyama, Takamitsu Nakamura, Takahiro Ebi, Kouzou Matsumoto, Hiroyuki Kurata* 35

February 14th, Wednesday

- 2-12 Stabilization of C₆₀ Nanoparticles by Protein Adsorption
○Shigeru Deguchi, Tomoko Yamazaki, Sada-atsu Mukai, Mikiko Tsudome, Koki Horikoshi 36

☆☆☆☆☆☆Coffee Break (15 : 00-15 : 15) ☆☆☆☆☆☆

General lecture (15 : 15-16 : 00)

Science of Nanocarbons

- 2-13 Deactivation properties of singlet oxygen by nano-carbon materials
○Kazuhiro Yanagi, Shingo Okubo, Toshiya Okazaki, Yasumitsu Miyata, Hiromichi Kataura 37
- 2-14 Light-Assisted Oxidation of Single-Wall Carbon Nanohorns for Biological Uses
○Minfang Zhang, Masako Yudasaka, Kumiko Ajima, Sumio Iijima 38
- 2-15 Molecular dynamics of phase transition of water inside a carbon nanotube
○Junichiro Shiomi, Tatsuto Kimura, Shigeo Maruyama 39

Poster preview (16 : 00-17 : 00)

Poster session (17 : 00-18 : 20)

Properties of Nanotubes

- 2P-1 Far-Infrared Absorption Peak in Single-Walled Carbon Nanotubes and Its Correlation with Tube Lengths
○Hirotaka Suzuki, Nima Akima, Hidekazu Shimotani, Yoshihiro Iwasa 91
- 2P-2 Photoluminescence of Larger Diameter Double-Walled Carbon Nanotubes Synthesized from C₆₀ Peapods
○Toshiya Okazaki, Zujin Shi, Takeshi Saito, Hideaki Wakabayashi, Kazu Suenaga, Sumio Iijima 92
- 2P-3 Chirality-sensitive in-situ observation of CVD growth of single-walled carbon nanotubes by Raman spectroscopy
○Masaya Tazawa, Daisuke Takagi, Yoshikazu Homma, Satoru Suzuki, Yoshihiro Kobayashi 93
- 2P-4 Determining Molar Absorbance Coefficients of Single-Walled Carbon Nanotubes
○Shota Kuwahara, Toshiki Sugai, Hisanori Shinohara 94
- 2P-5 Photoinduced electron transfer between single-wall carbon nanotubes and C₆₀ dispersed in D₂O
○Koji Inada, Yasuyuki Araki, Sandanayaka Atula, Osamu Ito 95
- 2P-6 ESR study of boron-doped multiwall carbon nanotubes
○Shigenori Numao, Shunji Bandow, Sumio Iijima 96
- 2P-7 FT-IR study of adsorption of H₂O on SWNTs prepared in Super-Growth technique
○Hiroyuki Yokoi, Hirosuke Akimaru, Akinori Kanetake, Noritaka Kuroda, Yuhei Hayamizu, Kenji Hata 97
- 2P-8 ¹³C NMR study of C₆₀-peapods
○Kazuyuki Matsuda, Yutaka Maniwa, Hiromichi Kataura, Shinzo Suzuki, Yohji Achiba 98
- 2P-9 Polarization dependence of photoluminescence excitation spectra of single-walled carbon nanotubes in UV-Vis range
○Yuhei Miyauchi, Shigeo Maruyama 99

Applications of Nanotubes

- 2P-10 Individual solubilization of single-walled carbon nanotubes using totally aromatic polyimides
○Masahiro Shigeta, Kouhei Hirayama, Tsuyohiko Fujigaya, Naotoshi Nakashima 100
- 2P-11 The relationship between the optical property and physical property of dispersed SWNTs under various pH conditions
○Toru Ishii, Teruo Takahashi, Catalin Romeo Luculescu, Katsumi Uchida, Tadahi Ishii, Hirofumi Yajima 101
- 2P-12 Dispersion Behavior and Spectroscopic Properties of the Polymorphic Forms of Carbon Nanotubes in Biopolymer Aqueous Solutions
○Noriko Maeda, Katsumi Uchida, Tadahi Ishii, Hirofumi Yajima 102
- 2P-13 Reduction kinetics of cytochrome *c* through single-walled carbon nanotubes
○Koji Matsuura, Takeshi Saito, Satoshi Ohshima, Motoo Yumura, Sumio Iijima 103
- 2P-14 Preparation of Single-Walled Carbon Nanotube-Organosilicon Hybrids and Their Field Emission Properties
○Yutaka Maeda, Tadashi Hasegawa, Yoshinori Sato, Kazuyuki Tohji, Masahiro Kako, Takatsugu Wakahara, Takeshi Akasaka, Jing Lu, Shigeru Nagase 104
- 2P-15 Assembly and Fluorescence Visualization of Carbon Nanotubes
○Fumihito Arai, Moeto Nagai, Akio Shimizu, Akihiko Ishijima, Toshio Fukuda 105
- 2P-16 Self-Organized Single-Walled Carbon Nanotubes with Honeycomb Structures
○Hisayoshi Takamori, Tsuyohiko Fujigaya, Yasuro Niidome, Naotoshi Nakashima 106

February 14th, Wednesday

Endohedral Nanotubes

- 2P-17** Raman spectroscopic study on size-selected linear polyyne molecules inside single-wall carbon nanotubes
○*D. Nishide, T. Wakabayashi, T. Sugai, R. Kitaura, H. Kataura, Y. Achiba, H. Shinohara* 107
- 2P-18** Synthesis and Characterization of C₆₀ and C₇₀ Double-Wall Carbon Nanopeapods
○*Guoqing Ning, Naoki Kishi, Haruya Okimoto, Masahiro Shiraishi, Toshiki Sugai, Hisanori Shinohara* 108
- 2P-19** Structure and phase behavior of quasi-one-dimensional water
○*Daisuke Takaiwa, Kenichiro Koga, Hideki Tanaka* 109
- 2P-20** Phase behavior of simple fluids in cylindrical and slit pores
○*Yoshinobu Hamada, Kenichiro Koga, Hideki Tanaka* 110
- 2P-21** Structural Characterization of Single-Wall Carbon Nanotubes and Fullerene-Nanopeapods by X-ray Diffraction Measurement
○*Yuko Kato, Ryo Kitaura, Takao Akachi, Shinobu Aoyagi, Eiji Nishibori, Makoto Sakata, Hisanori Shinohara* 111
- 2P-22** HR-TEM observations of structural isomers of C₈₂ with the C₂ symmetry
○*Hideaki Wakabayashi, Shingo Okubo, Masanori Koshino, Yuta Sato, Takeshi Saito, Toshiya Okazaki, Kazu Suenaga* 112
- 2P-23** Enhanced Structural Stability of C₆₀-Peapods toward Thermal Oxidation and Electron Beam Irradiation
○*Masahiro Shiraishi, Shota Kuwahara, Daisuke Nishide, Yasuhiro Ito, Ryo Kitaura, Toshiki Sugai, Hisanori Shinohara* 113
- 2P-24** Synthesis and Characterization of Carbon Nanotubes Encapsulating Metal Complexes
○*Daisuke Ogawa, Masashi Ishida, Daisuke Nishide, Ryo Kitaura, Toshiki Sugai, Hisanori Shinohara* 114
- 2P-25** Energetics of Ice Nanotubes inside Carbon Nanotubes
○*Takahiro Kurita, Susumu Okada, Atsushi Oshiyama* 115

Chemistry of Fullerenes

- 2P-26** Synthesis of water-soluble cationic porphyrin-C₆₀ hybrids toward efficient photo cleavage of DNA
○*Takahiro Yoshida, Takashi Hirota, Kensuke Okuda* 116
- 2P-27** Synthesis of Thiolated [60]Fullerene Derivative via Nitrofullerene Intermediate and Its Application to Thin Film Formation on Au
○*Masaru Sekido, Hirokazu Fukidome, Masamichi Yoshimura, Kazuyuki Ueda, Masatomi Ohno* 117
- 2P-28** Synthesis and Photophysical Properties of [60]Fullerene Adducts Carrying Oligocarbazole Moieties (2)
○*Takashi Konno, Yosuke Nakamura, Satoru Watanabe, Masato Suzuki, Jun Nishimura* 118
- 2P-29** Two New Metalloporphyrin Dimers: Molecular Scaffold for C₆₀ and C₇₀
○*Sumanta Bhattacharya, Kazuyuki Tominaga, Takahide Kimura, Hidemitsu Uno, Naoki Komatsu* 119
- 2P-30** Polymerization during mechanochemical oxidation under oxygen atmosphere
○*Hiroto Watanabe, Yuichi Ishiyama, Yusuke Tajima, Mamoru Senna* 120
- 2P-31** Extraordinarily Large Association Constants of Azulenes with Fullerenes
○*Naoki Komatsu, Sumanta Bhattacharya, A. F. M. Mustafizur Rahman, Takahide Kimura* 121
- 2P-32** Polymer Chain Length Effects on Temperature-Responsive Phase Transition Behaviors of [60]Fullerene End-Bonded Poly(*N*-isopropylacrylamide)
○*Atsushi Tamura, Katsumi Uchida, Hirofumi Yajima* 122
- 2P-33** Physicochemical property of water-soluble fullerene-chitosan conjugate
○*Yoshifumi Mishima, Katsumasa Nemoto, Hitoshi Sashiwa, Katsumi Uchida, Hirofumi Yajima* 123
- 2P-34** Abundance of C₆₀ revisited
○*Yusuke Ueno, Susumu Saito* 124

Metallofullerenes

- 2P-35** Synthesis and Characterization of Carbene Derivatives of La₂@C₈₀
○*Chika Someya, Michio Yamada, Takatsugu Wakahara, Takahiro Tsuchiya, Yutaka Maeda, Takeshi Akasaka, Naomi Mizorogi, Shigeru Nagase* 125
- 2P-36** Magnetic Properties of Solvent-Free M@C₈₂(I) (M = Y, La, Lu) Metallofullerene Solids
○*Takao Akachi, Yasuhiro Ito, Hitomi Takahashi, Hisashi Umemoto, Takashi Inoue, Shunji Bandow, Wataru Fujita, Kunio Awaga, Ryo Kitaura, Toshiki Sugai, Hisanori Shinohara* 126
- 2P-37** Element Specific Magnetization Measurements of ErY-Metallofullerenes by Soft X-ray Magnetic Circular Dichroism
○*Haruya Okimoto, Ryo Kitaura, Yutaka Kitamura, Yasuhiro Ito, Daisuke Ogawa, Takao Akachi, Naoki Imazu, Toshiki Sugai, Tomohiro Matsushita, Takayuki Muro, Hitoshi Osawa, Tetsuya Nakamura, Hisanori Shinohara* 127
- 2P-38** Development of Pulsed Ion Valve for High-resolution Ion Mobility Measurement
○*Toshiki Sugai, Hisanori Shinohara* 128

February 14th, Wednesday

2P-39 Variation of Electronic Properties in Gd@C₈₂ Metallofullerene Induced by Polyhydroxylation
○*Jun Tang, Gengmei Xing, Yuliang Zhao, Long Jing, Xingfa Gao, Ryotaro Kumashiro, Katsumi Tanigaki*

129

February 15th, Thursday

Special lectures: 25 min (Presentation) + 5 min (discussion)

General lecture: 10 min (Presentation) + 5 min (discussion)

Poster previews: 1 min (Presentation), no discussion

Special lecture (9 : 00-9 : 30)

- 3S-5 Dispersion of Carbon Nanotubes and Development of Transparent Conductive Coatings
Yuzo Sumita 5

General lecture (9 : 30-10 : 30)

Formation and Purification of Nanotubes

- 3-1 Competing Growth of Horizontally-Aligned SWNTs between Surface Atomic Arrangement and Surface Steps on Sapphire
○*Kenta Imamoto, Hiroki Ago, Naoki Ishigami, Ryota Ohdo, Naoyasu Uehara, Masaharu Tsuji* 40
- 3-2 Optical Enrichment of SWNTs through Preferential Extraction with Pyridine-based Chiral Diporphyrin Nano-tweezers
○*Xiaobin Peng, Naoki Komatsu, Takahide Kimura, Atsuhiko Osuka* 41
- 3-3 Radical chemical vapor deposition of vertically aligned CNTs at low temperatures using sizeclassified Co particles for LSI interconnects
○*Daisuke Yokoyama, Takayuki Iwasaki, Tsuyoshi Yoshida, Shintaro Sato, Mizuhisa Nihei, Yuji Awano, Hiroshi Kawarada* 42
- 3-4 Electrochemical growth of Pd nanostructures for the synthesis of multiwalled carbon nanotubes
○*Rakesh K. Joshi, Masamichi Yoshimura, Kazuyuki Ueda* 43

☆☆☆☆☆☆ Coffee Break (10 : 30-10 : 45) ☆☆☆☆☆☆

General lecture (10 : 45-11 : 45)

Applications of Nanotubes

- 3-5 Carbon Nanotube Growth by Remote Plasma CVD for Via Interconnects
○*Naoshi Sakuma, Masayuki Katagiri, Tadashi Sakai, Mariko Suzuki, Mizuhisa Nihei, Shintaro Sato, Takashi Hyakushima, Yuji Awano* 44
- 3-6 Area Selective Deposition of Carbon Nanotubes by Optical Tweezers for Optical Devices Applications
○*Ken Kashiwagi, Shinji Yamashita, Sze Yun Set* 45
- 3-7 Reduction of contact resistance by chemical doping in carbon nanotube FETs
○*Yosuke Noshio, Yutaka Ohno, Shigeru Kishimoto, Takashi Mizutani* 46
- 3-8 Ultra sensitive, room temperature NO₂ detection using single-wall carbon nanotube networks prepared by a simple method
○*Annamalai Karthigeyan, Nobutsugu Minami, Konstantin Iakoubovskii* 47

☆☆☆☆☆☆ Lunch Time (11 : 45-13 : 00) ☆☆☆☆☆☆

Special lecture (13 : 00-13 : 30)

- 3S-6 Phase transitions of water and simple liquids in carbon nanotubes
Kenichiro Koga 6

General lecture (13 : 30-14 : 00)

Formation and Purification of Nanotubes

- 3-9 Single-walled Carbon Nanotubes from Gold-group Catalysts
○*Daisuke Takagi, Yoshikazu Homma, Hiroki Hibino, Satoru Suzuki, Yoshihiro Kobayashi* 48
- 3-10 Synthesis of Diameter-Controlled Carbon Nanotubes Using Centrifugally Classified Nanoparticle Catalysts
○*Takashi Inoue, Itaru Gunjishima, Atsuto Okamoto* 49

Poster preview (14 : 00-15 : 00)

Poster session (15 : 00-16 : 20)

Formation and Purification of Nanotubes

- 3P-1 Growth of Carbon nanotubes on Si substrates using alcohol gas source in a high vacuum
○*Kenji Tanioku, Tomoyuki Shiraiwa, Takahiro Maruyama, Shigeya Naritsuka* 130

February 15th, Thursday

3P-2	Study of Carbon Source Gas Separation for Fabrication of Carbon Nanotubes ○Takeshi Hikata, Kazuhiko Hayashi, Ken-ichi Sato, Tomoyuki Mizukoshi, Yoshiaki Sakurai, Itsuo Ishigami, Takaaki Aoki, Toshio Seki, Jiro Matsuo	131
3P-3	Effect of metallicity on the diameter distribution of single walled carbon nanotubes synthesized by catalytic ACCVD ○Krishnendu Bhattacharyya, Yoshiyuki Suda, Yosuke Sakai, Hirotake Sugawara, Atsushi Okita, Takeshi Saito, Atsushi Ozeki, Masayuki Maekawa, Junichi Takayama	132
3P-4	Production of SWNTs by AC arc discharge in H ₂ -Ar-CH ₄ mixture gas ○Masafumi Shibata, Xinluo Zhao, Sakae Inoue, Yosinori Ando	133
3P-5	The effect of SiO ₂ thickness on the growth of SWNTs ○Toshiya Murakami, Takahiro Tokuda, Yuki Hasebe, Kengo Higashi, Kenji Kisoda, Koji Nishio, Toshiyuki Isshiki, Hiroshi Harima	134
3P-6	Recovery of carbon nanotubes dispersed with amphiphilic oligopeptides in water ○Atsushi Yamamoto, Shin-ya Masuhara, Yoshihiro Furukawa, Ryosaku Kawabata, Kishio Hidaka, Masao Kamahori, Shin Ono	135
3P-7	Separation of Metallic and Semiconducting Single-Walled Carbon Nanotubes by Electric Field ○Yoshikazu Wakizaka, Ken-ichi Nakayama, Satoshi Tanaka, Yoshiaki Sakurai, Yasuo Kanematsu, Masaaki Yokoyama	136
3P-8	Synthesis of vertical-aligned carbon nanotubes on SiO ₂ /Si substrate by microwave plasma chemical vapor deposition using CH ₄ /H ₂ gasses ○T. Naitou, A. Watanabe, Y. Hayashi, T. Tokunaga, K. Kaneko	137
3P-9	Size control of catalytic nanoparticles by thermal treatment toward diameter control of singlewalled carbon nanotubes ○Akira Yamazaki, Goo-Hwan Jeong, Satoru Suzuki, Hideyuki Yoshimura, Yoshihiro Kobayashi	138
3P-10	Production, Purification and Characterization of Double-Wall Carbon Nanotubes Synthesized by Hydrogen Arc Discharge ○Naoki Imazu, Masahiro Shiraishi, Naoki Kishi, Ryo Kitaura, Toshiki Sugai, Takeshi Hashimoto, Xinluo Zhao, Yoshinori Ando, Hisanori Shinohara	139

Applications of Nanotubes

3P-11	Cytotoxicological Studies of Carbon Nanotube Particles with Cultured Animal Cells. ~Standardrization for in vitro test~ Yuki Morioka, Takao Saito, Michiko Kusunoki, Motohiro Yamamoto, ○Katsuya Kato	140
3P-12	In situ TEM study on field emission from an isolated CNT:Field enhancement depending on emitter-anode gap ○Kensuke Okumura, Kazuyuki Seko, Koji Asaka, Yahachi Saito	141
3P-13	Field emission microscopy of MWNTs deposited with aluminum ○Tetsuya Yamashita, Tomohiro Matsukawa, Kazuyuki Seko, Koji Asaka, Hitoshi Nakahara, Yahachi Saito	142
3P-14	Reactive Carbon Nanotube Solubilizers - Individual solubilization and Pulsed Laser Irradiation ○Kaori Narimatsu, Tsuyohiko Fujigaya, Yasuro Niidome, Naotoshi Nakashima	143
3P-15	Separation of Semiconducting-Enriched Single-Walled Carbon Nanotubes using a Long Alkyl- Chain Benzenediazonium Compound ○Shouhei Toyoda, Yoshifumi Yamaguchi, Masataka Hiwatashi, Yasuhiko Tomonari, Hiroto Murakami, Naotoshi Nakashima	144
3P-16	Carbon Nanotube-coating on Photografted Polymer Films ○Shinsuke Haraguchi, Yoshifumi Yamaguchi, Tsuyohiko Fujigaya, Yasuro Niidome, Naotoshi Nakashima	145
3P-17	Role of van der Waals Interaction during DC Electrodeposition of Carbon Nanotubes ○Takanori Mastumoto, Masahito Sano	146

Nanohorns

3P-18	Development of DMFC Stack Cell using Catalytic-Metal-Particles Dispersed Arc-Soot ○Kenji Shinohara, Keisuke Higashi, Yuki Izumi, Masanobu Yamamoto, Shinichiro Oke, Hirohumi Takikawa, Nobuyoshi Aoyagi, Takashi Okawa, Toshihiro Sakakibara, Sotaro Nakamura, Syuichi Sugawara, Kazuo Yoshikawa, Koji Miura, Shigeo Ito, Tatsuo Yamaura	147
3P-19	Photoinduced Charge-Separation of Chemically Modified Carbon Nanohorns ○Osamu Ito, Atula Sandanayaka, Yasuyuki Araki, Masako Yudasaka, Sumio Iijima, Nikos Tagmatarchis	148
3P-20	Production of single-wall carbon nanohorns with high purity ○Takeshi Azami, Ryota Yuge, Daisuke Kasuya, Tsutomu Yoshitake, Yoshimi Kubo, Masako Yudasaka, Sumio Iijima	149
3P-21	Arc-Soot Electrode with Highly Dispersed RuO ₂ for Electrochemical Capacitor ○Masanobu Yamamoto, Keisuke Higashi, Kenji Shinohara, Sinichiro Oke, Hirofumi Takikawa, Xiaojun He, Shigeo Itoh, Tatsuo Yamaura, Kouji Miura, Kazuo Yoshikawa	150

February 15th, Thursday

3P-22	Magnetism of O ₂ adsorbed in SWNH: evaluation of adsorption space ○Hitomi Takahashi, Shunji Bandow, Sumio Iijima	151
3P-23	Boron nano-particles supported arc-generated arc-generated nanohorns ○Takayuki Inagaki, Shunji Bandow, Sumio Iijima	152
3P-24	High yeild production of small diameter carbon nanohorns by means of DC arc discharge and their characterization ○Takayuki Inagaki, Manabu Harada, Shunji Bandow, Sumio Iijima	153
Metallofullerenes		
3P-25	Formation of Nitrogen Atom Endohedral Fullerenes Using a Multipole Mirror-Type Electron Cyclotron Resonance Discharge Plasma ○Shigeyuki Abe, Hiroyasu Ishida, Shohei Nishigaki, Toshiro Kaneko, Rikizo Hatakeyama	154
3P-26	Effects of Parameters on Synthesis of Nitrogen Atom Encapsulated Fullerenes Using an RF plasma ○Shohei Nishigaki, Shigeyuki Abe, Toshiro Kaneko, Rikizo Hatakeyama	155
3P-27	Ultraviolet Photoelectron Spectroscopy of Lu ₂ @C ₈₂ (II) ○Takafumi Miyazaki, Masayuki Kato, Konosuke Furukawa, Ryohei Sumii, Hisashi Umemoto, Haruya Okimoto, Toshiki Sugai, Hisanori Shinohara, Shojun Hino	156
3P-28	¹³ C NMR Study of Pr ₂ @C ₈₀ ○Manabu Ito, Shiho Nagaoka, Takeshi Kodama, Yoko Miyake, Shinzo Suzuki, Koichi Kikuchi, Yohji Achiba	157
3P-29	Fluorescence Properties of Erbium-Metal-Carbide Metallofullerenes: (Er ₂ C ₂)@C _{2n} ○Masahiro Akachi, Yasuhiro Ito, Ryo Kitaura, Toshiki Sugai, Hisanori Shinohara	158
Carbon Nanoparticles		
3P-30	Electronic and magnetic properties of acid-adsorbed nanoporous activated carbon fibers ○Hao Sijia, Kazuyuki Takai, Toshiaki Enoki	159
3P-31	Chemical Control of Nanodiamond Surface Leading to Control of the Water Dispersibility ○Tatsuya Takimoto, Naoki Kadota, Yoichi Morita, Shuji Aonuma, Takahide Kimura, Naoki Komatsu	160
3P-32	Encapsulation of La in Spherical Graphytic Shells by Arc Discharge ○Kazunori Yamamoto, Takatsugu Wakahara, Takeshi Akasaka	161
Miscellaneous		
3P-33	Effect of annealed temperature on the capacitance of electrochemical capacitors ○X.J. He, M. Yamamoto, K. Higashi, K. Shinohara, S. Oke, H. Takikawa, S. Itoh, T. Yamaura, K. Miura, K. Yoshikawa	162
3P-34	Fully-automated CVD system for gram scale production of Super-growth SWNTs -A step toward industrial-scale mass production- ○Don N. Futaba, Tatsunori Namai, Tatsuki Hiraoka, Kenji Hata, Takeo Yamada, Motoo Yumura, Sumio Iijima	163
3P-35	Mass Production of Carbon Nanotwist and its Field Emission ○Y.Hosokawa, R.Sugiura, H.Shiki, H.Takikawa, T.Ina, S.Itoh, T.Yamaura	164
3P-36	Methodology for Fabricating LB Films of Fullerene ○Yasuhiro F. Miura, Atsushi Yamashita, Issei Matsuoka, Mitsutaka Urushibata, Michio Sugi	165
3P-37	Comparison of evolved gas by some pretreatment methods of CNT ○Shinji Fukumoto, Toyohito Wada, Yasushi Suzuki	166
3P-38	An XRD study of multiwalled carbon nanotubes' diameter ○Atsuhiko Kunishige, Tohru Kawamoto, Shoichi Kase, Yoshiyuki Sumiyama	167

特別講演
Special Lecture

1S - 1 ~ 1S - 2

2S - 3 ~ 2S - 4

3S - 5 ~ 3S - 6

IS-1

Quantum Chemical Molecular Dynamics Simulations of Fullerene and Carbon Nanotube Self-Assembly

Stephan Irle,¹ Guishan Zheng,² Zhi Wang,² Benjamin Finck,² and Keiji Morokuma^{2,3}

¹*Institute for Advanced Research and Department of Chemistry, Nagoya University, Nagoya 464-8602, Japan*

²*Cherry L. Emerson Center for Scientific Computation and Department of Chemistry, Emory University, Atlanta, GA 30322, U.S.A.*

³*Fukui Institute for Fundamental Chemistry, Kyoto University, Kyoto 606-8103, Japan*

“The maintenance of organization in nature is not – and cannot be – achieved by central management; order can only be maintained by self-organization” [1]. With this realization at the end of the last century we have come to recognize that fundamental understanding of nanostructure formation processes requires modeling of dissipative systems open to energy and interaction with environment. Molecular dynamics simulations of this type based on the basis of the density functional tight binding (DFTB) quantum chemical method have recently shown that fullerene formation is a dynamic self-assembly process far from thermodynamic equilibrium, with fullerene cages emerging as dissipative structures during the cooling of hot carbon vapor.[2]

In an extension of these fullerene formation studies we present quantum chemical molecular dynamics simulations of metallofullerene [3] formation and synthesis of carbon nanotubes from SiC [4] and from carbon-containing feedstock gases in the presence of transition metal (TM) catalysts,[5] using parameters developed in the Morokuma group.[6] Regarding nanotube formation, these simulations suggest that growth of the sidewalls is likely made possible by the presence of polyene chains attached to the ends of the nucleated cap, similar as in the case of “octopus on the rock” structures during fullerene formation. We present statistical analysis of pure carbon vapor dynamics and TM-catalyzed CNT growth simulations in the light of the importance of the polyene chains for carbon accretion.

[1] C. K. Briebacher, G. Nicolis, and P. Schuster, *Self-Organization in the Physico-Chemical and Life Sciences*, Report EUR 16546 (European Commission, 1995).

[2] S. Irle, G. Zheng, Z. Wang, K. Morokuma, *J. Phys. Chem. B* **110**, 21135 (2006)

[3] Z. Wang, B. Finck, G. Zheng, S. Irle, K. Morokuma, in preparation

[4] S. Irle, Z. Wang, G. Zheng, K. Morokuma, M. Kusunoki, *J. Chem. Phys.* **125**, 044702 (2006)

[5] G. Zheng, S. Irle, K. Morokuma, in preparation

[6] G. Zheng, G. Zheng, H. Witek, P. Bobadova-Parvanova, S. Irle, D. G. Musaev, R. Prabhakar, K. Morokuma, M. Elstner, C. Köhler, and T. Frauenheim, *J. Chem. Theory Comput.*, submitted.

Corresponding Authors: Stephan Irle and Keiji Morokuma

TEL: +81-75-711-7631, FAX: +81-75-781-4757, E-mail: stephan@euch4e.chem.emory.edu & morokuma@emory.edu

Novel Approaches for Materialization of Supramolecular Fullerenes

Takashi Nakanishi

*Organic Nanomaterials Center (ONC), and International Center for Young Scientists (ICYS),
National Institute for Materials Science (NIMS)
1-1 Namiki, Tsukuba, Ibaraki 305-0044, Japan*

Chemical modification of fullerenes, functionalization of fullerene-based materials using their unique chemical and physical features is achievable through alignment and arrangement of fullerene units in predictable way. As my research target, new fullerene derivatives were synthesized and stimulated to self-organize into supramolecular assemblies and fine-tune of the intermolecular interactions. In this study, I describe three attractive examples of functional fullerene molecules and fullerene materials from the points of supramolecular designs: i) fullerene polymorphism [1]; ii) fullerene nanowires at molecular level [2]; iii) room temperature liquid fullerenes [3].

Novel hierarchical supramolecular fullerene architectures with controlled dimensionality were demonstrated in these assemblies [1]. In different solvents, a fullerene derivative with three long alkyl chains forms hierarchically ordered assemblies with well-defined 0, 1, 2 and 3D architectures such as vesicles, fibers, disks and cones. XRD, FTIR and DSC analyses support the hypothesis that the fundamental structural sub-unit of the supramolecular assemblies consists of a self-organized interdigitated bilayer.

The fullerene derivative bearing long alkyl chains epitaxially adsorbs on HOPG substrate forming well-ordered 1D lamellar structure captured by AFM [2]. Within the lamellae, the fullerene moieties are organized in a zigzag fashion imaged by STM. This is a novel approach to direct the assembly of fullerenes at a solid surface in a predictable way.

In the course of above studies, I discovered serendipitously that fulleropyrrolidines substituted with 2,4,6-tris(alkyloxy)phenyl group exhibit a fluid phase at room temperature [3]. The liquid fullerenes show a dramatic decrease in viscosity with an increase in the length of the alkyl chains (Fig. 1). They are single component nanocarbon materials with high fluidity, which showed the potential use in materials applications.

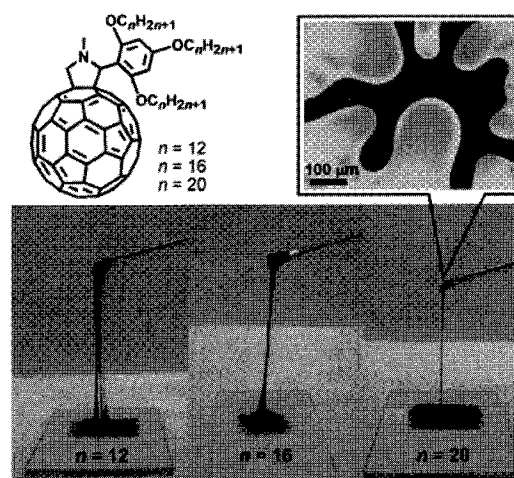


Fig. 1 Chemical structures of room temperature liquid fullerenes and photographs to show their fluidity.

[1] T. Nakanishi, et.al., *Chem. Commun.*, (48), 5982–5984 (2005) *selected as a hot article*.

[2] T. Nakanishi, et.al., *J. Am. Chem. Soc.*, **128** (19), 6328–6329 (2006).

[3] T. Nakanishi, et.al., *J. Am. Chem. Soc.*, **128** (32), 10384–10385 (2006).

Corresponding Author: Dr. Takashi Nakanishi

Tel: +81-29-860-4740, Fax: +81-29-860-4706, e-mail: NAKANISHI.Takashi@nims.go.jp

Structures of Endohedral Metallofullerenes

Shigeru Nagase

*Department of Theoretical Molecular Science, Institute for Molecular Science
Okazaki 444-8585, Japan*

Endohedral metallofullerenes have long attracted wide interest because electron transfer from metal atoms to carbon cages leads to unique electronic and magnetic properties as well as new reactions, enriching the chemistry of fullerenes in the material, catalytic and biomedical applications [1]. Thus, the properties, reactivities, and chemical modification of endohedral metallofullerenes have been extensively investigated both experimentally and theoretically. For these investigations and applications, however, it is fundamental to determine the cage structures and metal positions of endohedral metallofullerenes.

It is widely accepted that the maximum-entropy-method (MEM)/Rietveld analysis of synchrotron X-ray powder diffraction data is powerful for structural determination of endohedral metallofullerenes [2]. Since the first application to $Y@C_{82}$ in 1995, the endohedral structures of many representative metallofullerenes such as $Sc@C_{82}$, $La@C_{82}$, $Eu@C_{82}$, $Gd@C_{82}$, $Sc_2@C_{66}$, $Sc_2@C_{84}$, $La_2@C_{80}$, $Sc_2C_2@C_{84}$, $Y_2C_2@C_{82}$, and $Sc_3@C_{82}$ have been determined by the MEM/Rietveld method. However, these structures do not always correspond to energy minima or most stable structures.

In this talk, it is first discussed how cage structures and metal positions are determined. Next reported are the cage structures and metal positions of $Sc_3@C_{82}$, $Sc_2@C_{84}$, $Eu@C_{82}$, and $Gd@C_{82}$ that are recently determined through a close interplay of experiment (X-ray crystal analysis and NMR data) and theoretical calculations [3]. It is remarkable that these cage structures and metal positions are quite different from those obtained by the MEM/Rietveld analysis [4]. It is also reported how encapsulated metal atoms affect the reactivities of endohedral metallofullerenes and how the metal position and motion are controllable by exohedral chemical functionalization [5].

References

- [1] For reviews, (a) H. Shinohara, *Rep. Prog. Phys.*, **63**, 843 (2000). (b) *Endofullerenes: A New Family of Carbon Clusters*; T. Akasaka and S. Nagase (Eds.), Kluwer Academic, Dordrecht, 2002.
- [2] For reviews, M. Takata, E. Nishibori, M. Sakata and H. Shinohara, *Struct. Chem.*, **14**, 23 (2003). (b) M. Takata, E. Nishibori, M. Sakata and H. Shinohara, *Struct. Bonding*, **109**, 59 (2004).
- [3] (a) Y. Iiduka et al., *J. Am. Chem. Soc.*, **127**, 12500 (2005). (b) Y. Iiduka et al., *Chem. Commun.*, 2057 (2006). (c) M. Yamada et al., *J. Am. Chem. Soc.*, **128**, 1400 (2006). (d) N. Mizorogi and S. Nagase, *Chem. Phys. Lett.*, **431**, 110 (2006). For a recent Japanese review, (e) T. Akasaka and S. Nagase, *J. Crystallography Soc. Jpn.*, **48**, 230-236 (2006).
- [4] For the recent MEM/Rietveld analysis of Sc_3C_{82} , E. Nishibori et al., *J. Phys. Chem. B*, **110**, 19215 (2006).
- [5] For a recent Japanese review, T. Akasaka and S. Nagase, *Gendai Kagaku*, No. **422**, 51 (2006).

Corresponding Author: Shigeru Nagase

TEL: +81-564-55-7300, FAX: +81-564-4660, E-mail: nagase@ims.ac.jp

Present status of SWCNT mass production & future problems

○ Junzo yana¹, Takeji Murai¹, Yuzo Nakagawa¹, Shuichi Shiraki¹,
Takeshi Saito², Satoshi Ohshima², Motoo Yumura², Sumio Iijima²,

¹Business Development & Resource Management, Nikkiso Co.,Ltd.
Tokyo 150-8677, Japan

²Research Center for Advanced Carbon Materials, National Institute of
Advanced Industrial Science and Technology (AIST)
Tsukuba 305-8565, Japan

Since the carbon nanotubes (CNT) were introduced on Nature in 1991, various studies have been initiated in different fields by many researchers because of their unique and dreamlike characteristics.[1] However, in spite of such sensational advent of CNT, we have not seen any traces of changes in our industries by development of new product utilizing CNT. This was due to difficulty of utilizing CNT by itself, and unavailability of CNT of high enough purity and quality for industrial use without refining, although CNT's unique characteristics were well recognized. We describe here about single-walled carbon nanotube (SWCNT) available in the past and the high quality SWCNT available now, requiring almost no refining for industrial use.

The description includes purity, crystallization, diameter fluctuation production repeatability of this high quality SWCNT. We further describe the current trend regarding safety the necessary assignments to cope with for industrial use, such as debundling, dispersion functionalization and evaluation methods.

The topic of SWCNT described here is produced by Nikkiso's industrial production size CVD (Chemical Vapor Deposition) reactor developed successfully, utilizing the Enhanced Direct-Injection-Pyrolytic-Synthesis (e-DIPS) process technology of AIST. Here we report the present status of our achievement of large scale production of this high quality SWCNT which is quite different from those available in the past and that requires almost no refining. As no refining is required, problems due to process failure and cost on SWCNT for refining can be avoided, which means we can now consider SWCNT as the useful material in the industries. From this success, we can expect rapid developments also in Japan for SWCNT applications and evaluation, dispersion or functionalization technique's. The US was considered to be much advanced in these areas.

[1] S.Iijima, Nature, 354, 56 (1991)

Corresponding Author : Junzo Yana

TEL: +81-3-3443-3738, FAX: +81-3-3440-3661, E-mail: j.yana@nikkiso.co.jp

3S-5

Dispersion of Carbon Nanotubes and Development of Transparent Conductive Coatings

Yuzo Sumita (President, SUMITA Nanotechnologies Inc.)

ABSTRACT

Outline of the latest development situation of the transparent conductive coatings containing carbon nanotubes (CNT) done by speaker's group is reported. The key process for making the better coatings is sufficient dispersing of CNT into the required media, because CNT is produced and supplied as the cohered bundle complexes of super fine nano fibers entangling each other. In this lecture, firstly dispersing technology and selection of the suitable CNT for getting the desired properties of the coated layer and then features of three types of coatings (water-born, solvent-based and UV-curable) as well as the film properties coated by each of them are introduced. There is a trade-off relationship between the electro-conductivity (surface resistivity) and the total light transmission of the CNT coated film layer. The average balance level between them obtained by the coatings using MW-CNT on PET film so far is: total light transmission=85% and surface resistivity = $10^6\sim 10^7 \Omega/\square$ (thickness of coated layer is $0.3\sim 0.5 \mu\text{m}$). The light transmission of the coatings using SW-CNT is improved up to 87~90%. The level of conductivity may differ depending upon the kind of used base film: for instance, (better) TAC>Acrylic>PC>PET (worse). And better conductivity is usually obtained by using higher transparency film. And also it was found out that post treatment of the coated layer, such as heating, pressing, stretching or washing by solvent, can elevate its conductivity up to 10-100 times level. But such the post treatment has some limitation. Even such the treatment applied, the conductivity of the CNT coated film remains still in the antistatic or semi-conductive level under the conventional simple coating layer forming processes. Therefore, in order to produce the film having higher conductivity (less than $10^2 \Omega/\square$) and higher transparency (more than 85%) to be applied for replacing ITO sputtering film, development of more advanced new film forming technology is required.

3S-6

Phase transitions of water and simple liquids in carbon nanotubes

Kenichiro Koga

*Department of Chemistry, Faculty of Science, Okayama University,
Tsushima-Naka 3-1-1, Okayama, 700-8530, Japan*

Abstract: What have been predicted by theoretical calculations are reviewed about structures and phase transitions of water and spherical particles in carbon nanotubes. Structure of water at low temperatures is mainly determined by hydrogen bonds such that formation of a perfect four-coordinated network is realized whereas that of spherical particles such as argon and C₆₀ is determined by close packing. Nevertheless the two classes of systems under one-dimensional confinement exhibit striking similarity in phase behavior. Computer simulation studies of water confined in the carbon nanotube have shown that the confined water freezes into one-dimensional crystalline structures, often called ice nanotubes, and exhibits the phase behavior of continuous and discontinuous melting and freezing that any bulk system has never shown [1]. The theoretical prediction was followed by experimental observation of ice nanotubes in carbon nanotubes [2]. Recent theoretical studies reveal that there are more ordered structures of water inside carbon nanotubes including helical and filled ice nanotubes [3]. It is shown for a model system of argon in carbon nanotubes that the first ten close-packed phases are in one-to-one correspondence with the first ten ways of folding a triangular lattice, each being characterized by a roll-up vector like the single-walled carbon nanotube [4]. Phase diagrams in pressure-diameter plane and temperature-diameter plane are obtained by inherent-structure calculation and molecular dynamics simulation. The phase boundaries dividing two adjacent phases are infinitely sharp in the low-temperature limit but are blurred as temperature is increased. Existence of such phase boundaries explains rich, diameter-sensitive phase behavior unique for cylindrically confined systems.

- References:** [1] K. Koga, G.T. Gao, X.C. Zeng, H. Tanaka, *Nature*, **412**, 802 (2001).
[2] Y. Maniwa et al., *J. Phys. Soc. Jpn.*, **71**, 2863 (2002).
[3] D. Takaiwa, K. Koga, H. Tanaka, *Mol. Simulat.*, accepted.
[4] K. Koga and H. Tanaka, *J. Chem. Phys.*, **124**, 131103 (2006).

Corresponding Author: Kenichiro Koga

E-mail: koga@cc.okayama-u.ac.jp

Tel&Fax: 086-251-7904

一般講演
General Lecture

1-1 ~ 1-18

2-1 ~ 2-15

3-1 ~ 3-10

Super-Growth Single-Walled Carbon Nanotube Forest: An Ideal Graphene Surface Material with a Surface Area Over 1200 m²/g

Tatsuki Hiraoka¹, OTakeo Yamada¹, Kenji Hata¹, Don N. Futaba¹, Jin Miyawaki²,
Masako Yudasaka^{2,3}, Motoo Yumura¹ and Sumio Iijima^{1,2}

¹ *Research Center for Advanced Carbon Materials, National Institute of Advanced Industrial Science and Technology (AIST), Tsukuba, 305-8565, Japan*

² *NEC Corporation, Tsukuba, 305-8501, Japan*

³ *Japan Science and Technology Agency, Tsukuba 305-8501, Japan*

The solid surface is the interface where the interaction between the bulk and the surrounding environment takes place. Naturally, the amount of solid surface (i.e. surface area) determines how much these interactions (i.e. adsorption) can occur. The ability to utilize this interface is pivotal in numerous applications ranging from sensors, filters, to energy storage. Consequently, the synthesis and study of materials with large surface area, such as porous silica-based, alumina-based, and activated carbon materials have garnered significant attention. However, of these materials only activated carbon enjoys both a high surface area and electrical conductivity. Therefore, they are currently prominent in these important applications which require both qualities.

Single-walled carbon nanotubes (SWNTs), because of their high predicted surface area (1315 m²/g) and their excellent crystallinity and conductivity, are candidates as substitutes for next generation devices. But, reports¹ of the surface area for commercial-grade SWNTs (HiPco) have been disappointingly low (~600 m²/g). Here, we report the near ideal surface area of SWNT forests synthesized by the Super-growth method². Brunauer-Emmett-Teller surface area analysis revealed specific surface areas over 1200 m²/g for closed SWNT forests and over 2000 m²/g after exposing the inner tube surface³. These near-ideal level quantities (comparable to activated carbon) represent a significant improvement over previous reports and extend the scientific and practical use of SWNTS toward surface area and conducting related applications while being reliable, scalable, and retaining the intrinsic properties of SWNTs.

References

- [1] C. Yang, K. Kaneko, M. Yudasaka, S. Iijima, *Nano. Lett.* **4**, 385 (2002).
- [2] K. Hata, D. N. Futaba, K. Mizuno, T. Namai, M. Yumura, S. Iijima, *Science.*, **40**, 397 (2004).
- [3] J. Fan, M. Yudasaka, J. Miyawaki, K. Ajima, K. Murata, S. Iijima, *J. Phys. Chem. B* **110**, 1587 (2006).

Corresponding Author: Takeo Yamada

E-mail: takeo-yamada@aist.go.jp

Internal structure of vertically aligned single-walled carbon nanotubes

○Erik Einarsson¹, Hidetsugu Shiozawa², Christian Kramberger², Mark H. Rummeli²,
Alex Grüneis², Thomas Pichler², Shigeo Maruyama¹

¹*Dept. of Mechanical Engineering, The University of Tokyo, Tokyo 113-8656, Japan*

²*Inst. for Solid State & Materials Research (IFW) Dresden, D-01171 Dresden, Germany*

In this study we investigated the internal structure of vertically aligned single-walled carbon nanotube (VA-SWNT) films produced by the alcohol catalytic CVD method [1,2]. Freestanding VA-SWNT films were obtained using a hot-water assisted film transfer method [3], and observed by transmission electron microscopy. Due to the film alignment, observation along the alignment direction showed many bundle

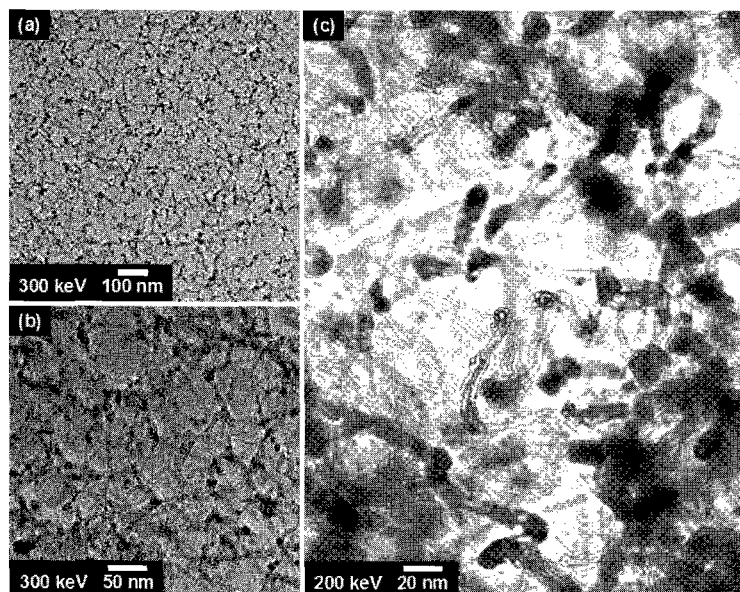


Fig. 1: TEM micrographs of VA-SWNTs (plan view).

cross-sections, revealing the film consists of very small bundles [4] (3-10 SWNTs per bundle), as shown in Figure 1. The degree of alignment of the SWNTs in the film was determined by high-resolution X-ray absorbance to be $\sim 25^\circ$ from normal [4], which is in good agreement with an earlier study [5] of anisotropic optical absorbance of the VA-SWNTs.

[1] S. Maruyama *et al.*, Chem. Phys. Lett. **360** (2002) 229.

[2] Y. Murakami *et al.*, Chem. Phys. Lett. **385** (2004) 298.

[3] Y. Murakami and S. Maruyama, Chem. Phys. Lett. **422** (2006) 575.

[4] E. Einarsson *et al.*, unpublished.

[5] Y. Murakami *et al.*, Phys. Rev. Lett. **94** (2005) 087402.

Corresponding Author: S. Maruyama **E-mail:** maruyama@photon.t.u-tokyo.ac.jp

Tel&Fax: +81-03-5841-6983

Current-Induced Structural Change of Fullerene-Encapsulated Single Wall Carbon Nanotubes

Hiroshi Somada¹, Yuya Yoshikawa¹, Atsuko Nagataki^{1,3}, Seiji Akita^{1,4},
Yoshikazu Nakayama^{1,2,3,4}

¹*Department of Physics and Electronics, Graduate School of Engineering, Osaka Prefecture University, 1-1 Gakuen-cho, Naka-ku, Sakai, Osaka 599-8531, Japan.*

²*Department of Mechanical Engineering, Graduate School of Engineering, Osaka University, 2-1 Yamadaoka, Suita, Osaka 565-0871, Japan*

³*Handai Frontier Research Center, Graduate School of Engineering, Osaka University, 2-1 Yamadaoka, Suita, Osaka 565-0871, Japan*

⁴*CREST, Japan Science and Technology Agency*

We have investigated the current-induced structural change of fullerene-encapsulated single wall nanotubes (peapod). The nanotubes were aligned and protruded from the edge of a Pt-coated Si substrate to prepare a nanotube cartridge. The nanotube cartridge and a Pt-coated Si tip were set on the manipulation stages installed in a transmission electron microscope (TEM). A nanotube with 3-nm diameter in the cartridge was attached on the Si tip and bent with a kink by manipulation of the Si tip. A voltage was applied to flow the current through the nanotube.

Figure 1 shows the sequential TEM images showing the change of the peapod as a function of the current. The polymerization of fullerenes started at 0.35 $\mu\text{A}/\text{nm}$ (circumferential current density) (a), the size of the fullerenes located inside and outside of the nanotube became large with increasing the current from 0.8 to 2.1 $\mu\text{A}/\text{nm}$ (b), the two inner nanotubes grew newly from the both ends with a low temperature (c), the fusion of the grown fullerenes with the nanotube was completed at the currents at 2.1 $\mu\text{A}/\text{nm}$ (d), the sublimation started after (d) and the kink disappeared at 2.5 $\mu\text{A}/\text{nm}$ (e) and then the sublimation proceeded to reduce the diameter (f) and finally cut the nanotube where the current density increased from 2.5 to 5.5 $\mu\text{A}/\text{nm}$.

This sequential change of the structure is due to the increase of the temperature and it is estimated to be $\sim 1100^\circ\text{C}$ for (a), $\sim 1200^\circ\text{C}$ for (b), $\sim 1500^\circ\text{C}$ for (c), (d) and $< 2400^\circ\text{C}$ for (e), (f) from the previous works. The growth of new nanotubes in (c) might occur at $\sim 1100^\circ\text{C}$.

Acknowledgement This work was partially supported by a Grant-in-Aid for Scientific Research from the Japan Society for the Promotion of Science.

Corresponding Author: Yoshikazu Nakayama

E-mail: nakayama@mech.eng.osaka-u.ac.jp, **Tel&Fax:** 06-6879-7307

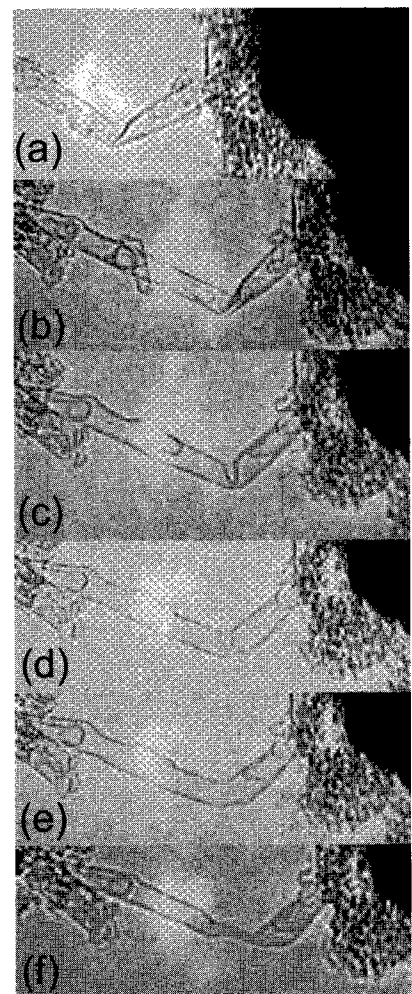


Fig.1 (a)-(f) sequential TEM images of current-induced structural change of a peapod.

Factors Affecting on Electronic Properties of CNTs-FETs

○Ryotaro Kumashiro¹, Nobuya Hiroshiba¹, Hiroataka Ohashi¹, Rikizo Hatakeyama² and
Katsumi Tanigaki¹

¹ *Department of Physics, Graduate School of Science, Tohoku University, Sendai, Japan*

² *Department of Electronic Engineering, Graduate School of Engineering,
Tohoku University, Sendai, Japan*

Carbon nanotubes (CNTs) having semiconducting properties are promising as electronic materials for nano-scale devices in the future, and the electrical properties of CNTs are of significantly fundamental and practical interests. It is well known that the field effect transistors (FETs) fabricated using semiconducting CNTs show high performance in terms of the mobility. However, it is also known that some serious problems in CNTs-FETs exist, such as control in the electron/hole carriers, atmospheric effects, large hysteresis in I_{SD} - V_G action (Fig.1). For their applications to electronic devices, it is required to overcome these problems in CNTs-FETs.

Especially in the case of the large hysteresis of I_{SD} - V_G curves, among the above problems, possible origins have been suggested, e.g. structural defects in CNTs, the interfacial problems between CNTs and gate insulators as well as contact on the source/drain electrodes. However, the details have not yet been elucidated. It has been known that the quality of CNTs, the amounts of structural defects and the order of tube diameter, strongly depends on the sample preparation methods as important parameters for controlling CNTs property. In this meeting, we will present comparison of the FET properties of various CNTs samples having different characters and will discuss the origin of various phenomena appearing in CNTs-FETs actions.

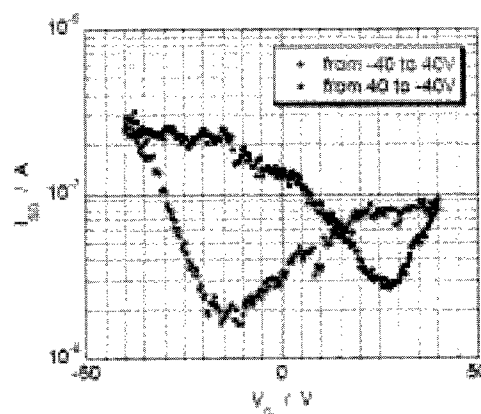


Figure 1. I_{SD} - V_G Curve of Single Wall CNTs -FETs.

Corresponding Author: Ryoraro Kumashiro, **E-mail:** rkuma@sspns.phys.tohoku.ac.jp
Tel&Fax: +81-22-795-6470

Negative differential resistance transport through C_{60} , C_{70} and C_{84} encapsulated double-walled carbon nanotubes

○Y. F. Li, T. Kaneko, and R. Hatakeyama

Department of Electronic Engineering, Tohoku University, Sendai 980-8579, Japan

Fullerenes such as C_{60} and carbon nanotubes have attracted great attention as promising candidates in fabricating new functional electronic devices. Here, we report novel electric transport properties of nanodevices fabricated using C_{60} , C_{70} and C_{84} encapsulated metallic double-walled carbon nanotubes (DWNTs). The fabrication of various fullerenes encapsulated DWNTs has been realized by both plasma irradiation and vapor diffusion methods. A series of electronic measurements in FET configurations indicate that all the fullerene-encapsulated DWNT devices exhibit strong distinct negative differential resistance (NDR) behavior. Figure 1 gives a V_{DS} - I_{DS} characteristic with NDR behavior for C_{84} @DWNTs. The high peak-to-valley ratio (PVR) up to the range of $10^3 \sim 10^4$ is observed for most of devices at room temperature. The fullerene species and applied gate voltages show a great influence on the peak voltage position [1]. With an increase in the size of fullerenes, the peak voltages give rise to a linear decrease from ~ 6.1 V (C_{60} @DWNTs) to ~ 2.7 V (C_{84} @DWNTs), as shown in Fig. 2. In addition, at high drain-source bias $V_{DS} > 6$ V, the measured current tends to be completely dominated by Coulomb oscillation peaks, exhibiting a strong single-electron tunneling phenomena at room temperature.

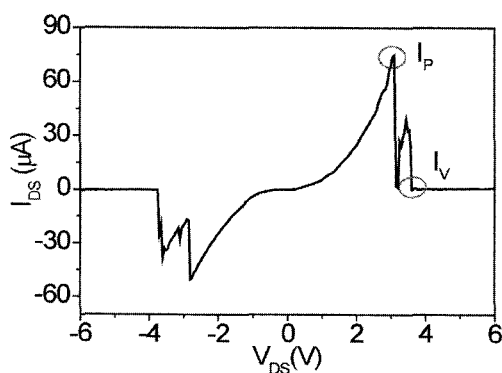


Fig.1 Characteristic of I_{DS} - V_{DS} for C_{84} @DWNTs

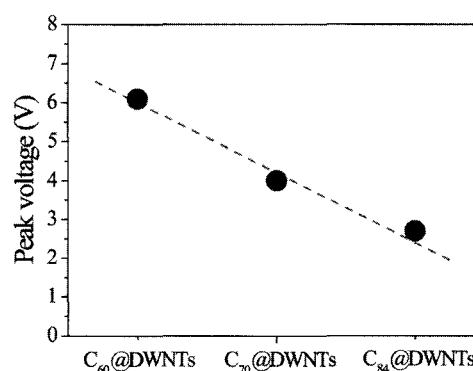


Fig.2 Peak voltages for different fullerenes encapsulated DWNTs

[1] Y.F. Li et al., Abstract of the 31st Fullerene-Nanotubes General Symposium, 3-17 (2006).

Corresponding Author: Yongfeng Li

Tel : 81-22-795-7046, FAX: 81-22-263-9225, E-mail: yfli@plasma.ecei.tohoku.ac.jp

Electric Polarization of Cylindrical Carbon-Nanotube Capacitor

○Kazuyuki Uchida, Susumu Okada, Kenji Shiraishi, and Atsushi Oshiyama

*Center for Computational Sciences and Institute of Physics, University of Tsukuba,
1-1-1 Tennodai, Tsukuba 305-8577, Japan*

*CREST, Japan Science and Technology (JST) Agency, 4-1-8 Honcho, Kawaguchi,
Saitama 332-0012, Japan*

Abstract: We theoretically investigated electric polarization of a coaxial-cylindrical carbon-nanotube (CNT) capacitor, by using first-principles approaches with the enforced Fermi-energy difference (EFED) method [1-2] which was recently developed by the author and co-workers. We exhibit that the capacitance of the system shows two kinds of quantum effects: The capacitance value is larger than its classical expectation, and the capacitance shows drastic and characteristic bias dependence.

We show that they are the reflections of the quantum-mechanical spill of the accumulated charge, and the van-Hove's singularities in the density of states (DOS) of the quasi-one dimensional CNT electrodes, respectively. We analyze the mechanism of the charge spill in detail. We also explain how the coaxial-cylindrical geometry of the present capacitor is reflected on these quantum effects. We believe that this kind of quantum effects in a series of CNT capacitors can be utilized for designing novel nano-electronic devices with varieties of functional characteristics.

This work is partly supported by CREST, JST. The numerical calculations were performed with the Tokyo *Ab-initio* Program Package (TAPP), which has been developed by our group [3-4].

References:

- [1] K. Uchida, H. Kageshima, and H. Inokawa, *e-J. Surf, Sci. Nanotech.* **3**, 453 (2005).
- [2] K. Uchida, H. Kageshima, and H. Inokawa, *Phys. Rev. B* **74**, 035408 (2006).
- [3] M. Tsukada, et al., *Computer Program Package (TAPP)*, University of Tokyo, Tokyo, Japan, 1983-2006.
- [4] J. Yamauchi, M. Tsukada, S. Watanabe, and O. Sugino, *Phys. Rev. B* **54**, 5586 (1996).

Corresponding Author: Kazuyuki Uchida

E-mail: kuchida@comas.frsc.tsukuba.ac.jp

Tel: 029-853-5600-8233

Energetics and Electronic Structures of Carbon Nanotubes with Adatom-Vacancy Pairs

○Susumu Okada

*Institute of Physics and Center for Computational Sciences, University of Tsukuba,
Tennodai, Tsukuba 305-8577, Japan
CREST, JST, 4-1-8 Honcho, Kawaguchi, Saitama 332-0012, Japan*

Atomic imperfections in nanotubes are known to play crucial role to determine their electronic properties near the Fermi level. The atomic defects (e.g. vacancies and interstitials) induces particular electron states of which wave functions are localized near the defects with lone pair character resulting in gap states at/near energy gap of the nanotubes. Recently, low-energy electron and phonon irradiations cause a new class of atomic defects on single-walled carbon nanotubes with peculiar geometric and electronic properties: The defects are completely healed under the elevated temperature of about 1000K. The fact indicates that the number of carbon atoms on this damage/healing process is preserved. Moreover, the metal-semiconductor transition was found to take place on the process. In the present work, we perform first-principles total-energy calculations on single-walled zigzag carbon nanotubes to explore a possible structural model of the defects and to elucidate the energetics and electronic properties of the nanotubes.

Figure 1 shows the optimized structures of the (9,0) nanotube with the defect which consists of a pair of a monovacancy and an adatom. Formation energies of these defects are found to be 8.09 eV and 8.59 eV for symmetric and asymmetric defects, respectively. Based on the constraint minimization scheme, it is found that the reaction barriers for the damage and healing are about 10 eV and 2 eV, respectively. Thus the structure is a possible candidate for the damaged nanotubes by the low-energy electron and phonon irradiations. As shown in Fig. 2, the metal-semiconductor transition takes place on the damaged nanotubes. It is found that two states emerge in the energy gap of the nanotube: For the symmetric case, the states lack their dispersion reflecting their localized character. In sharp contrast, for the asymmetric case, one of two states possesses considerable dispersion indicating the substantial mixing of localized state and π states.

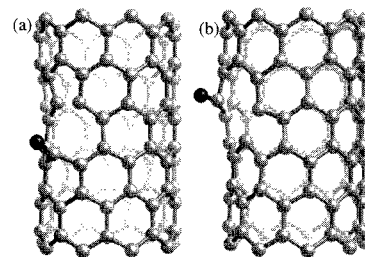


Fig.1: Structures of (9,0) tube with (a) a symmetric defect and (b) an asymmetric defect.

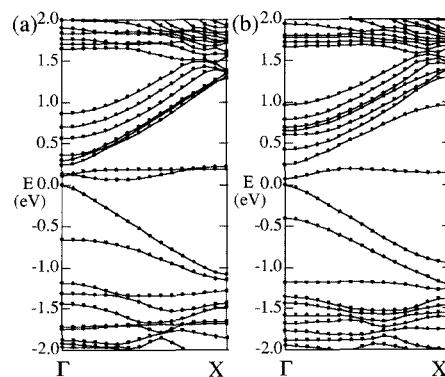


Fig. 2: Electronic structures of (9,0) nanotube with (a) symmetric defect and (b) asymmetric defect.

Corresponding Author: Susumu Okada
E-mail: sokada@comas.frsc.tsukuba.ac.jp
Tel&Fax: 029-853-5921/029-853-5924

Exciton effect on Raman spectra of single wall carbon nanotubes**R. Saito[○](1), J. Jiang(2), K. Sato(1), J. S. Park(1)***(1) Department of Physics, Tohoku University and CREST JST, Sendai 980-8578**(2) Department of Physics, North Carolina State University, Raleigh, NC 27695-7518,
USA*

For photo-excited electron and hole pair, a strong, attractive Coulomb interaction is expected to form a spatially bounded exciton. Because of localization of the wave function in the real space, we expect that a strong optical transition appears. However, in our previous calculation with use of a free pair of electron and hole, the Raman intensity reproduces the type, diameter and chirality dependence of Raman intensity such as RBM and G band for (n,m) single wall carbon nanotubes. Thus we need to investigate why the previous calculation works well for explaining the (n,m) dependence Raman spectra.

Here we solve the Bethe-Salpeter equation for calculating the exciton energy and wave functions. Using the exciton wavefunction, we make programs to calculate exciton-photon and exciton-phonon matrix element to calculate the Raman intensity for the giving (n,m) values and the excitation energies.

The calculated results show that the exciton-phonon interaction is similar to the electron-phonon interaction since the matrix element is a smooth function in the k space. However the exciton-phonon matrix element becomes 100 times larger to electron-hole picture reflecting the localization behavior. In this paper, we will show the Raman intensity of RBM and G bands and compared with the results by free electron and hole picture.

This work is partially supported by MEXT grant, (No. 16076201).

References: J. Jiang et al., Phys. Rev. B, in press.

Corresponding Author: Riichiro Saito

E-mail: rsaito@flex.phys.tohoku.ac.jp

Tel&Fax: 022-795-7754, 6445

Characterization of double-wall carbon nanotubes by absorption, photoluminescence, and Raman spectroscopies

○Konstantin Iakoubovskii, Nobutsugu Minami, Taro Ueno, Said Kazaoui, Yasumitsu Miyata and Hiromichi Kataura

Nanotechnology Research Institute, National Institute of Advanced Industrial Science and Technology (AIST), 1-1-1 Higashi, Tsukuba, Ibaraki 305-8565, Japan

We report a comprehensive and self-consistent optical study of double-wall carbon nanotubes (DWNTs) grown by chemical vapor deposition, using optical absorption, photoluminescence (PL) and Raman spectroscopies. PL mapping (Fig. 1) in the extended IR range [1] reveals a bimodal pattern of PL excitation/emission (S_{22}/S_{11}) peaks characteristic of the DWNT structure. Application of in situ perturbations, namely UV illumination, electrochemical doping or ozone treatment (Fig. 1a) revealed that the outer shells are more sensitive to those perturbations than the inner shells, another confirmation of the double-wall structure. In particular, this allowed us to decompose, in Fig. 1b, the total DWNT absorption into the contributions of the inner and outer shells, to assign the spectral features to the bandgap transitions in the semiconducting/metallic (S/M) outer/inner (o/i) tubes as S_{11}^o , S_{11}^i , M_{11}^o , etc, and to estimate the filling ratio of DWNTs ($\sim 100\%$) and the metallic fraction of the outer tubes ($\sim 50\%$) on several assumptions. PL quenching due to interaction between the inner and outer DWNT shells will also be discussed.

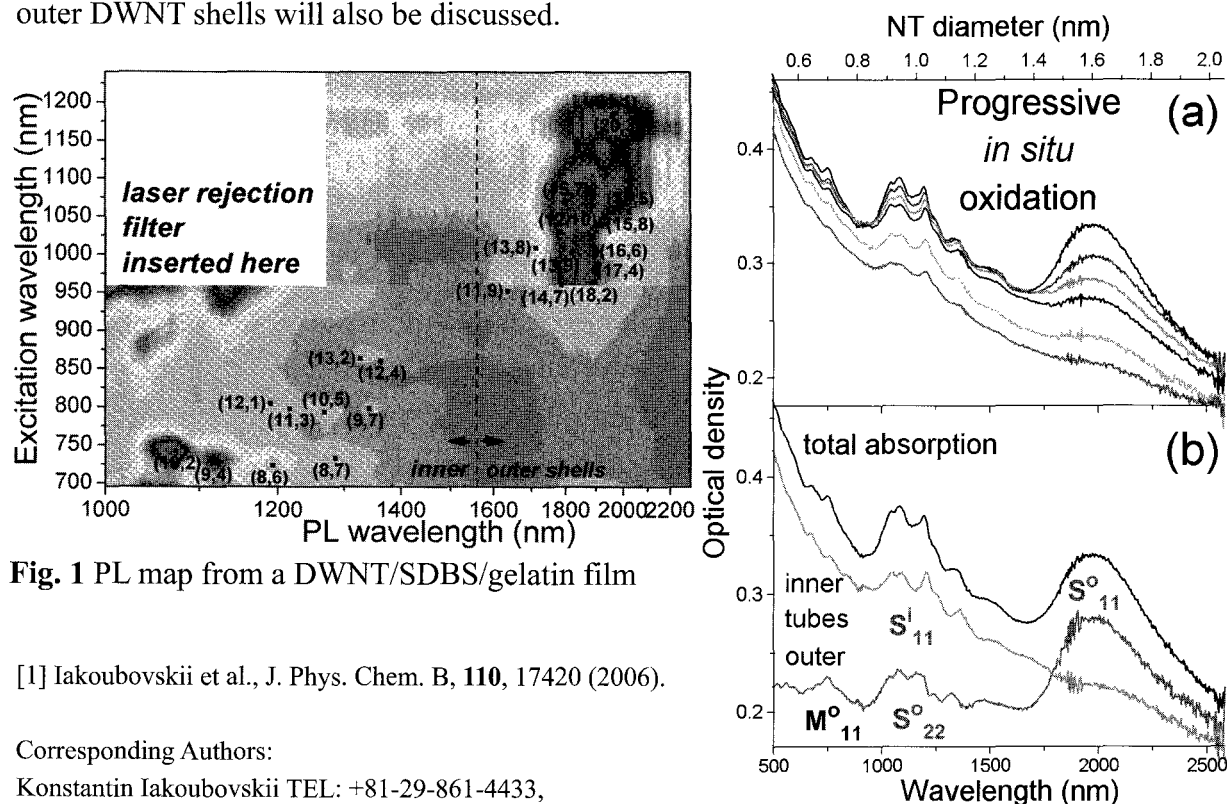


Fig. 1 PL map from a DWNT/SDBS/gelatin film

[1] Iakoubovskii et al., J. Phys. Chem. B, **110**, 17420 (2006).

Corresponding Authors:

Konstantin Iakoubovskii TEL: +81-29-861-4433,
 FAX: +81-29-861-4433, E-mail: k.iakoubovskii@aist.go.jp
 Nobutsugu Minami TEL: +81-29-861-9385,
 FAX: +81-29-861-6309, E-mail: n.minami@aist.go.jp

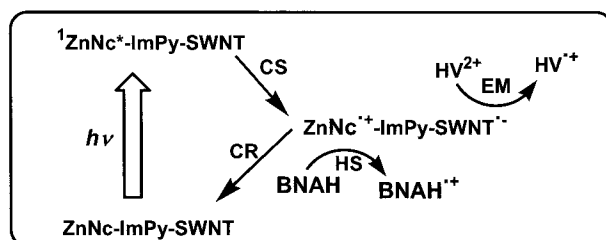
Fig.2 (a) Evolution of DWNT absorption spectra during progressive oxidation by UV-created ozone. (b) Decomposition of the spectrum into the components.

Photoinduced Charge Separation of Chemically Modified Carbon Nanotubes

○Osamu Ito, Atula Sandanayaka, Yasuyuki Araki, Francis D'Souza

Institute of Multidisciplinary Research for Advanced Materials, Tohoku University, Sendai 980-8577, Japan, Wichita University, USA.

Photoinduced electron transfer processes of chemically modified SWCNTs have been extensively studied aiming the solar energy conversion. In our previous supramolecular approach for chemically modified fullerenes, we succeeded in construction of artificial photosynthetic models. In this presentation, we extend this approach to SWCNT.¹⁾ Zinc naphthalocyanine (ZnNc), which is good photosensitizing electron donor with sharp absorption band due to its radical cation at 980 nm, was attached to SWCNT via pyrene-imidazole, giving homogeneous solution as shown in Fig. 1. Upon the light illumination in the presence of viologen dication (V^{2+}) with appropriate hole shifter, accumulation of the radical cation $V^{\bullet+}$ (620 nm band) as electron pool was observed (Fig. 1), suggesting charge-separation between SWCNT and ZnNc followed by the electron and hole migration. By the transient absorption spectra shown in Fig. 2, the initial charge-separation producing $ZnNc^{\bullet+}$ was confirmed by the 980 nm band; additional 1400 nm band can be thought as trapped electron in SWCNT. Fluorescence lifetime shortening of ZnNc shown in Fig. 3 indicates that the charge-separation takes place via the singlet excited state of ZnNc as shown in Scheme belows. Similar photosensitized charge-separation / electron (hole) migration systems could be contracted using zinc porphyrins and other aromatic hydro-carbons with high electron donor ability.



[1] M. El-Khouly, D'Souza, O. Ito, et al., *ChemPhysChem*. **2003**, *4*, 474.

Corresponding Author: Osamu Ito

TEL FAX: +81-22-217-5608, E-mail: ito@tagen.tohoku.ac.jp

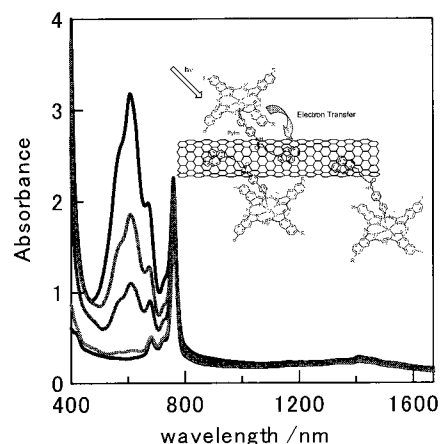


Fig. 1. Accumulation of $V^{\bullet+}$ by the light illumination of ZnNc on SWCNT in the presence V^{2+} and BNAH in THF.

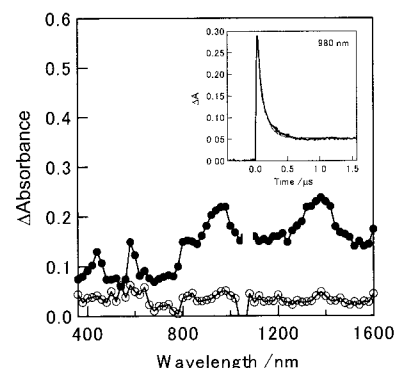


Fig. 2. Transient absorption spectra of ZnNc on SWCNT.

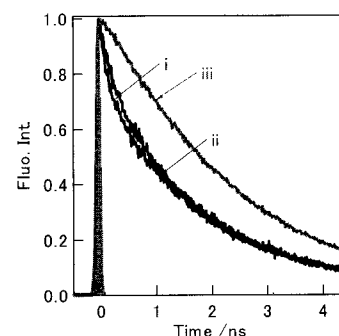


Fig. 3. Fluorescence time profile of ZnNc on SWCNT in THF.

Diameter-Dependent Dissipation of Vibration Energy of Cantilevered Multiwall Carbon Nanotubes

○Shintaro Sawaya¹, Yoshikazu Nakayama^{1,2,3} and Seiji Akita^{1,3}

¹Department of Physics and Electronics, Graduate School of Engineering, Osaka Prefecture University, 1-1 Gakuen-cho, Naka-ku, Sakai, Osaka 599-8531, Japan.

²Department of Mechanical Engineering, Graduate School of Engineering, Osaka University, 2-1 Yamadaoka, Suita, Osaka 565-0871, Japan

³CREST, Japan Science and Technology Agency

Cantilever miniaturization is crucial to realize highly sensitive force sensor based on resonant frequency shift of cantilevers. Carbon nanotubes (CNTs) are one of the promising candidates for this application because of their light weight, high aspect ratio, and extraordinary mechanical properties.[1,2] In order to realize higher sensitivity, the detailed analysis of vibration of CNT cantilevers should be required. In this study, we have investigated the vibration of multiwall CNTs in terms of dissipation of vibration energy.

Nanotubes examined were classified into six groups of multiwall CNTs synthesized by catalytic chemical vapor deposition (CVD) method. Cantilevered CNTs were vibrated mechanically using a piezo device in the SEM ($\sim 10^{-5}$ Pa) at room temperature. The average Young's modulus for each groups measured from resonant frequencies increases from 0.1 to 0.7 TPa with increasing the G/D ratio measured from the Raman spectroscopy. Thus, the well developed sp^2 network strongly contributes to the mechanical strength of CNTs. The quality factor, Q , determined from the resonant curve corresponds to the inverse of vibration-energy dissipation. The CVD grown CNTs show the Q factors of 100 ~ 500 depending on the groups. As shown in Fig. 1, the $1/Q$ value corresponding to the dissipation increases with increasing the tube diameter, while the $1/Q$ value is independent of the specific Young's modulus. This implies that the interlayer interaction rather than the defects in the sp^2 network affects the energy loss of the vibrating CNT cantilever. This is because the inner CNT layers act as a damper due to the weak interlayer coupling, and the defect dependence of the energy loss is screened by the loss derived from the interlayer interaction. Thus, the vibration energy of the CVD grown multiwall CNT cantilevers is mainly dissipated at the interlayer interaction.

Acknowledgement This work was partially supported by a Grant-in-Aid for Scientific Research from the Japan Society for the Promotion of Science.

[1] M. Nishio et al, Appl. Phys. Lett. **86**, 133111(2005).

[2] M. Nishio et al, J. Vac. Sci. Tech. B **23**, 1975 (2005).

Corresponding Author: Seiji Akita,

E-mail: akita@pe.osakafu-u.ac.jp, **Tel&Fax:** 072-254-9265

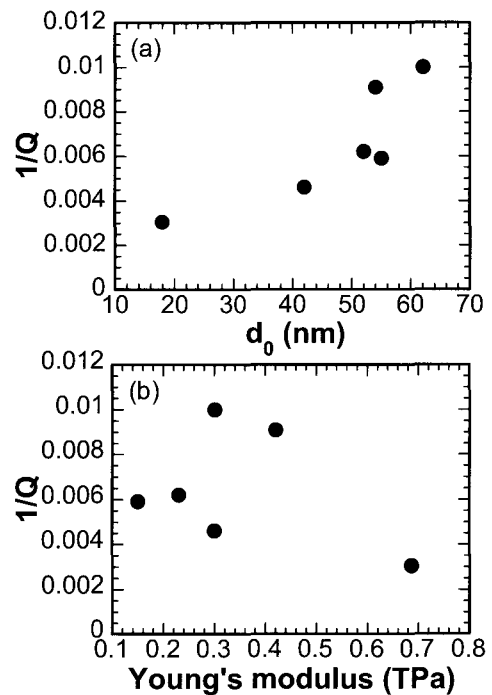


Fig. 1 (a) Diameter dependence of $1/Q$ and (b) Young's modulus dependence of $1/Q$.

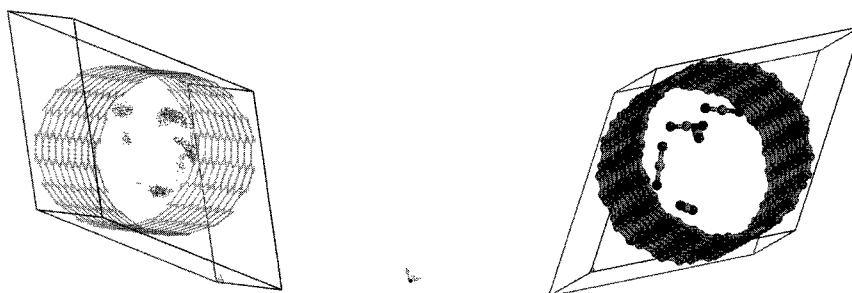
Effect of Adsorption of various gas molecules on the electronic structure of single walled CNT

O Abhijit Chatterjee

*Accelrys K.K., Nishishinbashi TS Bldg. 11F, 3-3-1 Nishishinbashi, Minato-ku, Tokyo
105-0003, Japan.*

Abstract

Since the discovery of the structure of Carbon nanotubes (CNTs)¹, much effort has been devoted to finding uses of these structures in applications ranging from field-emission devices to other nanodevices². Kong et al³ proposed for the first time the use of CNTs as gas sensors. A recent study of Maiti et al⁴ has investigated the semiconducting single-walled nanotubes as gas sensors. NH₃ binds only weakly with CNTs, yet can change the conductance significantly. This discrepancy has been explained by assuming that the NH₃ binds at defects. This work explains the mechanism of gas sensing of NH₃ and proposes practical methods for increasing sensitivity. The present communication is aimed to explore here the interaction of CNT with different gas molecules starting from O₂, N₂, H₂, CO₂, NO₂ to have an understanding first of the adsorption behavior of the selected gases in defect free CNT using Grand Canonical Monte Carlo simulation (GCMC). Once the adsorption local minima are identified a first principle calculation using DMol3 of Accelrys is performed to rationalize the change in electronic structure due to adsorption of simple gases. A reactivity index study⁵ was performed to formulate a priori rule for the gas sorption in CNTs.



The Monte Carlo simulation results using Sorption module of Accelrys is shown for CO₂.

References

1. S. Iijima, Nature 354, 56 (1991).
2. W. a. de Heer, A. Chaterlam nd D. Ugarte, Science 270, 1179 (1995).
3. J. Kong, N. R. Franklin, c. Chou, M.G. Chaplin, S. Peng, K. Cho and H. Dai, Science 287, 622 (2000).
4. J. Andzelm, N. Govind and A. Maiti, Chem. Phys. Lett. 421, 58 (2006).
5. A. Chatterjee, T. Ebina and F. Mizukami, J. Phys. Chem. B 109, 7306 (2005).
- 6.

Corresponding Author: Abhijit Chatterjee

E-mail: achatterjee@accelrys.com

Tel: 03-3578-3861, Fax: 03-3578-3873.

First principles calculations for nanotube disruption by oxygen molecule

○Takazumi Kawai, Yoshiyuki Miyamoto

*Fundamental and Environmental Research Laboratories, NEC Corporation
34 Miyukigaoka, Tsukuba 305-8501, Japan*

The oxidation processes are widely used for the purification or cap opening of carbon nanotubes. Recently, some experiments showed that the nanotubes are selectively oxidized depending not only on tube diameter but also on chirality[1-3]. Understanding of the atomic mechanisms of nanotube oxidation helps us to pick out nanotubes with intended chirality from the mixture.

Here, we focus on the destructive deformation process, where an oxygen molecule chemisorbed on nanotube surface breaks up the original C-C bonding. The reaction barriers for the process increase for nanotubes with larger diameter. Furthermore, armchair nanotubes have smaller reaction barriers compared to zigzag nanotubes with similar diameter. The local curvature near the breaking bond is one of the important factors. For armchair nanotubes, the broken C-C bond is perpendicular to the tube axis, and the curvature radius equal to the tube radius. On the other hand, the broken bond of zigzag nanotubes has 30 degrees tilt from perpendicular direction, and then the local curvature radius near the bond is much larger than those of armchair nanotubes. Since the larger strain due to the large curvature decrease the reaction barriers for C-C bond breakup, the armchair nanotubes with relatively small diameters are easily broken by the oxidation process compared to the zigzag nanotubes. We will also discuss the hole-doping effect, which may correspond to the oxidation in some solution.

[1] E.Menna, et al, Phys. Rev. B 68 (2003) 193412R.

[2] W.Zhou, et al, Chem. Phys. Lett. 350 (2001) 6.

[3] Y.Miyata, et al, J. Phys. Chem. B110, (2006) 25.

Corresponding Author: Takazumi kawai

E-mail: t-kawai@da.jp.nec.com

Tel&Fax: 029-850-1554

Structural change in MWCNTs pressurized under H₂ gas atmosphere

○ Atsuko Nakayama, Shigenori Numao, Satoshi Nakano*, Shunji Bandow, Sumio Iijima

Department of Materials Science and Engineering, 21st century COE Nanofactory, Meijo University, 1-501 Shiogamaguchi, Nagoya 468-8502, Japan

**National Institute for Materials Science, 1-1 Namiki, Tsukuba 305-0044, Japan*

Hydrogen molecule has a stable hydrogen bond with large ionization energy and the magnitude of electron affinity is close to that of carbon; we could not expect the charge-transfer interaction between graphite and H₂, inducing the intercalation, unless carbon and H₂ are in some special condition. Unstable electron state in the layered structure can be caused by pressurization. Recently we have found that pressurization of graphite and H₂ has also occurred the intercalation¹. We could understand that the pressurization causes the changes in the C-C π bond composing of the in-plane structure and the *van der Waals* bond working between the interlayers. These facts have motivated us to investigate whether multi-walled carbon- nanotubes (MWCNTs) accepts H₂ under pressure.

In this study, *in-situ* observation of structural change in MWCNTs pressurized with H₂ (H₂-MWCNTs) has been performed at the pressure up to 2.5 GPa at room temperature with a diamond anvil cell. The MWCNTs were prepared by radio frequency (RF) plasma vaporization². In order to remove the tips of MWCNTs and make the opened structure, they were heat-treated at 675 °C for 75 min under a mixed gases atmosphere of O₂ and Ar (1:4 by pressure). Angle-dispersive x-ray diffraction patterns were taken using synchrotron radiation beams monochromatized to energy of 20 keV at Photon Factory (PF) in High Energy Accelerator Research Organization (KEK).

According to the x-ray diffraction patterns, the peaks observed in the range from 5 to 30 degrees of 2θ angles were assigned to 002, a mixture of 100 and 101, 004 and 110 reflections. The peak positions were individually analyzed by fitting of the diffraction patterns with Gaussian functions. The pressure changes in 2θ angles of the 002 and 110 reflections indicate that the *a*-axis length become lengthen by pressurization up to 1.1 GPa in contrast to the monotonous contraction in the *c*-axis length.

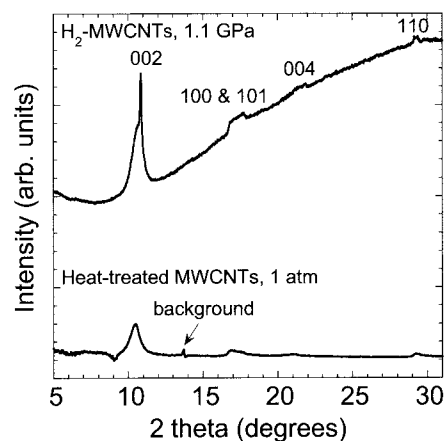


Fig. 1. X-ray diffraction patterns of heat-treated MWCNTs and

[1] A. Nakayama *et al.*, Special Issue of the Rev. of High Pressure Science and Technology, **14**, 222 (2004).

[2] A. Koshio *et al.*, Chem. Phys. Lett. **356**, 595 (2002).

Corresponding Author: Atsuko Nakayama, E-mail: atsuko@ccmfs.meijo-u.ac.jp, Tel&Fax: 052-834-4001

Visualization of CNT networks in CNT/polymer nanocomposites by ADF-STEM

○Tohoru Matsubara, Kaoru Shoda, Kousuke Itou, Atsuhiko Kunishige and
Yoshiyuki Sumiyama

UBE Scientific Analysis Laboratory, Inc., Tokiwadai, Ube, Yamaguchi 755-0001, Japan

Carbon nanotubes (CNTs) in CNT/polymer nanocomposites play important roles on their electronic, mechanical, and thermal properties. To evaluate and improve the properties of the nanocomposites, it is necessary to identify the dispersion of individual CNTs and their agglomerates in polymer matrix. Although transmission electron microscopy (TEM) is indispensable for the observation of CNTs, it is difficult to distinguish CNTs from polymer matrix because of small difference in contrast between them [1].

In this study, we have used annular dark-field scanning transmission electron microscopy (ADF-STEM) and visualized CNT networks in nanocomposites by examining the effect of detection angles on their image contrast, which can control scattered electrons on ADF detector.

A commercially available surface electroconductive resin sheet was sectioned using an ultra-microtome for plan-view TEM observation, as shown in Fig. 1(a). It is difficult to evaluate the CNT networks in the image. On the other hand, Figure 1(b) shows a high angle ADF-STEM (HAADF-STEM) image, as known as Z-contrast image, identifying individual CNTs as bright lines and their agglomerates as bright areas. In addition, as decreasing the detection angles, ADF-STEM images, shown in Figs.1(c) and 1(d), provide significant improvement in contrast. It is assumed that the ADF-STEM images are mainly formed from the elastically scattered electrons of CNTs and allow us to visualize individual CNTs, as we will discuss in detail.

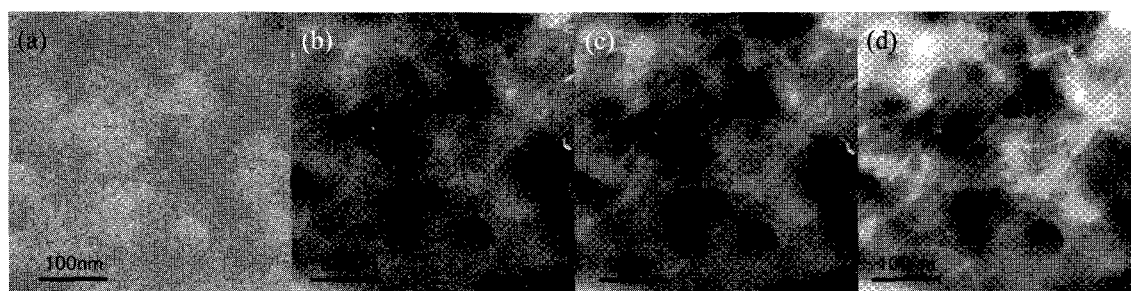


Fig. 1 Plan-view (a) TEM image and (b)-(d)ADF-STEM images of CNT/polymer nanocomposites. Detection angles: (b) 87 – mrad (c) 44 - 116 mrad (d) 18 – 47 mrad.

References: 1) J. Loos et. al.: *Ultramicroscopy* **104** (2005) 160.

Corresponding Author: Tohoru Matsubara

E-mail: t.matsubara@ube-ind.co.jp

Tel&Fax: +81-836-51-8195, +81-836-51-8196

Unique Optical Properties of DNA-dissolved Carbon Nanotubes

○Yuichi Noguchi, Tsuyohiko Fujigaya, Yasuro Niidome, Naotoshi Nakashima

*Department of Applied Chemistry, Graduate School of Engineering, Kyushu University,
744 Motoooka, Nishi-ku, Fukuoka 819-0395, Japan*

We have already reported that double-stranded DNAs and RNAs are able to dissolve single walled carbon nanotubes (SWNTs) in water^{1, 2}). Here, we examined optical and structural characterizations for aqueous solutions of DNA / SWNTs and found interesting pH response. Water solutions of DNA / SWNTs were prepared by sonication with a bath type ultrasonifer at a temperature below 10 °C, and subsequent centrifugation at 250000 g. The pH (pH = 5.8, 6.4, 7.0, 8.0) was adjusted with phosphate buffered saline. The optical and structural analysis of the composites were performed using visible-near-IR absorption spectrophotometry, near-IR photoluminescence (PL) spectrophotometry, and atomic force microscope. The DNA / SWNTs in phosphate buffer (pH = 5.8) exhibit only one intense luminescence peak, which can be attributed to the (6,5) chirality of SWNTs (Fig.1). 2D-mapping of PL showed strong pH dependence. Details will be reported at the meeting.

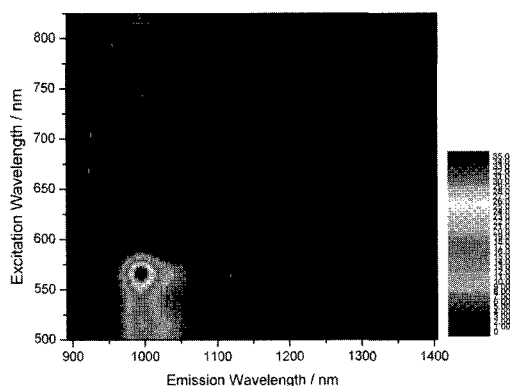


Fig. 1 2D mapping of photoluminescence spectra of aqueous solution of ds-DNA / CNT at pH 5.8. Optical cell length is 1 cm.

References: 1) N. Nakashima et al., *Chem. Lett.*, **32**, 456 (2003). 2) N. Nakashima et al., *Chem Phys. Lett.* **419**, 574 (2006).

Corresponding Author: Naotoshi Nakashima

E-mail: nakashima-tcm@mbox.nc.kyushu-u.ac.jp

Tel&Fax: +81-92-802-2840

Improved Ultrasonic Dispersion of Carbon Nanotubes

Hiroshi Saito and Masahito Sano

*Department of Polymer Science and Engineering, Yamagata University
4-3-16 Jyonan, Yonezawa, Yamagata 992-8510 JAPAN*

Dispersing carbon nanotubes (CNTs) in solvents is extremely important for fundamental characterization as well as many practical applications. Yet, this is a challenging task by the following reasons. The highly extended π -electron on an atomically smooth surface causes the CNTs highly non-wettable by any solvents. Poor wettability implies that a CNT does not mix with solvent molecules. Also, the shape and size of CNTs makes van der Waals (VDW) interaction exceptionally strong. It takes a huge energy to separate the adhered CNTs, and even in the case of separated CNTs, they tend to coagulate immediately. In order to disperse CNTs, therefore, it is necessary to make the CNT surface wettable (wetting), disintegrate the CNT aggregates (disintegration), and prevent from re-coagulating each other (stabilization).

Most studies of so-called “CNT dispersions” involve covalent functionalization, additions of surfactants like SDS or polymers, introduction of electrostatic charges through acid treatments, and partial destruction by heat or mechanical forces. All of these techniques belong to stabilization. However, stabilization alone is not sufficient for dispersion, as easily verified by the fact that nothing happens by simply adding SDS to water containing CNTs. Most often, ultrasonic is used to force solvent molecules to have direct contact with the CNT surface and to disintegrate CNT bundles. Despite of the important role played by ultrasonic, hardly any studies have been done to improve dispersion ability or to characterize its effect on chiral CNTs.

One of the problems in ultrasonic dispersion is the existence of air bubbles or adsorbed air layers around CNTs. Air layers are formed around the CNT surface when CNTs are first introduced in water. Also air bubbles that produced during ultrasonic treatments can be trapped on the CNTs. Due to the wave nature of ultrasonic, nearly all the incoming ultrasonic waves are reflected at the air-solvent interface and cannot reach the CNT surface. This problem is circumvented by an addition of anti-foaming agents. At the meeting, we report the effects of agents on the dispersed amount and a possibility of chirality dependence enhancement.

Corresponding Author: Masahito Sano

E-mail: mass@yz.yamagata-u.ac.jp, Tel&Fax: +81-(0)238-26-3072

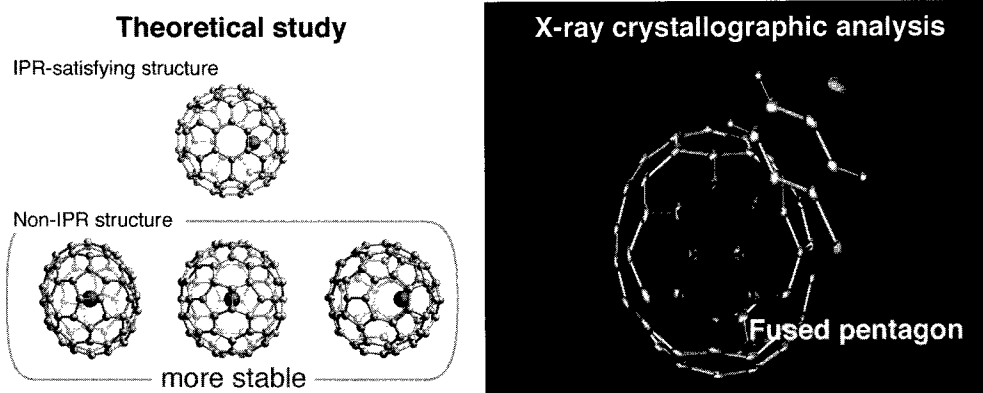
La@C₇₂ Having a Non-IPR Carbon Cage

○Hidefumi Nikawa¹, Takashi Kikuchi¹, Takatsugu Wakahara¹, Tsukasa Nakahodo¹, G. M. Aminur Rahman¹, Takahiro Tsuchiya¹, Yutaka Maeda², Takeshi Akasaka¹, Kenji Yoza³, Ernst Horn⁴, Kazunori Yamamoto⁵, Naomi Mizorogi⁶, Zdenek Slanina⁶, and Shigeru Nagase⁶

¹Center for Tsukuba Advanced Research Alliance, University of Tsukuba, Tsukuba, Ibaraki 305-8577, Japan, ²Department of Chemistry, Tokyo Gakugei University, Koganei, Tokyo 184-8501, Japan, ³Bruker AXS K.K., Yokohama, Kanagawa 221-0022, Japan, ⁴Department of Chemistry, Rikkyo University, Tokyo 171-8501, Japan, ⁵Power Reactor & Nuclear Fuel Development Corporation, Tokai, Ibaraki 319-1100, Japan, ⁶Theoretical Molecular Science, Institute for Molecular Science, Okazaki, Aichi 444-8585, Japan

Fullerenes have an even number of three-coordinate carbon atoms (n) and consist of 12 pentagonal and $(n/2 - 10)$ hexagonal carbon rings (e.g., C₆₀ has 12 pentagons and 20 hexagons). It has been established as the isolated-pentagon rule (IPR) that all pentagons are isolated in the most stable fullerene. Since the first proposal by Kroto in 1987, the IPR has proved particularly valuable in unraveling cage structures of higher fullerenes and metallofullerenes. Recently, Sc₂@C₆₆ and Sc₃N@C₆₈ have been reported as the examples of endohedral metallofullerenes having a non-IPR cage. Since no IPR-satisfying cage structure is available for C₆₆ and C₆₈, it remains still an open question whether metallofullerenes that have a non-IPR cage are isolable or not.

For C₇₂, there is only one IPR-satisfying structure with D_{6d} symmetry. Theoretical investigation of C₇₂ and Ca@C₇₂ suggests that non-IPR cage structures are more stable than the IPR-satisfying one. Recently, Shinohara et al. reported the NMR study on La₂@C₇₂, which indicates that La₂@C₇₂ has a non-IPR cage. However, there is no conclusive evidence for the structural characterization. Meanwhile, we succeeded in the extraction, isolation, and characterization of a missing metallofullerene La@C₇₄ as a derivative, La@C₇₄(C₆H₃Cl₂) [1]. This derivative method opened a way for the experimental structural investigation of unconventional metallofullerenes. We herein report the first structural determination of a monometallofullerene derivative, La@C₇₂(C₆H₃Cl₂), that has a non-IPR cage by spectroscopic and X-ray crystallographic analysis [2]. In addition, the unique electronic properties and high reactivity of La@C₇₂ are discussed on the basis of the theoretical study.



References:

- [1] Nikawa, H.; Kikuchi, T. *et al. J. Am. Chem. Soc.* **2005**, *127*, 9684-9685.
 [2] Wakahara, T.; Nikawa, H. *et al. J. Am. Chem. Soc.* **2006**, *128*, 14228-14229.

Corresponding Author: Takeshi Akasaka

E-mail: akasaka@tara.tsukuba.ac.jp

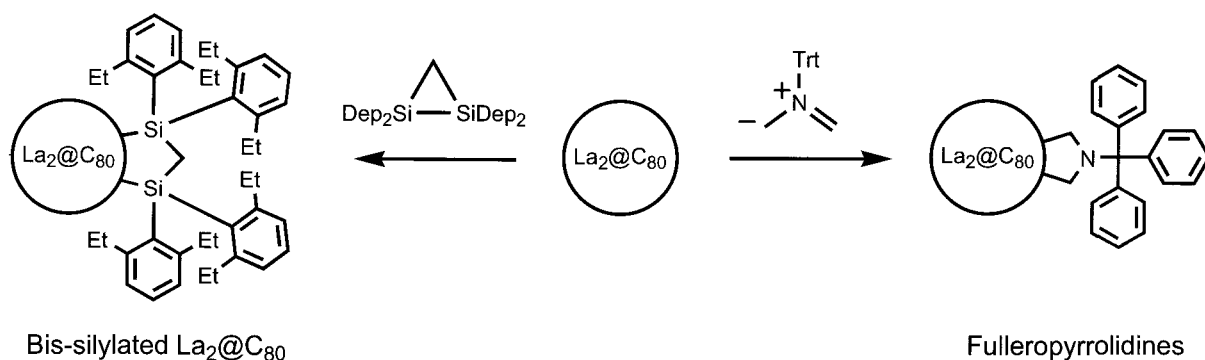
Tel&Fax: +81-29-853-6409

Motion of the La Atoms in $\text{La}_2@C_{80}$ Derivatives

○Michio Yamada,¹ Tsukasa Nakahodo,¹ Takatsugu Wakahara,¹ Takahiro Tsuchiya,¹ Yutaka Maeda,² Takeshi Akasaka,¹ Kenji Yoza,³ Naomi Mizorogi,⁴ and Shigeru Nagase⁴

¹Center for Tsukuba Advanced Research Alliance, University of Tsukuba, Tsukuba, Ibaraki 305-8577, Japan, ²Department of Chemistry, Tokyo Gakugei University, Koganei, Tokyo 184-8501, Japan, ³Bruker AXS K. K., Yokohama, Kanagawa 221-0022, Japan, ⁴Department of Theoretical Molecular Science, Institute for Molecular Science, Okazaki, Aichi 444-8585, Japan

Abstract: Among many kinds of metallofullerenes, $M_2@C_{80}$ has attracted special attention for the dynamics of the encapsulated metal atoms because of their three-dimensional random motion.^{1,2} To control the motion of atoms within a cage may be very valuable in designing functional molecular devices with new electronic or magnetic properties.^{3,4} Recently, we have reported the silicon-derivative of $Ce_2@C_{80}$, in which the motion of metal atoms are restricted by the electron-donation from the silyl group to the fullerene cage.⁵ Meanwhile, theoretical calculation predicts that the random motion of the encapsulated metal atoms remains in a Diels-Alder adduct of $M_2@C_{80}$.⁶ Herein we report the synthesis and full characterization of $\text{La}_2@C_{80}(\text{Dep}_2\text{Si})_2\text{CH}_2$ (Dep = 2,6-diethylphenyl), and two regioisomers of $\text{La}_2@C_{80}(\text{CH}_2)_2\text{NTrt}$ (Trt = triphenylmethyl). We found that the fulleropyrrolidines show the different motion of the metal atoms from the bis-silylated $\text{La}_2@C_{80}$.



References: (1) Akasaka, T. et al., *Angew. Chem., Int. Ed. Engl.* **1997**, *36*, 1643. (2) Shimotani, H.; et al., *J. Am. Chem. Soc.* **2004**, *126*, 364. (3) Balzani, V. et al., *Angew. Chem. Int. Ed.* **2000**, *39*, 3348. (4) Molecular Machines Special Issue. *Acc. Chem. Res.* **2001**, *34*, 409. (5) Yamada, M. et al., *J. Am. Chem. Soc.* **2005**, *127*, 14570. (6) Kobayashi, K. et al., *Chem. Phys. Lett.* **2003**, *374*, 562.

Corresponding Author: Takeshi Akasaka, E-mail: akasaka@tara.tsukuba.ac.jp, Tel&Fax: +81-298-53-6409

Structure of Scandium Carbide-encapsulated Metallofullerene

○Yuko Iiduka,¹ Takatsugu Wakahara,¹ Koji Nakajima,¹ Takahiro Tsuchiya,¹ Yutaka Maeda,² Tsukasa Nakahodo,³ Takeshi Akasaka,^{*,1} Kenji Yoza,⁴ Michael T. H. Liu,⁵ Naomi Mizorogi⁶ and Shigeru Nagase^{*,6}

¹Center for Tsukuba Advanced Research Alliance, University of Tsukuba, ²Department of Chemistry, Tokyo Gakugei University, ³Department of Applied Chemistry, Kinki University, ⁴Bruker AXS K. K., ⁵Department of Chemistry, University of Prince Edward Island, ⁶Department of Theoretical Molecular Science, Institute for Molecular Science

Metal carbide-encapsulated metallofullerenes have attracted special attention because of encapsulation of the C₂ unit together with several metal atoms.^{1,2} Recently, some of dimetallofullerenes such as Sc₂C₈₄³ and Y₂C₈₄⁴ have been investigated by ¹³C NMR spectroscopy. As a result, it is found that Sc₂C₈₄(III) and Y₂C₈₄(I, II, III) are not normal M₂@C₈₄ types, but M₂C₂@C₈₂ types encapsulating metal carbide. Furthermore, these structures for Sc₂C₂@C₈₂(III) and Y₂C₂@C₈₂(III) have been confirmed by the MEM (maximum entropy method)/Rietveld analysis of synchrotron X-ray powder diffraction data.⁵ To promote better understanding of the endohedral structure of Sc₂C₂@C₈₂(III), we herein report the structural determination of Sc₂C₂@C₈₂(III) by means of theoretical calculation and X-ray single-crystal structure analysis.

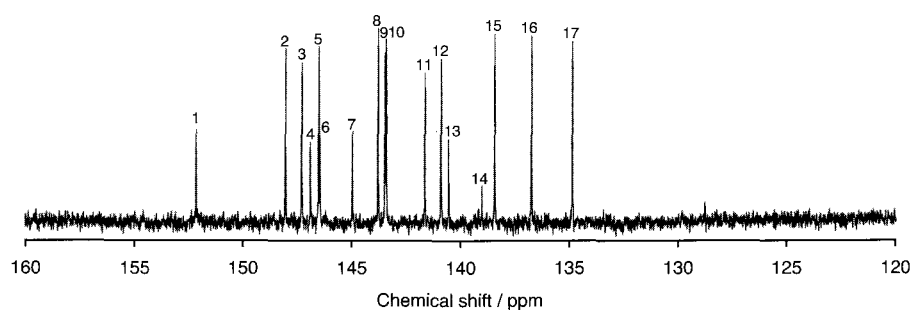


Figure. ¹³C NMR spectrum of Sc₂C₂@C₈₂(III) with C_{3v} symmetry.

References: (1) Nishibori, E. et al., *Angew. Chem. Int. Ed.* **2001**, *40*, 2998. (2) Iiduka, Y. et al., *J. Am. Chem. Soc.* **2005**, *127*, 12500. (3) Iiduka, Y. et al., *Chem. Commun.* **2006**, 2057. (4) Inoue, T. et al., *Chem. Phys. Lett.* **2003**, *382*, 226. (5) Nishibori, E. et al., *Chem. Phys. Lett.* *in press*.

Corresponding author: Takeshi Akasaka, Tel & Fax: +81-29-853-6409, E-mail: akasaka@tara.tsukuba.ac.jp

2-4

Characterization of Metallofullerenes and Fullerene Nano-peapods by Synchrotron Radiation: Soft X-ray Magnetic Circular Dichroism Spectroscopy and X-ray Diffraction.

Ryo Kitaura^{1,2}, Haruya Okimoto^{1,2}, Yuko Kato^{1,2}, Tetsuya Nakamura³, Eiji Nishibori⁴, Shinobu Aoyagi⁴, Makoto Sakata⁴, Hisanori Shinohara^{1,2}

¹Department of Chemistry, Nagoya University, Nagoya 444-8602, Japan

²Institute for Advanced Research, Nagoya University, and CREST/JST

³JASRI-the Spring-8, Hyogo 679-5198, Japan

⁴Department of Applied Physics, Nagoya University, Nagoya 444-8602, Japan

Metallofullerenes and fullerene nano-peapods have attracted wide range of researchers owing to their specific structure and properties. In most cases, synthetic yield of endohedral metallofullerenes (especially di- and tri-metallofullerenes) and therefore fullerene nano-peapods is very low, which have prevented us from investigating structure and properties of these novel compounds. Characterization using high brilliance synchrotron radiation is a very powerful method, which needs only little amount of samples. Here we report characterization of Dy- and Er-metallofullerene and the corresponding nano-peapods by using synchrotron soft x-ray magnetic circular dichroism spectroscopy (SXMCD) and x-ray diffraction (XRD).

Temperature dependence of MCD spectra of metallofullerenes and nano-peapods clearly shows that the reciprocal magnetization of encapsulated lanthanide ions are proportional to temperature, namely, follows Curie-Weiss law. Determined Weiss temperature of these ions are relatively small ($-10 \sim 5$ K), which represents that magnetic interaction between encapsulated ions are weak. Sum rule analyses of observed spectra show that the orbital moment of encapsulated atoms is greatly reduced compared to free trivalent lanthanide atoms. This moment reduction is also evidenced by determined Curie constants. Spectra simulation suggests that this moment reduction originates from crystal field and orbital hybridization effects. We will also report structural analyses of metallofullerenes and nano-peapods using X-ray diffraction and discuss about correlation between the structure and magnetic properties.

Corresponding Author: Hisanori Shinohara

TEL: +81-52-789-2482, FAX: +81-52-789-1169, E-mail: noris@cc.nagoya-u.ac.jp

Structure and Electronic Properties of $(\text{NaH})_x\text{C}_{60}$ Compounds(II)

○Takashi Naniki , Satoru Motohashi , Hironori Ogata

Dept. of Materials Chemistry, Hosei University

3-7-2 Kajino cho, Koganei, Tokyo, 184-8584. Japan

Since the discovery of superconductivity in $\text{Na}_x\text{X}_y\text{C}_{60}$ ($\text{X}=\text{N}:T_c=12\text{K}$, $\text{X}=\text{H}:T_c=15\text{K}$), there has been many interests in the structure and the electronic states of the Na-X-C_{60} ternary systems. It has been suggested that nitrogen or hydrogen in the systems contribute not only to a spacer which suppress the structural instability but also to the electronic states near the Fermi level.

In the present work, $(\text{NaH})_x\text{C}_{60}$ compounds ($x=1\sim 10$) were synthesized, and their structures and electronic properties were investigated by powder X-ray diffraction, magnetic susceptibility and solid state NMR measurements.

Stoichiometric amounts of C_{60} and NaH were mixed and ground in a mortar and sealed into ESR quartz tubes in a glove box. These were heated in a furnace at 290°C for 100minutes.

Figure 1 shows the solid state $^1\text{H-NMR}$ spectra of $(\text{NaH})_x\text{C}_{60}$ ($x=1,3\sim 8$) compounds at room temperature. It was found that anionic hydrogen exist in the crystals for $x\geq 3$.

Detail results on the crystal structures and correlation between structures and electronic properties of these materials will be discussed in the presentation.

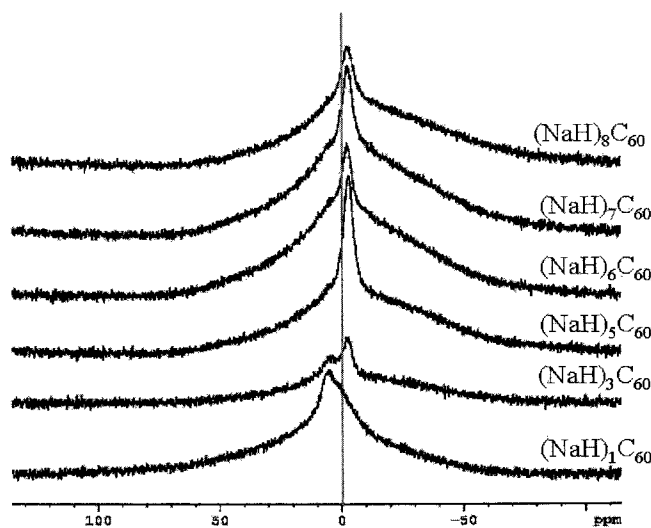


Fig 1. Solid state $^1\text{H-NMR}$ spectra of $(\text{NaH})_x\text{C}_{60}$ ($x=1,3\sim 8$) compounds at r.t.

[1] K.Imaeda et al, Solid State Communication, Vol99, No7, 479-482(1996)

Corresponding Author: Hironori Ogata, E-mail: hogata@hosei.ac.jp
Tel&Fax: 042-387-6229

Analyses of the carrier injection barrier of C₆₀ FET devices with Au source/drain electrodes modified by 1-alkanethiol

○Takayuki Nagano¹, Yohei Ohta¹, Naoko Kawasaki¹, Ryo Nouchi², Yoshihiro Kubozono¹, Akihiko Fujiwara³, Shojun Hino⁴

¹Department of Chemistry, Okayama University, Okayama 700-8530, Japan

²CREST, Japan Science and Technology Agency, Kawaguchi, 322-0012, Japan

³Japan Advanced Institute for Science and Technology, Ishikawa 923-1292, Japan

⁴Graduate School of Science and Engineering, Ehime University, Ehime 790-8577, Japan

In field-effect transistor (FET) devices with organic molecules, the interface between the active layer and the source/drain electrodes is found to be very important for the effective carrier injection.^{1,2} In this study, we have fabricated and characterized the C₆₀ FET devices with Au source/drain electrodes modified by various types of 1-alkanethiols in order to clarify quantitatively the electronic structure of the interface produced by a contact of C₆₀ thin films and their electrodes. Figure 1 shows drain current I_D versus drain voltage V_{DS} plots of the C₆₀ FET device with Au electrodes modified by 1-hexadecanethiol (C₁₆H₃₃SH). The I_D - V_{DS} plots shows a concave-up nonlinearity in low V_{DS} region, showing that the plots are remarkably affected by the carrier-injection barrier. We have tried to determine the barrier height ϕ_B in this device on the basis of the thermionic emission model.³ The ϕ_B value of 0.63 eV determined is 1/2 of the value (= 1.3 eV) predicted from the energy levels of electrodes and C₆₀.

Furthermore, the electronic structure of the C₆₀ thin films on the Au modified by 1-hexadecanethiol was studied by using of ultraviolet photoelectron spectroscopy under high vacuum. The shift of peaks for molecular orbitals of C₆₀ was plotted as a function of film thickness.

[1] T. Yasuda et al. *Appl. Phys. Lett.* **85**, 2098 (2004).

[2] T. Nishikawa et al. *J. Appl. Phys.* **97**, 104509 (2005).

[3] S. M. Sze, *Semiconductor devices* (John Wiley & Sons Inc., NY, 2002) Chap. 7.

Corresponding Author: Takayuki Nagano

E-mail: t-nagano@cc.okayama-u.ac.jp

Tel: +81-86-251-7850, **Fax:** +81-86-251-7853

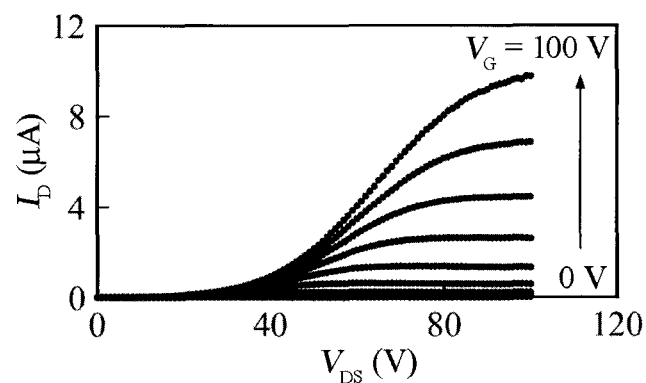


Fig.1. The I_D - V_{DS} plots for the C₆₀ FET device with Au source/drain electrodes modified by 1-hexadecanethiol.

Electrochemical and Photoelectrochemical Properties of Buckyferrocenes on Electrodes

○Katsuhiko Kanaizuka, Yutaka Matsuo, and Eiichi Nakamura

Nakamura Functional Carbon Cluster Project, ERATO, Japan Science and Technology Agency, Hongo, Bunkyo-ku, Tokyo 113-0033, Japan

The donor-chromophore-fullerene (D-C-F) molecule shows high conversion efficiency from photoenergy to electric energy when applied in a solar cell. However, in general elaborate multi-step synthesis is required to obtain D-C-F molecules and the total yields are quite low. We have reported the synthesis and characterizations of penta-adducts of fullerenes and their metal complexes (bucky metallocenes) in high yields.¹ Buckyferrocene is a hybrid molecule of fullerene and ferrocene, which shows reversible multiple redox based on the fullerene and ferrocene. It should be noted that if these unique materials can be immobilized at an electrode surface, many intriguing devices should be created.

We will report on preparation method of buckyferrocene self-assembled monolayers (SAMs) on indium tin oxide (ITO) electrodes (Fig. 1) and photoelectrochemical properties of SAMs. The ITO electrodes modified with these molecules showed the high performance of photocurrent generation.

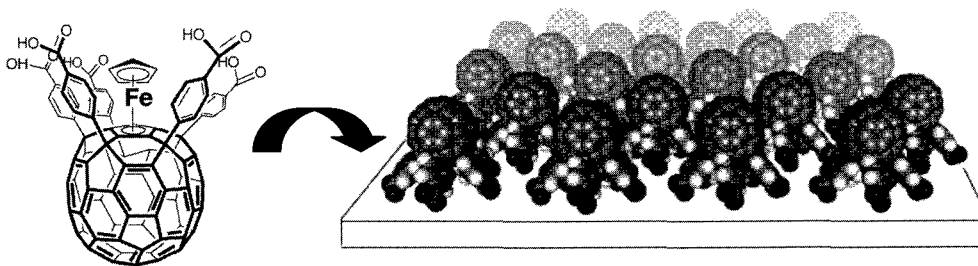


Fig. 1. Structure of the buckyferrocene used for film preparation (left) and image of the film on an indium tin oxide electrode (right)

References:

[1] E. Nakamura, *at al. J. Am. Chem. Soc.* **2002**, *124*, 9354.

E-mail: nakamura@chem.s.u-tokyo.ac.jp; matsuo@chem.s.u-tokyo.ac.jp

Fullerene derivatives have antioxidant activity but no metal-dependent prooxidant activity

○Shigeo Nakamura¹, Eriko Satake¹, Masashi Hatanaka¹, Kyoko Takahashi¹,
Kenji Matsubayashi², Tadahiko Mashino¹

¹Kyoritsu University of Pharmacy, 1-5-30 Shibakoen, Minato-ku, Tokyo 105-8512

²Vitamin C60 BioResearch Corporation, 1-8-7, Kyobashi, Chuo-ku, Tokyo 104-0031

Some biological activities of water-soluble fullerene derivatives are related to the redox-active properties. We examined the superoxide($O_2^{\cdot-}$)-quenching activity of $C_{62}(COOH)_4$ (**1**). When xanthine oxidase was added to the solution to generate $O_2^{\cdot-}$, cyt. *c* was reduced and the absorbance at 550 nm increased. The increase of the absorbance at 550 nm was suppressed by the addition of **1**. Fullerene derivative **1** also relieved the growth inhibition of *E. coli* by $O_2^{\cdot-}$ -generator such as paraquat.

Many antioxidants are known to have both antioxidant activity and prooxidant activity. For example, in the presence of metal ion, ascorbic acid reduces Cu^{2+} to Cu^+ , and Cu^+ reacts with O_2 to produce active oxygens. We examined the prooxidant activity of **1** evaluated by the $\cdot OH$ -dependent production of HCHO from DMSO. In contrast to the case of ascorbic acid, **1** did not show the prooxidant activity (Fig. 1). Radical Sponge®, a fullerene containing cosmetic ingredient, had also no prooxidant activity.

This result suggests that fullerene derivatives are excellent antioxidants that have no prooxidant activity.

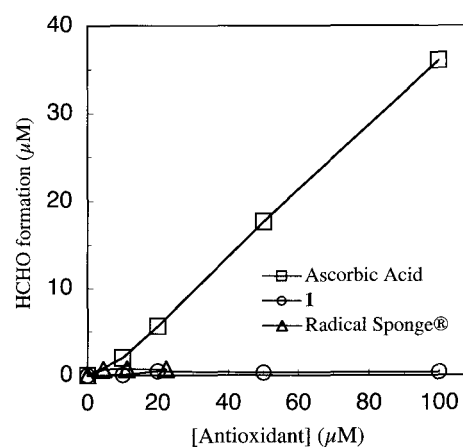
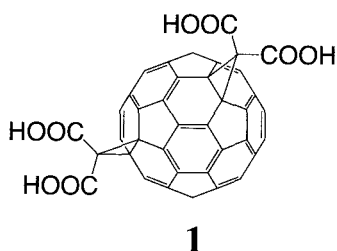


Fig. 1 Prooxidant activity of antioxidants in the presence of Cu^{2+}

Corresponding Author: Tadahiko Mashino

E-mail: mashino-td@kyoritsu-ph.ac.jp

Tel: +81-3-5400-2694, Fax: +81-3-5400-2691

A New Route to Water-Soluble Fullerenol and its Application to CMP Slurry

OKen Kokubo^{1*}, Syogo Shirakawa¹, Kenji Matsubayashi²,
Terutake Hayashi³, Takashi Miyoshi³, and Takumi Oshima¹

¹*Division of Applied Chemistry, Graduate School of Engineering, Osaka University,
Suita, Osaka 565-0871, Japan*

²*Vitamin C60 BioResearch Corporation, 1-8-7 Kyobashi, Chuo-ku, Tokyo 104-0031, Japan*

³*Department of Mechanical Engineering, Graduate School of Engineering, Osaka University*

Water-soluble fullerene has attracted much attention in the field of life science, as medicine or cosmetic, in view of its high antioxidant activity [1]. The polyhydroxyl fullerene, so-called fullerenol, is one of the most accessible candidates for the water-soluble fullerene and several synthetic methods, *e.g.*, Oleum [2] and TBAH [3] methods, have already been reported. However, the low water solubility due to the insufficiently substituted hydroxyl groups or the inevitable Na ion contamination by treatment of NaOH may result in some obstacles in the practical use. Recently, we developed the two step synthetic method for milky white fullerenols with 36–40 hydroxyl groups (estimated average) by heating adequately pre-hydroxylated C₆₀ in H₂O₂ aqueous solution [4,5].

In this study, we improved our previous method by employing two liquids phase oxidation method with phase transfer catalyst and obtained C₆₀(OH)₄₄•8H₂O in one step from pristine C₆₀ (Table 1). We also report a novel application of our fullerenols to chemical mechanical polishing (CMP), which is a planarization nanotechnology for Ultra LSI.

Table 1. Effects of Phase Transfer Catalyst on Two Liquids Phase Oxidation Synthesis of Fullerenol^a

Catalyst	Equiv ^d	Temp / °C	Conv / % ^e	Yield / % ^f	
				As produced	Purified ^g
None	–	60	0	0	0
TBAB ^b	6.15	60	13	– (78)	– (49)
TBAH ^c	3.08	60	80	77 (173)	44 (98)
TBAH	6.15	60	100	89 (199)	47 (105)
TBAH	6.15	rt	61	52 (117)	21 (47)

a) A toluene solution of C₆₀ (100 mg) was treated with 30% H₂O₂ aqueous solution for 12 h. b) Tetra-*n*-butyl ammonium bromide. c) Tetra-*n*-butyl ammonium hydroxide. d) Based on C₆₀. e) Determined by HPLC. f) Isolated yield based on the estimated formula: C₆₀(OH)₄₄•8H₂O. The values in parentheses are the yield in weight (mg). g) After column chromatography on Florisil followed by re-precipitation.

[1] Takada, H.; Kokubo, K.; Matsubayashi, K.; Oshima, T. *Biosci, Biotech, Biochem.* **2006**, *70*, 3088.

[2] Chiang, L. Y.; Wang, L.-Y.; Swirczewski, J. W.; Soled, S.; Cameron, S. *J. Org. Chem.* **1994**, *59*, 3960.

[3] Li, J.; Takeuchi, A.; Ozawa, M.; Li, X.; Saigo, K.; Kitazawa, K. *J. Chem. Soc., Chem. Commun.* **1993**, 1785.

[4] Kokubo, K. *et al.*, Abstracts of The 28th Fullerene-Nanotubes General Symposium, p.105, 2005.

[5] Tategaki, H. *et al.*, Abstracts of The 30th Fullerene-Nanotubes General Symposium, p.149, 2006.

Corresponding Author: Ken Kokubo

TEL: +81-6-6879-4592, FAX: +81-6-6879-4593, E-mail: kokubo@chem.eng.osaka-u.ac.jp

Ionization and fragmentation of solid C₆₀ by femtosecond laser ablation

○T. Kobayashi, T. Kato, Y. Matsuo, M. Kurata-Nishimura, J. Kawai, and Y. Hayashizaki

RIKEN, 2-1 Hirosawa, Wako, Saitama, 351-0198 Japan

Dynamical behavior of C₆₀ after laser excitation has been extensively studied in the gas phase*¹. We report here ionization and fragmentation of solid C₆₀ ablated on the surface of a silicon plate. Femtosecond laser ablation (fsLA) has been performed with a femtosecond laser system (400nm, 200fs) at laser intensity in the range between 10¹¹ and 10¹² W/cm². A reflectron time-of-flight (TOF) mass spectrometer is used to measure mass distribution of ions produced by laser ablation.

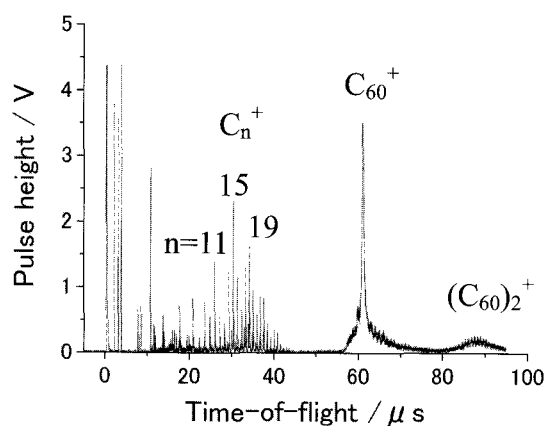


Figure 1 A TOF spectrum of ions produced by fsLA of C₆₀ at 6.2×10^{11} W/cm².

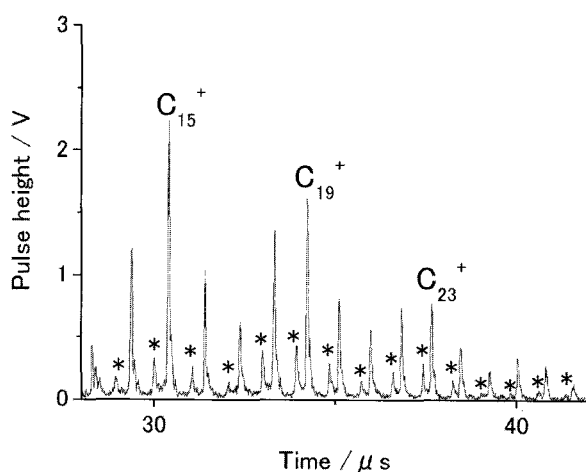


Figure 2 A part of Figure 1 is expanded. Metastable peaks are indicated by asterisks.

As shown in Fig.1, many fragment ions C_n⁺ (n≤30) have been observed as well as C₆₀⁺ ion and the dimer ion. These fragment ions have never been observed by femtosecond photoexcitation of C₆₀ in the gas phase because of the poor coupling of electronic excitation energy into vibrational degrees of freedom*². Figure 2 is the expansion of a part of Fig.1 in the range for C_n⁺ (13≤n≤28). The presence of metastable dissociation is clear in the figure. Since the dissociation energies of C₃ or C₅ from monocyclic C_n⁺ cluster ions (≤5.6eV) are smaller than that for C₂ from C₆₀⁺*³ (~10eV), the result is not consistent with the fact that C₆₀⁺ and C_{60-2n}⁺ complete dissociation during their flight in the acceleration region. We suggest that the initial structure of C_n⁺ ions just after fsLA is different from the monocyclic ring form of well-studied C_n⁺ cluster ions.

*¹ C. Lifshitz, Int.J.Mass Spectrom., **200**, 423 (2000).

*²M.Tchaplyguine,K.Hoffmann,O.Dühr, H. Hohmann, G. Korn, H. Rottke, M. Wittmann, I.V. Hertel, and E.E.B. Campbell, J.Chem.Phys., **112**, 2781 (2000).

*³ M.B. Sowa-Resat, P.A. Hintz, and S.L. Anderson, J. Phys. Chem., **99**, 10736 (1995).

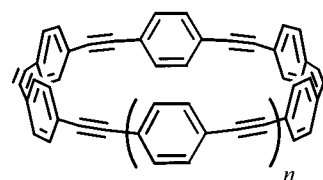
Tohru Kobayashi: tokoba@riken.jp, Tel: 048-467-8527

Cyclic [5]Paraphenyleneacetylene: Synthesis, Properties and Its Supramolecular Properties

○Takeshi Kawase, Yoshitaka Nishiyama, Takamitsu Nakamura, Takahiro Ebi, Kouzou Matsumoto, Hiroyuki Kurata
Graduate School of Science, Osaka University

New carbon allotropes having three-dimensional structures such as fullerenes, carbon nanotubes, fullerene-peapod, have been discovered and have attracted much attention. Therefore, the nature of the concave-convex π - π interaction between the curved graphene sheets should be important in the formation and properties of these materials.

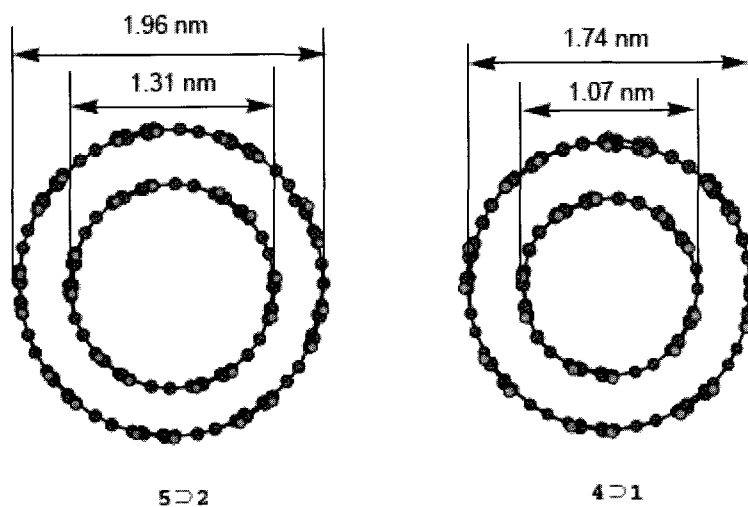
Recently we have reported the synthesis of cyclic [6]- to [9]paraphenyleneacetylene (CPPA) **2-5**. These compounds have smooth belt-shaped structures similar to a cut piece of carbon nanotube, and thus may be termed “carbon nanorings”, and [6]CPPA (**2**) with a 1.32-nm diameter forms unusually stable inclusion complexes with C₆₀ [association constant (K_a) = $(1.6 \pm 0.3) \times 10^4$ L mol⁻¹ at 30 °C in benzene]. We have also found that **2** can be



1: $n = 0$, 2: $n = 1$, 3: $n = 2$,
4: $n = 3$, 5: $n = 4$

accommodated in the cavity of [9]CPPA (**5**) with a 1.96-nm diameter to construct a novel ring-in-ring complex (K_a = ca. 40 L mol⁻¹ at 30 °C in CDCl₃).^[1] To explore the properties of curved conjugated systems, we have synthesized [5]CPPA (**1**), the smallest member of this class, and examined the complexation with [8]CPPA (**4**). The spectral properties of **1** are well correlated with their molecular strains. ¹H NMR chemical shifts of **1** in the mixture with **4** vary with temperatures and the ratio of the compounds. The results clearly indicate the formation of a ring-in-ring complex

4⊃**1** in the CDCl₃ solution. The thermodynamic parameters are also calculated from the K_a values at variety of temperatures to be ΔH = 0.75 kcal mol⁻¹ and ΔS = 16 cal mol⁻¹ K⁻¹. Although **4**⊃**1** has small contact area, the K_a value [$(9.2 \pm 1.4) \times 10^3$ L mol⁻¹ at 30 °C in CDCl₃] is about 200 times larger than that of **5**⊃**2**. The results clearly indicate the participation of the electrostatic attractive rather than the dispersion force.^[2]



[1] T. Kawase, H. Kurata, *Chem. Rev.*, **106**, 5250-5273 (2006).

[2] T. Kawase, Y. Nishiyama, T. Nakamura, T. Ebi, K. Matsumoto, H. Kurata, M. Oda, *Angew. Chem. Int. Ed.*, **46**, (2007) in press.

Stabilization of C₆₀ Nanoparticles by Protein Adsorption

○Shigeru Deguchi, Tomoko Yamazaki, Sada-atsu Mukai, Mikiko Tsudome, and Koki Horikoshi

Extremobiosphere Research Center, Japan Agency for Marine-Earth Science and Technology (JAMSTEC), 2-15 Natsushima-cho, Yokosuka 237-0061, Japan.

Fullerenes are currently of great interest in many areas of science and technology due to their unique chemical and physical properties, but many of the potential applications are hampered because fullerenes are soluble in the limited range of solvents. Various attempts have been made to modify fullerenes chemically to surmount the limitations, including synthesis of water-soluble fullerene derivatives and their applications for medical, cosmetic, and biotechnological purposes. Several groups including us found that the nanoparticles of fullerenes disperse stably in water even without the aid of dispersing agents such as surfactant.¹⁻⁴⁾ The finding holds promises as a totally new strategy for fullerenes functionalization.

The C₆₀ nanoparticles in aqueous dispersions are stabilized kinetically by electrostatic repulsion between the surface charges, and are destabilized and flocculate rapidly upon addition of electrolytes. The dispersion stability of C₆₀ has been studied extensively as to electrolyte concentration, pH, and preparation procedure. However, not much is known as to the dispersion stability of the C₆₀ nanoparticles in the physiological environments, which has direct relevance for studying biological activities and toxicological effects of the C₆₀ nanoparticles.

Dispersion stability of nanoparticles of C₆₀ under a model condition simulating a physiological environment is studied by dynamic light scattering (DLS).⁵⁾ Special attention was paid on the possible stabilizing effects of human serum albumin (HSA), which is the major component of blood plasma and serves as a carrier of hydrophobic compounds such as fatty acids, bilirubin and hormones. While the C₆₀ nanoparticles flocculate and precipitate out rapidly in a phosphate buffered saline, we found that addition of HSA at the concentrations higher than 1 mg/mL suppresses the flocculation completely. The DLS results suggest that the HSA molecules adsorb onto the surfaces of the C₆₀ nanoparticles, thereby forming a protective layer and prevent the salt-induced flocculation. The results indicate that the interaction between the C₆₀ nanoparticles and proteins affects the dispersion stability significantly, and are of significant implications for the on-going efforts to evaluate the cytotoxicity of the C₆₀ nanoparticles.

1) S. Deguchi, R. G. Alargova, K. Tsujii, *Langmuir*, **2001**, 17, 6013-6017. 2) R. G. Alargova, S. Deguchi, K. Tsujii, *J. Am. Chem. Soc.*, **2001**, 123, 10460-10467. 3) S. Deguchi, S. Mukai, M. Tsudome, K. Horikoshi, *Adv. Mater.*, **2006**, 18, 729-732. 4) S. Deguchi, S. Mukai, *Chem. Lett.*, **2006**, 35, 396-397. 5) S. Deguchi, T. Yamazaki, S. Mukai, R. Usami, K. Horikoshi, *submitted*.

Corresponding Author: Shigeru Deguchi

E-mail: shigeru.deguchi@jamstec.go.jp

Tel: +81-46-867-9679 / **Fax:** +81-46-867-9715

Deactivation Properties of Singlet Oxygen by Nano-Carbon Materials

Kazuhiro YANAGI,^a Shingo OKUBO,^b Toshiya OKAZAKI,^b Yasumitsu MIYATA,^a
Hiromichi KATAURA^a

^a*Nanotechnology Research Institute and* ^b*Research Center for Advanced Carbon Materials, National Institute of Advanced Industrial Science and Technology (AIST), 1-1-1 Higashi, Tsukuba, Ibaraki 305-8562, Japan*

Abstract: Singlet oxygen [$^1\text{O}_2(^1\Delta_g)$], here denoted as $^1\text{O}_2$, is one of the electrically activated reactive oxygen species known to be implicated in the inactivation of proteins by peroxidation of biological lipids and in damaging DNA. Evaluation of the deactivation properties of $^1\text{O}_2$ in natural pigments is important for understanding their roles in protecting biological systems against this reactive molecule. In this context, clarification of the reactivity of nano-carbon materials with $^1\text{O}_2$ should contribute to their practical biological applications. In this study, the total rate constants (sum of physical quenching and chemical reaction, k_q+k_r) of $^1\text{O}_2$ by various fullerenes (C_{60} , C_{70} , C_{76} , C_{82} , La@C_{82} , Ce@C_{82} , $\text{Ce}_2@\text{C}_{80}$) and carbon nanohorns were determined. It is revealed that the $^1\text{O}_2$ quenching capabilities of C_{82} and endohedral metallofullerenes are comparable to that of β -carotene, a well-known strong $^1\text{O}_2$ quencher (Figure 1). Although the rate constant by SWNHs is smaller than C_{82} and metallofullerenes, it is also clarified that SWNHs have remarkable $^1\text{O}_2$ deactivation capability. The unique $^1\text{O}_2$ quenching by metallofullerenes can be explainable in terms of a combination of energy and charge transfer processes. The origin of the remarkable efficiency of SWNHs for $^1\text{O}_2$ deactivation is ascribed to the unique curvature of the graphitic tube in their horn shaped structure.

References: K. Yanagi et al. *Chem. Phys. Lett.* **431** (2006) 145. K. Yanagi et al. (submitted in 2006).

Corresponding Author:

Kazuhiro Yanagi E-mail:
k-yanagi@aist.go.jp

Tel&Fax: 029-861-3132,
029-861-2786

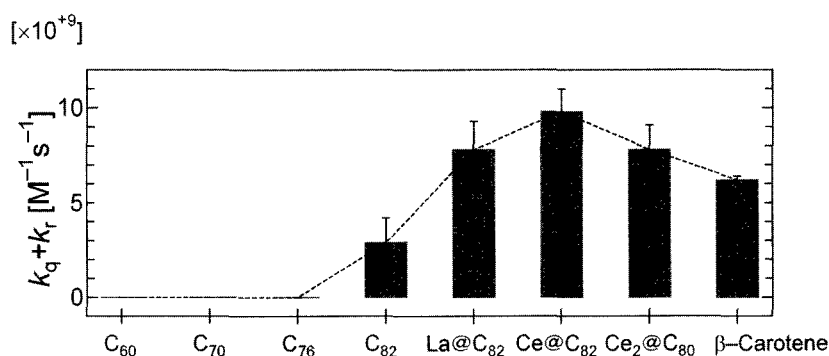


Fig. 1 Deactivation rate constants of $^1\text{O}_2$ by fullerenes

Light-Assisted Oxidation of Single-Wall Carbon Nanohorns for Biological Uses

OMinfang Zhang¹, Masako Yudasaka^{1,2}, Kumiko Ajima¹, Sumio Iijima^{1,2,3}

¹*SORST-JST, c/o NEC, 34 Miyukigaoka, Tsukuba, Ibaraki 305-8501, Japan*

²*NEC, 34 Miyukigaoka, Tsukuba, Ibaraki 305-8501, Japan*

³*Meijo Univ. 1-501 Shiogamaguchi, Tenpaku-ku, Nagoya 468-8502, Japan*

The large surface areas and plentiful inner nanospaces of single-wall carbon nanohorns (SWNHs) suggest several potential applications for material storage extending to various fields including drug delivery systems (DDS). For these applications, the cap removal or hole-opening is a crucial technique. Materials are incorporated inside tubes through holes, and chemical modifications are possible at hole-edges, which is important in the chemical and biological applications. We show in this report that light-assisted oxidation (LAOx) is useful in opening holes with large pore volumes and generating functional groups abundantly at hole-edges.

In LAOx, SWNHs were dispersed in H₂O₂ solution at 70°C, and the light from a Xe Lamp (wavelength: 250-2000 nm) was irradiated for a couple of hours. By this treatment, the holes were opened and the largest adsorption-capacity inside SWNHs was achieved. More important point of LAOx was that the abundant –COOH groups were available at the holes edges. The –COOH groups thus created were demonstrated to react with BSA protein via diimide-activated amidation under ambient conditions. The LAOx-NH-BSA conjugates were highly dispersive in aqueous solutions of phosphate buffer saline, which was confirmed by dynamic light scattering measurements. Owing much on the dispersion improvement, the uptake of LAOx-NH-BSA by the human lung cancer cells was observed with a confocal laser scanning microscope. The flow cytometric analysis was also carried out, which showed that the uptake quantity of LAOx-NH-BSA by the cells was larger than that of BSA alone, suggesting that SWNHs would be useful in delivering biological materials such as protein.

We consider that LAOx would be also effective to other carbon nanotubes, and thus their potential applications might be extended to biology and chemistry easily.

Corresponding authors: M. Zhang, minfang@frl.cl.nec.co.jp, M. Yudasaka, yudasaka@frl.cl.nec.co.jp

Tel: 0081-29-856-1940, Fax: 0081-298-50-1366

Molecular dynamics of phase transition of water inside a carbon nanotube

○Junichiro Shiomi¹, Tatsuto Kimura² and Shigeo Maruyama¹

¹Department of Mechanical Engineering, The University of Tokyo
7-3-1 Hongo, Bunkyo-ku, Tokyo 113-8656, Japan

²Department of Mechanical Engineering, Kanagawa University
3-27-1 Kanagawa-ku, Yokohama-shi, Kanagawa 221-8686, Japan

The first order phase transition of a water cluster confined in a single-walled carbon nanotube (SWNT) to an ice-nanotube [1] has been investigated by using a classical molecular dynamics (MD) method. The MD model takes into account not only the water-water and water carbon interactions, but also carbon-carbon interactions. By cooling or heating the cast SWNT with constant heat flux, the transition between a water cluster and an ice-nanotube was monitored through the structure factor and potential energies (Fig. 1). As the result, the transition temperature and its diameter dependence obtained by the simulations agree surprisingly well with those of previously reported experiments [2] as shown in Fig. 2. The transition temperature of the ice-nanotube was observed to take a maximum value of around room temperature with the number of the ice-ring members $n=5$. Potential energy contribution to the phase change is generally dominated by that of the intrinsic water-water interaction, while that of water-carbon interaction plays a significant role on determining the dependence of transition temperature on the nanotube diameter.

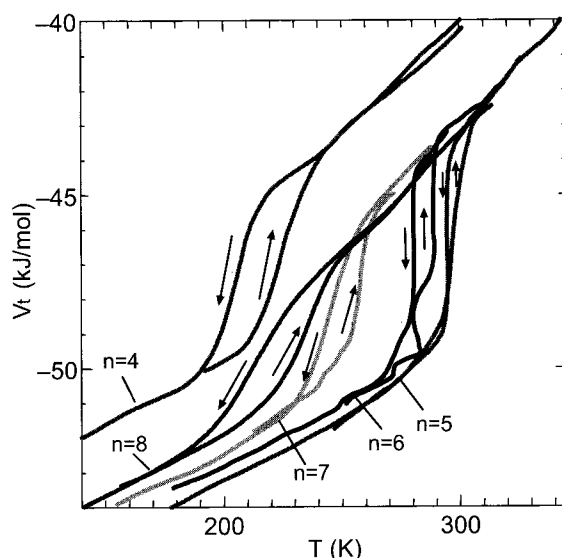


Fig. 1 Temperature dependence of the average potential energy for various numbers of ice-ring members (n). Hysteresis is highlighted by plotting the profiles of cooling and heating processes.

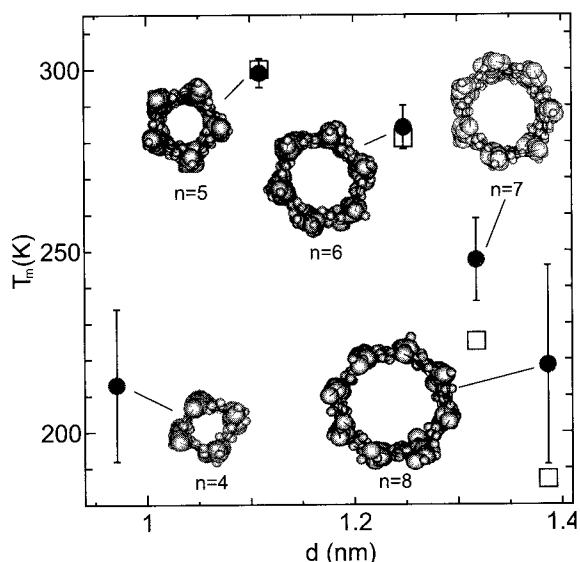


Fig. 2 The transition temperature for various values of n (or nanotube-diameter). The simulations (circles) are compared with the experiments (squares) [2]. The error bars indicate the extent of the hysteresis.

[1] K. Koga *et al.*, *Nature*, **412** (2001) 802.

[2] Y. Maniwa *et al.*, *Chem. Phys. Lett.*, **401**, (2005) 534.

Corresponding author: Shigeo Maruyama

E-mail: maruyama@photon.t.u-tokyo.ac.jp

Competing Growth of Horizontally-Aligned SWNTs between Surface Atomic Arrangement and Surface Steps on Sapphire

○Kenta Imamoto,¹ Hiroki Ago,^{*,1,2} Naoki Ishigami,¹ Ryota Ohdo,¹
Naoyasu Uehara,¹ Masaharu Tsuji^{1,2}

¹Graduate School of Engineering Sciences, Kyushu University, Fukuoka 816-8580, Japan

²Institute for Materials Chemistry and Engineering, Kyushu University and CREST-JST, Fukuoka 816-8580, Japan

Effects of substrate on geometry of single-walled carbon nanotubes (SWNTs), such as orientation, diameter, and chirality, are of great interest in relation with the epitaxial nanotube growth. Recently, we discovered a new method to align SWNTs by using a single-crystalline sapphire substrate (R- and A-faces), which we call “atomic arrangement-programmed (AAP) growth”. Anisotropic interaction between SWNT and surface atoms of sapphire is considered to be the main driving-force for the nanotubes alignment. On the other hand, “step-templated growth” was also reported for C-face sapphire by Ismach et al [2]. Interestingly, in our case, the SWNT growth direction was not related to the step direction [1].

How do the AAP and step-templated growth correlate on sapphire surface? To clarify the influence of the atomic arrangement and surface steps, we have investigated the nanotube growth on various A-face substrates by systematically controlling step height and its direction. We found that there is competition between AAP growth and step-templated growth on the A-face sapphire. When the surface step is single-atom level (0.16 nm), SWNTs were aligned parallel to m-axis, which is dominated by the surface atomic arrangement (Fig. 1ab). When the step height is higher, SWNTs growth direction was determined by the step direction (Fig. 1cd). Our new finding may offer designed networks of SWNTs based on the combination of the AAP and step-templated growth.

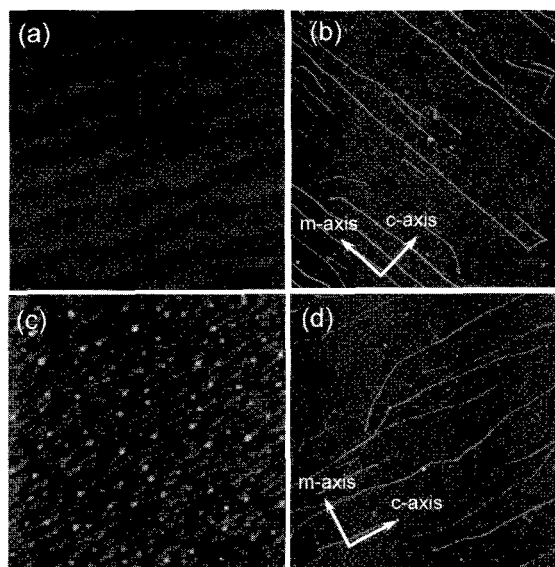


Fig. 1 AFM images of surface structures of the A-face sapphire substrates before and after the nanotube growth. On the single-atomic steps with height of 0.16 nm (a), SWNTs were aligned parallel to m-axis (b). The higher steps with 0.32-0.48 nm height (c) gave SWNT alignment perpendicular to m-axis (d).

Acknowledgements: This work is supported by Grant-in-aid for Scientific Research from MEXT (#18681020), Industrial Technology Research Program in 2005 from NEDO, CREST-JST, and Joint Project of Chemical Synthesis Core Research Institutions.

References: [1] H. Ago *et al.*, *Chem. Phys. Lett.*, **408**, 433 (2005).; H. Ago *et al.*, *Chem. Phys. Lett.*, **421**, 399 (2006). [2] A. Ismach *et al.*, *Ang. Chem. Int. Ed.*, **43**, 6140 (2004).

Corresponding Author: Hiroki Ago (Tel&Fax: +81-92-583-7817, E-mail: ago@cm.kyushu-u.ac.jp)

Optical Enrichment of SWNTs through Preferential Extraction with Pyridine-based Chiral Diporphyrin Nano-tweezers

Xiaobin Peng^{1,2}, Naoki Komatsu¹, Takahide Kimura¹ AND Atsuhiro Osuka³

¹ Department of Chemistry, Shiga University of Medical Science, Seta, Otsu 520-2192, Japan

² International Innovation Organization, Kyoto University, Nishikyo-ku, Kyoto 615- 8520, Japan.

³ Department of Chemistry, Graduate School of Science, Kyoto University, Sakyo-ku, Kyoto 606-8502, Japan

In the last conference, we reported optically active single-walled carbon nanotubes (SWNTs) obtained through the preferential extraction with *m*-phenylene-based chiral diporphyrin nano-tweezers **1** (Fig. 1).[1] Other than the recognition of the helicity of SWNTs, the chiral nano-tweezers also exhibited preference to the SWNTs with relatively larger diameters. In order to obtain higher selectivity in both helicity and chirality, we changed the spacer of the nano-tweezers from *m*-phenylene to pyridine to give the smaller cavity and examined the extraction of SWNTs.

The amount of SWNTs extracted by **2** increased remarkably than that extracted by **1**. After **2** was removed completely from the **2**-SWNTs complex, the SWNTs were dissolved into D₂O/SDBS solution with the aid of tip-sonication and the resulting supernatant was subjected to CD spectroscopic analysis.

As shown in Fig. 2, the CDs of SWNTs extracted with (*R*)- or (*S*)-**2** were opposite and symmetrical, indicating that the extracted SWNTs are optically active and that **2** discriminates the helical structure of SWNTs. The CD intensity of SWNTs extracted with **2** was much larger than that of SWNTs extracted by (*R*)-**1**, when their CDs were measured at the same concentration. This clearly shows that the discriminating ability of **2** to the helical structure is larger than that of **1**. We will also describe the chirality selectivity of **2** different from that of **1**.

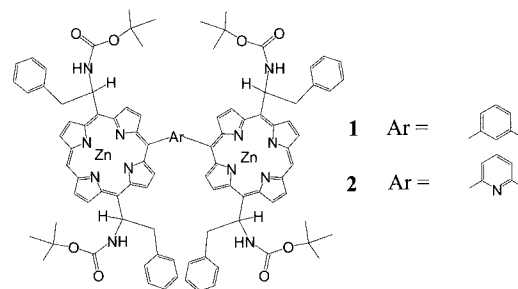


Fig. 1 Diporphyrin nano-tweezers

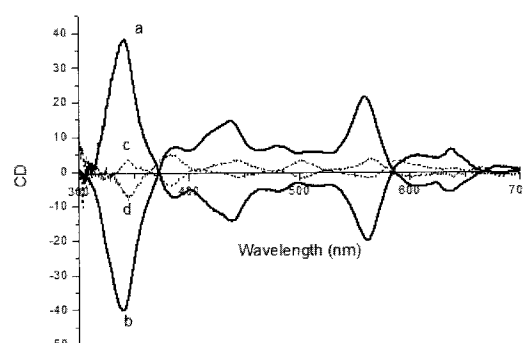


Fig. 2 CD spectra of the extracted SWNTs (After the chiral diporphyrins was washed up.) at same concentration in D₂O, a and b: extracted by (*S*)-**2** and (*R*)-**2**, c and d: extracted by (*S*)-**1** and (*R*)-**1**

[1] N. Komatsu, X. Peng, T. Shimawaki, S. Aonuma, T. Kimura, A. Osuka, The 31st Fullerene-Nanotubes General Symposium.

Corresponding Author: Naoki Komatsu

Tel: +81-77-548-2102, **Fax:** +81-77-548-2405, **E-mail:** nkomatsu@belle.shiga-med.ac.jp

3-3

Radical chemical vapor deposition of vertically aligned CNTs at low temperatures using size-classified Co particles for LSI interconnects

○Daisuke Yokoyama¹, Takayuki Iwasaki¹, Tsuyoshi Yoshida¹, Shintaro Sato²,
Mizuhisa Nihei², Yuji Awano² and Hiroshi Kawarada¹

¹*School of Science and Engineering, Waseda university, Tokyo 169-8555, Japan*

²*MIRAI-Selete, Atsugi 243-0197, Japan*

Carbon nanotube (CNT) is one of promising materials for future LSI interconnects because of its unique properties such as high current density exceeding 10^9 A/cm², high thermal conductivity and ballistic transport. For interconnect application, it is essential to synthesize densely-packed CNT-bundles at a low temperature below 400°C [1].

In this study, we report the synthesis of vertically aligned CNTs from via structure at 390°C by radical chemical vapor deposition [2]. The growth temperature was measured by a pyrometer. The Co catalyst particles were size classified using impactor [3] and the average diameter of particles was 3.8nm. Figure 1(a) shows an SEM image of grown CNTs in a hole with a diameter of 2μm. The diameter of grown CNTs ranges 5 to 10 nm and the density is 1.6×10^{11} cm⁻², which corresponds to one-tenth of the close-packed density. A TEM image shown in Fig. 1(b) indicates that a CNT grown at a low temperature of 390°C maintains a hollow structure. Therefore, this growth method is expected to be useful for future multi-layer interconnects of LSI.

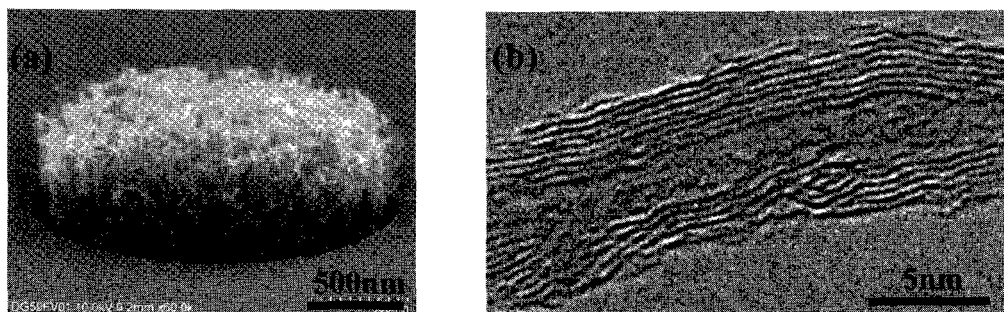


Fig.1 (a) SEM and (b) TEM images of CNTs grown at 390°C from via structure.

Acknowledgements: This work was completed as part of the MIRAI Project supported by NEDO.

[1] M. Nihei, et al., Jpn.J.Appl.Phys. 43 1856 (2004)

[2] T. Iwasaki, et al., New. Diam. Front. C. Tec. 16, 177 (2006)

[3] S. Sato, et al., Proc. IEEE Int. Interconnect Technol. Conf. 2006, 230 (2006)

Corresponding Author: H. Kawarada

E-mail : kawarada@waseda.ac.jp Tel&Fax : +81-3-5286-3391

Electrochemical growth of Pd nanostructures for the synthesis of multiwalled carbon nanotubes

Rakesh K. Joshi ○, Masamishi Yoshimura and Kazuyuki Ueda

*Nano High Tech Research Centre, Toyota Technological Institute Hisakata 2-Chome,
Tempaku-Ku, Nagoya 4688511, Japan*

Abstract:

Palladium nanostructures with variation in shape and size have been synthesized using electrochemical deposition method. The experimentally observed linear variation of peak current in cyclic and linear sweep voltammetry with square root of scan rate suggests that the electrode reaction is controlled by diffusion, which is mass transport of electroactive species to the surface of the electrode across a concentration gradient. Field emission scanning electron microscope (FESEM) was used to visualize the Pd nanostructures on various substrates. EDX shows the presence of Pd in the films whereas XRD studies confirm the formation of metallic Pd nanostructures with f.c.c. structure. As direct application of these electrochemically grown Pd nanostructures they have been used as catalyst for the growth of multiwalled carbon nanotube (MWNT). The nanotubes filled with PdH_{0.649} have been observed using high resolution transmission electron microscopy. Development of Pd into PdH_{0.649} during the growth of MWNT has been studied. Dependence of Pd nanoparticle shape on the architecture of MWNTs is studied. Raman spectroscopy has been used to study the graphite structure of the partial filled MWNTs.

Corresponding author: Rakesh Kumar Joshi

E-mail: rakesh@toyota-ti.ac.jp

Tel: (052)809-1852, Fax: (052)809-1853

Carbon Nanotube Growth by Remote Plasma CVD for Via Interconnects

○N. Sakuma, M. Katagiri, T. Sakai, M. Suzuki,
M. Nihei, S. Sato, T. Hyakushima, Y. Awano

*1, Komukai Thoshiba-cho, Saiwai-ku, Kawasaki, 212-8582, Japan
MIRAI-Selete (Semiconductor Leading Edge Technologies, Inc.)*

Carbon nanotubes (CNTs) are expected as a future LSI via interconnect material, since their excellent properties such as high current density exceeding 10^9 A/cm², high thermal conductivity such as diamond, and ballistic transport along the tube. For LSI via interconnects¹⁾, it is required to grow the CNTs by CVD at temperatures less than 400°C. In this paper, we report the growth temperature lowering down to 430°C by reducing ion densities, based on surface wave type remote plasma CVD. CNT bundles successfully grown in via arrays using the remote CVD are also shown.

Plasma CVD method is to be suitable for low temperature deposition of CNTs. However, ions generated in the plasma are said to cause damages in CNT graphite walls. We have applied dual ion traps to reduce ion flows near the substrate holder. One is a dielectric (quartz) cup trap that has holes at the bottom to control gas flow. Another is a metal mesh gate above the substrate holder, which is grounded to the holder. Applying these traps, ion density measured by Langmuir probe was decreased to about 1/1000. As a result, the growth temperature of CNT was able to be lowered to 430°C. Figure 1 shows SEM image of the CNTs grown in 2.5μm via hole arrays formed in SiO₂ layer at growth temperature of 430°C.

In summary, we have confirmed that reduction of ion density in plasma CVD is effective to lower the growth temperature of CNTs. Also, CNT bundles were able to grow in vias at 430°C by using the ion reduced remote plasma CVD system.

Acknowledgement: This work has been performed as a part of the MIRAI-Project, which is supported by NEDO.

References: 1) M. Nihei et al., SSDM2006, pp. 140.

Corresponding author: Naoshi Sakuma

E-mail: sakuma.naoshi@selete.co.jp

Tel: +81-44-549-2213, **Fax:** +81-44-520-1501

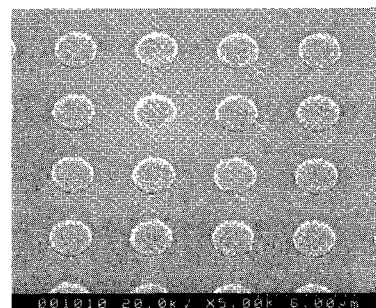


Fig.1. SEM image of CNT bundles in via hole arrays.

Area Selective Deposition of Carbon Nanotubes by Optical Tweezers for Optical Devices Applications

○¹Ken Kashiwagi, ¹Shinji Yamashita, ²Sze Yun Set

¹ *Department of Electronic Engineering, Graduate School of Engineering,
The University of Tokyo, 7-3-1 Hongo, Bunkyo-ku, Tokyo 113-8656, JAPAN.*

² *Alnair Laboratories Corporation, YK Building-2F, 2-4-7 Mishuku, Setagaya-ku, Tokyo
154-0005, JAPAN.*

Abstract: Since carbon nanotubes (CNTs) were adopted as a saturable absorber [1], photonics applications of CNTs have been intensively studied [2,3]. However, handling CNTs method is not well developed. In this paper, we propose and demonstrate area selective deposition of CNTs onto optical fibers ends by optical tweezers.

Optical tweezers is a technique to trap micro-, nano-sized objects due to the gradient force of a light at a focused spot. Figure 1 shows the experimental setup. A light from laser diode at the wavelength of 1560nm was amplified by a high-power erbium-doped fiber amplifier (EDFA). The light incidents into CNTs dispersed dimethylformamide (DMF) solution through a cleaved fiber end which serves as the focused spot of optical tweezers. By using 21.5dBm output power, CNTs were deposited just around the fiber core end. Selective area deposition is confirmed by microscope image and microscopic raman spectra which are shown in Fig. 2.

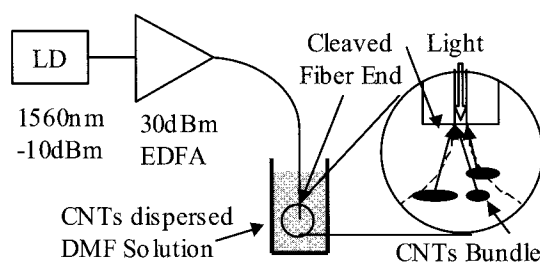


Fig. 1 Experimental setup

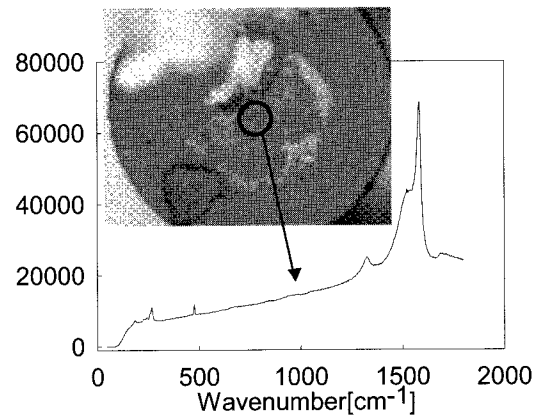


Fig. 2 Microscope image and raman spectra

References: [1] S.Y. Set, et al., *J. Lightw. Technol.*, vol.22, no.1, pp.51-56, 2004.

[2] S. Yamashita, et al., *Opt. Lett.*, vol.29, no.14, 1581-1583, 2004.

[3] Y. Sakakibara, et al., *Jpn. J. Appl. Phys.*, vol.42, L494-496, 2003.

Corresponding Author : Ken Kashiwagi

E-mail : kashiwagi@sagnac.t.u-tokyo.ac.jp **Tel :** 03-5841-6783(Tel) 03-5841-6025(Fax)

Reduction of contact resistance by chemical doping in carbon nanotube FETs

Yosuke Nosho¹, Yutaka Ohno^{1,2}, Shigeru Kishimoto^{1,3}, and Takashi Mizutani^{1,4}

¹Dept. of Quantum Eng., Nagoya Univ., Furo-cho, Chikusa-ku, Nagoya 464-8603, Japan

²PRESTO/JST, 4-1-8 Honcho, Kawaguchi, Saitama 332-0012, Japan

³Venture Business Laboratory, Nagoya Univ., Furo-cho, Chikusa-ku, Nagoya 464-8601, Japan

⁴Institute for Advanced Res., Nagoya Univ., Furo-cho, Chikusa-ku, Nagoya 464-8601, Japan

Carrier doping is one of the most important technologies to improve the performance of nanotube FETs. In this study, we have found that the chemical doping with F₄TCNQ (tetrafluorotetracyano-*p*-quinodimethane) [1] is effective to reduce not only channel resistance (R_{chan}) but also contact resistance (R_C) in *p*-type carbon nanotube FETs.

We employed the transfer line model (TLM) technique to evaluate R_C and R_{chan} separately [2]. For the TLM measurement, we fabricated multi-probe devices with different channel lengths (inset of Fig. 1). After synthesis of SWNTs, gold contacts were formed on an individual SWNT. The device was annealed in vacuum to obtain uniform R_C of each electrode. The chemical doping was carried out by spin coating with isopropyl alcohol solution of F₄TCNQ.

Figure 1 shows the results of TLM measurement before and after the doping. In the TLM plot, the intercept and slope give $2R_C$ and R_{chan} per unit length, respectively. R_C and R_{chan} were reduced by 92 % and 30 %, respectively. In Schottky barrier transistors such as nanotube FETs, the reduction of the R_C has been one of important issues. Present results suggest that the chemical doping is promising for improving the device performances.

We have applied the chemical doping to top-gate nanotube FETs. Drain current and transconductance increased by more than one order of magnitude. The reduction of the R_C is dominant factor for the improvement of the device performances.

References:

- [1] T. Takenobu *et al.*, Adv. Mater. **17**, 2430 (2005).
[2] F. Nihey *et al.*, 6th International Conference on the Science and Application of Nanotubes, P215 (2005).

Corresponding author: Yutaka Ohno

E-mail: yohn@nuee.nagoya-u.ac.jp

Phone & Fax: +81-52-789-5387

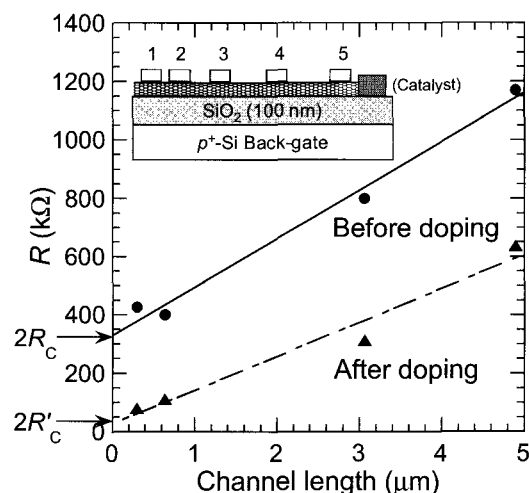


Fig. 1 TLM data before and after the doping. Inset is schematic device structure of fabricated multi-probe device.

Ultra sensitive, room temperature NO₂ detection using single-wall carbon nanotube networks prepared by a simple method

○Annamalai Karthigeyan, Nobutsugu Minami, Konstantin Iakoubovskii

Nanotechnology Research Institute, National Institute of Advanced Industrial Science and Technology (AIST), 1-1-1 Higashi, Tsukuba, Ibaraki 305-8565, Japan

The exceptional properties of single wall carbon nanotubes (SWNT) as gas sensing material [1] have generated growing interest among gas sensor researchers. Sensors with individual SWNT or its ensembles (mats or networks) were reported for NO₂ detection, but they suffer from major drawbacks such as complex fabrication processes involving highly sophisticated techniques, irreproducibility and low yield.

Here we have developed an ultra sensitive NO₂ sensor based on SWNT networks. An aqueous SWNT dispersion with a cellulose derivative used as a dispersant [2] was spin coated on to a quartz substrate, followed by heat treatment, creating a well individualized SWNT network as observed by AFM. Interdigitated gold electrodes with a gap width of 100 μm were deposited on nanotube networks. Conductivity based gas responses of SWNT networks were measured at room temperature for different concentrations of NO₂, a representative toxic gas. Initial base line and recovery (after NO₂ exposure) to the base line was achieved by UV-induced photodesorption. We demonstrate that the sensor is capable of detecting an NO₂ concentration of 50 ppb or less and shows almost no base line drift after multiple NO₂ exposures (Fig.1). From an application viewpoint, we stress that the simple fabrication process, reproducible results and room temperature operation (and thus the lower power consumption as compared with existing metal oxide sensors) bode well for industrial mass production and broad uses.

[1] J. Kong, N. R. Franklin, C. Zhou, M. G. Chapline, S. Peng, K. Cho, H. Dai, *Science* **87**, 622, (2000).

[2] N. Minami, Y. Kim, K. Miyashita, S. Kazaoui, B. Nalini, *Appl. Phys. Lett.* **88**, 093123 (2006).

Corresponding Authors:

Nobutsugu MINAMI
E-mail: n.minami@aist.go.jp
Tel: +81-29-861-9385
Fax: +81-29-861-6309

Annamalai KARTHIGEYAN
E-mail: a-karthigeyan@aist.go.jp
Tel&Fax +81-29-861-4433

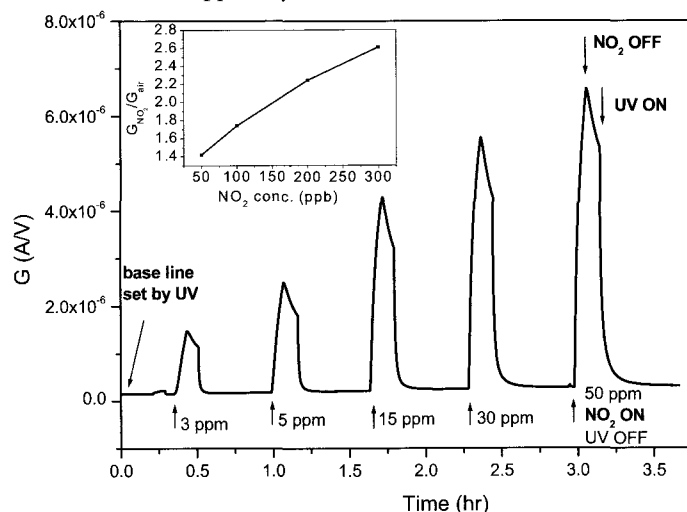


Fig. 1 Conductivity changes by NO₂ exposure (3-50ppm). For photodesorption, UV was turned on 5min after the termination of each gas exposure and then turned off before the next exposure. (Inset) ppb level responses.

Single-walled Carbon Nanotubes from Gold-group Catalysts

○Daisuke Takagi¹, Yoshikazu Homma^{1,3}, Hiroki Hibino²,
Satoru Suzuki^{2,3}, Yoshihiro Kobayashi^{2,3}

¹*Department of Physics, Tokyo University of Science, Shinjuku, Tokyo 162-8601, Japan*

²*NTT Basic Research Laboratories, NTT Corporation, Atsugi, Kanagawa 243-0198, Japan*

³*CREST, JST, Kawaguchi, Saitama332-0012, Japan*

Iron-group elements (Fe, Co, and Ni) and their alloys (Fe-Co, Co-Mo, etc.) have been used as catalysts for single-walled carbon nanotube (SWCNT) synthesis in chemical vapor deposition (CVD). In this report, we show that gold-group elements (Au, Ag, and Cu) and platinum-group elements (Pt and Pd) act as excellent catalysts for SWCNT synthesis when an activation processing is applied [1].

We synthesized SWCNTs by using gold-group elements as catalysts with alcohol CVD. Catalyst particles of gold-group elements must be nano size (1-5 nm in diameter) and contamination-free for SWCNT synthesis. Atmospheric heating at 800-900°C is the key process to activate gold-group elements for SWCNT synthesis. It results in contamination-free metal catalysts. The grown SWCNTs and catalyst particles were characterized by SEM, TEM, AFM, EDX, and Raman spectroscopy.

TEM images and Raman spectra of carbon materials from activated Au catalysts are shown in Figs. 1 and 2, respectively (in Fig. 2, signals of carbon materials from Ag and Cu are also shown). TEM images indicate that materials grown from activated Au were composed of single-walled tubes. In Raman spectra, radial breathing mode (RBM) signals are clearly detected. These results prove that the Au nanoparticles surely catalyze SWCNT synthesis. The activation process was effective for Ag and Cu, and also to iron-group elements, and platinum-group elements, yielding a high density of SWCNTs in all cases.

The fact that SWCNTs can be synthesized efficiently without iron-group elements has a significant meaning. The catalytic function for SWCNT synthesis is not specific to iron-group elements. The SWCNT growth mechanism from the catalyst metal should be reconsidered taking this fact into account. Since these novel catalysts are non-ferromagnetic, and some of them can produce nanowires too, they will open up new applications of SWCNTs.

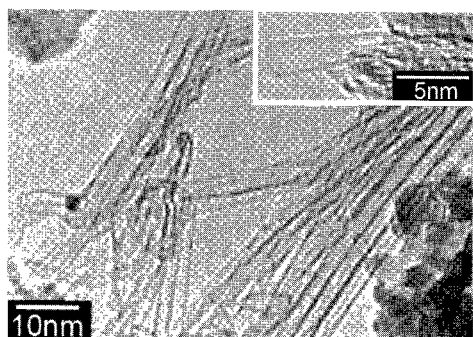


Fig. 1 TEM images of SWCNTs from Au

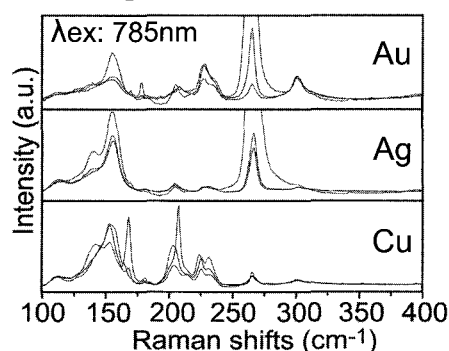


Fig. 2 Raman spectra of SWCNTs from gold-group

[1] D. Takagi, *et al.*, Nano Lett., in press

Corresponding Author: Daisuke Takagi

TEL: +81-3-5228-8244, FAX +81-3-5261-1023, E-mail: daisuke@will.brl.ntt.co.jp

Synthesis of Diameter-Controlled Carbon Nanotubes Using Centrifugally Classified Nanoparticle Catalysts

○Takashi Inoue, Itaru Gunjishima, Atsuto Okamoto

Toyota Central R&D Laboratories, Inc., Nagakute, Aichi, 480-1192, Japan

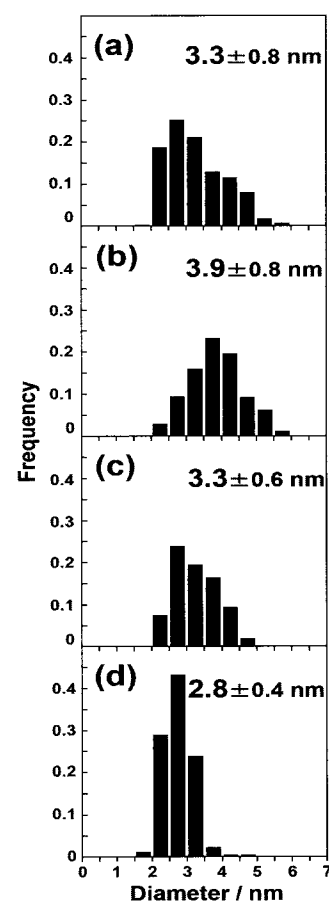
Fe based catalytic nanoparticles covered with ligand molecules were highly size classified via a centrifugal classification technique to improve diameter controllability of carbon nanotubes (CNTs). The centrifugal classification of nanoparticles is facilitated by fractional precipitations through the sequential addition of ethanol to a hexane solution containing the nanoparticles. The diameter of nanoparticles was evaluated by both TEM and XRD. As shown in Figure, the mean diameter of each classified nanoparticle gradually decreased with increasing ratio of ethanol to hexane (EtOH/hexane) and the standard deviation of diameter was successfully reduced. An XRD peak originated from high diameter uniformity of nanoparticles was found at low 2θ . The peaks show great sensitivity to small changes of mean diameter of nanoparticles. This indicates that this analysis has comparable potential to conventional TEM for diameter evaluation of the nanoparticles at small size region. We will show the results of CNT growth using the classified nanoparticles.

Acknowledgment: The authors would like to thank Dr. S. Yamamuro and Prof. K. Sumiyama (Nagoya Institute of Technology) for helpful discussion and support in the preparation of nanoparticles.

Corresponding Author: Takashi Inoue

E-mail: inouet@mosk.tytlabs.co.jp

Tel / Fax: 0561-63-6972 / 6507



Diameter distribution of (a) as-synthesized nanoparticle and centrifugally classified nanoparticles: (b) NP3.9, (c) NP3.3, and (d) NP2.8, which were obtained at EtOH/hexane = 0.65, 0.82, and 1.20, respectively.

ポスター発表
Poster Preview

1P-1 ~ 1P-40

2P-1 ~ 2P-39

3P-1 ~ 3P-38

1P-1

Origin of Linear Relationship between CH₂/NH/O-(n,n)SWCNT Reaction Energies and Sidewall Curvature

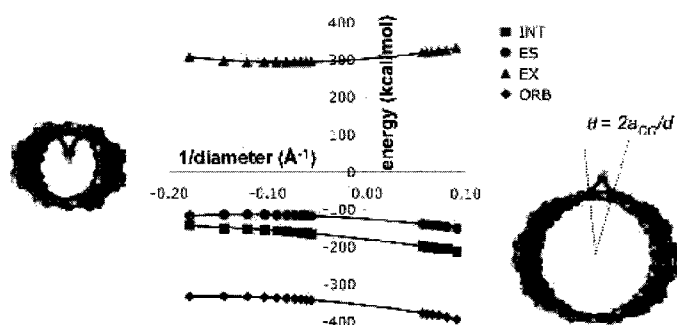
Guishan Zheng,¹ Zhi Wang,¹ *Stephan Irle,² and Keiji Morokuma^{1,3}

¹*Cherry L. Emerson Center for Scientific Computation and Department of Chemistry, Emory University, Atlanta, GA 30322, U.S.A.*

²*Institute for Advanced Research and Department of Chemistry, Nagoya University, Nagoya 464-8602, Japan*

³*Fukui Institute for Fundamental Chemistry, Kyoto University, Kyoto 606-8103, Japan*

The origin of the linear relationship between the reaction energy of the CH₂/NH/O exo and endo additions to armchair (n,n) single-walled carbon nanotubes (SWCNTs) and the inverse tube diameter (1/d) measuring sidewall curvature was elucidated using density functional theory (DFT) and density functional tight binding (DFTB) methods for finite-size SWCNTs models with n=3,4,...,13. A nearly perfect linear relationship between ΔE and 1/d all through exo- (positive curvature) and endohedral (negative curvature) additions is due to cancellation between the quadratic contributions of the SWCNT deformation energy (DEF(SWCNT)) and the interaction energy (INT) between the deformed SWCNT and CH₂/NH/O adducts. Energy decomposition analysis (EDA) shows that the quadratic contributions in electrostatic (ES), exchange (EX) and orbital (ORB) terms mostly cancel each other making INT weakly quadratic and that the linear 1/d-dependence of INT, and therefore of ΔE , is a reflection of the 1/d-dependence of the back-donative orbital interaction of b₁ symmetry from the occupied CH₂/NH/O p _{π} orbital to the vacant C=C π^* LUMO of the SWCNT. We also discuss the origin of the two isomers (open and 3-membered ring) of the exohedral addition product and explain the behavior of their associated minima on the C-C potential energy surfaces with changing d.[1]



[1] G. Zheng, Z. Wang, S. Irle, and K. Morokuma, *J. Am. Chem. Soc.*, in press.

Corresponding Authors: Stephan Irle and Keiji Morokuma

TEL: +81-75-711-7631, FAX: +81-75-781-4757, E-mail: stephan@euch4e.chem.emory.edu & morokuma@emory.edu

1P-2

High-Speed Screening of Carbon Nanotube

Yoshiyuki Miyamoto○

*Fundamental and Environmental Research Laboratories, NEC, 34 Miyukigaoka,
Tsukuba, 305-8501*

And

CREST, Japan Science and Technology Agency, 4-1-8 Honcho, Kawaguchi, Saitama 332-0012.

In this presentation, I will show first-principles simulation of electron-ion dynamics of nano-object under existence of external electric field. The combination of the time-dependent density functional theory for valence electrons and classical Newton dynamics for ions [1] are applied. This type of simulation will be useful for nano-device simulation under consideration of electric field needed for nano-device operation.

First, I show computational method and examination of numerical accuracy in a test case, *i.e.*, disintegration of a hydrogen atom under an extreme electric field.

Then I show time-evolution of electric field which is suddenly applied perpendicular to an axis of a (10,10) nanotube. Simulation showed a significant reduction/enhancement of the field within few femtoseconds inside/outside of the carbon nanotubes. Figure 1 shows how applied electric field (0.3 eV per Å) is modified by (10,10) nanotube.

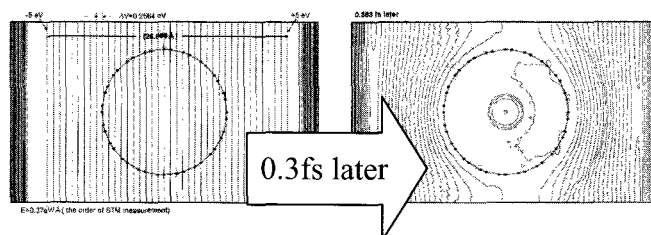


Figure 1. Time evolution of electric field with an intensity of 0.3 eV/Å. (Left) Contour lines of the bias when the field is suddenly applied, and (Right) the contour lines 0.36 fs later. Cross sections of the (10,10) nanotubes are also shown as a circle and black dots.

References:

[1] O. Sugino and Y. Miyamoto, Phys. Rev. **B59**, 2579 (1998); *ibid*, Phys Rev **B66**, 089901(E) (2002).

Corresponding Author: Yoshiyuki Miyamoto

E-mail: y-miyamoto@ce.jp.nec.com

Tel&Fax: +81-29-850-1586 & +81-29-850-2647

Chirality Dependence of G'-band Intensity on Raman Spectra of Single Wall Carbon Nanotubes

* Jin Sung Park¹⁾, Riichiro Saito¹⁾, Kentaro Sato¹⁾, Jie Jiang¹⁾, Ki Kang Kim²⁾,
Young Hee Lee²⁾, Gene Dresselhaus³⁾, Mildred S. Dresselhaus^{4), 5)}

¹⁾Department of Physics, Tohoku University and CREST JST, Sendai 980-8578, Japan

²⁾Department of Physics, Sungkyunkwan University, Suwon, 440-746, Korea

³⁾Francis Bitter Magnet Laboratory, ⁴⁾Department of Electrical Engineering and ⁵⁾Computer Science, Department of Physics, Massachusetts Institute of Technology, Cambridge, MA 02139-4307, USA

We recently observed that the G'-band intensity of the Raman spectra for single wall carbon nanotubes (SWNT) depends on chirality. Especially the G'-band intensity for the metallic (m-) SWNTs is generally stronger than that of the semiconducting (s-) SWNTs. In order to understand this finding, we have calculated two phonon scattering processes for the G'-band intensity by using extended tight-binding model [1]. The G'-band is an overtone Raman spectra of the iTO phonon mode around the K point of 2D graphite Brillouin zone. In order to obtain the Raman intensity, we calculate both the electron-phonon and electron-photon interaction matrix elements in the numerator of the Raman intensity formula. Further we also take account of the Raman resonance width (hereafter γ value [2]) in the denominator. The calculated results show that the G'-band intensity of m-SWNTs is stronger than that of s-SWNTs in large diameter range (> 1.0 nm). As for smaller diameter region, we can not say that the m-SWNT always gives a strong G'-band intensity compared with s-SWNT. When we investigate each contribution to the Raman intensity, the electron-phonon matrix elements for the iTO phonon at the K point and γ values have a strong chirality and diameter dependence especially for the smaller diameter region. A simple explanation for a strong G'-band intensity for the m-SWNT for the larger diameter region is that the electron-phonon matrix elements for the iTO phonon have larger value in the metallic SWNTs rather than the semiconducting SWNTs in the larger diameter range. The calculated results are directly compared with G'-band Raman measurement for SWNTs with metal-semiconductor nanotubes separation [3].

Reference:

- 1) J. Jiang, R. Saito, Ge. G. Samsonidze, S. G. Chou, A. Jorio, G. Dresselhaus, and M. S. Dresselhaus, Phys. Rev. B, 72, 235408 (2005)
- 2) J. S. Park, Y. Oyama, R. Saito, W. Izumida, J. Jiang, K. Sato, C. Fantini, A. Jorio, G. Dresselhaus, and M. S. Dresselhaus, Phys. Rev. B, 74, 165414 (2006)
- 3) K. H. An, J. S. Park, C-. M. Yang, S. Y. Jeong, S. C. Lim, C. Kang, J. H. Son, M. S. Jeong and Y. H. Lee, J. Am. Chem. Soc. 127(14), 5196 (2005)

*Email address: park@flex.phys.tohoku.ac.jp

1P-4

Pressure dependence of photoluminescence spectra in single-walled carbon nanotubes dispersed in D₂O with deoxycholic acid

S. Sakoda¹, M. Ichida^{1, 2}, Y. Miyata^{3, 4}, H. Kataura⁴,
K. Mizuno^{1, 2}, and H. Ando^{1, 2}

¹Graduate school of Nature Science, Konan University

²Quantum Nano-Technology Laboratory, Konan University

³Department of Physics, Tokyo Metropolitan University

⁴Nanotechnology Research Institute, AIST

Optical measurement under hydrostatic pressure is one of powerful tools for studying electronic states and electron-lattice interaction. Recently, photoluminescence (PL) spectra of single-walled carbon nanotubes (SWNTs) under high pressure have been measured by some groups [1,2]. Deacon et al. have reported that the pressure shifts of PL peaks are resulted from a uniaxial strain effect depending on the chirality and environmental effects [2]. However, since the PL in SWNTs is due to the exciton transition, we need to take into account the exciton effect in the PL under high pressure. In this study, we report pressure dependence of PL spectra in SWNTs in micelles.

SWNTs (purified HiPco and laser-ablation tubes) were dispersed in D₂O with deoxycholic acid. IR PL spectra were measured using Ar-ion laser and 0.3 m monochromator equipped with liquid-nitrogen cooled InGaAs array. Hydrostatic pressure was applied using diamond-anvil cell.

Fig. 1 shows PL peak energies as a function of pressure. Applying pressure, all peaks shift to the lower energy side. Although the absolute value of pressure coefficient ($|dE/dP|$) tends to be large for smaller tube diameter, it also depends on the tube chirality. We will discuss the pressure effect connecting with the exciton transition.

[1] R. B. Capaz et al., Phys. Status Solidi B 241, 3352 (2004).

[2] R. S. Deacon et al., Phys. Rev. B 74, 201402 (2006).

Corresponding Author: Masao Ichida

E-mail: ichida@konan-u.ac.jp

TEL: 078-435-2679

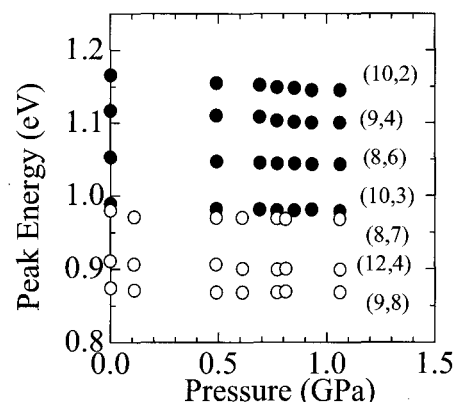


Fig. 1: Peak energies of HiPco (solid circles) and LA tubes (open circles) as a function of pressure.

1P-5

Electronic structures and magnetic moments at edges of graphene ribbon

* Hirofumi Sakashita and Tatsuki Oda

Graduate School of Natural Science and Technology, Kanazawa University

Kanazawa, Ishikawa, 920-1192, Japan

Carbon materials such as carbon nanotube (CNT) attract attention as one of the new materials in the next generation. The surface, defect, and edge of carbon materials are important in electronic conductivity and growth of materials, etc. When a catalyst is adsorbed at an edge in growing of CNTs, we are interested in the change of the electronic structure. The catalyst such as iron, nickel, cobalt, has usually magnetic moment and the magnetism should be taken into account in the electronic structure.

In the investigation of edges for carbon materials, Fujita and his co-workers found that there are localized electronic state('edge stat') in graphene ribbon which have the zigzag edges terminated by single hydrogen atoms[1]. These states make sharp peak at the Fermi level in the density of states, introducing an instability in the materials.

We have investigated the electronic structures at edges on graphene ribbons with and without adsorbing an iron atom by the first-principles calculation in the Kohn-Sham theory. We use a pseudopotential plane wave method and a generalized gradient approximation. We have calculated electronic structures of the systems having zigzag and armchair edges, respectively. Furthermore, we have investigated the magnetic system and non-magnetic one. We have determined the most stable position of the iron atom adsorbed for zigzag and armchair edges, respectively.

We have analyzed electronic structures by the local density of states which is projected on each p_x, p_y, p_z atomic orbital. For a non-magnetic system, the electronic state at the Fermi level has a component of the p_z orbitals located on the carbon atoms for the zigzag edge which is terminated by single hydrogen. Their components originate a sharp peak in the density of states. Without hydrogen terminations, dangling bonds (p_x and p_y orbital) also make sharp peak at the Fermi level. In the magnetic system, the armchair edge has no magnetic moment but the zigzag edge has. The orbital of dangling bonds is pushed up above the Fermi level and become an unoccupied orbital. This means that magnetism stabilizes the electronic states at the Fermi level. The unoccupied electronic states are broadened in the density of states when an iron atom adsorbed at an edge of graphene ribbon. The magnetic moment on carbon atom decreases when an iron atom comes near the zigzag edge.

We will present the atom and electronic structures in the graphene ribbon with iron atoms on the symposium.

Reference

[1] M. Fujita, K. Wakabayashi, K. Nakada, and K. Kusakabe, J. Phys. Soc. Jpn. **65**, 1920 (1996)

Corresponding Author : Hirofumi Sakashita

E-mail : sakasita@cphys.s.kanazawa-u.ac.jp

Tel & Fax +81-76-264-5676 , +81-76-264-5740

Theory of superconductivity in carbon nanotubes and graphene

K. Sasaki¹, J. Jiang², R. Saito¹, S. Onari³ and Y. Tanaka³

¹*Department of Physics, Tohoku University and CREST, JST, Sendai 980-8576, Japan*

²*Department of Physics, North Carolina State University, Raleigh, North Carolina 27695, USA*

³*Department of Applied Physics, Nagoya University, Nagoya 464-8603, Japan*

The energy spectrum of the π -electrons near the Fermi level consists of not only delocalized bulk states but also localized edge states [1]. Theoretically, edge states are zero energy eigenstates at the Fermi energy (flat-band). Experimentally, a direct measurement by scanning tunneling microscopy and spectroscopy of graphite edge has been observed a sharp peak of local density of states near the Fermi energy [2], which can be identified as the edge states. An interesting point is that the peak is located not just at the Fermi energy but below it by about 20 meV. We explain this by next nearest-neighbor (NNN) hopping process that is not considered in the original nearest-neighbor tight-binding Hamiltonian. The NNN gives a finite bandwidth to the edge states [3].

The edge states play a decisive role at the interface between nanotube and an electronic contact because they enhance the local density of states. The contact is also important for emergence of superconductivity observed in multi-walled carbon nanotubes [4]. Thus, it is valuable to examine the effect of the edge states on the superconductivity. Using the Eliashberg equation, we obtain an appreciable superconducting transition temperature for the edge states[5]. As a result, a metallic zigzag nanotube having open boundaries can be regarded as a natural Superconductor/Normal metal/Superconductor junction system, in which superconducting states are developed locally at both ends of the nanotube and a normal metal exists in the middle. In this case, a signal of the edge state superconductivity appears as the Josephson current which is sensitive to the bandwidth, the position of the Fermi energy and the length of a nanotube.

[1] M. Fujita *et al.*, *J. Phys. Soc. Jpn.* **65**, 1920 (1996).

[2] Y. Niimi *et al.*, *Appl. Surf. Sci.* **241**, 43 (2005); Y. Kobayashi *et al.*, *Phys. Rev. B* **71**, 193406 (2005).

[3] K. Sasaki, S. Murakami and R. Saito, *Appl. Phys. Lett.* **88**, 113110 (2006).

[4] I. Takesue *et al.*, *Phys. Rev. Lett.* **96**, 057001 (2006).

[5] K. Sasaki *et al.*, arXiv:cond-mat/0611452

Corresponding Author: Ken-ichi Sasaki, E-mail: sasaken@flex.phys.tohoku.ac.jp

Electronic Structures of Functionalized Single-Walled Carbon Nanotubes

○Yoshikazu Kobayashi¹⁾, Hiroyuki Fueno¹⁾, Kazuyoshi Tanaka^{1), 2)},
Tomokazu Umeyama¹⁾, and Hiroshi Imahori¹⁾

¹⁾*Department of Molecular Engineering, Graduate School of Engineering,
Kyoto University, Kyoto, 615-8510, Japan*

²⁾*CREST, Japan Science and Technology Agency (JST), Japan*

Carbon nanotubes (CNTs) modified with functional groups have recently been studied both experimentally and theoretically. For instance, Umeyama et al. synthesized functionalized CNTs and proposed that every functional group on the sidewall affects the electronic properties of the original CNT [1]. Here we have theoretically investigated the electronic structures on the functionalized single-walled CNT (SWCNT) with the use of CRYSTAL03 program package under the one-dimensional periodic boundary condition along the tube axis **T** by employing the DFT method with the STO-5G basis set. Three types; (a) plain SWCNT, (b) that modified with a five-membered ring, and (c) with a three-membered ring (see Fig. 1) for both SWCNTs (10, 5) and (13, 1) have been considered here as the models for those prepared in ref. 1.

It has been found that change in the electronic structures of SWCNTs depends on the functional groups and that the density of states (DOS) is smeared with generation of the 'impurity' levels. Deformation of the CNT surface has also been predicted.

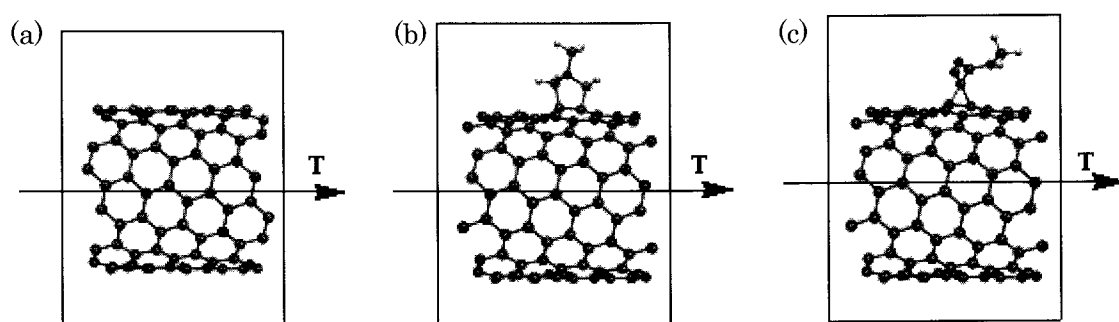


Fig. 1. Unit cells of (a) plain SWCNT, and (b), (c) functionalized SWCNT.

References:

[1] T. Umeyama et al., *31th Fullerene-Nanotube General Symposium*, **31**, 52 (2006)

Corresponding Author: Yoshikazu Kobayashi

E-mail: yoshikazu@t17bunnshikou.mbox.media.kyoto-u.ac.jp

Tel: +81-75-383-2551 & **FAX:** +81-75-383-2556

Coulomb gap increase in SWNT single-electron transistors induced by low-energy irradiation

○Junichi Hashimoto¹, Satoru Suzuki^{2,3}, Toshio Ogino^{1,3}, Yoshihiro Kobayashi^{2,3}

¹*Department of Electrical and Computer Engineering Yokohama National University
Tokiwadai 79-5, Hodogayaku, Yokohama 240-8501, Japan*

²*NTT Basic Research Laboratories, NTT Corporation, Atsugi, Kanagawa 243-0198, Japan*

³*CREST/JST, Japan Science and Technology Corporation*

Our previous studies have shown that low-energy (20 eV – 20 keV) electron and photon irradiation in a vacuum causes damage in single-walled carbon nanotubes (SWNTs), which can be reversibly restored [1]. The irradiation damage was found to significantly affect the electric properties of SWNTs. The irradiation converts the electric properties of metallic SWNTs to semiconducting [2]. Intense irradiation almost extinguishes the electric conductivity of SWNTs [3]. In this work, we focused on irradiation effects on Coulomb blockade characteristics of SWNT single-electron transistors (SETs).

SWNTs were grown on a SiO₂/Si substrate by the ethanol CVD method and FET devices were fabricated by patterning metal electrodes on the SWNTs. A part of the SWNT was irradiated by 20-keV electrons with an electron-beam lithography system. The pressure during the irradiation was less than 5×10^{-5} Pa. SET characteristics of the devices were measured in a vacuum at temperatures ranging from 40 K to room temperature.

Figure 1 shows Coulomb blockade characteristics of a device at 40 K before and after irradiation. This device showed SET characteristics before the irradiation, and the initial Coulomb gap was estimated to be about 0.09 V. After the irradiation at a dose of about 0.25 C/cm², the Coulomb gap significantly increased to 0.54 V, probably because a small dot was

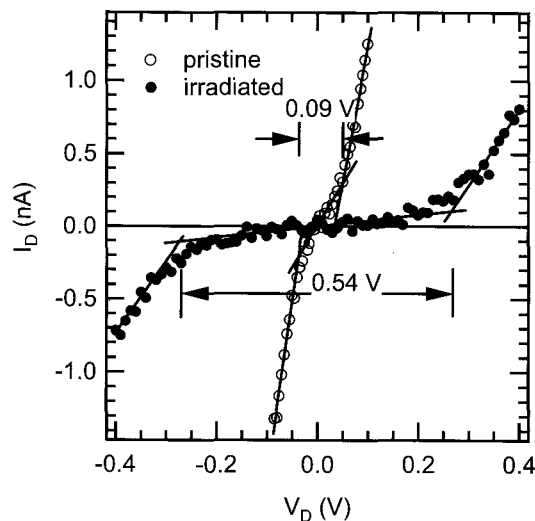


Fig. 1. Coulomb gap characteristics of a SWNT-SET before and after irradiation.

formed in the SWNT channel by the low-energy irradiation-induced defects. Low-energy irradiation would be very effective for fabricating SWNT-SETs operating at high temperatures.

References

- [1] S. Suzuki, et al., Chem. Phys. Lett. 430 (2006) 370., and references therein.
- [2] A. Vijayaraghavan, et al., Nano Lett. 5 (2005) 1575.
- [3] S. Suzuki et al., Jpn. J. Appl. Phys. 44 (2005) L1498.

Corresponding Author: Satoru Suzuki

TEL: +81-46-240-4711, FAX:+81-46-240-4711

E-mail: ssuzuki@will.brl.ntt.co.jp

Conversion of metallic SWNT-FETs to semiconducting at room temperature by low-energy irradiation

○Satoru Suzuki^{1,3}, Junichi Hashimoto², Toshio Ogino^{2,3}, Yoshihiro Kobayashi^{1,3}

¹NTT Basic Research Laboratories, NTT Corporation, Atsugi, Kanagawa 243-0198, Japan

²Department of Electrical and Computer Engineering Yokohama National University
Tokiwadai 79-5, Hodogayaku, Yokohama 240-8501, Japan

³CREST/JST, Japan Science and Technology Corporation

We have reported that low-energy (20 eV – 20 keV) electron and photon irradiation in a vacuum damage single-walled carbon nanotubes (SWNTs) and that the irradiation-induced defects have unique properties [1]. Moreover, the electric properties of metallic (gate-insensitive) SWNTs were found to be converted to semiconducting (highly gate-sensitive), simply by electron irradiation in a scanning electron microscope (SEM) [2]. The nominal bandgap observed in the electric properties can also be widened by increasing the irradiation dose [2]. In the previous study, however, the irradiation-induced semiconducting properties were apparently observed only at low temperature (40 K), not at room temperature. In this study, we succeeded in converting room-temperature (RT) electric properties of a metallic SWNT-FET to semiconducting by local electron irradiation of a part of the SWNT.

SWNTs were grown from patterned Co catalyst on a SiO₂/Si substrate by the ethanol CVD method. SWNT-FETs were fabricated by depositing Pd electrodes on the SWNTs by conventional lithographic and lift-off methods. In our previous studies, whole devices were irradiated by the normal SEM observation. In this study, the irradiation was concentrated on a part of the SWNT using an electron beam lithography system. The electron energy was set to 20 keV. The pressure of the specimen chamber during the irradiation was better than 5×10^{-5} Pa.

Figure 1 shows the RT gate voltage (V_G) characteristics of a SWNT-FET before and after the irradiation. Before the irradiation, the device was gate-insensitive, meaning that the SWNT was metallic. On the other hand, after exposure of up to ~ 0.25 C/cm², the device

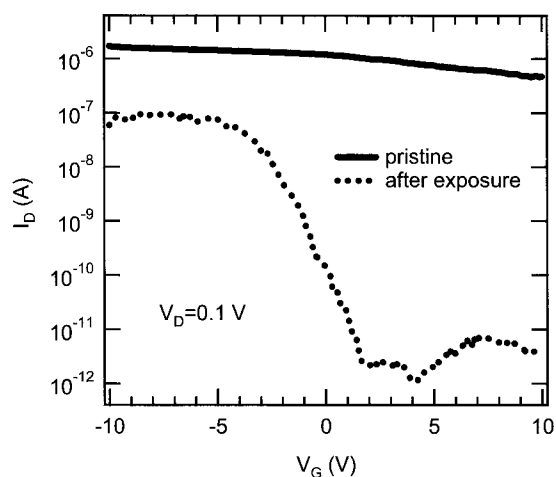


Fig. 1. RT gate characteristics of an initially metallic SWNT device.

clearly showed p-type semiconducting characteristics. The on/off ratio reaches $10^4 \sim 10^5$. The transition behavior can be explained by defect-induced barrier formation and gate-induced band bending.

References

- [1] S. Suzuki, et al., Chem. Phys. Lett. 430 (2006) 370 – 374, and references therein.
[2] A. Vijayaraghavan, et al., Nano Lett. 5 (2005) 1575-1579.

Corresponding Author: Satoru Suzuki

TEL: +81-46-240-4711,

FAX: +81-46-240-4711

E-mail: ssuzuki@will.brl.ntt.co.jp

1P-10

Bond Curvature Dependent Oxidation Process in Single-Wall Carbon Nanotubes

○Yasumitsu Miyata^{1,2}, Takazumi Kawai³, Yoshiyuki Miyamoto³, Kazuhiro Yanagi²,
Yutaka Maniwa^{1,4}, Hiromichi Kataura²

¹*Department of Physics, Tokyo Metropolitan University, 1-1 Minami-Osawa, Hachioji,
Tokyo 192-0397, Japan*

²*Nanotechnology Research Institute (NRI), National Institute of Advanced Industrial
Science and Technology (AIST), 1-1-1 Higashi, Tsukuba 305-8562, Japan*

³*Fundamental and Environmental Research Laboratories, NEC Corporation
34 Miyukigaoka, Tsukuba, 305-8501, JAPAN*

⁴*CREST, Japan Science and Technology Corporation (JST), Japan*

It is well known that thinner single-wall carbon nanotubes (SWCNTs) are less stable due to the curvature effect. Indeed, the thinner SWCNTs burn faster than thicker ones when they are heated in air. One can expect that “bond curvature” could be a good scale of probabilities of oxygen chemisorptions on several C-C sites, and subsequent bond breaking on each site. However, to our knowledge, there is no detailed report about the oxidation process of SWCNTs from the view point of “bond curvature”.

In this work, we have investigated the diameter and chirality dependence of the oxidation rate of SWCNTs. We have measured radial breathing mode Raman spectra of SWCNTs in the oxidation process in air and in hydrogen peroxide. Chirality assignment based on the result of the previous work[1] made it possible to estimate the oxidation rate of each chirality. We found that the oxidation rate depends on the largest bond curvature in three kinds of C-C bonds in SWCNT, in the case of oxidation in the air. On the other hand, for the oxidation in hydrogen peroxide, the oxidation rate depends simply on the average nanotube curvature. The difference in oxidation process could be explained by the difference in the internal energy of oxygen. The bond-curvature dependent oxidation process in air was well reproduced by the theoretical calculation.

[1] H. Telg, et al., Phys. Rev. Lett. 93, 177401 (2004).

Corresponding Author: Hiromichi Kataura

E-mail: h-kataura@aist.go.jp

TEL: 029-861-2551, Fax: 029-861-2786

1P-11

Orientalional control of carbon nanotube growth by plasma-enhanced hot filament chemical vapor deposition

Chien-Chao Chiu○, Masamichi Yoshimura, Kazuyuki Ueda

*Nano High-Tech research center, Toyota Technological Institute, Tempaku, 2-12-1
Hisakata, Nagoya 468-8511, Japan*

Abstract:

Single-walled carbon nanotubes (SWNTs) and carbon nanotubes (CNTs) array [1] were grown by plasma-enhanced hot-filament chemical vapor deposition (PE-HFCVD). The Fe film with the thickness of 0.13-5 nm was pre-coated on 500 nm SiO₂ by arc plasma gun deposition (ULVAC). The size of catalytic nano-particles, which would affect the diameter of CNT, was controlled by the thickness of Fe film. We have newly developed a combined system of PECVD and HFCVD, where CH₄ was decomposed sequentially through microwave plasma and hot W filament. Figure 1 shows scanning electron microscope image of high density SWNTs grown without hot filament. By turning on hot filament, the CNTs array can be grown at a low reactive pressure (~2 torr). Figure 2 shows the SEM image of the CNTs array with the thickness of 50 μm. This fact indicates that after the decomposition by microwave plasma, the hot filament also plays an important role on the pyrolysis of decomposed hydrocarbide for providing carbon atoms on the catalytic metal particles.

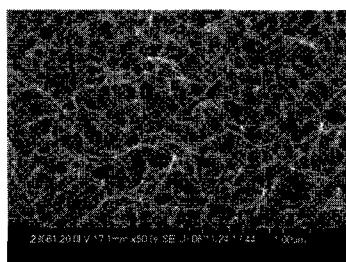


Fig.1 The SEM image of SWNT

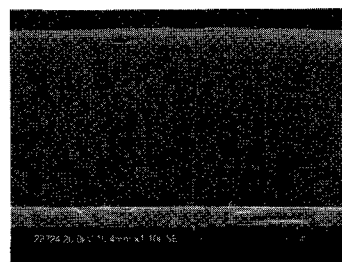


Fig.2 The SEM image of CNTs array

References: 1. Y. Xu, E. Flor, H. Schmidt, R. E. Smalley, R. H Hauge, Appl. Phys. Lett. 89 (2006) 123116.

Corresponding Author: Chien-Chao Chiu

E-mail: kc@toyota-ti.ac.jp

Tel: (052)809-1852, **Fax:** (052)809-1853

Aligned growth of single-walled carbon nanotubes due to interaction with sapphire substrates

○Akira Yamazaki^{1,2}, Daisuke Takagi³, Suzuki Satoru^{1,4}, Jeong Goo-Hwan*^{1,4}, Hideyuki Yoshimura², Yoshikazu Homma^{3,4}, Yoshihiro Kobayashi^{1,4}

¹NTT Basic Research Laboratories, NTT Corporation, Japan

²Department of Physics, Meiji University, Japan

³Department of Physics, Tokyo University of Science, Japan

⁴JST/CREST, Japan Science and Technology Corporation

*Present address: Department of Physics, Göteborg University, Sweden

There have been several reports on aligned growth of single-walled carbon nanotubes (SWNTs) on sapphire substrates [1,2]. But the alignment mechanism of the SWNTs has not been understood in detail. In this paper, we examine the interaction of catalyst nanoparticles and SWNTs with sapphire substrates and discuss the alignment mechanism based on the observed results.

Figure 1 shows an SEM image from a SWNT-growing sapphire substrate with trench structures fabricated by usual photolithography. The aligned SWNTs occasionally bend suddenly and the bending nodes tend to locate especially around the edge boundary of the trench. Moreover, *in-situ* observation of growing SWNTs using SEM showed that the bending nodes created in growing SWNTs do not move as the growth proceeds. This growth behavior is not compatible with the root growth mechanism, in which growing SWNTs slide on the substrate surface and the bending nodes should move. Therefore, a tip-growth mechanism must be responsible for the aligned growth.

Figure 2 compares the diameters of aligned SWNTs grown using ferritin, Co-ferritin and Fe-Dps as catalysts. The diameters were evaluated from AFM images and Raman spectra obtained with excitation laser wavelengths of 532, 633 and 785 nm. The SWNT diameters evaluated from the Raman spectra are significantly larger than these in the AFM results. A strong interaction between SWNTs and sapphire substrate may cause this discrepancy, which would be consistent with tip-growth mechanism.

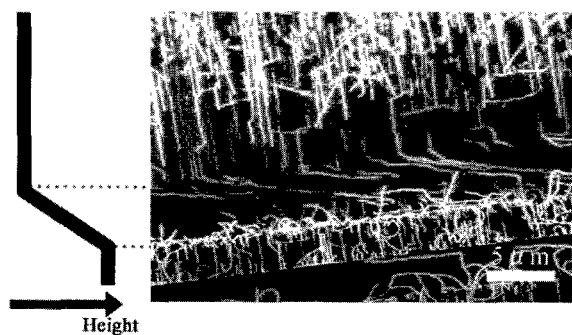


Fig. 1. SEM image of aligned SWNTs around a trench fabricated on sapphire substrate and a cross-sectional view of the height profile.

References: [1] S. Han et al., *JACS* 127 (2005) 5294.

Corresponding Author: Akira Yamazaki

E-mail: a.yama@will.brl.ntt.co.jp Tel. & Fax.: +81-46-240-4070/4718

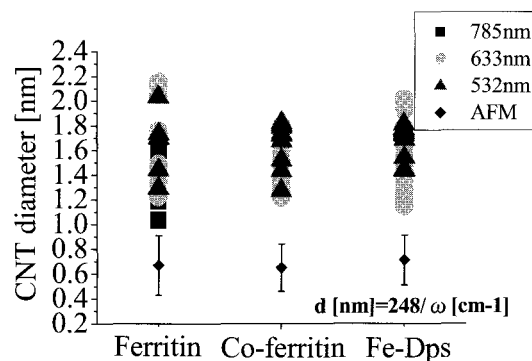


Fig. 2. Diameter distribution of SWNTs grown from various catalyst particles, evaluated from AFM images and Raman spectra

[2] H. Ago et al., *CPL* 408 (2005) 433.

Growth of carbon nanotube on Si substrate using pulse arc plasma as carbon source

○Tomoyuki Shiraiwa¹, Yoshiaki Kato¹, Kenji Tanioku¹, Suzuka Nishimura^{2,3},
Takahiro Maruyama^{1,3} and Shigeya Naritsuka^{1,3}

¹Dept. of Materials Science and Engineering, Meijo Univ., Nagoya 468-8502 Japan

²Dept. of Materials Science and Engineering, Syonan Institute of Technology Univ.,
Fujisawa 251-8511, Japan

³Meijo Univ. 21st CENTURY COE program "Nano Factory", Nagoya 468-8502 Japan

To clarify growth mechanism of carbon nanotube (CNT), low speed growth in a high vacuum is effective, because *in situ* observation technique, such as scanning electron microscopy (SEM) and electron diffraction, can be utilized during growth. In this study, in order to achieve CNT growth in a high vacuum, we carried out CNT growth using pulse arc plasma as carbon source. Pulse arc plasma source can supply atomic-like carbon at very slow rate onto catalyst-coated substrates in an ultra-high vacuum (UHV). We observed a radial breathing mode (RBM) peak in Raman spectra for the samples grown by this technique.

Co (thickness: ~1nm)/SiO₂/Si substrates were used for CNT growth. After the substrates were heated up to the growth temperature, carbon was evaporated using a pulse arc plasma gun in ultrahigh vacuum (UHV) chamber (the base pressure: ~1.0 × 10⁻⁶ Pa). During the growth, one discharge pulse was shot every 1 second, and 6000 pulses (180 nm in thickness) of carbon were totally evaporated. After the growth, the samples were characterized by SEM and microscopic Raman spectroscopy (Ar laser: 514.5nm).

Raman spectra of as-grown sample showed that G/D ratio was 0.9 and full width at half-maximum (FWHM) of G-band peak was rather broad. Although these suggest inclusion of large amount of amorphous carbon in the product, a radial breathing mode (RBM) peak was observed at 119 cm⁻¹, as shown in Fig. 1. After purification of the as-grown sample by heating at 400 °C in air, the RBM peak became distinct. These results indicate that CNTs can be grown by using pulse arc plasma as carbon source for CNT growth. A possibility of CNT growth by pulse arc plasma was demonstrated.

Corresponding Author: Takahiro Maruyama

E-mail: takamaru@ccmfs.meijo-u.ac.jp

Tel: +81-52-838-2386, Fax: +81-52-832-1172

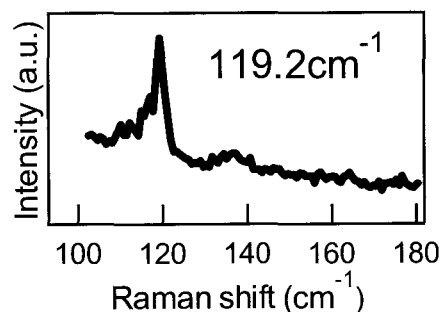


Fig.1 Raman spectrum of low-frequency region of as-grown sample.

Dielectrophoresis separation of single-walled carbon nanotubes

○Shigeo Maruyama¹ Junichiro Shiomi¹, Yuhei Miyauchi¹, Yuan Lin² and Gustav Amberg²

¹*Department of Mechanical Engineering, The University of Tokyo
7-3-1 Hongo, Bunkyo-ku, Tokyo 113-8656, Japan*

²*KTH-Mechanics, Osquarsbacke 18, Stockholm, 100 44 Sweden*

Dielectrophoresis (DEP) has a strong potential to realize the separation of semiconducting and metallic SWNTs [1]. The yield of metallic SWNTs is observed to depend strongly on the frequency of the applied electric field and surfactant concentration [2]. While many studies have been devoted to understand the dielectrophoretic nature of SWNTs, investigations of the integrated systems are essential on controlling and optimizing the system towards actual applications. At the first phase of the project, we have simulated SWNTs in an SDBS solution and quantified the influence of electrothermal (ET) force caused by the temperature dependence of the permittivity and conductivity of the surfactant solution (Fig. 1) [3]. DEP, Brownian and ET force fields were computed by solving the electric field with a finite element method. The results indicate that, within the commonly used parameter range, the ET effect can have a significant influence on the overall transport of semiconducting SWNTs (Fig. 2). The ET force typically attracts the semiconducting SWNTs to the electrodes and hence interferes with the separation of metallic and semiconducting SWNTs. In the current study, we further investigate the phenomenon by experimentally performing the dielectrophoresis separation. The work focuses on probing the spatial distribution of the semiconducting and metallic SWNTs based on Raman spectroscopy.

[1] R. Krupke et al., *Science*, **301** (2003) 347.

[2] R. Krupke et al., *Nano Lett.*, **4** (2004) 1395.

[3] Y. Lin, et al. (to be submitted).

Corresponding author: Shigeo Maruyama

E-mail: maruyama@photon.t.u-tokyo.ac.jp

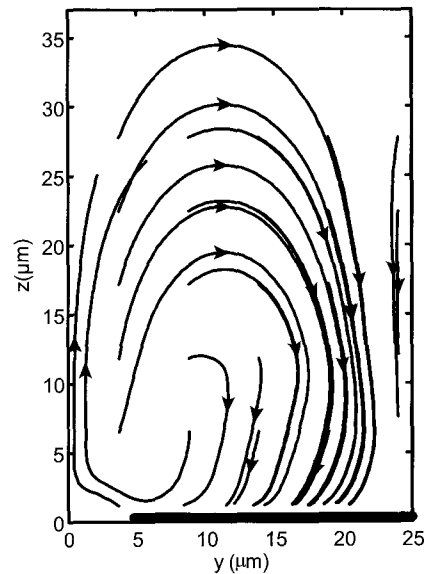


Fig. 1 Streamlines of the ET flow in 0.1 % SDBS solution subjected to an AC electric field ($f=300$ kHz). The right half of the cross-section of the 3D field ($50\mu\text{m} \times 50\mu\text{m} \times 50\mu\text{m}$) is shown. $(y, z)=(0, 0)$ is the center of the gap between the two electrodes (thick line).

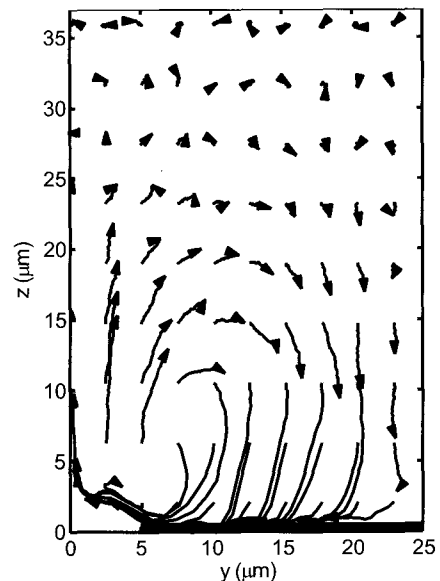


Fig. 2 Traces of semiconducting SWNTs. The simulation conditions are the same as in Fig. 1.

Effect of hydrogen on increasing of the diameters of
single-wall carbon nanotubes

○Masahiro Hayakawa, Shunji Bandow, Sumio Iijima

*Department of Materials Science and Engineering Meijo University,
1-501 Shiogamaguchi, Tenpaku, Nagoya 468-8502, Japan*

Single-wall carbon nanotubes (SWNTs) can be prepared with high yield by the vaporization of a metal catalyzed composite carbon rod using a laser ablation technique at 1200 °C [1]. Although it normally conducts in a pure Ar flux, we examined this method in a mixture gas of Ar and H₂ (3 % of H₂ balance gas) by using a bi-metallic Fe-Ni catalyst (0.6 atomic % with respect to C for each case). According to the TEM observation, it was found that the diameter distribution of SWNTs synthesized in a mixture flux had somewhat larger diameter than the normal ones. In addition, this tendency can be accelerated when the sample is prepared from the composite rod including 0.1 atomic % of boron. Recently, the study of the encapsulation of macromolecules in the nano-space is often carried out for the bio-chemical purpose. For such a purpose, large diameter nanotubes is required as a candidate for the capsule. The current research tendency certainly indicate the direction for enlarging the tube size. We were able to obtain a large diameter nanotubes by method of using the balance gas of Ar including 3% of H₂, but it should be noted that the quantity of amorphous carbon particles increases. Further study is needed.

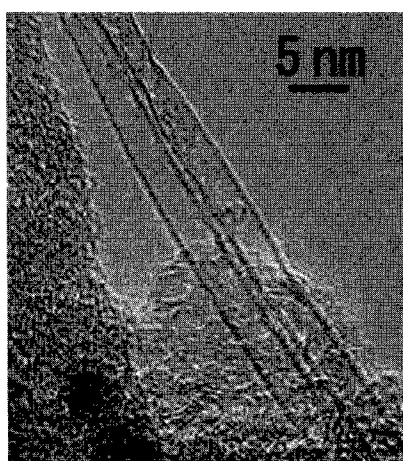


Fig.1. Transmission electron micrograph taken for SWNTs produced from Fe-Ni containing carbon target in the balance gas of Ar including 3 % of H₂.

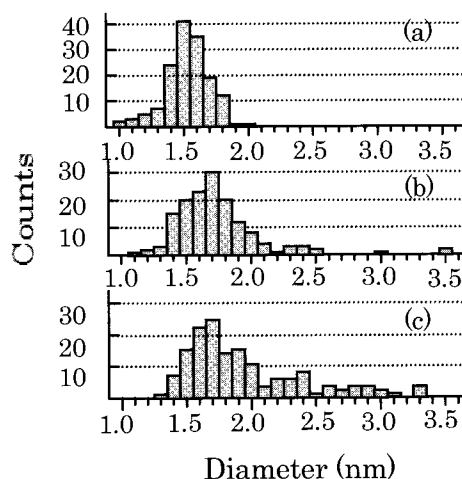


Fig.2. Tube diameter distribution determined from TEM observations. Distributions are (a) for Fe-Ni catalyzed target in Ar, (b) Fe-Ni in Ar + H₂ (3 %) and (c) Fe-Ni-B(0.1atom%) in Ar + H₂ (3 %). Concentrations of Fe and Ni are 0.6 atomic % with respect to C for each case.

[1] A. Thess et al., Science **273**, 483 (1996).

Corresponding : Masahiro Hayakawa, **E-mail:** m0534026@ccmailg.meijo-u.ac.jp, **Fax & voice:** +81-52-834-4001.

Growth and Synthesis of Single-Wall Carbon Nanotubes within Mesoporous Materials by Catalyst-supported Chemical Vapor Deposition

○K. Kobayashi¹, R. Kitaura¹, T. Sugai¹, Y. Kumai³, Y. Goto³, S. Inagaki³ and
H. Shinohara^{1,2}

¹Department of Chemistry, Nagoya University, Nagoya 464-8062, Japan

²Institute for Advanced Research, Nagoya University, and CREST/JST

³Toyota Central R&D Labs., Inc., Nagakute, Aichi, 480-1192, Japan

The catalyst-supported chemical vapor deposition (CCVD) by using nanometer-sized metal particles, which are supported on microporous materials such as zeolites, has been extensively investigated as a promising method for growth of single-wall carbon nanotubes (SWNTs). However, SWNTs produced by CCVD usually have a large diameter distribution because of the mul-size distribution of supported metal particles. To prepare metal particles with an uniform size distribution is essential to produce SWNTs having a narrow diameter distribution. This ultimately leads us to prepare SWNTs with a desired chirality. Mesoporous materials such as MCM41 [1] and FSM16 [2] provide us suitable nano-sized ordered space to prepare regulated nano-sized metal particles [3]. Here, we report the growth of SWNTs by CCVD by using Rh/Pd and Fe/Co particles supported on the mesoporous materials.

A mixture solution of Rh chloride/Pd chloride or Fe acetate/Co acetate was used as a source of catalyst metals which were mixed with a powder of MCM41 and FSM16. The Rh/Pd chlorides, which are incorporated in mesopores, were reduced by a high temperature H₂ reaction or UV irradiation in an H₂O/EtOH atmosphere, and the Fe/Co acetates were pyrolytically decomposed. Figures 1(a) and (b) show a transmission electron microscopy (TEM) image and the selected area electron diffraction (SAED) pattern of Rh/Pd particles supported on MCM41, respectively. The TEM image and SAED pattern clearly indicates the presence of size-ordered Rh/Pd particles (about 3-4 nm) from one-dimensional arrays along the mesopore of MCM41.

Prior to alcohol CCVD, the Rh/Pd particles were treated at 573 K in air to the enhance the catalyst activity [4]. The alcohol CCVD was carried out at 1273 K under an Ar gas flow for 30 min. Obtained SWNTs were characterized by TEM observations and Raman spectroscopy.

We will discuss the correlation between the size distribution of SWNTs so prepared and pore sizes of the mesoporous materials.

[1] C. T. Kresge et al., *Nature*, **959**, 710 (1992). [2] T. Yanagisawa et al., *Bull. Chem. Soc. Jpn.*, **63**, 988 (1990)., S. Inagaki et al., *Chem. Commun.*, 680 (1993) [3] A. Fukuoka et al., *Microporous Mesoporous Mat.*, **48**, 171 (2001). [4] D. Takagi et al., *Nano Lett.*, in press (2006).

Corresponding Author : Hisanori Shinohara

TEL: +81-52-789-2482, FAX:+81-52-789-1169, E-mail: noris@cc.nagoya-u.ac.jp

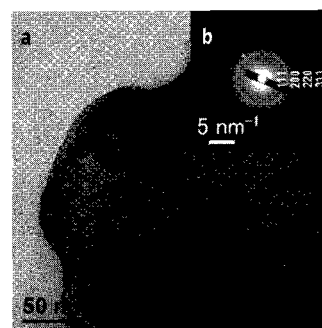


Fig. 1 (a) TEM image and (b) SAED pattern of Rh/Pd particles in MCM41 before CCVD

Control of Location and Orientation of Single-Walled Carbon Nanotubes on Sapphire Surface

○Ryota Ohdo,¹ Hiroki Ago,^{*,1,2} Masashi Shingawa,¹ Naoki Ishigami,¹
Masaharu Tsuji,^{1,2} Tatsuya Ikuta,³ Koji Takahashi³

¹Graduate School of Engineering Sciences, Kyushu University, Fukuoka 816-8580, Japan

²Institute for Materials Chemistry and Engineering, Kyushu University and CREST-JST

³Graduate School of Engineering, Kyushu University

For the realization of nanoelectronics applications of single-walled carbon nanotubes (SWNTs), such as field-effect transistors, nonvolatile memories, and chemical sensors, it is important to establish a means to integrate a large number of SWNTs. In our previous work, we succeeded to grow horizontally-aligned SWNTs on R- and A-faces of sapphire substrates (α -Al₂O₃), probably due to the anisotropic interaction between nanotubes and sapphire surface [1]. Here, we have patterned the iron nanoparticle catalyst based on an electron-beam lithography technique [2] and tried to realize an integrated network of SWNTs on a sapphire substrate, which will enable the control of both the position and direction of SWNTs.

To selectively deposit the iron nanoparticle catalyst on a sapphire substrate, the resist film was patterned by electron-beam lithography with 1 μ m square holes. Then, the substrate was immersed in the colloidal solution of iron nanoparticles with either 4 nm or 12 nm diameter, followed by the removal of the resist film. Several surface treatments were studied to anchor the iron nanoparticle effectively, and the pattern of iron nanoparticles was obtained (Fig. 1a). Nanotubes were grown from the patterned catalyst by chemical vapor deposition (CVD). The iron nanoparticles were found to diffuse at the high reaction temperatures, resulting in the disappearance of the catalyst pattern. By optimizing the reaction condition and carbon feedstock, the patterned growth of SWNTs has been realized as shown in Fig. 1b.

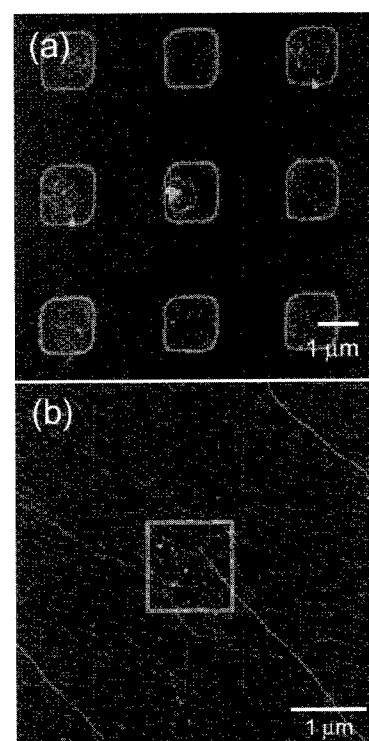


Fig. 1 AFM images of the iron nanoparticles patterned on sapphire surface (a) and the resulting aligned SWNTs (b). The square shows the original catalyst pattern.

Acknowledgements: This work is supported by Industrial Technology Research Program in 2005 from NEDO, Grant-in-aid for Scientific Research from MEXT (#18681020), Joint Project of Chemical Synthesis Core Research Institutions, and CREST-JST.

References: [1] H. Ago, K. Nakamura, K. Ikeda, N. Uehara, N. Ishigami, M. Tsuji, *Chem. Phys. Lett.*, **408**, 433 (2005). [2] H. Ago, J. Qi, K. Tsukagoshi, K. Murata, S. Ohshima, Y. Aoyagi, M. Yumura, *J. Electroanal. Chem.*, **559**, 25 (2003).

Corresponding Author: Hiroki Ago (Tel&Fax: +81-92-583-7817, E-mail: ago@cm.kyushu-u.ac.jp)

Chemistry of Water-Oxidation during CVD Growth of Single- and Double-Walled Carbon Nanotubes over Fe-Mo/MgO Catalyst

○Naoki Yoshihara,¹ Hiroki Ago,*^{1,2} and Masaharu Tsuji^{1,2}

¹Graduate School of Engineering Sciences, Kyushu University, Fukuoka 816-8580, Japan

²Institute for Materials Chemistry and Engineering, Kyushu University, Fukuoka 816-8580 and CREST-JST, Japan

The high-yield growth of single- and double-walled carbon nanotubes (SWNTs, DWNTs) is essential for applications in composites and energy devices. We analyzed the change in the gas composition during the methane chemical vapor deposition (CVD) growth of SWNTs and DWNTs for their high-yield synthesis and found that addition of Mo to Fe/MgO increases the initial methane conversion and prevents from the rapid deactivation [1]. We also confirmed that an appropriate amount of water vapor increases the nanotube yield mainly due to extension of the catalyst lifetime [1], as reported by Hata et al [2]. The chemistry of the water-assisted nanotube growth is interesting and important for the high-yield growth, but it is still unclear. Here, we report on the mechanism of water-oxidation based on the analysis of the effluent gas.

Fig. 1 shows the time dependence of methane conversion and carbon monoxide (CO) concentration determined from the effluent gas. Only a trace amount of carbon dioxide (CO₂) was observed with the concentration of ~50 ppm. It is interesting to note that the emission of CO gas was observed even in the water-free CVD process in a initial few minutes. This initial CO emission was found to be due to the reduction of the iron oxide catalyst.

In the case of the water-assisted CVD, both the initial and equilibrium CO concentrations were higher than those of the water-free CVD condition. The difference of the equilibrium CO concentration is ascribed to the water-oxidation of amorphous carbon, which contributes to the improvement of the nanotube yield. The equilibrium CO concentration suggests that the formation of carbon precipitate (including nanotubes and amorphous carbon) is much faster than the water-oxidation; roughly 1/1000 of the as-formed carbon precipitate was oxidized by water.

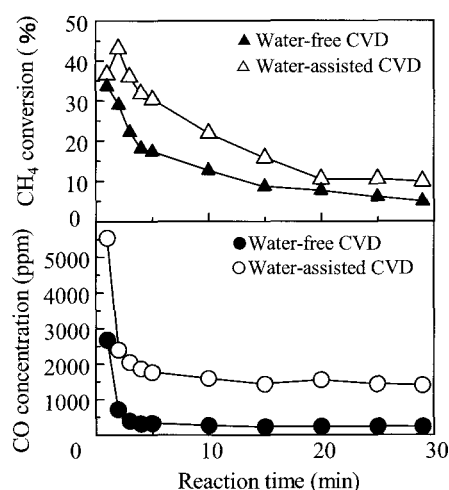


Fig. 1 Time dependence of the methane conversion and carbon monoxide concentration. Lines are guide for eyes.

Acknowledgements: Part of this work is supported by CREST-JST, Joint Project of Chemical Synthesis Core Research Institutions, and Industrial Technology Research Program in 2005 from NEDO.

References: [1] H. Ago, N. Uehara, N. Yoshihara, M. Tsuji, M. Yumura, N. Tomonaga, T. Setoguchi, *Carbon*, **44**, 2912 (2006). [2] K. Hata, D. N. Futaba, K. Mizuno, T. Namai, M. Yumura, S. Iijima, *Science*, **306**, 1362 (2004).

Corresponding Author: Hiroki Ago (Tel&Fax: +81-92-583-7817, E-mail: ago@cm.kyushu-u.ac.jp)

Low-temperature growth of carbon nanotubes by alcohol CCVD (II)

Ken Hiasa¹, Shogo Suzuki¹, Hideki Sato¹, Koichi Hata¹, Kazuo Kajiwara¹, Yahachi Saito²

¹ Graduate School of Eng., Mie University, 1577 Kurima-machiya-cho, Tsu 514-8507, Japan

² Graduate School of Eng., Nagoya University, Furo-cho, Nagoya 464-8603, Japan

We reported that it is possible to grow carbon nanotubes (CNTs) by an alcohol catalytic chemical vapor deposition (ACCVD) method at low temperature (<500 °C), which is favorable for nanoelectronics applications [1]. Here we report results of studies that were carried out to clarify the temperature dependence of CNT growth by ACCVD method.

The CNT growth was carried out by a horizontally fixed quartz tube reactor (2 inches in diameter) using ethanol (99.5% purity) as carbon feedstock. Si (100) wafer (*n*-type, 10x10 mm²) with Co-Al bilayer film deposited by vacuum evaporation was used as a substrate for CNT growth. Co (2 nm) was deposited onto Al film (20 nm) that was previously deposited onto the Si wafer. Growth time was 30 min and ethanol pressure was 40 Torr.

Figure 1 is an Arrhenius plot, where the thickness of CNT layers is shown as a function of the reciprocal of growth temperature. In this graph, some regions that show different temperature dependence can be confirmed. The temperature dependence of the CNT layer thickness is weak at the range less than 550 °C. The thickness steeply increases at the range between 550 and 700 °C and then decreases at >700 °C. The CNTs grown in this study were multi-walled containing many double-walled CNTs. Activation energy estimated from the Arrhenius plot at 550-700 °C was 219 kJ/mol, which is close to standard heat of formation for ethanol (235.3 kJ/mol). This indicates that the CNT growth at this range is dominated by thermal decomposition of ethanol. On the other hand, the activation energy at <550 °C is 41 kJ/mol, which is not enough for thermal decomposition. At the low growth temperature range, activation of catalyst film is more important for the CNT growth.

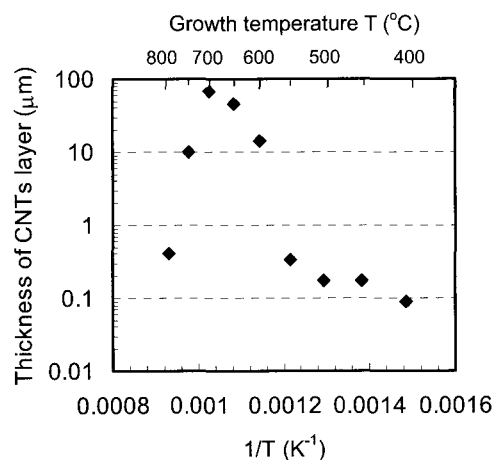


Fig. 1 Growth temperature dependence of CNT layer thickness.

[1] K. Hiasa, T. Nakagita, H. Sato, K. Hata, Y. Saito, *Abst. The 30th Commemorative Fullerene-Nanotubes General Symposium*, 1P-25.

Corresponding author: Hideki Sato

E-mail : sato@elec.mie-u.ac.jp Tel&Fax : +81-59-231-9404

Half-centimeter long vertically aligned carbon nanotubes using optimized radical CVD conditions and study of CO₂ effects

○ Takayuki Iwasaki¹, Tasuku Maki¹, Tsuyoshi Yoshida¹, Takumi Aikawa¹, Tatsuhiro Nozue², Daiyu Kondo², Akio Kawabata², Shintaro Sato², Mizuhisa Nihei², Yuji Awano², and Hiroshi Kawarada¹

¹*School of Science and Engineering, Waseda university, Tokyo 169-8555, Japan*

²*MIRAI-Selete, Atsugi 243-0197, Japan*

Millimeter-long vertically aligned single-walled carbon nanotubes (SWNTs) have been synthesized using our unique radical CVD apparatus at a low temperature of 600°C [1,2]. The growth rate, however, was not high because catalyst activity depends strongly on the growth temperature. To achieve the growth of long CNTs with higher growth rates, investigation of optimized conditions is required.

In this study, we optimized radical CVD conditions such as growth temperature, CH₄/H₂ ratio and total gas flow rate for CNT growth with higher growth rates. Figure 1 shows the growth rate of CNTs variation with growth temperature. Highest growth rate was obtained at 680-690°C, and Fig. 2 indicates 5.3mm-long vertically aligned CNTs grown at 690°C. Moreover, CO₂ effects on the ultra long CNT growth were investigated. At 650°C, CO₂ promoted the CNT growth. In contrast, CNT growth was saturated within a few hours at a higher temperature of 690°C, which was probably caused by the difference in the reactivity of oxygen derived from CO₂ with the catalyst particles.

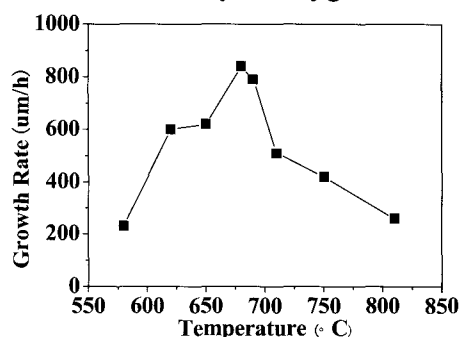


Fig.1 Growth rate of CNTs variation with growth temperature

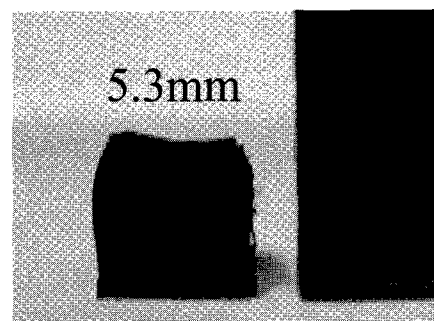


Fig.2 5 mm-long vertically aligned CNTs

Acknowledgements: This work was completed as part of the MIRAI Project supported by NEDO.

[1] T. Iwasaki, New. Diam. Front. C. Tec. 16, 177(2006)

[2] T. Iwasaki, J. Phys. Chem. B 109, 19556 (2005)

Corresponding Author : T. Iwasaki

E-mail : iwasaki@kaw.comm.waseda.ac.jp

Tel&Fax : +81-3-5286-3391

1P-21

Toxicological study of single-wall carbon nanohorns

○ Jin Miyawaki,¹ Masako Yudasaka,^{1,2} Takeshi Azami,² Yoshimi Kubo,²
and Sumio Iijima^{1,2,3}

¹*JST/SORST, c/o NEC, 34 Miyukigaoka, Tsukuba, Ibaraki 305-8501, Japan*

²*NEC, 34 Miyukigaoka, Tsukuba, Ibaraki 305-8501, Japan*

³*Meijo Univ., 1-501 Shiogamaguchi, Tenpaku, Nagoya 468-8502, Japan*

To realize drug delivery system using single-wall carbon nanohorns (SWNHs) [1], and to assess health risk for SWNH users, toxicological information has to be fully elucidated. Here, we report preliminary but extensive results of toxicity tests of SWNHs.

Outermost organs, such as skin and eyes, could be most frequently exposed to SWNHs; skin sensitization and skin/eye irritation tests for as-grown SWNHs proved nonstimulative. Next, there is a risk that we breathe in fluffy SWNHs; an intratracheal instillation test for rats revealed that while anthracosis was observed, as-grown SWNHs rarely damaged lung tissues for 90-days test period. We also assessed biodistribution and toxicity after an intravenous injection of hole-opened SWNHs (oxNHs) at a dose of 6 mg/kg. Body weight gain of mice after the administration did not show statistical difference from the control, suggesting that oxNHs at this dosage are likely to be nontoxic for mice. Histopathological examinations showed that pigmentations due to oxNHs observed in liver and spleen did not induce any inflammations, cell degenerations, or necroses. Furthermore, an alleviation of pigmentation grade in pulmonary blood vessels accompanied with vessel-wall thickening was observed 6-month after the administration, suggesting a possibility of long-term clearance of oxNHs from lung. Finally, negative mutagenicity suggests that as-grown SWNHs are not carcinogenic.

Although comprehensive toxicological assessments, including chronic and genetic toxicities, are still required, these *in vivo* results and *in vitro* examinations [2,3] strongly suggest non/low-toxicity of SWNHs.

References: [1] S. Iijima et al., *Chem. Phys. Lett.*, **309**, 165 (1999). [2] T. Murakami et al., *Mol. Pharm.*, **1**, 399 (2004). [3] K. Ajima et al., *Mol Pharm.*, **2**, 475 (2005).

Corresponding Authors: Jin Miyawaki and Masako Yudasaka, E-mail: jin_m@frl.cl.nec.co.jp (Miyawaki), yudasaka@frl.cl.nec.co.jp (Yudasaka), TEL: +81-29-856-1940, FAX: +81-29-850-1366

Closing Rates of Holes in Single-Wall Carbon Nanohorns at Various Heating Temperature

○ Jing Fan¹, Masako Yudasaka^{1,2}, Jin Miyawaki¹, Ryota Yuge²,
Takazumi Kawai², Sumio Iijima^{1,2,3}

1) SORST/JST, NEC Corporation, 34 Miyukigaoka, Tsukuba 305-8501, Japan

2) NEC Corporation, 34 Miyukigaoka, Tsukuba 305-8501, Japan

3) Meijo University, 1-501 Shiogamaguchi, Tenpaku-ku, Nagoya 468-8502, Japan

A previous report showed that holes at tips of single-wall carbon nanohorns (SWNHs) can be closed by heat treatments of 1200°C in Ar, which were evidenced by the N₂ adsorption measurement [1]. In this study, we investigated the hole-closing temperatures (from 600~1200 °C) and hole closing rates.

To open the holes, SWNHs were oxidized in flowing air by slow combustion method [2] with target temperatures, (Tox) of 400, 450, 500, or 550 °C (NHox). For closing the holes, NHox was heat-treated (HT) at 600, 800, 1000, or 1200 °C in Ar for 3 h. The hole closing was examined by measuring xylene-adsorption quantity (Q) using thermogravimetric equipment. The Q value decreased with the HT temperature (Fig 1), which exhibited the numbers of closed holes increased with the HT temperature. When Tox was higher than 500 °C, the hole closing mainly occurred at HT 1200 °C. To analyze the hole closing rate, we heat-treated NHox (Tox of 450 °C) at HT 1000 or 1200 °C for different periods. As a result, a quick and a slow closing process were found. (Fig 2). Tentatively, we assume that these two different-rate processes reflect the holes with different diameters.

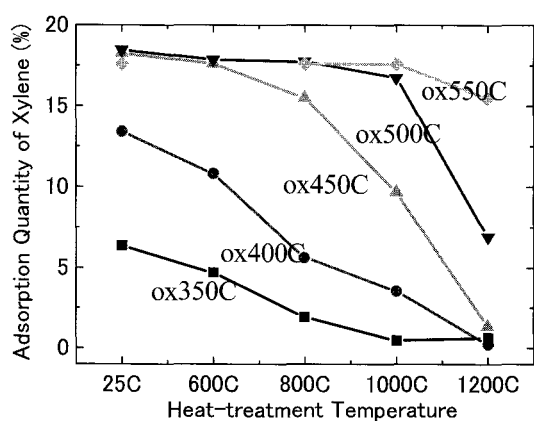


Fig. 1 Adsorption quantities of xylene by NHox after HT at various temperatures.

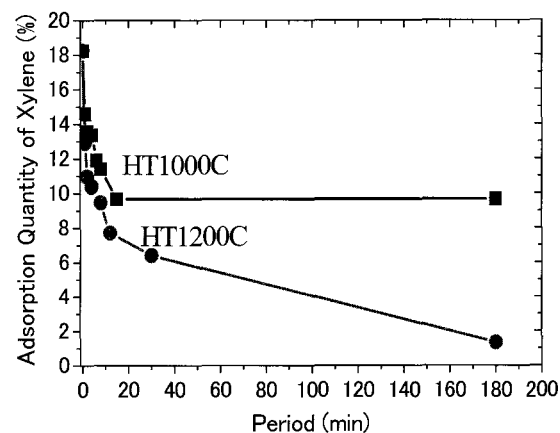


Fig. 2. Adsorption quantities of xylene by NHox450 after HT at 1000 and 1200°C for various periods.

References:

[1] J. Miyawaki et al., submitted.

[2] J. Fan et al., *J. Phys. Chem. B* **110** (2006) 1587-91.

Corresponding Author: Yudasaka Masako

E-mail: yudasaka@frl.cl.nec.co.jp Tel:+0081-29-850-1190; Fax: +0081-29-850-1366.

Streptavidin-modified Single Wall Carbon Nanohorns

O Xu Jianxun,¹ Yudasaka Masako,¹ Iijima Sumio^{1,2}¹*JST/SORST, c/o NEC, 34 Miyukigaoka, Tsukuba, Ibaraki 305-8501, Japan*²*Meijo University, 1-501 Shiogamaguchi, Tenpaku-ku, Nagoya 468-8502, Japan*

Single Wall Carbon Nanohorns (SWNHs) are a new kind of nano-carbon material, which are of horn-like structure with 2~5 nm diameter and usually exist in an aggregate form with monodispersive diameter of around 80~100 nm.¹ SWNHs aggregate emerges as an attractive candidate for drug delivery system (DDS). Until now, there have been plenty of reports on this field, including controlled hole-open on SWNHs, drug incorporation and release, surface chemical modification and bio-properties *in vitro/vivo*.² On the way to realize the potential DDS application of SWNHs aggregate, chemical modification on the surface is the pivot point, to make the aggregate water-soluble, bio-compatible and disease- area specific.

In this study, we used a protein streptavidin to chemically modify SWNHs. The obtained protein-wrapped SWNHs were well-dispersed and stable in water. Recently, light-assisted oxidization of SWNHs using hydrogen peroxide was developed in our group.³ By this method, a lot of carboxylic groups can be introduced on the edges of the nano-sized holes on SWNHs, providing active sites for further reactions. In the present work, so-oxidized SWNHs suspended in phosphate buffer solution (PBS: PH 7.4, 1/15 M; SWNHs: 0.3 mg/ml) were used to react with amine-PEO₃-Biotin (0.01 mg/ml) overnight under stir. Carbodiimide hydrochloride (EDC, 5 mg/ml) and *N*-hydroxysufosuccinimide (S-NHS, 2.5 mg/ml) were added as catalysts. The obtained solution was filtered and rinsed with DI water carefully to get rid of unreacted amine-PEO₃-Biotin, EDC and S-NHS. The black powders on the filter membrane were re-suspended in PBS to react with the tagged-protein streptavidin-Alexa 488 (0.1 mg/ml) for one hour under stir in darkness. Biotin (2.5 µg/ml) was mixed with the above solution for one more hour to specifically bind with streptavidin. After filtering the solution, unreacted proteins and biotins were washed away thoroughly. Protein-modified SWNHs were checked by transmission electron microscopy (TEM) and confocal fluorescence microscopy. As shown in the figures, the modified SWNHs are coated by streptavidins and show strong fluorescence.



Fig 1. TEM image of modified SWNHs (Mag = 110 K).



Fig 2. Confocal fluorescence image of modified SWNHs (100 X).

References:

1. M. Zhang, M. Yudasaka, J. Miyawaki, J. Fan, S. Iijima *J. Phys. Chem. B* **2005**, *109*, 22201;
2. K. Ajima, M. Yudasaka, T. Murakami, A. Maigne, K. Shiba, S. Iijima *Mol. Pharm.* **2005**, *2*, 475; therein cited;
3. M Zhang, *et al* unpublished.

Corresponding Author: Yudasaka Masako; **E-mail:** yudasaka@frl.cl.nec.co.jp;

Tel: 029-856-1940; **Fax:** 029-850-1366

Formation Mechanism of Single-Wall Carbon Nanohorn Aggregates Hybridized with Carbon Nanocapsules

Keita Kobayashi, Akira Koshio, Yutaka Takahashi, and ○Fumio Kokai

Graduate School of Engineering, Mie University, 1577 Kurimamachiya-cho, Tsu, Mie 514-8507, Japan

Single-wall carbon nanohorn (SWNH) particles with diameters of 80–100 nm are nearly spherical aggregates of many tubule-like structures made of graphene sheets [1]. One end of the tubule located in the outer region of the particle has a horn-shaped tip. Room-temperature CO₂ laser vaporization of graphite can produce SWNH particles with a high yield of more than 90% in Ar gas. For the formation mechanism, it was suggested that nanohorn structures were grown from the nucleation of cones in liquid-like particles [2]. On the other hand, the formation of tubule-like nanohorn structures and their aggregation in Ar gas was suggested to be important for the formation mechanism [3].

Sano et al. [4] reported the generation of a new hybrid structure, a SWNH particle including a Ni-encapsulated carbon nanocapsule (CNC) in its center, by a submerged arc method. However, the major product was Ni-encapsulated CNCs and the yield of the SWNH particles hybridized with CNCs was very low (less than 1%).

In this work, we report a high-yield (~70%) fabrication of SWNH aggregates hybridized with CNCs by laser vaporization at room temperature. Iron or nickel was mixed with graphite with a content from 5 to 30 at.% and then pressed to form pellets. A continuous wave Nd:YAG laser (500 W peak power) was used for laser vaporization in the presence of Ar gas of 0.1–0.3 MPa. The products obtained were hybridized SWNH particles and other nanocarbon materials. Controlling the Ar gas pressure and the element content in a laser-irradiation graphite target containing Fe or Ni enabled us to fabricate SWNH particles including metal- or carbide-containing CNCs with the high yield of approximately 70%. The sizes of hybridized SWNH particles were larger than those of unhybridized ones. We also found that the sizes of CNCs encapsulated by SWNHs were smaller than those of CNCs alone. We will discuss the growth of hybridized SWNH aggregates from the formation of tubule-like nanohorn structures and their aggregation around molten carbon-metal particles in Ar gas.

[1] S. Iijima et al. *Chem. Phys. Lett.* 309, 165 (1999).

[2] F. Kokai et al. *Appl. Surf. Sci.* 197-198, 650 (2002).

[3] F. Kokai et al. *Carbon* 42, 2515 (2004).

[4] N. Sano et al. *Carbon* 42, 95 (2004).

Corresponding author: Fumio Kokai

E-mail: kokai@chem.mie-u.ac.jp **Tel:** +81-59-231-9422 **Fax:** +81-59-231-9424

Effect of solvents on CDDP incorporation into SWNHs

○ Kumiko Ajima¹, Masako Yudasaka^{1,2} and Sumio Iijima^{1,2,3}

¹JST/SORST, c/o NEC, 34 Miyukigaoka, Tsukuba, Ibaraki 305-8501, Japan

²NEC, 34 Miyukigaoka, Tsukuba, Ibaraki 305-8501, Japan

³Meijo Univ., 1-501 Shiogamaguchi, Tenpaku, Nagoya 468-8502, Japan

We have been studying applications of single-wall carbon nanohorns (SWNHs) to drug delivery systems (DDS). Previous experiments showed incorporation of cisplatin (CDDP), an anticancer drug, into hole-opened SWNHs (NHox) by the precipitation method using *N,N*-dimethylformamide (DMF), and their anticancer effect in vitro [1,2]. However, the anticancer effect of CDDP-DMF@NHox against human lung-cancer cells was comparable with that of CDDP [2]. We show in this report that the anticancer effect was improved greatly by using H₂O instead of DMF in preparing CDDP@NHox.

Thermogravimetric analysis indicated that the CDDP quantity in CDDP@NHox prepared by using H₂O (CDDP-H₂O@NHox) was about 20wt% which was almost equal to that of CDDP-DMF@NHox. However, X-ray diffraction patterns of CDDP-H₂O@NHox revealed that most of the CDDP was incorporated inside NHox (Figure 1), while CDDP-DMF@NHox had non-incorporated CDDP (crystals) outside NHox. In addition, its cytotoxicity evaluated by using WST-1 assay showed that the anticancer effect of CDDP-H₂O@NHox was stronger than that of CDDP (Figure 2). We will discuss about the effects of solvent on CDDP@NHox in the presentation.

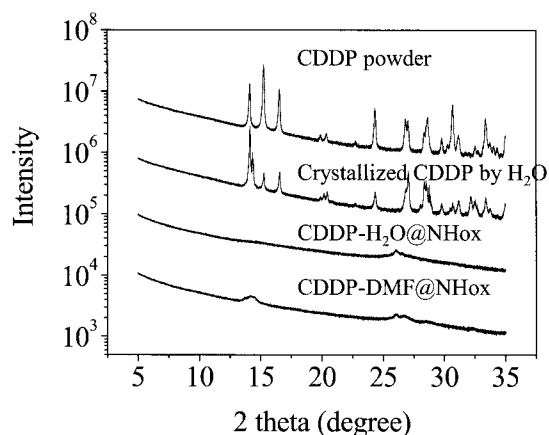


Figure 1. X-ray diffraction patterns of CDDP and CDDP@NHox.

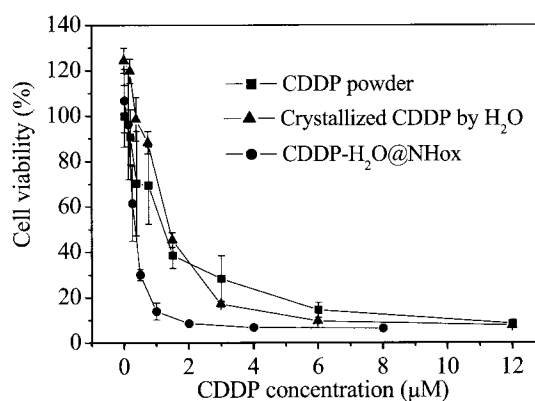


Figure 2. Cell viability of human lung-cancer cells incubated with CDDP or CDDP@NHox.

References :

[1] K. Ajima, et al. *Mol. Pharm.* **2**, 475 (2005). [2] K. Ajima, et al. *J. Phys. Chem. B* **110**, 5773 (2006).

Corresponding author: Kumiko Ajima, Masako Yudasaka

E-mail: kumikoajima@frl.cl.nec.co.jp, yudasaka@frl.cl.nec.co.jp

Tel: +81-(0)29-856-1940, Fax: +81-(0)29-850-1366.

1P-26

Hydrogen production by steam reforming of methane at low temperature using EuPt catalyst supported on single-wall carbon nanohorns

○Ryota Yuge¹, Katsuyuki Murata², Masako Yudasaka^{1,2}, Yoshimi Kubo¹, Tsutomu Yoshitake¹, and Sumio Iijima^{1,2,3}

¹*NEC, 34 Miyukigaoka, Tsukuba 305-8501, Japan*

²*SORST-JST, 34 Miyukigaoka, Tsukuba 305-8501, Japan*

³*Meijo University, 1-501 Shiogamaguchi, Tenpaku-ku, Nagoya, 468-8502, Japan*

Generating hydrogen by reforming methane with steam (RMS) is utilized extensively at industrial technology. However, one of the most disadvantages of RMS is its high operating temperature, about 800°C. Accordingly, the development of new catalysts worked in low temperature is key issue for RMS. We previously reported that EuPt supported single-wall carbon nanohorn (SWNH) generated hydrogen by RMS at 300°C without emitting carbon monoxide, and the hydrogen quantity thus generated was comparable with that produced by using one of the conventional catalysts of Ni/Al₂O₃ at 800°C [1]. We show in this report how the EuPt/SWNH catalyst was so effective in producing hydrogen.

The EuPt/SWNH catalyst was prepared by the previous reported method [1]. Namely, hexa-ammine Pt(IV) and SWNH were mixed in ethanol, followed by filtration and reduction in H₂. The obtained Pt/SWNH was dispersed in an ethanol solution of Eu nitrate, and dried.

The RMS-catalyst effect of EuPt/SWNH was remarkable, but not those of Pt/SWNH and Eu/SWNH [1]. We increased the Eu quantity while keeping the Pt quantity constant (4%), then the generated-hydrogen quantities increased drastically in a low Eu-quantity range, but soon saturated when the Eu quantity became 1% or higher. Arrhenius-type plots of the generated-hydrogen quantity vs 1/T showed that activation energies of EuPt/SWNH were similar to that of Pt/SWNH. These and other results indicated that Pt was the major RMS catalysts, and Eu had a function of increasing the effective methane-quantity through enhancing the methane-adsorption capacity of SWNHs [1, 2]. Details are shown in the presentation.

Acknowledgement:

We thank T. Azami and D. Kasuya for preparing SWNH samples.

Reference:

[1] K. Murata et al. *Carbon* **44**, 799 (2006).

[2] K. Murata et al. *Adv. Mater.* **16**, 1520 (2004).

Corresponding Author: M. Yudasaka and R. Yuge.

TEL: +81-29-850-1566, FAX: +81-29-856-6137 E-mail: yudasaka@frl.cl.nec.co.jp, ryuge@frl.cl.nec.co.jp

**Drug-loaded single-walled carbon nanohorns
dispersed with a polyethylene glycol-peptide conjugate**

○Sachiko Matsumura^{1,2}, Masako Yudasaka^{1,3}, Sumio Iijima^{1,3,4}, Kiyotaka Shiba^{2,5}

¹*SORST-JST, c/o NEC, Miyukigaoka, Tsukuba, Ibaraki 305-8501, Japan*

²*Cancer Institute, Japanese Foundation for Cancer Research, Ariake, Koto-ku, Tokyo
135-8550, Japan*

³*NEC, Miyukigaoka, Tsukuba, Ibaraki 305-8501, Japan*

⁴*Meijo University, Shiogamaguchi, Tenpaku-ku, Nagoya 468-8502, Japan*

⁵*CREST-JST, c/o Cancer Institute, Japanese Foundation for Cancer Research, Ariake,
Koto-ku, Tokyo 135-8550, Japan*

Single-walled carbon nanohorns (SWNHs) are spherical aggregates with a diameter of about approximately 100 nm. The oxidized SWNHs (oxSWNHs) with that have nano-sized holes on their surfaces have been shown to can be loaded with various molecules both inside and outside, indicating their potentiality for a therefore they are potential materials as a drug delivery carrier. Previous reports studies have showed shown that the oxSWNHs can bewere loaded with some small drugsdexamethasone and cisplatin, and that the loaded drugs are were gradually slowly releasedreleased into aqueous environments.[1,2] On the other hand, the agglomeration of SWNHs in physiological conditions is an unacceptable behavior as a drug carrier. To solve this problem, we decided to use polyethylene glycol (PEG) as a surface modifiermodification is advantageous, because the materials modified with PEG has been widely used to endow various materials with are expected to change into ones with not only better solubility but alsoand lower immunogenicity. Murakami et al. have found that the conjugates of PEG and a hydrophobic drug endowed oxSWNHs with dispersibility in aqueous media.[3] In this case, the hydrophobic drug works as a binder for SWNHs. In this study, we , however, a non-drug binder will contribute to the increased availability of SWNHs as a drug carrier. focused on aA peptide aptamer, NHBP-1, which specifically binds to the surfaces of SWNHs,,[4] can be an alternative binder for PEG modification of SWNHs, as a binder.. In this presentation, weWe will report the preparation of the drug-loaded SWNHs that were dispersible in physiological conditions by using a conjugate of PEG and NHBP-1 (PEG-NHBP).

The PEG-NHBP was synthesized by coupling between the N-terminus of NHBP-1 and PEG *via* an amide linkage. Two types of drug-loaded oxSWNHs were prepared: one contained doxorubicin and another did cisplatin. By mixing with PEG-NHBP, cisplatin-loaded oxSWNHs, in which cisplatin existed inside of the tubes, were well dispersed in physiological conditions. The *in vitro* and *vivo* studies will also be reported.

[1] T. Murakami, J. Fan, M. Yudasaka, S. Iijima, K. Shiba, *Mol. Pharmaceutics*, **1**, 399 (2004).

[2] K. Ajima, M. Yudasaka, T. Murakami, A. Maigné, K. Shiba, S. Iijima, *Mol. Pharmaceutics*, **2**, 475 (2005).

[3] T. Murakami, J. Fan, M. Yudasaka, S. Iijima, K. Shiba, *Mol. Pharmaceutics*, **3**, 407 (2006).

[4] D. Kase, J. L. Kulp, III, M. Yudasaka, J. S. Evans, S. Iijima, K. Shiba, *Langmuir*, **20**, 8939 (2004).

Corresponding Author: Sachiko Matsumura

TEL: +81-3-3520-0111, FAX: +81-3-3570-0461, E-mail: sachiko.matsumura@jfcf.or.jp

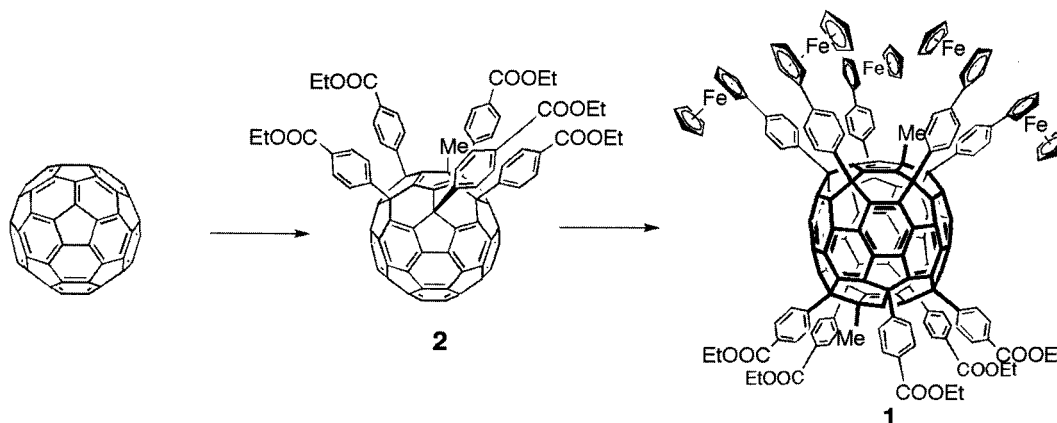
Synthesis and Characterization of Deca(organo)[60]fullerenes Containing Five Ferrocenyl Groups

○Takahiko Ichiki, Yutaka Matsuo, and Eiichi Nakamura

Department of Chemistry, The University of Tokyo and Nakamura Functional Carbon Cluster Project, ERATO, Japan Science and Technology Agency, Hongo, Bunkyo-ku, Tokyo 113-0033, Japan

Regioselective multiple addition reactions to [60]fullerene are of great importance in fullerene chemistry. Recently, we have reported a synthesis of deca(organo)[60]fullerenes.^[1] This procedure provides a powerful method for a multiple functionalization of the [60]fullerene. Since various organocopper reagents can be employed for this addition reaction, versatile functional groups are introduced to the [60]fullerene.

Here we report a synthesis of a pentaferrocenyl derivative, $C_{60}(C_6H_4COOEt)_5Me(C_5H_4FeCp)_5Me$ (**1**). The synthesis was started with conversion of C_{60} into $C_{60}(C_6H_4COOEt)_5Me$ (**2**) by means of regioselective five-fold addition of a functionalized organocopper reagent.^[2] The compound **2** was treated with a ferrocenylphenyl copper reagent in pyridine to obtain **1**, which was characterized by MALDI-TOF-MS, ¹H NMR, UV-vis, and electrochemical analyses.



References:

[1] Matsuo, Y.; Tahara, K.; Sawamura, M.; Nakamura, E. *J. Am. Chem. Soc.* **2004**, *126*, 8725. [2] Zhong, Y.-W.; Matsuo, Y.; Nakamura, E. *Org. Lett.* **2006**, *8*, 1463.

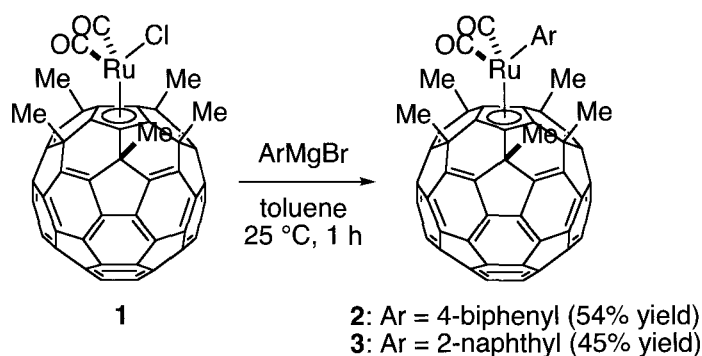
E-mail: nakamura@chem.s.u-tokyo.ac.jp; matsuo@chem.s.u-tokyo.ac.jp

Synthesis and Electrochemistry of Fullerene-Metal-Arene Conjugated Systems

○ Takeshi Nanao, Yutaka Matsuo, and Eiichi Nakamura

Department of Chemistry, The University of Tokyo and Nakamura Functional Carbon Cluster Project, ERATO, Japan Science and Technology Agency, Hongo, Bunkyo-ku, Tokyo 113-0033, Japan

Incorporation of organic π -electron conjugated system with transition metal d-electron system has attracted interest of chemists and physicists. Here we report the reaction of $\text{Ru}(\text{C}_{60}\text{Me}_5)\text{Cl}(\text{CO})_2$ (**1**)^[1] with 4-biphenyl and 2-naphthyl Grignard reagents in toluene yielding ruthenium-aryl complexes, $\text{Ru}(\text{C}_{60}\text{Me}_5)(4\text{-biphenyl})(\text{CO})_2$ (**2**) and $\text{Ru}(\text{C}_{60}\text{Me}_5)(2\text{-naphthyl})(\text{CO})_2$ (**3**). Complexes **2** and **3** were found to undergo reversible three-electron reduction at the fullerene part. We will discuss electronic interaction between fullerene and arenes through the transition metal conjugation system.



	Reduction potential (vs Fc/Fc ⁺)		
	$E_{1/2}^{\text{red1}}$	$E_{1/2}^{\text{red2}}$	$E_{1/2}^{\text{red3}}$
$\text{Ru}(\text{C}_{60}\text{Me}_5)(4\text{-biphenyl})(\text{CO})_2$ (2)	-1.34	-1.95	-2.61
$\text{Ru}(\text{C}_{60}\text{Me}_5)(2\text{-naphthyl})(\text{CO})_2$ (3)	-1.41	-2.02	-2.70
$\text{Ru}(\text{C}_{60}\text{Me}_5)\text{Cl}(\text{CO})_2$ (1) ^a	-1.30 ^b	^c	^c

^a ref 1 ^b Irreversible reduction (E_p value) ^c Not observed

References:

[1] Matsuo, Y.; Nakamura, E. *J. Am. Chem. Soc.* **2004**, *126*, 8725.

E-mail: nakamura@chem.s.u-tokyo.ac.jp; matsuo@chem.s.u-tokyo.ac.jp

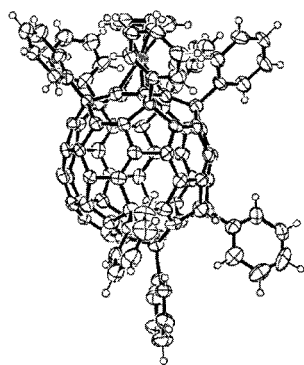
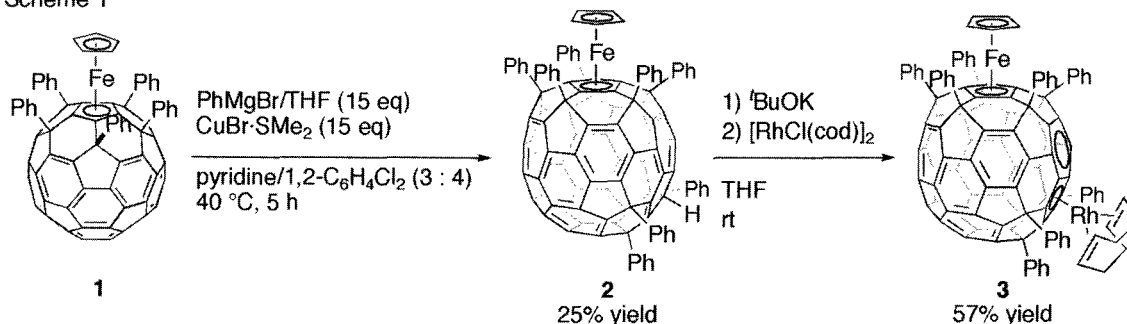
Synthesis of Heterodinuclear Metal Complexes of Octa(organo)[60]fullerenes

○Takahiro Nakae, Yutaka Matsuo, and Eiichi Nakamura

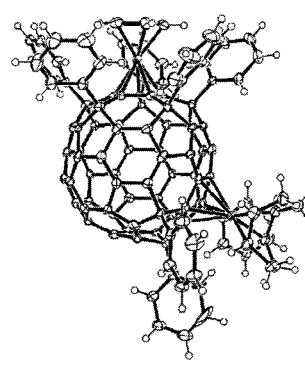
Nakamura Functional Carbon Cluster Project, ERATO, Japan Science and Technology Agency (JST), The University of Tokyo, Hongo, Bunkyo-ku, Tokyo 113-0033, Japan

Octa(organo)[60]fullerenes, which have a hemispherical aromatic system, have potential utilities in materials science, because of their unique π -electron conjugated system and ability to form hybrids with transition metal atoms.^[1] Conjugate addition of phenylcopper reagents to $\text{Fe}(\text{C}_{60}\text{Ph}_5)\text{Cp}$ (**1**) in pyridine afforded an iron-octa(organo)[60]fullerene complex **2** as a major product. Since **2** has an indene moiety, it can act as an η^5 -indenyl-type ligand. For example, a ligand exchange reaction of potassium salt of **2** with $[\text{RhCl}(\text{cod})]_2$ gave a corresponding Rh-Fe heterodinuclear fullerene complex **3** in a moderate yield.

Scheme 1



ORTEP drawing of **2**



ORTEP drawing of **3**

References:

[1] Y. Matsuo, K. Tahara, M. Sawamura, and E. Nakamura *J. Am. Chem. Soc.*, **126**, 8725 (2004).

Corresponding Author: Eiichi Nakamura and Yutaka Matsuo

E-mail: nakamura@chem.s.u-tokyo.ac.jp. TEL/FAX: +81-3-5800-6889

Regioselective Octa- and Deca-additions of Pyridine-modified Organocopper Reagent to [60]Fullerene

○Yutaka Matsuo, Kazukuni Tahara, Kouhei Morita, Keiko Matsuo,
and Eiichi Nakamura

Nakamura Functional Carbon Cluster Project, ERATO, Japan Science and Technology Agency, Hongo, Bunkyo-ku, Tokyo 113-0033, Japan, and Department of Chemistry, The University of Tokyo, Hongo, Bunkyo-ku, Tokyo 113-0033, Japan

A pyridine-modified arylcopper reagent undergoes octa- and deca-addition to [60]fullerene in one-step in good yields on a 20-mg to 1-g scale (eq. 1). The regioselectivity and the number of the aryl groups introduced could be controlled by the amount of pyridine and by the installation of an *ortho*-methyl group of the incoming phenyl group. The deca-adduct could be further converted to the corresponding double-decker metallocene (Figure 1) and other compounds of materials interest.

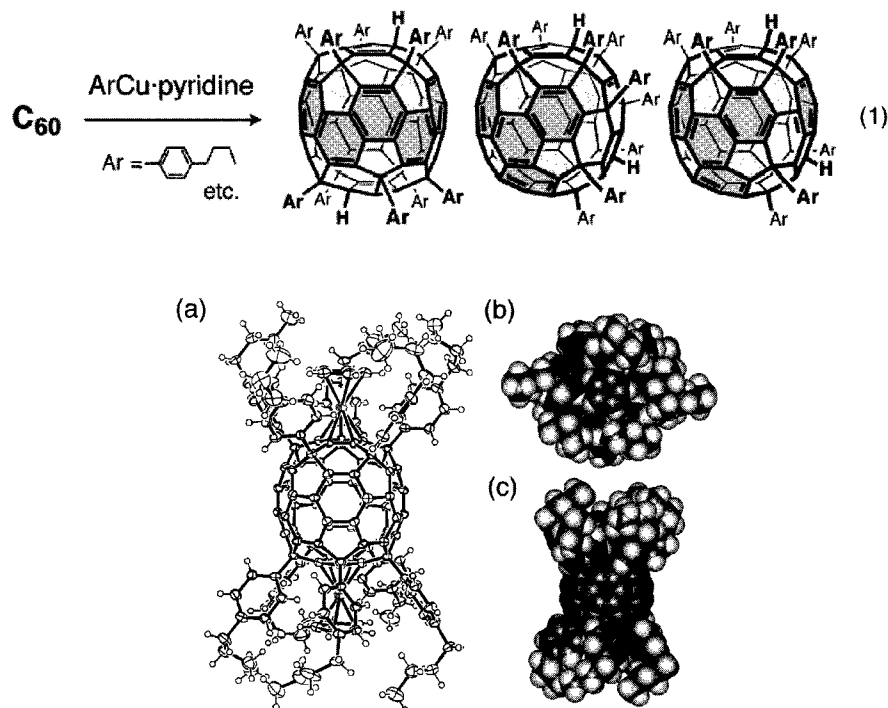


Figure 1. Crystal structure of $\text{Ru}_2[\text{C}_{60}(\text{C}_6\text{H}_4\text{-}^n\text{Bu})_{10}]\text{Cp}_2$. (a) ORTEP drawing. (b) and (c) CPK models.

Corresponding Author: Yutaka Matsuo and Eiichi Nakamura

E-mail: matsuo@chem.s.u-tokyo.ac.jp; TEL/FAX: +81-3-5841-1476

Encapsulation of a He Atom inside an Open Cage C₆₀ and Synthesis of He@C₆₀

○Fumiyuki Tanabe¹, Sadayuki Mori¹, Koichi Komatsu^{1,2},
Michihisa Murata¹, and Yasujiro Murata^{1,3}

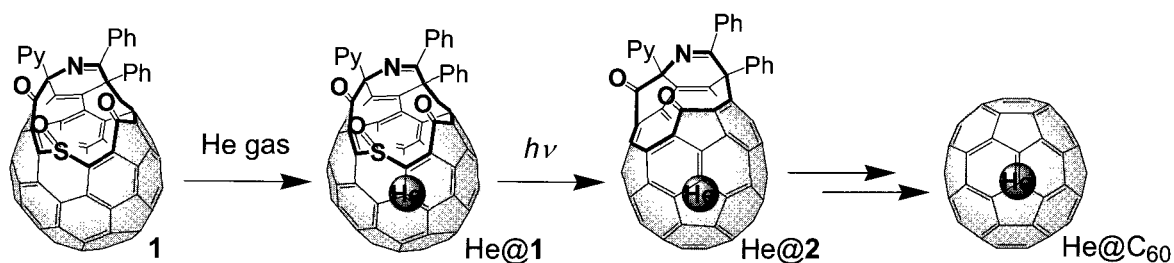
¹*Institute for Chemical Research, Kyoto University, Uji, Kyoto 611-0011, Japan*

²*Fukui University of Technology, Fukui 910-8505, Japan*

³*PRESTO, Japan Science and Technology Agency (JST), Japan*

Endohedral fullerenes are of considerable interest because of their properties and potential use in applications. However, the production of endohedral metallofullerenes has relied only on the physical method that yields only milligram quantities of pure product after laborious isolation procedures. Saunders et al. achieved the insertion of a He atom into C₆₀ by high-pressure/high-temperature treatment (3000 atm, 650 °C), but the incorporation ratio was limited to only 0.04 ~ 2.1%^{1,2}. We report herein the synthesis of He@C₆₀ using alternative method using a series of organic reactions, so-called “molecular surgery”^{3,4}.

An insertion of a He atom into open-cage fullerene derivative **1** having a 13-membered-ring orifice was carried out by heating a solution of **1** in *o*-dichlorobenzene at 150 °C under He atmosphere (850 atm) for 5 hours. Then the orifice size was reduced to a 12-membered ring by photochemical elimination of SO to give a mixture of empty **2** and He@**2**, whose orifice is small enough to prevent the He escape. The APCI mass spectrum of the resulting product revealed that a He atom was encapsulated inside the cage of **2** in ca. 40% yield. The orifice of He@**2** was completely closed by two-step reactions to afford He@C₆₀ as a mixture with empty C₆₀. The ¹³C NMR spectrum and an attempt to isolation of He@C₆₀ will be also reported.



(1) Sanders, M.; Cross, R. J.; Jiménez-Vázquez, H. A.; Shimshi, R.; Khong, A. *Science* **1996**, 271, 1693. (2) Cross, R. J.; Khong, A.; Saunders, M. *J. Org. Chem.* **2003**, 125, 7152. (3) Komatsu, K.; Murata, Y.; Murata, M. *Science* **2005**, 307, 238. (4) Murata, M.; Murata, Y.; Komatsu, K. *J. Am. Chem. Soc.* **2006**, 128, 8024.

Corresponding Author: Yasujiro Murata

TEL: +81-774-38-3173, FAX: +81-774-38-3178, E-mail: yasujiro@scl.kyoto-u.ac.jp

Fabrication of field-effect transistor devices with Langmuir-Blodgett films of fullerodendron

○Naoko Kawasaki¹, Takayuki Nagano¹, Yoshihiro Kubozono¹,
Yuuki Sako², Yutaka Takaguchi²,
Akihiko Fujiwara³, Shojun Hino⁴, Chih-Chien Chu⁵, and Toyoko Imae⁵

¹Department of Chemistry, Okayama University, Okayama 700-8530, Japan

²Graduate School of Environmental Science, Okayama University, Okayama 700-8530, Japan

³Japan Advance Institute of Science and Technology, Ishikawa 923-1292, Japan

⁴Graduate School of Science and Engineering, Ehime University, Ehime 790-8577, Japan

⁵Faculty of Science and Technology, Keio University, Yokohama 223-8522, Japan

We previously reported field-effect transistors (FETs) with fullerodendron (Fig. 1) films formed by spin-coating process [1]. The field-effect mobility, μ , of the device reaches $1.7 \times 10^{-3} \text{ cm}^2 \text{ V}^{-1} \text{ s}^{-1}$. This study suggested a significance of highly-ordered arrangement of C_{60} moieties for the high-performance FET devices. We have fabricated FETs with Langmuir-Blodgett (LB) films of fullerodendron molecules, since the fullerodendron LB films are known to be highly ordered on various surfaces [2].

The LB films with five-monolayers of fullerodendron were formed on SiO_2/Si wafers. The source and drain electrodes were formed on the LB films by thermal deposition of gold. The FET properties were measured under a vacuum of 10^{-6} Torr. Figure 2 shows typical output characteristics of the FET device with the LB films. The μ value of the device was found to be $2.7 \times 10^{-3} \text{ cm}^2 \text{ V}^{-1} \text{ s}^{-1}$ at 300 K. This value is higher than the highest one obtained in the devices fabricated by spin-coating process. The high μ value can be attributable to the improvement of conduction path by a formation of ordered structures of C_{60} moieties.

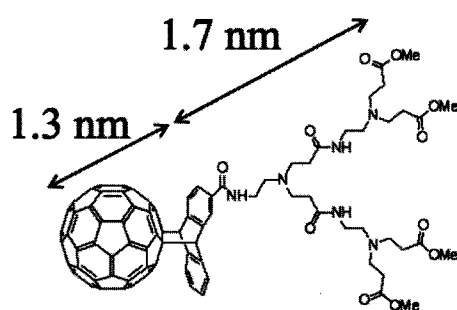


Fig. 1. The structure of fullerodendron.

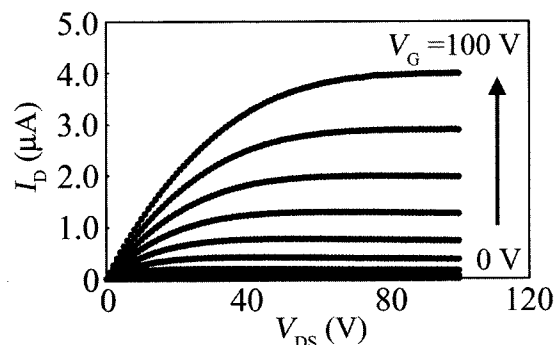


Fig. 2. I_D - V_{DS} plots of fullerodendron FET.

References: [1] Kusai et al., *Appl. Phys. Lett.* **88**, 173509 (2006).

[2] Hirano et al., *Langmuir* **21**, 272 (2005).

Corresponding Author: Naoko Kawasaki

E-mail: naoko-k@cc.okayama-u.ac.jp

Tel: +81-86-251-7850, **Fax:** +81-86-251-7853

TEM and Raman Spectroscopy Analyses of Fullerene Derivative Nanowhiskers and Fullerene Nanotubes

○Kun'ichi Miyazawa,¹ Cherry Ringor,¹ Tadahiko Mashino² and Shigeo Nakamura²

¹Fuel Cell Materials Center, National Institute for Materials Science, 1-1, Namiki, Tsukuba, Ibaraki, 305-0044, Japan

²Kyoritsu University of Pharmacy, 1-5-30, Shibakoen, Minato-ku, Tokyo, 105-8512, Japan

It has been shown that the C₆₀ fullerene nanowhiskers prepared by the liquid-liquid interfacial precipitation method [1] using a C₆₀-saturated *m*-xylene solution and isopropyl alcohol (IPA) have a solvated hexagonal structure [2,3]. The solvated hexagonal structure of C₆₀ nanowhiskers (C₆₀NWs) turns to cubic structure by drying in air. It has been also shown that the solvated C₆₀ nanotubes (C₆₀NTs) with tubular structure have a hexagonal structure and turn to cubic structure by losing the contained solvent in air [3]. The structure of hexagonal C₆₀NWs is considered to be explained by the model of Ramm et al. [4]. Fig.1 shows a hexagonal structure model for a C₆₀NW which is viewed along the c-axis that is parallel to the whisker growth axis. The model shows that nanochannels with a diameter of about 0.8 nm are formed along the c-axis. Hence, it is expected that linear arrays of various atoms could be prepared by filling the nanochannels. For this purpose, it is necessary to stabilize the hexagonal structure in air. It is suggested that the hexagonal crystal structure of the C₆₀NWs can be stabilized by dissolving larger C₆₀ derivative molecules into the matrix of C₆₀NWs. For example, C₆₀ nanowhiskers with a composition of C₆₀ – 4.2 mol% C₆₀[C(COOC₂H₅)₂] showed electron diffraction patterns that could be indexed by a hexagonal structure [5]. On the other hand, a Raman profile (Fig.2) for a whisker of C₆₀(6,7-dimethoxytetralin) showed a A_g(2) peak of 1460 cm⁻¹ which is very close to that of one-dimensionally polymerized C₆₀. Detailed discussions about the crystal structure and the Raman profile of C₆₀ derivative nanowhiskers will be presented.

Part of this research was financially supported by a Grant in Aid for Scientific Research of the Ministry of Education, Culture, Sports, Science and Technology of Japan (Project No.17201027 and No.17651076).

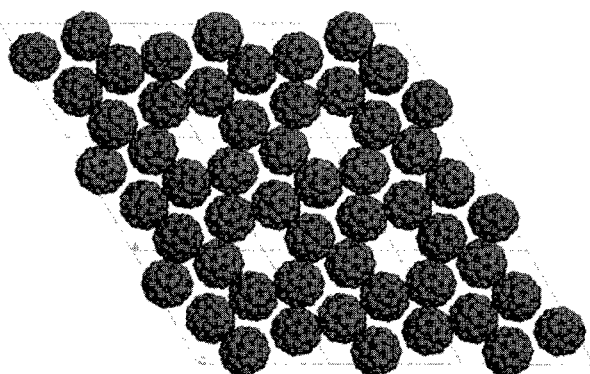


Fig.1 Structural model of hexagonal C₆₀ nanowhisker viewed along its c-axis.

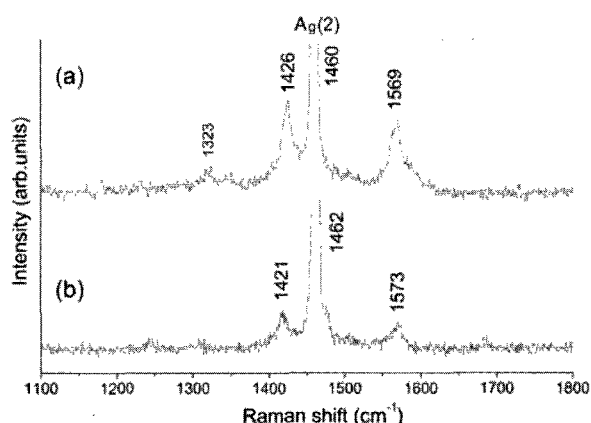


Fig.2 Raman spectra for (a) whisker of C₆₀(6,7-dimethoxytetralin) and (b) pristine C₆₀ powder.

- [1] K.Miyazawa, Y.Kuwasaki, A.Obayashi and M.Kuwabara, *J.Mater.Res.*, **17**[1](2002)83,
 [2] J.Minato and K.Miyazawa, *Carbon*, **43**(2005)2837
 [3] J.Minato and K.Miyazawa, *Diamond & Related Materials*, **15** (2006) 1151,
 [4]M.Ramm, P.Luger, D.Zobel, W.Duczek and J.C.A.Boeyens, *Crys. Res. Technol.*, **31** (1996)43.
 [5] K.Miyazawa, J.Minato, T.Mashino, S.Nakamura, M.Fujino and T.Suga, *NUKLEONIKA*,
51 Supplement 1(2006)S41.

Corresponding Author : Kun'ichi Miyazawa

E-mail : miyazawa.kunichi@nims.go.jp, Tel +81-(0)29-860-4528, Fax +81-(0)29-860-4667

Enhanced Growth of C₆₀ Nanotubes by Illumination with UV Light

○Cherry Ringor¹, Kun'ichi Miyazawa¹ and Tohru Awane²

¹*Fuel Cell Materials Center, National Institute for Materials Science, 1-1 Namiki,
Tsukuba, Ibaraki, 305-0044, Japan*

²*Materials Analysis Station, National Institute for Materials Science, 1-2-1 Sengen,
Tsukuba, Ibaraki, 305-0044, Japan*

Nanotubes composed of C₆₀ fullerenes have been synthesized by the liquid-liquid interfacial precipitation method using pyridine and isopropyl alcohol (IPA) as solvents [1]. It has also been reported that the growth of nanotubes are assisted by illumination with visible light between wavelengths of 600-625 nm [2,3]. Subsequent work by [4] used UV light with a wavelength of 302 nm to irradiate the C₆₀-saturated pyridine solution to accelerate the growth of the nanotubes. Using a small-scale set-up (using bottles with 10 ml capacity), the method successfully produced about 25% yield of nanotubes within 7 days or more. However, in such scenario, it is difficult to generate sufficient amount of nanotubes to be used for further studies of their unique chemical and physical properties and for developing useful products and devices. We provide an improved method to grow high yield of nanotubes of as much as 100% within a span of 1-3 days using the same materials previously reported and have scaled-up the method using 100 ml bottles to produce gram quantities of nanotubes. By mixing different amounts of C₆₀-saturated pyridine and IPA and controlling the growth temperature, it is possible to produce considerable amount of nanotubes. It was found that 1:10, 1:9, 1:8 ratios of C₆₀-pyridine:IPA and 5°C growth temperature are the most efficient experimental conditions compared to 1:7, 1:6, 1:5, 1:4, and 1:3 ratios and 10-15°C temperatures. A detailed analytical method and structural characterization of the C₆₀ nanotubes will be presented.

[1] K. Miyazawa, J. Minato, M. Fujino, and T. Suga, *Diamond Relat. Mater.*, **15**, 1143-1146 (2006).

[2] K. Kobayashi, M. Tachibana, and K. Kojima, *J. Cryst. Growth*, **274**, 617-621 (2005).

[3] T. Tachibana, K. Kobayashi, T. Uchida, K. Kojima, M. Tanimura, and K. Miyazawa, *Chem. Phys. Lett.*, **374**, 279-285 (2003).

[4] J. Minato and K. Miyazawa, *Diamond Relat. Mater.*, **15**, 1151-1154 (2006)

Corresponding Author : Cherry Ringor

E-mail : RINGOR.cherry@nims.go.jp

Tel&Fax : +81-(0)29-860-4667

Theoretical Study of Electronic and Transport Properties of Fullerene as a Molecular Device

○Shinji Usui, Yoshihisa Ohshima, Shoji Hirose, Tetsuo Kitajima

Cybernet System Co., Ltd. New Business Development Department

The molecular based electric device has been attracted much attention for a candidate of approaches to overcome the limitation of the conventional silicon-based device. Fullerenes and carbon nanotubes related compounds are believed to be active components for the molecular device since they directly provide well-defined nano-scale systems. A detailed understanding of such fullerenes and nanotubes based devices will provide essential insights to create and develop such devices. Based on these backgrounds, we report here the results of electric and transport properties of fullerene (C_{60}) as a molecular device using a theoretical first-principle method.

When one C_{60} allocates between the two metal electrodes, the metal-fullerene-metal system will have tunneling current due to the size of fullerene molecule. In order to describe such a quantum transport problem, Atomistix ToolKit[1-4] which implements the methods of combination of density functional theory (DFT) and the nonequilibrium Green's function's (NEGFs) technique, was used to analyze electric and transport properties. The calculated system in this study is shown in Fig. 1. The model system consists of two semi-infinite gold electrodes and one C_{60} molecule whose five-membered ring part faces onto the center of the Au(111) surface. The calculated I-V character is shown in Fig. 2. The slope of I-V curve is large at the low bias, while the slope changes over the bias at 0.2V. In the presentation, the detail transport behavior and its mechanism will be discussed.

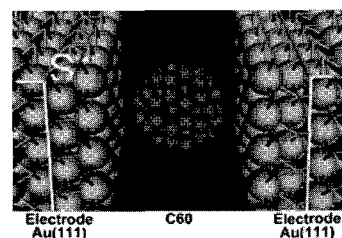


Fig. 1 Model for C_{60} based molecular device.

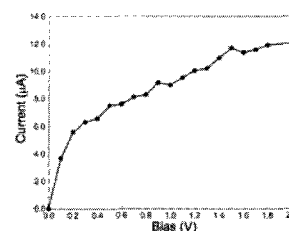


Fig. 2 Calculated I-V character.

References: [1] <http://www.atomistix.com/>, see also <http://www.cybernet.co.jp/nanotech/atomistix/>

[2] M. Brandbyge, J.-L. Mozos, P. Ordejón, J. Taylor, and K. Stokbro, *Phys. Rev. B* **65**, 165401 (2002).

[3] J.M. Soler, E. Artacho, J.D. Gale, A. García, J. Junquera, P. Ordejón, and D. Sánchez-Portal, *J. Phys. Condens. Matter* **14**, 2745 (2002).

[4] J. Taylor, H. Guo, and J. Wang, *Phys. Rev. B* **63**, 245407 (2001).

Corresponding Author: Shinji Usui, **E-mail:** s-usui@cybernet.co.jp

Electrical Properties of FET devices with C₆₀ Nano-Whiskers

○ K.Ogawa¹, H.Tsuji¹, N.Aoki^{1,2}, and Y.Ochiai^{1,2}

¹ Graduate School of Science and Technology, Chiba University, 1-33 Yayoi-cho,
Inage-ku, Chiba 263-8522, Japan

² Department of Electronics and Mechanical Engineering, Chiba University

A new type of C₆₀ needle, or “nano-whisker”, has been obtained by the liquid-liquid interfacial precipitation (LLIP) method [1]. Typical C₆₀ nano-whiskers (C₆₀NW) that we obtain by LLIP are typically less than 0.3 μm in diameter and more than 50 μm in length (Fig. 1). From recent researches, C₆₀NW exhibit a hexagonal crystal structure and is formed soltate with a solvent (*m*-xylene). In this work, we have fabricated C₆₀ nano-whisker based FETs (C₆₀NW-FETs) keeping a hexagonal crystal structure, and have investigated their electrical properties.

For fabricating the C₆₀ NW-FET device structure in our study [2], we have used a Si wafer as the substrate, with a thermally-grown SiO₂ insulating top layer. The source and drain electrodes were fabricated on the surface of SiO₂ layer. C₆₀ NW was used to bridge the two electrodes, by using amicropipette to instill solution containing NWs in a glove box filled with N₂ gass. Their FET characteristics were then measured in N₂ atmosphere without exposing the devices to the ambient atmosphere.

Gate-voltage characteristics ($I_{SD}-V_G$) is shown in Fig. 2. From this data, the carrier mobility of this C₆₀ NW-FET can be roughly estimated to be $4 \times 10^{-3} \text{ cm}^2 \text{ V}^{-1} \text{ s}^{-1}$.

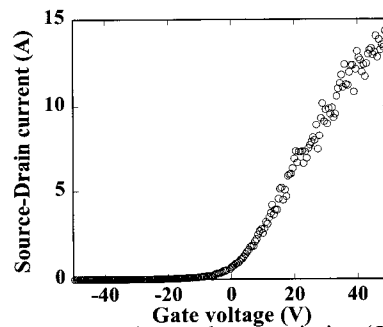
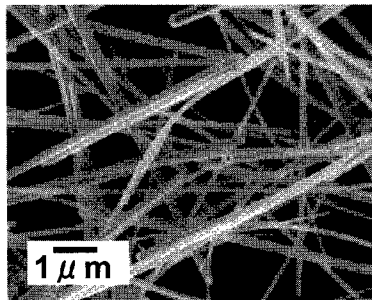


Fig. 1, SEM image showing typical C₆₀ NW Fig. 2, Gate-voltage characteristics ($I_{SD}-V_G$)

[1] K.Miyazawa, Y.Kuwasaki, A.Obayashi, and M.Kuwabara: J. Mater. Res. **17**, 83 (2002)

[2] K.Ogawa, T.Kato, A.Ikegami, H.tsuji, N.Aoki, Y.Ochiai, and J.P.Bird: Appl. Phys. Lett. **88**, 112109 (2006)

Corresponding author: Yuichi Ochiai

E-mail: ochiai@faculty.chiba-u.ac.jp

Tel.043-290-3428, Fax.043-290-3427

Electronic transport properties of electron beam irradiated C₆₀ polymers

○ H.Tsuji¹, K.Ogawa¹, K.Ryuzaki², N.Aoki¹, J.Onoe², and Y.Ochiai¹

1) Chiba University, Yayoi, Inage-Ku, Chiba 263-8522, Japan

2) Tokyo Institute of Technology, O-okayama, Meguro, Tokyo 152-8550 Japan

Recently, Onoe et al found that a peanut-shaped C₆₀ polymer, which exhibits metallic *I-V* characteristics at room temperature in air, is formed from a C₆₀ irradiated by a 3-kV electron-beam [1]. In the present work, we have examined the electronic transport properties of the peanut-shaped C₆₀ polymer in the range of 9~400 K, and applied the polymer to a field-effect transistor (FET).

Figure 1 shows a Arrhenius plot of the electrical resistivity of the C₆₀ polymers on a CsI substrate. The resistivity was obtained to be 0.73 Ωcm at room temperature (RT). It is interesting to note that the slope was changed drastically at around 90 K and becomes almost flat below 90K.

Figure 2 shows the FET characteristics of the C₆₀ polymers. A thin SiO₂ layer on a p-type Si wafer was used as a substrate. The RT resistivity was obtained to be 8.0×10⁴ Ωcm at V_g=0 V. There was a large difference in resistivity on between CsI and SiO₂/Si substrates.

Details of these electrical properties will be discussed at the symposium.

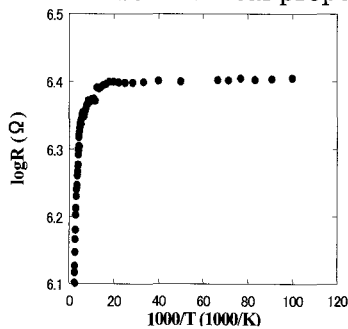


Fig. 1, Resistance of polymer C₆₀ on CsI

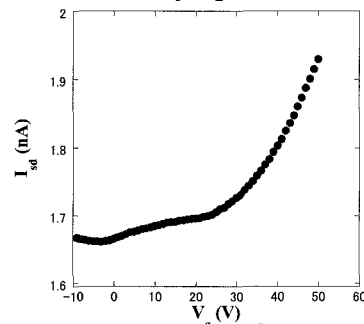


Fig. 2, Vg dependence of polymer C₆₀ FET

[1] J. Onoe, T. Nakayama, M. Aono, and T. Hara, Appl. Phys. Lett. 82, 595 (2003).

Corresponding Author: Y.Ochiai

E-mail: ochiai@faculty.chiba-u.ac.jp Tel.043-290-3428, Fax.043-290-3427

Synthesis of polymerized C₆₀ films by irradiation of a free electron laser during a deposition

○Nobuyuki Iwata, Ryo Nokariya, Shingo Ando, Reo Koyaizu, Hiroshi Yamamoto

*Department of Electronics & Computer Science,
College of Science & Technology, Nihon University*

Since the polymerization of C₆₀ films was carried out by a phototransformation first, the possibility of a three-dimensional (3D) polymerized phase has been discussed. The purposes of this work are to develop a novel photon-assisted process for C₆₀ polymerization and to synthesize 3D C₆₀ polymers by free electron laser (FEL) irradiation. In the last presentation we reported that the polymerization was took place just on the surface of a pressed bulk sample, depending on FEL wavelength probably due to the different absorption coefficient and a degree of electronic excitation [1]. In this presentation to obtain 3D C₆₀ polymers, FEL was irradiated during deposition of C₆₀ molecules on substrates. The deposition and irradiation time was 30 min. The fundamental wavelength was 1350 nm, including 3rd (450 nm) and 5th (270 nm) harmonics. The irradiations through a quartz BK7 window were carried out under the pressure of 470 MPa in a vacuum chamber at around 10⁻⁶ Torr.

Figure 1 shows the Raman shift of an Ag(2)-derived mode. The wave number of the peak of the non-irradiated pristine C₆₀ was 1469 cm⁻¹(dotted line), while that of the irradiated C₆₀ (solid line) changed to 1461 cm⁻¹, indicating the polymerization of the deposited film. Growth condition dependence of degree of polymerization will be discussed.

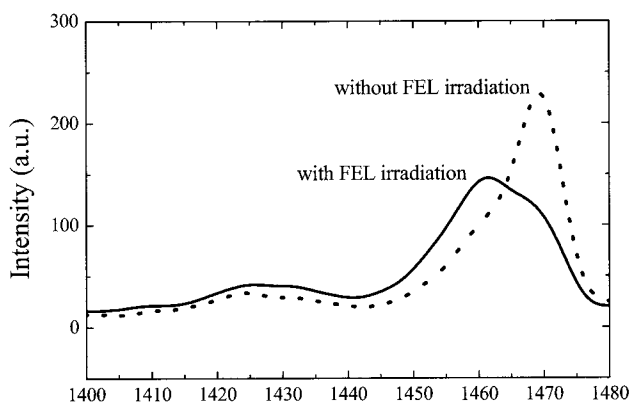


Fig.1 Raman shift of C60 film with and without FEL irradiation

[1] 31th the F&NT symposium 2P-19

1P-40

Structure and Physical Properties of Charge transfer C₆₁H₂(dihydrofulleroid) Compounds

○Takayuki Iwase , Satoru Motohashi , Yasutaka Aihara , Shihori Seto, Hironori Ogata

*Dept.of Materials Chemistry,Hosei University
3-7-2 Kajino cho,Koganei,Tokyo,184-8584,Japan*

We report here the structure and physical properties of TDAE (tetrakis(dimethylamino)ethylene)-C₆₁H₂ and TMBI(1,1',3,3'-tetramethyl- $\Delta^{2,2'}$ -bi(imidazolidine))-C₆₁H₂ charge transfer compounds. TDAE-C₆₁H₂ was prepared by mixing method without solvent. The diffraction profile can be indexed with a orthorhombic lattice(space group:P222) of lattice constants of $a=13.012\text{ \AA}$, $b=14.747\text{ \AA}$, $c=15.767\text{ \AA}$. Figure 1 shows the temperature dependence of the product of the magnetic susceptibility with temperature for TDAE-C₆₁H₂ compound. The value of χT decreases approximately linearly with decreasing temperature and no evidence of magnetic transition is observed to 2K.

Detailed results on the structure and magnetic properties including the results of solid state NMR of TDAE-C₆₁H₂ and TMBI-C₆₁H₂ will be discussed in the presentation.

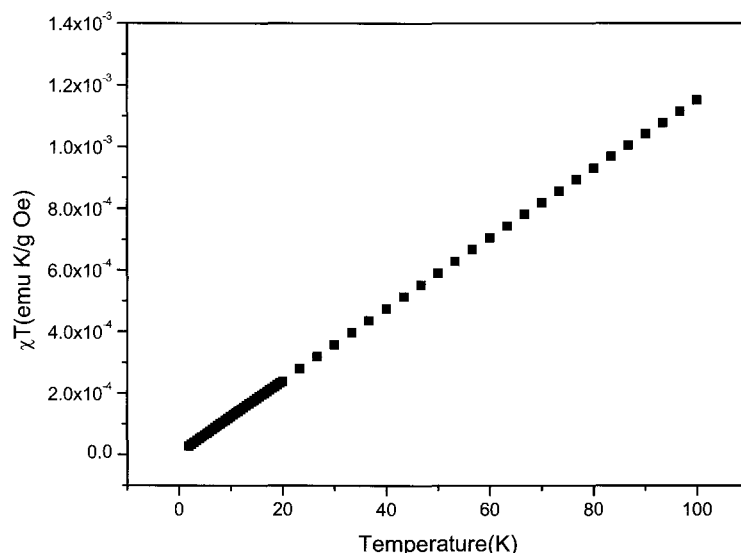


Fig.1 Temperature dependence of χT for TDAE-C₆₁H₂ compound

Corresponding Author:Hironori Ogata, E-mail:hogata@hosei.ac.jp

Tel&Fax:042-387-6229

2P-1

Far-Infrared Absorption Peak in Single-Walled Carbon Nanotubes and Its Correlation with Tube Lengths

○H.Suzuki¹, N.Akima¹, H.Shimotani¹, Y.Iwasa¹

¹Institute for Materials Research, Sendai 980-8577, Japan

Background: In our previous poster, we reported that the peak position which appeared clearly in far-infrared (FIR) region shifted to higher frequency with shortening of average lengths of SWNTs. The FIR peak structure is caused by plasmon resonance of metallic tubes, of which position is dependent on the length [1]. In this poster, we will make poster presentation that is drawn about study to estimate the average length from FIR peak position quantitatively by fitting analysis and discuss about contribution of bundling effect or diameter that is important in study of plasmon resonance of metallic SWNTs as well as length.

Experiment: We sorted DNA-wrapped HiPco SWNTs (DNA-CNTs) [2] and SDS-encased CoMoCat SWNTs (SDS-CNTs) [3] in aqueous solution by length through ultracentrifugation nondestructively. The DNA-CNTs solution was dropped on SiO₂ substrate and SDS-CNTs were embedded in PVA. The absorption spectra of these samples were measured. Since these SWNTs were isolated completely, absorption spectra of individual SWNTs could be obtained and bundling effect should be estimated through comparison of these spectra with bundled SWNTs spectra. Correlation between FIR peak position and SWNTs diameter also can be established as considering the difference in the peak position of SDS-CNTs and DNA-CNTs because HiPco SWNTs and CoMoCat SWNTs have different diameter distribution respectively.

Fitting Analysis: We fitted these FIR spectra using an effective medium theory assuming an ellipsoid model of SWNT, and obtained average length as fitting parameters. The FIR peak position was exclusively dependent on average length. It was found that the length dependence of the peak position was qualitatively but not quantitatively understood in terms of the plasmon resonance of finite sized SWNTs.

References:

[1] N. Akima, et al., Adv. Mat. **18**, 1166 (2006).

[2] M. Zheng, et al., Nat. Mat **2**, 338 (2003).

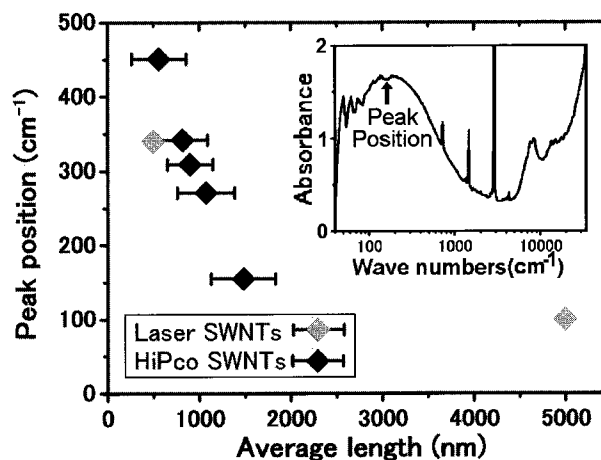
[3] B. Kitiyanan, et al., Chem. Phys. Lett **317**, 497 (2000).

Corresponding Author: Hiroataka Suzuki

TEL:+81-22-215-2032,

FAX:+81-22-215-2032,

E-mail: hsuzuki@imr.tohoku.ac.jp



Photoluminescence of Larger Diameter Double-Walled Carbon Nanotubes Synthesized from C₆₀ Peapods

○Toshiya Okazaki¹, Zujin Shi², Takeshi Saito¹, Hideaki Wakabayashi¹, Kazu Suenaga¹ and Sumio Iijima¹

¹Research Center for Advanced Carbon Materials, AIST, Tsukuba 305-8565, Japan

²Department of Chemistry, Peking University, Beijing 100871, P. R. China

Double-walled carbon nanotubes (DWNTs) have been expected for nanocomposites, field emission sources, nanotube bi-cables and electronic devices because of their superior mechanical properties, thermal conductivity and structural stability [1]. Optical application of DWNTs is also attractive because the inner core tube is protected from environment and its optical properties are preserved. We previously reported a detailed study of photoluminescence (PL) from the peapod-derived DWNTs, together with optical absorption and resonant Raman spectroscopy [2]. The SWNTs with diameter (d_t) ranging in ~ 1.2 - 1.4 nm were produced by the pulsed laser vaporization of a Fe-Ni containing carbon target and used for templates. Even though the optical absorption and the resonant Raman spectra exhibit characteristic features of DWNTs, no PL originated from the inner and the outer tubes were observed. This suppression is a consequence of an interlayer interaction between the inner and the outer tubes that efficiently quenches the PL signals of the DWNTs.

On the other hand, theoretical calculations predict that the interaction between the inner and outer shells in the DWNT strongly depends on the interlayer distance - naturally, the larger the distance being the weaker the interaction [3,4]. One might expect that larger diameter of the outer tubes results in the broader distribution of the interlayer spacing. Here we report optical behaviors of larger diameter DWNTs synthesized by annealing of C₆₀ peapods. The diameter of SWNTs used for templates ranges from 1.3-1.5 nm which were synthesized by the DC arc discharging method. In contrast to the previous result, the PL signals were observable from the inner tubes. It is therefore likely that the present sample contains a significant fraction of DWNTs with the larger interlayer distance and they can show PL signals.

[1] M. Endo, H. Muramatsu, T. Hayashi, Y. A. Kim, M. Terrones, M. S. Dresselhaus, *Nature* **433**, 476 (2005).

[2] T. Okazaki, S. Bandow, G. Tamura, Y. Fujita, K. Iakoubovskii, S. Kazaoui, N. Minami, T. Saito, K. Suenaga, S. Iijima, *Phys. Rev. B*, **74**, 153404 (2006).

[3] S. Okada and A. Oshiyama, *Phys. Rev. Lett.* **91**, 216801 (2003).

[4] W. Song, M. Ni, J. Lu, Z. Gao, S. Nagase, D. Yu, H. Ye, X. Zhang, *Chem. Phys. Lett.* **414**, 429 (2005).

Corresponding Author: Toshiya Okazaki

E-mail: toshi.okazaki@aist.go.jp, **Tel:** 029-861-4173, **Fax:** 029-861-4851

2P-3

Chirality-sensitive *in-situ* observation of CVD growth of single-walled carbon nanotubes by Raman spectroscopy

○M. Tazawa^{1,2}, D. Takagi^{2,3}, Y. Homma^{2,3}, S. Suzuki^{1,3}, Y. Kobayashi^{1,3}

¹NTT Basic Research Laboratories, NTT Corporation, Atsugi 243-0198, Japan

²Department of Physics, Tokyo University of Science, Shinzuyuku, Tokyo 162-8601, Japan

³CREST/JST, Japan Science and Technology Corporation

In-situ observation of single-walled carbon nanotube (SWNT) growth is useful approach for investigating the growth mechanism of SWNTs [1,2]. However, chiralities of growing SWNTs was not specified in these previous works. Here, we succeeded in measuring chirality-sensitive RBM signals during CVD growth of SWNTs by *in-situ* Raman spectroscopy and examined the diameter dependence of growth behavior.

SWNTs were synthesized by ethanol-CVD using Co film (0.5,2 Å) as the catalyst. The growth temperature was 650 °C and the ethanol gas pressure was 0.1-0.6 Torr. Raman spectra were measured *in situ* during the CVD growth (633-nm excitation wavelength, 2- μ m laser spot).

Figure 1 is a series of typical Raman spectra in the RBM frequency region. Each spectrum was integrated for 30 s and its intensity was normalized by the intensity of RBM signals at 190 cm^{-1} which were the most prominent peak in these spectra. It is clearly recognized that the RBM signals around 130-150 cm^{-1} from relatively thick SWNTs delay in appearing, compared with the signal at 190 cm^{-1} . This indicates that the incubation time of SWNT growth observed by Chiashi *et al.* [2] should depend on the chirality. Moreover, it was observed that growth conditions, such as catalyst film thickness, also significantly affect initial growth behaviors of SWNTs even if they have the same chirality. These chirality-sensitive growth behavior should be elucidated by a detailed analysis of *in-situ* Raman spectra in conjunction with an analysis of catalyst particle diameters.

References: [1]Y. Homma et al., APL 88 (2006) 023115.

[2]S. Chiashi et al., CPL 386(2004)89.

Corresponding Author: M. Tazawa

E-mail: tazawa@will.brl.ntt.co.jp

Tel&Fax: +81-46-240-4070 /4718

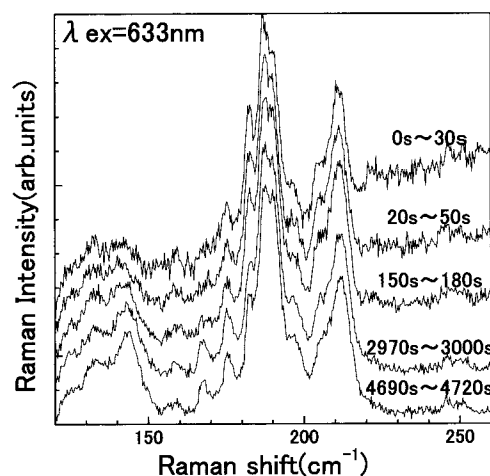


Fig.1 *In-situ* Raman spectra observed during CVD growth.

2P-4

Determining Molar Absorbance Coefficients of Single-Walled Carbon Nanotubes

○Shota Kuwahara, Toshiki Sugai and Hisanori Shinohara

Department of Chemistry, Nagoya University, Nagoya 464-8602, Japan

Dealing with carbon nanotubes (CNTs) as an individual “molecule” is very important for studying optical properties and chemical reactivity of CNTs, which also leads to standardize CNT’s evaluation. It has not been possible to study, for example, molar absorbance coefficient of individual CNTs quantitatively and to compare them with other nanomaterials, largely because that the number of CNTs in dispersed solution per unit volume has not been determined yet.

To evaluate the number of CNTs in unit volume, we have developed a new spray technique coupled with AFM observations [1]. Here we report molar absorbance coefficients of a single-wall carbon nanotube (SWNT) accrued from the present method. We found that the molar absorbance coefficient of a SWNT is 100 times as large as that of C_{60} and that the value is comparable to the recent study on weight absorbance coefficients [2]. The height-length distribution obtained by AFM observation also allows us to estimate the coefficient per carbon atom. The result shows that it is 10 times as small as that of C_{60} .

SWNTs of purified HiPco were dispersed in aqueous sodium dodecyl sulfate (SDS) surfactant [1 wt%] and were centrifuged at 197,000 g for 1 hour [3]. These samples were characterized by AFM (Veeco Digital Instruments NanoscopeIV), absorption spectroscopy (JASCO V-570) and spectrofluorometer (SHIMADZU). AFM samples were prepared by the spray technique with the suspension [1].

The AFM images show nanotube bundles together with thin uniform layers of SDS with a height of 2-3 nm. The ratio between observed amounts of SDS and that of nanotubes corresponds to the number density of nanotube bundles in the suspension by considering the concentration of SDS. The concentration estimated from this AFM technique with the absorbance at wavelength of 280 nm (π -plasmon) can provide a plot shown in Figure 1.

The molar absorbance coefficient of SWNTs (HiPco tubes) was estimated as 1.86×10^7 [L mol⁻¹ cm⁻¹], and the coefficient per carbon atoms was also estimated as 8.78×10^{-22} [L nc⁻¹ cm⁻¹]. These values enable us to deal with SWNTs as an individual “molecule”, which can also provide fair comparison of the molar coefficient of SWNTs with that of other π -conjugate compounds such as benzene and C_{60} molecules. These results show that molar coefficients increase as the number of carbon atoms or π electron increases; the number of π electrons of SWNTs contributed to π -plasmon is much larger than that of C_{60} .

References:

- [1] S. Kuwahara, et al.: *the 30th Fullerene-Nanotube Symposium*.
- [2] J. L. Bahr, et al.: *Chem. Comm.* 2001, 193.
- [3] M. J. O’Connell, et al.: *Science* **297** 593 (2002).

Corresponding Author: Hisanori Shinohara

E-mail: noris@cc.nagoya-u.ac.jp

TEL: +81-52-789-2482, FAX: +81-52-789-1169

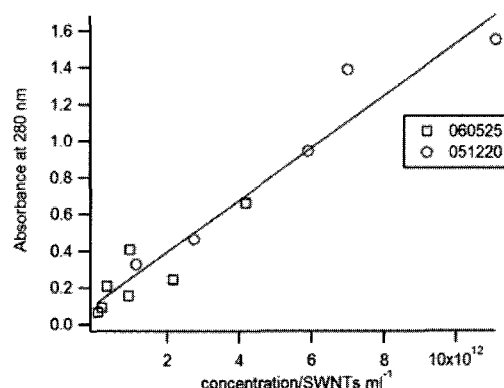


Figure 1: Optical Density at 280 nm of the SWNTs in SDS solution

2P-5

Photoinduced electron transfer between single-wall carbon nanotubes and C₆₀ dispersed in D₂O

Koji Inada, Yasuyuki Araki, Atula S.D. Sandanayaka, Osamu Ito
Institute of Multidisciplinary Research for Advanced Materials, Tohoku University

【Introduction】

Single-wall carbon nanotubes (SWNTs) have attracted much attention as photo devices¹⁾. In such devices, although SWNTs may be acting as acceptor, their donor ability seems to be still unknown. Therefore, it is important to clarify a critical role of SWNTs on the photoinduced electron transfer. Here, we have investigated photoinduced electron transfer between SWNTs and C₆₀/ γ -cyclodextrin (γ -CD) in carboxymethylcellulose (CMC)/ D₂O by laser flash photolysis method.

【Experiment】

1. HiPco SWNTs (1 mg) were added to a solution of CMC (0.1 mg) in D₂O (10 mg). The suspension was homogenized by stirring and sonicating. The supernatant was corrected after centrifuged (95000 G) to remove non-dispersible SWNTs.
2. C₆₀ (100 mg) was mixed with γ -CD (300 mg) by ball-mill for 20 h and extracted with 50 ml of D₂O. The supernatant was corrected after centrifugation (95000 G) to remove non-soluble C₆₀.
3. Transient absorption spectra of SWNTs and C₆₀/ γ -CD mixed solution were measured by 532 nm laser irradiate (1 mJ/ pulse, 10Hz).

【Result】

By ns laser light pulse (532 nm, 6 ns) irradiation, a peak around 740 nm (³C₆₀*/ γ -CD) was observed. With decaying 750 nm peak, new peaks appeared at 1080 nm, 1300 nm, 1500 nm as shown in Fig. (a). The new absorption band at 1080 nm can be attributed to the C₆₀^{·-}/ γ -CD. Another bands appeared over 1200 nm seem to be associated to the SWNTs because C₆₀/ γ -CD does not show any transition band in there wavelength regions. On the other hand, without SWNTs, system did not show any new rising peak as shown in Fig. (b). Therefore, this finding indicates that an electron transfer occurred from SWNTs to ³C₆₀*/ γ -CD yielding C₆₀^{·-}/ γ -CD and SWNTs cation. In this case, SWNTs acts as electron donor.

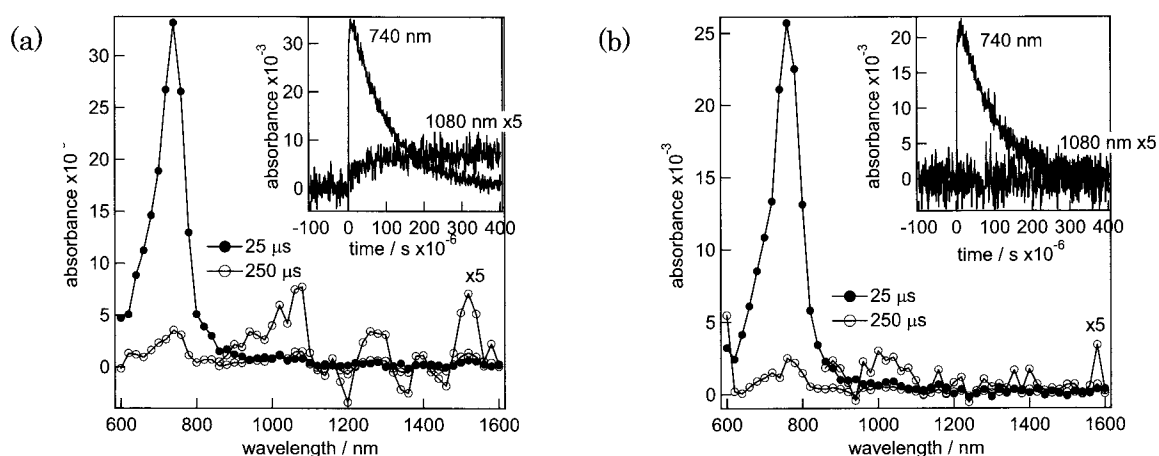


Figure. Transient absorption spectra of (a) SWNTs with C₆₀/ γ -CD in CMC/ D₂O, (b) C₆₀/ γ -CD in CMC/ D₂O at 25 μ s (●), 250 μ s (○). Inset: Absorption-time profiles at 740 nm and 1080 nm.

Reference

- 1) Said Barazzouk et al., *J. Phys. Chem. B*, **2004**, *108*, 17015.
- 2) Masuhara et al, *Bull. Chem. Soc. Jpn.*, **2000**, *73*, 2199

2P-6

ESR study of boron-doped multiwall carbon nanotubes

○Shigenori Numao, Shunji Bandow, Sumio Iijima

*Department of Materials Science and Engineering, Meijo University,
1-501 Shiogamaguchi, Tenpaku, Nagoya 468-8502, Japan*

In the previous study [1], we reported the production of high purity multiwall carbon nanotubes (MWNTs) with various innermost tube diameters, which can be controlled by the boron concentration in the carbon rod for RF-plasma vaporization. Although the burning temperatures of thus prepared MWNTs were decreased with increasing the boron concentration from 750 (0 % of B) to 710 °C (20 %), TEM and Raman scattering results indicated that the concentration of atomic defects is quite small.

In the present study, we examined the ESR of the MWNTs. Figure 1a shows the boron concentration dependence of ESR spectra. For 0 % sample (B0-NT), ESR spectrum can be fitted by two ESR components having the g -values of 2.015 and 2.005. We temporarily assigned these signals to the conduction ESR (CESR) from scrolled MWNTs ($g = 2.015$) and concentric MWNTs (2.005). By adding the boron, rather strong ESR feature by ca. 10 times was newly appearing at $g = 2.001$ (broad component, thick dotted line in Fig. 1a) together with a narrow component at $g = 2.002$ (integrated intensity is in the same order with CESR at $g = 2.0015$ and 2.005). Temperature dependences of these newly appearing signals are shown in Fig. 1b and ESR features are in Figs. 1c and d. Intensities of these ESR are decreased when the temperature is lower than ca. 140 K. The temperature dependences of χ_s are indicated in Fig. 1c and they are roughly fitted by $\chi_s \propto \sqrt{\Delta_e/k_B T} \exp(-\Delta_e/k_B T)$, where Δ_e corresponds to the effective energy gap from the E_F to the impurity states.

This expression is utilized to analyze the χ_s of a quasi-one-dimensional conductor. Hence we remind the boron doping to the carbon network. Detailed analyses will be presented.

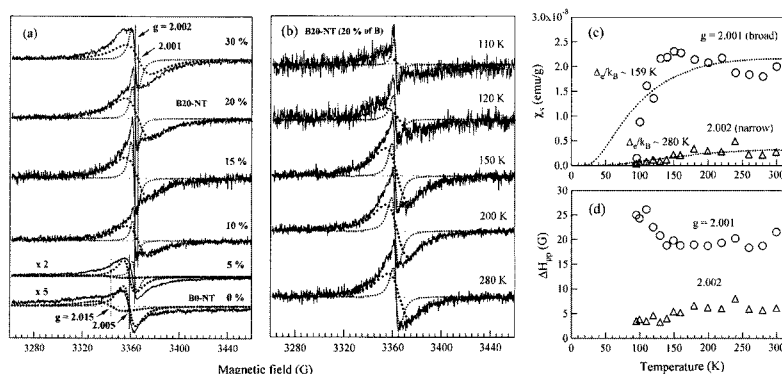


Fig. 1. Boron concentration (a), temperature dependences of ESR taken for MWNTs from 20 % of boron (b), temperature dependences of spin magnetic susceptibility χ_s of each simulated component (c) and ESR linewidth ΔH_{pp} .

[1] S. Numao et al., The 31st Fullerene Nanotubes General Symposium, July 12-14 (2006), Mie, **1P-19**.

Corresponding Author : Shigenori Numao

E-mail : m0534024@ccmailg.meijo-u.ac.jp **Tel&Fax :** +81-52-834-4001

FT-IR study of adsorption of H₂O on SWNTs prepared in Super-Growth technique

○Hiroyuki Yokoi¹, Hirosuke Akimaru¹, Akinori Kanetake², Noritaka Kuroda¹,
Yuhei Hayamizu³, Kenji Hata³

1Dept. of Materials Sci. and Eng., Kumamoto Univ., Kumamoto 860-8555

2Dept. of Mechanical Eng. and Materials Sci., Kumamoto Univ., Kumamoto 860-8555

*3Res. Ctr. for Advanced Carbon Materials, National Inst. of Advanced Industrial Sci.
and Technol., Tsukuba 305-8565*

It is known that adsorption of water molecules on semiconducting single-walled carbon nanotubes (SWNTs), which is pristinely of p-type, reduces electric conductivity. This phenomenon is attributed to doping of electrons to SWNTs from water molecules[1]. In this study, we have aimed to investigate the modification of the electric properties of SWNTs due to the adsorption of water molecules in detail using a FT-IR method. We have monitored spectral changes of SWNTs prepared in Super-Growth chemical vapor deposition by controlling the adsorption amount of water molecules on SWNTs. The employed SWNTs had diameters around 3 nm and an absorption peak attributed to the first subband gap of semiconducting SWNTs was observed at approximately 0.3 eV. It was observed that absorption structures disappeared when the SWNTs were exposed to humid atmosphere. In return, the Drude absorption was observed to be enhanced. With increasing the temperature of the SWNTs to 540 K in dry nitrogen gas, it was recognized that the absorption structure corresponding to the first subband gap was recovered and the Drude absorption was suppressed. We have also noticed that sharp absorption structures around 2900 cm⁻¹, which are assigned to C-H stretch mode[2], became smaller concurrently. These results suggest that adsorption of H₂O molecules on SWNTs causes C-H bonding and induce semiconductor-metal transition of SWNTs.

[1] Ranjit Pati et al. Appl. Phys. Lett. **81**, 2638 (2002).

[2] A.V. Ellis et al. Nano Lett. **3**, 279 (2003).

Corresponding Author: Hiroyuki Yokoi

E-mail: yokoihr@kumamoto-u.ac.jp

Tel: 096-342-3727, **Fax:** 096-342-3710

2P-8

^{13}C NMR Study of C_{60} -Peapods

○ Kazuyuki Matsuda¹, Yutaka Maniwa^{1,3}, Hiromichi Kataura²,
Shinzo Suzuki¹, and Yohji Achiba¹

¹ Faculty of Science, Tokyo Metropolitan University, 1-1 Minami-osawa, Hachioji,
Tokyo 192-0397, Japan

² Nanotechnology Research Institute, National Institute of Advanced Industrial Science
and Technology (AIST), Central 4, Higashi 1-1-1, Tsukuba, 305-8562, Japan

³CREST, Japan Science and Technology Corporation

Single-wall carbon nanotubes (SWNTs) encapsulate many kinds of materials in their inner hollow cavities with a typical diameter of one nanometer. Materials confined in such small cavities are expected to show novel features which cannot be observed in bulk materials. Among this class of materials, the SWNTs filled with fullerenes (e.g., C_{60}), so-called “peapods”, where fullerene molecules form a 1D linear chain inside SWNTs, has attracted considerably attention due to their unusual electronic and structural properties as well as their potential applications. In particular, the linear chains of fullerene molecules inside SWNTs are of interest for the fundamental study of 1D solid. In order to study dynamics of C_{60} molecules forming 1D chain inside SWNTs, we have performed ^{13}C NMR lineshape and spin-lattice relaxation time (T_1) measurements in a wide temperature range from 4.2 to 300 K with using high purity ^{13}C -enriched C_{60} encapsulated SWNT samples. At low temperatures, the ^{13}C NMR spectrum shows a typical chemical-shift -anisotropy powder lineshape for sp^2 -carbon. This lineshape is qualitatively the same as that observed in low temperature sc phase of bulk C_{60} crystal. Above ~ 30 K, the motionally narrowed ^{13}C NMR spectra are observed due to the rotational C_{60} molecules. This indicates that the rotational motions of C_{60} molecules are fast on the NMR time scale of $\sim 10^{-5}$ s. From the T_1 results, no evidence for the orientational phase transition was obtained, not as in the 3D crystalline C_{60} . This suggests that a 1D fluctuation effect play an important role in the orientational dynamics of C_{60} inside SWNTs.

Corresponding Author: Kazuyuki Matsuda

E-mail: matsuda@phys.metro-u.ac.jp

Tel: +81-426-77-2498

Fax: +81-426-77-2483

Polarization dependence of photoluminescence excitation spectra of single-walled carbon nanotubes in UV-Vis range

○Yuhei Miyauchi and Shigeo Maruyama

Department of Mechanical Engineering, The University of Tokyo, 7-3-1 Hongo, Bunkyo-ku, Tokyo 113-8656, Japan

Photoluminescence excitation (PLE) spectroscopy of single-walled carbon nanotubes (SWNTs) have been extensively studied for characterization of their unique electronic properties due to the one-dimensionality. In our previous studies, the excitonic phonon sideband due to strong exciton-phonon interaction was clearly identified with the expected isotope shift by comparing PLE spectra of SW¹³CNTs and normal SWNTs [1]. In addition to the direct identification of excitonic-phonon sideband, we have also found that some PL peaks for cross-polarized excitation to the nanotube axis can be clearly observed in the PLE spectra of isolated SWNTs by polarized PLE spectroscopy [2]. The measured resonance energies for perpendicular excitations were considerably larger than the qualitative values predicted within a single-particle theory. These results indicate a smaller exciton binding energy for perpendicular excitations than for parallel excitations.

In this study, we focus on polarized PLE spectra for UV-Vis range. As shown in Fig.1, we found that there exist small, but nonzero intensity tails above the distinct peaks for perpendicular excitation, and the PL intensities corresponding to the perpendicular excitation were even comparable to those for the parallel excitation in a certain energy region in near UV range. This result indicates that one can not neglect the contribution of perpendicular excitations in optical measurements of SWNTs for Vis to UV range beyond E_{22} absorption.

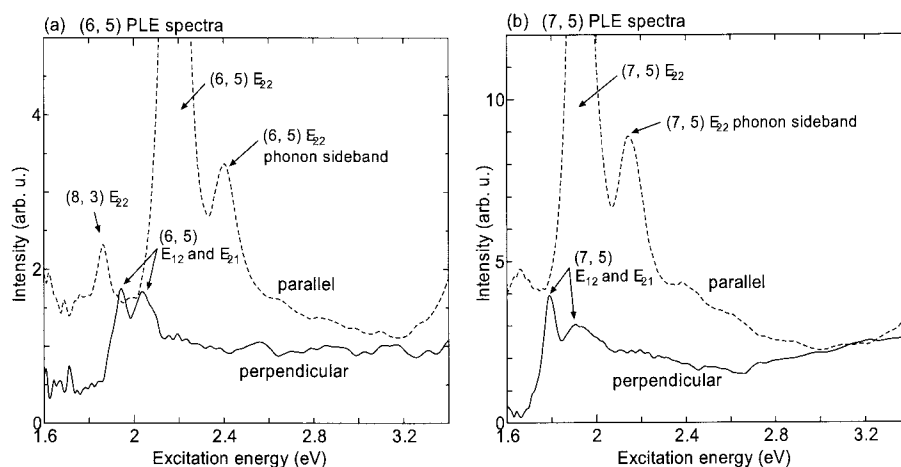


Fig. 1: Decomposed PLE spectra of (a) (6, 5) and (b) (7, 5) SWNTs for parallel (dotted line) and perpendicular (solid line) excitations. PLE spectra were measured along PL emission energies of 1.268 eV and 1.210 eV for (6, 5) and (7, 5) SWNTs, respectively.

[1] Y. Miyauchi, S. Maruyama, Phys. Rev. B, 74 (2006) 35415.

[2] Y. Miyauchi, M. Oba, S. Maruyama, Phys. Rev. B 74, (2006) 205440.

Corresponding Author: Shigeo Maruyama

E-mail: maruyama@photon.t.u-tokyo.ac.jp

2P-10

Individual solubilization of single-walled carbon nanotubes using totally aromatic polyimides

○Masahiro Shigeta, Kouhei Hirayama, Tsuyohiko Fujigaya, Naotoshi Nakashima

*Department of Applied Chemistry
Graduate School of Engineering, Kyushu University
744 Motoooka, Fukuoka 819-0395, Japan*

Carbon nanotubes (CNTs) have a high potential for applications in energy, electronics, IT and materials. However, their insolubility in solvents has hindered chemical approaches using CNTs. Our interest is focused on the fundamental properties and applications of soluble carbon nanotubes in aqueous and organic systems¹⁻³. Polymer wrapping is a powerful technique to construct CNTs-polymer composite materials. Polyimides are based on stiff aromatic backbones, and total aromatic polyimides are especially suitable polymers having unusual mechanical strength and high resistance to heat and chemical reactions. Combination of carbon nanotubes and polyimides is expected to play an important role in the development of novel nanocarbon composite polymers with high performance. We found that totally aromatic polyimides individually dissolve single-walled carbon nanotubes (SWNTs) in solutions.⁴ Here we report in detail the individual dissolution of SWNTs and the formation of organic gels of SWNTs using polyimides as solubilizers.

We synthesized several kinds of totally aromatic polyimides by the reactions of different tetracarboxylic dianhydride compounds and 4, 4'-diaminodiphenyl ether-2, 2'-disulfonic acid or 2, 2'-benzidinedisulfonic acid. Typical procedures for the solubilization of SWNTs are as follows. A certain amount of SWNTs was added to a solution of the polyimide, and the mixture was sonicated for 1 h, followed by centrifugation. Higher concentrations of SWNTs in polyimide solutions formed gels composed of individually dissolved SWNTs. The visible-near IR spectra of SWNTs/polyimides showed characteristic features assignable to individually dissolved SWNTs. We examined near-IR photoluminescence behaviors of the SWNTs/polyimide solutions. We also fabricated SWNTs/polyimide films by a casting method and characterized their spectral behaviors.

References:

1. N. Nakashima, *International J. Nanosci.* **2005**, *4*, 119-137
2. H. Murakami, N. Nakashima, *J. Nanosci. Nanotechnol.* **2006**, *6*, 16-27.
3. N. Nakashima, T. Fujigaya, H. Murakami, "Soluble Carbon Nanotubes", in "Chemistry of Carbon Nanotubes", eds, V. A. Basiuk, and E. V. Basiuk, American Scientific Publisher, in press.
4. M. Shigeta, M. Komatsu, N. Nakashima, *Chem. Phys. Lett.*, **2006**, *418*, 115-118.

Corresponding Author E-mail: nakashima-tcm@mbox.nc.kyushu-u.ac.jp

Tel&Fax: +81-92-802-2840

The relationship between the optical property and physical property of dispersed SWNTs under various pH conditions

OToru Ishii, Teruo Takahashi, Catalin Romeo Luculescu, Katsumi Uchida, Tadahiro Ishii, and Hirofumi Yajima

*Department of Applied Chemistry, Faculty of Science, Tokyo University of Science
12-1 Ichigaya Funagawara-machi, Shinjyuku-ku, Tokyo 162-0826, Japan*

It is known that optical properties of single-wall carbon nanotubes (SWNTs) are sensitive to external stimuli such as temperature or pH [1,2]. We have investigated pH effect on optical characteristics and dispersion states of SWNTs. Typical surfactants such as sodium dodecylsulfate (SDS) and polysaccharides such as carboxymethylcellulose (CMC) were used as dispersing agents. The spectroscopic properties of SWNTs dispersed using these agents were probed by UV-vis-NIR absorption, NIR photoluminescence and Raman scattering under various pH condition. Furthermore, the SWNTs molecular characteristics were analyzed with dynamic light scattering.

Absorption results indicated that the interband optical transitions originated from van Hove singularities were dependent on dispersing agent species and pH. Using SDS as a dispersing agent, the absorption peaks in the first semiconductive band range disappeared with decreasing pH, and aggregation of SWNTs was brought about at extremely high or low pH. On the other hand, SWNTs dispersed by CMC were stable at high pH above 3.5, where the absorption peaks remained unchanged. Nevertheless, at pH below 3.5, the SWNTs aggregation took place. The bleaching features of interband transition induced by protonation were significantly different between SDS and CMC systems. This result was ascribed to the discrepancy of the SWNTs dispersion mechanism between the SDS and CMC systems, in which the SWNTs would be dispersed in aqueous solution, accompanied by the formation of a micelle-like structure comprising inner core of SWNT and polymer wrapped SWNT, respectively.

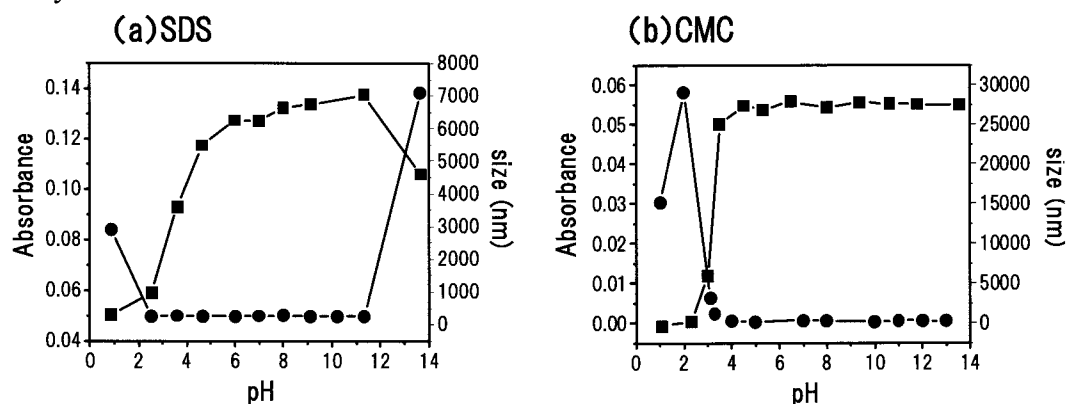


Fig. Plots of absorption intensity and cumulant diameter at various pH. (a)SDS, (b)CMC.

[1] P. Finnie, Y. Homma, and J. Lefebvre, *Phys. Rev. Lett.* **94**, 247401 (2005)

[2] M. S. Strano, C. A. Dyke, V. C. Moore, M. J. O'Connell, E. H. Haroz, J. Hubbard, M. Miller, K. Rialon, C. Kittrell, S. Ramesh, R. H. Hauge, R. E. Smalley, *J. Phys. Chem. B* **107**, 6979 (2003)

Corresponding Author: Hirofumi Yajima

TEL: +81-3-3260-4272(ext.5760), FAX: +81-3-5261-4631, E-mail: yajima@rs.kagu.tus.ac.jp

2P-12

Dispersion Behavior and Spectroscopic Properties of the Polymorphic Forms of Carbon Nanotubes in Biopolymer Aqueous Solutions

○Noriko Maeda, Katsumi Uchida, Tadahiro Ishii, and Hirofumi Yajima

*Department of Applied Chemistry, Faculty of Science, Tokyo University of Science
12-1 Funagawara-machi, Shinjyuku-ku, Tokyo 162-0826, Japan*

Carbon nanotubes (CNTs) have attracted a lot of attention as multifunctional material for its potential applications in various fields due to their unique structural and electronic properties. There exist the polymorphic forms of CNTs, such as single-walled carbon nanotubes (SWNTs), double-walled carbon nanotubes (DWNTs), multi-walled carbon nanotubes (MWNTs). Strong van der Waals force of CNT makes bundles among CNTs, which prevents CNTs from practical application and spectroscopic analysis. We have so far developed effective dispersion procedures for debundling SWNTs with some biopolymers such as chitosan and carboxymethylcellulose (CMC) in aqueous solutions, and then scrutinized the spectroscopic properties of the dispersed SWNTs, with reference to the dispersed SWNTs-surfactant solutions. In this paper, we have investigated the dispersion behavior for the polymorphic forms of CNTs including vapor-grown carbon fiber (VGCF) by using some biopolymers and surfactants as dispersants, in comparison with that of SWNT. SWNTs were obtained from Carbon Nanotechnologies, Inc., DWNTs from Nanocyl, Co., MWNTs from MTR Ltd., and VGCF from Showa Denko Co.. CNTs were added to each of dispersant aqueous solution, and homogenized by a tip type sonicator. The obtained black solution was ultracentrifugated to remove large bundles of CNTs. After centrifugation, the upper 80% supernatants were collected for further measurements. The dispersion and spectroscopic properties of the polymorphic forms of CNTs were measured by UV-vis NIR absorption, Raman, and photoluminescence spectroscopies and ζ -potential. The dispersion solution for all of polymorphic forms of CNTs with chitosan and CMC as dispersants indicated higher absorbances at 500 nm and ζ -potentials, compared to other dispersants. Consequently, chitosan and CMC were found to be effective dispersants for DWNT, MWNT, and VGCF, and CNT diameter size and aspect ratio are not responsible for the dispersion mechanism and behavior.

References:

[1]T.Takahashi et al. *Jpn.J.Appl.Phys* **43** (2004) 3636

[2]T.Takahashi et al. *Chem.Lett.* **11** (2005) 1516

Corresponding Author : Hirofumi Yajima

E-mail : yajima@rs.kagu.tus.ac.jp

Tel : +81-3-3260-4272(ext.5760) , **Fax**:+81-3-5261-4631

Reduction kinetics of cytochrome *c* through single-walled carbon nanotubes

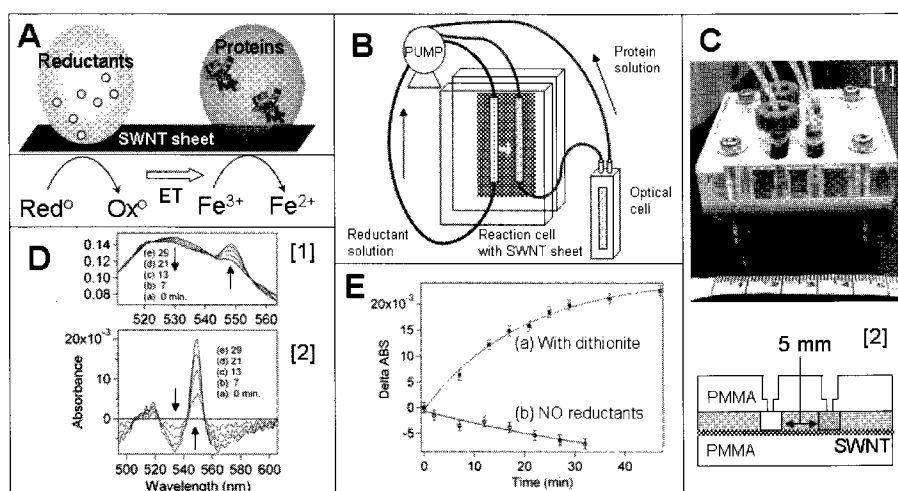
○Koji Matsuura, Takeshi Saito, Satoshi Ohshima, Motoo Yumura, and Sumio Iijima

Research Center for Advanced Carbon Materials, National Institute of Advanced Industrial Science and Technology (AIST), Tsukuba, 305-8565

We have previously reported electron transfer (ET) through a single-walled carbon nanotubes (SWNTs) sheet between two redox reactions as shown in Fig. A (1). However, several problems for the clarification of the reaction schemes still remained. Because of determination of the rate-determining step, kinetics of the reactions should be investigated.

To solve these problems, we have developed a flow-reaction system with an ET reaction cell including a SWNT sheet as shown in Fig. B (2). This system contains a pump, the reaction cell (Fig. C), and a quartz optical cell. By absorption spectral changes of 15~20 μM cytochrome *c* (cyt *c*), rates of the reduction were surveyed. For the reductant, we selected dithionite ($\text{Na}_2\text{S}_2\text{O}_4$), because the kinetics of direct mixing with cyt *c* are known ($k_{\text{obs(mix)}} = 24[\text{Na}_2\text{S}_2\text{O}_4]^{1/2} + 250[\text{Na}_2\text{S}_2\text{O}_4]$ (min^{-1})) (3).

In [1] and [2] of Fig. D, the time-resolved spectra of cyt *c* and the difference spectra from that of (a) 0 min after circulating 100 mM dithionite were shown, respectively. Calculated final concentration of the reduced forms was $\sim 2 \mu\text{M}$. Absorption at 550 nm in the difference spectra are shown in Fig. E. These data points were fitted by a single exponential curve. The rates ($k_{\text{obs}} = 0.05 \pm 0.01$ (min^{-1})) are similar in the conditions of 10 and 100 mM dithionite solutions. Our results suggest that the distance between the two solutions and morphology of the SWNT-bundles on the sheet would mainly affect the reduction kinetics of cyt *c*. By comparing the rate of the reduction and the amount of the reduced cyt *c*, the direct mixing of the reductant would be a minor effect. For the further understanding of the reduction scheme, we are researching the dependence of the kinetics on the SWNT sheets, reductants, and redox proteins.



Figures (A) Previous experimental system and a proposed reaction scheme.

(B) Schematic view of the developed flow-reaction system. Total volume of reductant and cyt *c* solutions was ca. 1.5 and 2.8 ml, respectively. Flow-rate was set at 1~3 ml/min.

(C) [1] A picture and [2] a cross-sectional figure of the developed reaction cell.

(D) [1] Time-resolved absorption spectra of cyt *c*. [2] Difference spectra. (a) 0 (ferric), (b) 7, (c) 13, (d) 21, and (e) 29 min after circulating at room temperature.

(E) Time-dependent changes of absorption at 550 nm in difference spectra with circulation of (a) 100 mM dithionite solution and (b) no reductants (control). The trace is an exponential fit of the points. The decrease of absorbance in the trace (b) is due to loss of the protein.

References: 1: Matsuura, K. et al. *31st Fullerene-Nanotubes General Symposium 2006*, 2P-52,

2: Saito, T. et al. *J. Phys. Chem. B* **2006**, 110, 5849-5851,

3: Lambeth, D. et al. *J. Biol. Chem.* **1973**, 248, 6095-6103,

Corresponding Author Koji Matsuura

E-mail koji-matsuura@aist.go.jp **Tel:** +81-29-861-4654; **Fax:** +81-29-861-4851

Preparation of Single-Walled Carbon Nanotube-Organosilicon Hybrids and Their Field Emission Properties

○Yutaka Maeda,^{1,2} Tadashi Hasegawa,¹ Yoshinori Sato,³ Kazuyuki Tohji,³ Masahiro Kako,⁴ Takatsugu Wakahara,⁵ Takeshi Akasaka,⁵ Jing Lu,⁶ Shigeru Nagase⁷

¹Department of Chemistry, Tokyo Gakugei University, Tokyo 184-8501, Japan, ²PRESTO, Japan Science and Technology Agency (JST), Japan, ³Graduate School of Environmental Studies, Tohoku University, Sendai 980-8579, Japan, ⁴Department of Chemistry, The University of Electro-Communications Tokyo 182-8585, Japan, ⁵Center for Tsukuba Advanced Research Alliance, University of Tsukuba, Tsukuba 305-8577, Japan, ⁶Department of Physics, Peking University, Beijing 100871, People's Republic of China, ⁷Department of Theoretical Molecular Science, Institute for Molecular Science, Okazaki 444-8585, Japan

SWNTs have been used as field emission sources of field emission display devices because of their unique structures and prominent stability.¹ It is well-known that adsorption of various gases on SWNTs leads to different field emission characteristics. Organosilicon compounds, in which extensive delocalization of σ electrons takes place along the silicon chain, have many unique and interesting electronic properties. We report here preparation of SWNTs-organosilicon hybrids and their field emission properties.

For preparation of SWNTs-organosilicon hybrids, covalent and non-covalent bonds formation was carried out. Irradiation of a degassed suspension of SWNTs with disilane resulted in formation silylated SWNTs (SWNTs-1).^{2,3} The field emission currents were measured as a function of applied voltage at a pressure of 1.0×10^{-7} Torr for spacer of 10 mm between a cathode of the SWNTs tips and an anode of the Faraday cup. Isosceles triangle shaped SWNTs tips were cut out from the mats of SWNTs, SWNTs-1, and SWNTs/1 (physisorption) using a razor, and were fixed on top of hair-pin shaped wires using Ag paste to measure the FE properties, respectively.

From the I-V characteristics, the turn-on voltage decreases from 400 to 200 V / 0.1 pA by silylation, and the field emission current increases from 10^{-8} to 10^{-6} A at a voltage of 500 V. We compared the field emission properties between SWNTs and SWNTs/1. SWNTs/1 shows a lower gate voltage (250 V / 0.1 pA) than SWNTs, suggesting that the intermolecular σ - π interaction between SWNTs and organosilicon compound also enhances effectively the field emission of SWNTs. To understand the above experimental results, we have also studied the interaction of SiH_2 and Si_2H_6 with the Semiconducting (10,0) SWNT and that of SiH_2 with the metallic (5,5) SWNT by using local density functional theory.

References: 1. Y. Saito, et al., **38**, 169 (2000). 2. Y. Maeda, et al., **68**, 6791 (2003). 2. Y. Maeda, et al., *Chem. Mater.* **18**, 4205 (2006).

Corresponding Author: Yutaka Maeda

E-mail: ymaeda@u-gakugei.ac.jp

Tel&Fax: +81-42-329-7512

Assembly and Fluorescence Visualization of Carbon Nanotubes

○Fumihito Arai¹, Moeto Nagai², Akio Shimizu³,
Akihiko Ishijima⁴, Toshio Fukuda²

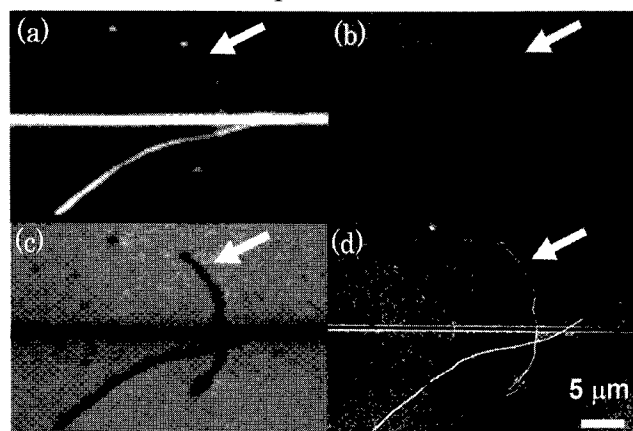
¹*Department of Bioengineering and Robotics, Tohoku University*

²*Department of Micro-Nano Systems Engineering, Nagoya University*

³*Department of Applied Physics, Nagoya University*

⁴*Institute of Multidisciplinary, Research for Advanced Materials, Tohoku University*

Abstract: We demonstrate visualization method of carbon nanotubes (CNTs) in water with fluorescent microscopy through quenching effect that cause a decrease of fluorescent intensity around CNTs. Reversal contrast in fluorescence imaging of the CNTs was observed in fluorescent dye solution. We could observe CNTs under a constant excitation light for more than ten minutes. Dielectrophoretic force was used for CNTs deposition onto electrodes that consist of transparent conductive film. Scanning electron microscope revealed that CNTs of 80 nm in diameter were observed with fluorescent microscopy. The positions of the CNTs tips were observed under optical microscope. It can be applied for biological sensing devises with nanomanipulation.



(a) Dark-field, (b) bright field, (c) fluorescent, and (d) scanning electron microscopy image of CNTs attached onto ITO electrode. The CNTs indicated by the red arrows are 80 nm in diameter.

Reference:

F Arai, M. Nagai, A. Shimizu, A. Ishijima, T. Fukuda, Fluorescence Visualization of Carbon Nanotubes Using Quenching Effect for Nanomanipulation, Proc. IEEE-NEMS, January 18-21, 2007 (To appear)

Corresponding Author: Fumihito Arai, Tohoku University, Japan

E-mail: arai@imech.mech.tohoku.ac.jp

Tel&Fax: +81-22-795-6966 (T), +81-22-795-6967 (F)

Self-Organized Single-Walled Carbon Nanotubes with Honeycomb Structures

○Hisayoshi Takamori, Tsuyohiko Fujigaya, Yasuro Niidome, and Naotoshi Nakashima

*Department of Applied Chemistry, Graduate School of Engineering, Kyushu University,
744 Motoooka, Nishi-ku, Fukuoka 819-0395, Japan*

Potential applications using carbon nanotubes (CNTs) are often limited due to their insolubility in many solvents due to strong intertube van der Waals interactions. Therefore, strategic approaches toward the solubilization of CNTs should be important for the applications of CNTs.¹⁻³ We report here the first finding that a simple solution casting of carbon nanotubes/lipid complex (complex **1**) produces self-organized honeycomb structures. The mixing of aqueous solution of single-walled carbon nanotubes (SWNTs) with aqueous molecular-bilayers of an artificial ammonium lipid produced a precipitate, which was collected to obtain complex **1** that is soluble in organic solvents. A simple solution casting of the complex **1** was found to produce self-organized honeycomb structures (**Figure 1-a**), whose cell sizes were controllable by changing experimental conditions. The lipid part of complex **1** was easily removed by an “ion exchange” method with maintaining the basic honeycomb structures (**Figure 1-b**). After the ion-exchange, the films with thinner skeletons exhibited dramatic decrease of the surface resistivity from insulating to (semi)conducting.

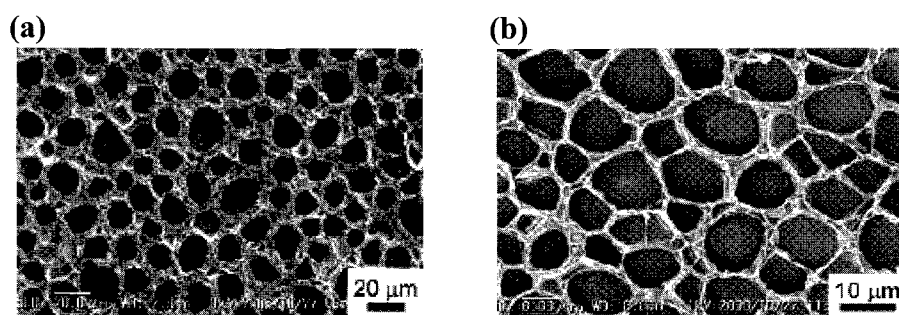


Figure 1. Typical SEM images for the films casting from a chloroform solution of complex **1** before (a) and after (b) the ion exchange.

References

- [1] N. Nakashima, *Int. J. Nanosci.* **2005**, *4*, 119-137.
- [2] H. Murakami, N. Nakashima, *J. Nanosci. Nanotechnol.* **2006**, *6*, 16-27.
- [3] N. Nakashima, T. Fujigaya, H. Murakami, “Soluble Carbon Nanotubes”, in “Chemistry of Carbon Nanotubes”, eds, V. A. Basiuk, and E. V. Basiuk, American Scientific Publisher, in press.

Corresponding Author : Naotoshi Nakashima

E-mail : nakashima-tcm@mbox.nc.kyushu-u.ac.jp

Tel & Fax : +81-92-802-2840

Raman spectroscopic study on size-selected linear polyynes inside single-wall carbon nanotubes

○D. Nishide¹, T. Wakabayashi², T. Sugai¹, R. Kitaura¹,
H. Kataura³, Y. Achiba⁴, and H. Shinohara¹

¹*Department of Chemistry, Nagoya University, Nagoya 464-8602, Japan*

²*Department of Chemistry, Kinki University, Higashi-Osaka 577-8502, Japan*

³*Nanotechnology Research Institute, AIST, Tsukuba 305-8562, Japan*

⁴*Department of Chemistry, Tokyo Metropolitan University, Hachioji 192-0397, Japan*

In interstellar space, there are many organic molecules/ions which are oftentimes unstable and reactive under conventional experimental conditions [1]. Especially, linear formed hydrocarbons, *i.e.* linear-polyynes ($C_{2n}H_2$, $n \geq 2$), are typical such molecules among them because of their simple structure and of an ideal π -conjugated electronic system. In experimental studies, however, the molecule has been thought to be unstable due to their high reactivity leading to polymerization. The instability of the molecules precludes such linear-polyynes from fundamental spectroscopic characterization.

Very recently, we have reported that linear-polyynes $C_{10}H_2$ molecules are successfully encapsulated inside single-wall carbon nanotubes (SWNTs) [2] and that labile polyynes can be treated in usual experimental field, *i.e.* in solid, under air, and at room temperature conditions

In the present study, we will focus on the following two points: 1) diameter dependence of SWNTs on encapsulation efficiency; and 2) length dependence of polyynes on the encapsulation. Three kinds of SWNTs films having different diameter distribution and four kinds of polyynes family, *i.e.* C_8H_2 , $C_{10}H_2$, $C_{12}H_2$, and $C_{14}H_2$, were produced and purified for the present study, which have been used to prepare several kinds of polyynes-peapods (polyynes-encapsulating SWNTs). Spectroscopic properties of polyynes molecules inside SWNTs will be discussed based on Raman spectroscopy.

References:

- [1] P. Ehrenfreund et al., *Annu. Rev. Astron. Astrophys.* **38** (2000) 427, and references therein.
- [2] D. Nishide et al., *Chem. Phys. Lett.* **428** (2006) 356.

Corresponding Author: Hisanori Shinohara

TEL: +81-52-789-2482 / FAX: +81-52-789-1169 / E-mail: noris@cc.nagoya-u.ac.jp

2P-18

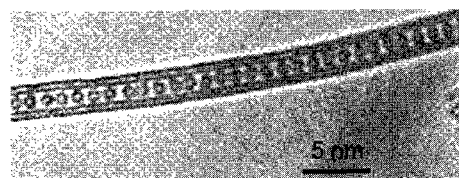
Synthesis and Characterization of C₆₀ and C₇₀ Double-Wall Carbon Nanopeapods

○Guoqing Ning^a, Naoki Kishi^b, Haruya Okimoto^b, Masahiro Shiraishi^b, Toshiki Sugai^b, Hisanori Shinohara^{a,b,*}

CREST, Japan Science and Technology Agency, c/o Department of Chemistry, Nagoya University, Nagoya 464-8602, Japan

Department of Chemistry and Institute for Advanced Research, Nagoya University, Nagoya 464-8602, Japan

Double-wall carbon nanotubes (DWNTs) encapsulating C₆₀ and C₇₀ fullerenes, the so-called (C₆₀)_n@DWNTs and (C₇₀)_n@DWNTs peapods, have been synthesized in high yield by the vapor reaction method¹. TEM observation and powder XRD analysis have confirmed a relatively high filling factor of the so-prepared fullerene peapods. Rotation of encapsulated C₇₀ molecules has clearly been observed, as shown in the image above, which indicates a weak interaction between fullerenes and DWNTs.



Washing treatment with ultrasonication has been able to completely remove C₇₀ molecules both inside and outside DWNTs, whereas without ultrasonication, only C₇₀ attached from outside were removed. Powder XRD and Raman spectra analyses were used to characterize the peapods prepared by different washing processes.

Based on a detailed experimental comparison, charge transfer between fullerenes and nanotubes² has been evidenced by upshift and downshift of Raman RBM peaks, respectively due to the fullerenes attached from outside together with the fullerenes encapsulated inside DWNTs.

Furthermore, an 1200 °C heat treatment in vacuum was performed on (C₆₀)_n@DWNTs peapods.² The observed different type of structural transformation upon such heat treatment shows that the interaction exerted between fullerenes and nanotubes varies on the encapsulation structures of fullerenes..

(1) Hirahara, K.; Suenaga, K.; Bandow, S.; Kato, H.; Okazaki, T.; Shinohara, H.; Iijima, S. *Phys. Rev. Lett.* **2000**, *85*, 5384.

(2) Bandow, S.; Takizawa, M.; Hirahara, K.; Yudasaka, M.; Iijima, S. *Chem. Phys. Lett.*, **2001**, *337*, 48.

Corresponding Author: Hisanori Shinohara, noris@cc.nagoya-u.ac.jp, TEL: +81-52-789-2482, FAX: +81-52-789-1169

2P-19

Structure and phase behavior of quasi-one-dimensional water

○Daisuke Takaiwa, Kenichiro Koga and Hideki Tanaka

*Department of Chemistry, Faculty of Science, Okayama University,
3-1-1 Tushima-naka, Okayama 700-8530, Japan*

A material confined in extremely narrow space may exhibit properties that the bulk material never does. When water is confined in carbon nanotubes, quasi-one-dimensional solids called "ice nanotubes" form spontaneously when temperature is lowered and moreover the freezing transition can be continuous, which suggests an existence of liquid-solid critical points in quasi-one-dimensional systems.¹ In the quasi-two-dimensional systems water may form a bilayer crystal and a bilayer amorphous, both resulting from a liquid via a first-order phase transition².

Molecular simulations and thermodynamics analyses are carried out to investigate water confined in a quasi-one-dimensional space surrounded by a hydrophobic wall. The structures of solid water under various thermodynamic conditions are classified in a systematic fashion.

Constant-temperature and constant-volume molecular simulations are carried out to seek novel structures of water at fixed densities corresponding to high pressure states. Several structures are found in this step and several related structures are implied as possible phases. Obtained structures of solid water can be classified into two closely-packed forms of solid water: one is N -gonal ice nanotubes and the other is N -helical ice nanotubes, both of the inner spaces being filled with water molecules^{3,4}.

References

- [1] K. Koga, G. T. Gao, H. Tanaka, and X. C. Zeng, *Nature* (London) **412**, 802 (2001).
- [2] K. Koga, X. C. Zeng, and H. Tanaka, *Phys. Rev. Lett.* **79**, 5262-5265 (1997).
- [3] D. Takaiwa, K. Koga, and H. Tanaka, in preparation.
- [4] D. Takaiwa, K. Koga, and H. Tanaka, *Mol. Simul.*, (accepted)

Corresponding Author : Daisuke Takaiwa

E-mail : dns18303@cc.okayama-u.ac.jp

Phase behavior of simple fluids in cylindrical and slit pore

○Yoshinobu Hamada, Kenichiro Koga, and Hideki Tanaka

Department of Chemistry, Okayama University, Okayama 700-8530, Japan

Abstract: When a fluid is confined in a nano pore, its properties are strongly affected by the pore size, shape, dimensionality, physical and chemical properties, etc. Structure and phase behavior of the fluid in such extreme confinement are qualitatively different from, and often much richer than, its bulk counterparts[1-3]. Our goal is to gain quantitative information on how each element that defines the pore is correlated with the phase behavior.

Components of the pressure tensor of a confined fluid are in general different from the equilibrium pressure of the bulk fluid, but how the pressure tensor is related with the bulk pressure has remained to be answered. It is found in the model systems that the component P_x of the pressure tensor in the direction parallel to the slit-pore wall or to the axis of the cylindrical pore is linearly correlated with the equilibrium pressure P of the bulk fluid only in a limited range of P , and the range decreases with decreasing the pore size.

It is always the case that the fluid in the hard pore with no potential field does not undergo a gas-liquid phase change, discontinuous or continuous, before the equilibrium bulk fluid does as the chemical potential is increased at fixed temperature. But the model potential field of a single-walled carbon nanotube is found to reverse the order, that is, a gas-to-liquid phase change occurs in the pore before it does in the bulk fluid. If a hard cylindrical pore has a uniform potential field with the value ($-0.832 A\epsilon$) of the carbon nanotube potential at the center of the pore, then the gas-liquid phase change of the confined fluid occurs at the chemical potential close to (but slightly larger than) the value at which the bulk phase transition occurs.

References:

- [1] L. D. Gelb and K. E. Gubbins and R. Radhakrishnan and M. Sliwinska-Bartkowiak, *Rep. Prog. Phys.*, **62**, (1999).
- [2] H. K. Christenson, *J. Phys.: Condens. Matter.*, **13**, R95 (2001).
- [3] K. Koga, G.T. Gao, H. Tanaka, and X.C. Zeng, *Nature*, **412**, 802 (2001)

Corresponding Author Yoshinobu Hamada

E-mail dns17351@cc.okayama-u.ac.jp

Structural Characterization of Single-Wall Carbon Nanotubes and Fullerene-Nanopeapods by X-ray Diffraction Measurement

Yuko Kato¹, Ryo Kitaura¹, Takao Akachi¹, Shinobu Aoyagi², Eiji Nishibori², Makoto Sakata², Hisanori Shinohara^{1,3*}

¹Department of Chemistry, Nagoya University, Nagoya 444-8602, Japan

²Department of Applied physics, Nagoya University, Nagoya 444-8602, Japan

³Institute for Advanced Research, Nagoya University, and CREST/JST

The so-called Nanopeapods have attracted wide range of researchers owing not only to their interesting low-dimensional structure but also to possible applications such as field effect transistors and molecular devices. Structural characterization of nanopeapods is very important to understand physical properties of the peapods in detail and to investigate application of peapods. Usually, characterization of synthesized peapods has been carried out by transmission electron microscope (TEM). However, TEM observation provides us only local structure information. Therefore, it has been difficult to determine important structural information such as diameter distribution of SWNTs, filling ratio of fullerene peas and mean inter-fullerene distances by TEM observation. X-ray diffraction is a complementary method, which provides us bulk structure information. Here we report structural characterization of SWNTs and nano-peapods by using XRD measurements.

SWNTs were prepared by the laser ablation method, and peapods were synthesized by putting purified fullerenes and open-ended SWNTs in quartz tube at 400~500 °C in vacuum. Prior to X-ray diffraction measurements, the peapods synthesized, (C₆₀)_n@SWNTs and (Y@C₈₂)_n@SWNTs, were heated in vacuum and sealed in a borosilicate capillary to remove adsorbed gases and water molecules. The x-ray wavelength used in this diffraction studies is 0.70927 Å (Mo K α).

Figure 1 shows XRD patterns of pristine SWNTs and (Y@C₈₂)@SWNT. Due to the encapsulation of Y@C₈₂ molecules, the intensity of 10 peaks, which are around $Q = 0.4$, have significantly decreased. On the other hand, a new peak arising from 1-dimensional regulated array of Y@C₈₂ appeared at around $Q = 0.6$. We have successfully simulated observed diffraction patterns by assuming cylindrical electron density and double shell electron density for SWNTs and encapsulated Y@C₈₂ molecules, respectively. From comparison between simulated and observed patterns, the filling ratio was determined. We will also discuss the reaction time dependence of fullerene filling ratio.

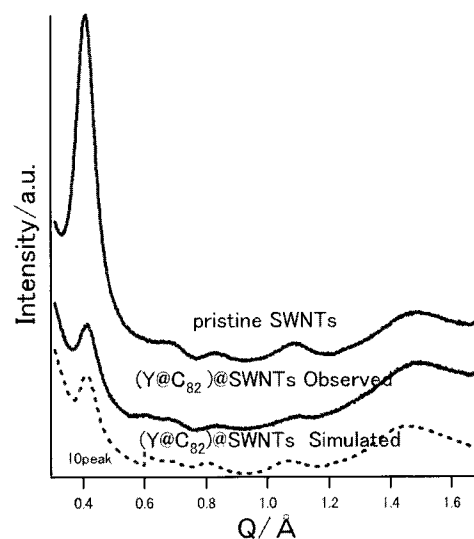


Figure 1. XRD patterns of pristine SWNTs and (Y@C₈₂)@SWNTs

Corresponding Author: Hisanori Shinohara

TEL: +81-52-789-2482, FAX: +81-52-789-1169, E-mail: noris@cc.nagoya-u.ac.jp

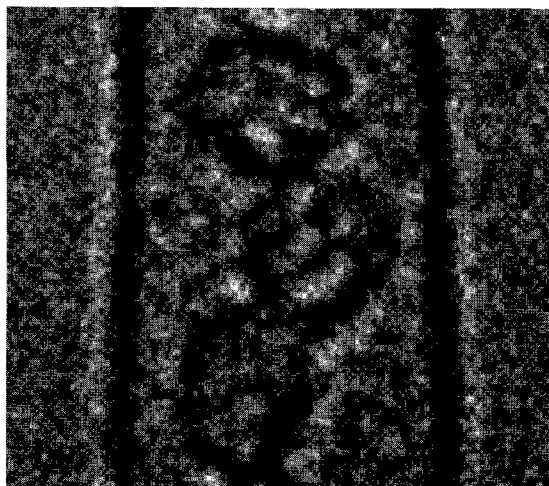
HR-TEM observations of structural isomers of C₈₂ with the C₂ symmetry

○Hideaki Wakabayashi, Shingo Okubo, Masanori Koshino¹, Yuta Sato, Takeshi Saito,
Toshiya Okazaki and Kazu Suenaga

Research Center for Advanced Carbon Materials, AIST, Tsukuba 305-8565, Japan
¹*ERATO-JST, AIST, Tsukuba 305-8565, Japan*

High-resolution transmission electron microscopy (HR-TEM) has been recently used to determine the structural isomers of metallofullerenes which were encapsulated in SWNTs [1, 2]. Since only the encapsulated metal atoms with larger atomic numbers were imaged by HR-TEM in these studies, the structures of fullerene cage have been unidentified. In order to identify the fullerene cage structure, the point resolution of HR-TEM should be pushed down to 0.14 nm. We have used the HR-TEM 2010F with a post-column Cs corrector so that the intra-molecular structure of fullerene cages can be recognized. The C₈₂ fullerene molecules with the C₂ symmetry were chosen and encapsulated into the SWNTs with larger diameters (1.6 ~ 2.2 nm) by the liquid phase.

Fig. 1 shows a typical HR-TEM image of the C₈₂ peapods in which the intra-molecular structures of encapsulated fullerenes are clearly visible. One should notice that the image contrast appeared in the fullerene cage is attributed to the moiré pattern with the graphene network of SWNT wall, therefore great caution should be taken to analyze the intra-cage structures in the HR-TEM images. The C₈₂ fullerenes occasionally rotate inside the SWNTs. This rotation enables a convincing analysis of the molecular structures because HR-TEM images of particular molecule with different orientations can be obtained. Comparison with the simulated HR-TEM images for three possible structural isomers of C₈₂ cage (C₂_1, C₂_3, C₂_5) was made.



[1] K. Suenaga, T. Okazaki, C.-R. Wang, S. Bandow, H. Shinohara and S. Iijima, *Physical Review Letters*, 90 (2003) 055506

[2] Y. Sato, T. Yumura, K. Suenaga, H. Moribe, D. Nishide, M. Ishida, H. Shinohara and S. Iijima, *Physical Review B* 73 (2006) 193401

Corresponding Author: Kazu Suenaga

E-mail: suenaga-kazu@aist.go.jp, **Tel:** 029-861-6850, **Fax:** 029-861-4860

Fig. 1 A typical HR-TEM image of C₈₂ peapod.

Enhanced Structural Stability of C₆₀-Peapods toward Thermal Oxidation and Electron Beam Irradiation

○M. Shiraishi, S. Kuwahara, D. Nishide, Y. Ito, R. Kitaura, T. Sugai, and H. Shinohara

Department of Chemistry, Nagoya University, Nagoya 464-8602, Japan

Thermal oxidation is one of the most powerful and effective methods for the purification of carbon nanotubes and also for enrichment of double-wall carbon nanotubes (DWNTs) [1]. To date, however, the detailed oxidation mechanism of carbon nanotubes has not been clarified yet. Furthermore, the so-called fullerene-nanopeapods are considered to be more resistant toward thermal oxidation and might have a higher mechanical stability than the pristine single-wall carbon nanotubes (SWNTs). In the present study, structural changes of fullerene encapsulated SWNTs against thermal heating and electron beam irradiation are investigated by using atomic force microscope (AFM) and transmission electron microscope (TEM) observations.

Synthesis and preparation of C₆₀-peapods were performed by the method already reported [2]. The sample substrates with C₆₀-peapods were heated in dry air at 500 °C for 10 min for oxidation. After cooling down to room temperature, morphological changes of the peapods were observed by AFM. This procedure was repeated for 4 times, *i.e.* peapods were heated for 40 minutes in total. The same samples were also observed by high-resolution TEM under 120 keV electron irradiation. As a reference, two kinds of undoped SWNTs (as-produce and purified) were also prepared, oxidized and characterized in a similar manner.

Figure 1 shows typical AFM images of (a) C₆₀-peapods and (b) pristine nanotubes before/after the thermal heating. Undoped SWNTs are decomposed almost completely by the oxidation at 500 °C, whereas only a little structural changes are occurring in C₆₀-peapods. The results suggest that the peapods have much higher oxidation stability than undoped SWNTs.

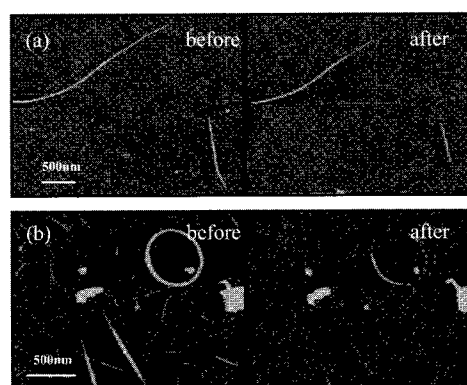


Fig.1: AFM images of (a) C₆₀-peapods and (b) undoped SWNTs before/after thermal heating.

References:

- [1] T. Sugai *et al.*, *Nano Lett.* **3** (2003) 769.
 [2] K. Hirahara *et al.*, *Phys. Rev. Lett.* **85** (2000) 5384.

Corresponding Author: H. Shinohara.

E-mail: noris@cc.nagoya-u.ac.jp **TEL:** +81-52-789-2482, **FAX:** +81-52-789-1169

Synthesis and Characterization of Carbon Nanotubes Encapsulating Metal Complexes

○D. Ogawa^{1,2}, M. Ishida¹, D. Nishide¹, R. Kitaura¹, T. Sugai^{1,3}, and H. Shinohara^{1,2,3}

¹*Department of Chemistry, Nagoya University, Nagoya 464-8602, Japan*

²*CREST, Japan Science and Technology Corporation, c/o Department of Chemistry, Nagoya University, Nagoya 464-8602, Japan*

³*Institute for Advanced Research, Nagoya University, Nagoya 464-8602, Japan*

Single-walled carbon nanotubes (SWNTs) can encapsulate various foreign molecules or compounds. Those newly formed materials are expected to have novel properties and functions[1]. In particular, SWNTs encapsulating metallofullerenes (so-called, “peapod”) have been attracting wide interests due to their unique properties originated from special interaction between metals and SWNTs through carbon cages. But, much metal-richer complexes and new synthesis methods are desired since the metal/carbon ratio and the filling ratio of the metallofullerenes are still not enough. Here, we present new synthesis of SWNTs encapsulating new metal complexes, $\text{Er}(\text{C}_5\text{H}_5)_3$ (ErCp_3) and Pd nano-rods, namely, $\text{ErCp}_3@$ SWNTs and $\text{Pd}@$ SWNTs, with the filling ratio higher than the previous reports[2].

ErCp_3 was encapsulated with the gas phase sublimation at 200 °C for 3 days, where the temperature is much lower than that for metallofullerenes. On the other hand, $\text{Pd}@$ SWNTs was synthesized through the newly developed liquid phase method. Aqueous solution of PdCl_2 was injected into SWNTs by capillary action in a vacuum. Further injection of PdCl_2 is performed by heat treatment at 80 °C in Ar for a day. PdCl_2 in SWNTs was reduced to Pd nano-rods by NaBH_4 .

Both $\text{ErCp}_3@$ SWNTs and $\text{Pd}@$ SWNTs were characterized with TEM and EDX (JEOL JEM-2100F). A TEM image of $\text{ErCp}_3@$ SWNTs (Fig.1) shows ErCp_3 as periodic dot-like contrasts along the SWNT. The distance between dots is 0.94 nm, which corresponds to the size of a ErCp_3 molecule (Fig.2). TEM images in Fig.3(a) and (b) show that PdCl_2 was converted into Pd nano-rods in SWNTs. During reduction, the weak fog-like contrast of PdCl_2 changed the strong rod-like contrast of Pd in SWNTs. This results revealed that “the aqueous solution methods” have high potential to insert various metals into SWNTs. The existence of both ErCp_3 and Pd was also confirmed by EDX.

Based on these results, we intend to perform further characterization of their structures and optical and magnetic properties, which should be utilized for promising devices.

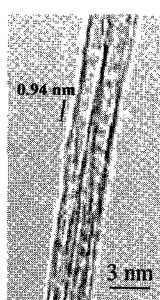


Fig.1 TEM image of $\text{ErCp}_3@$ SWNTs

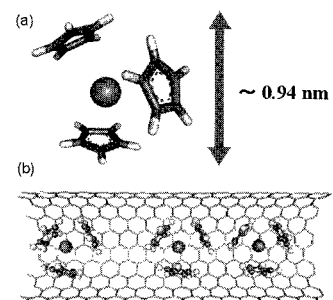


Fig.2 (a) ErCp_3 and (b) $\text{ErCp}_3@$ SWNTs

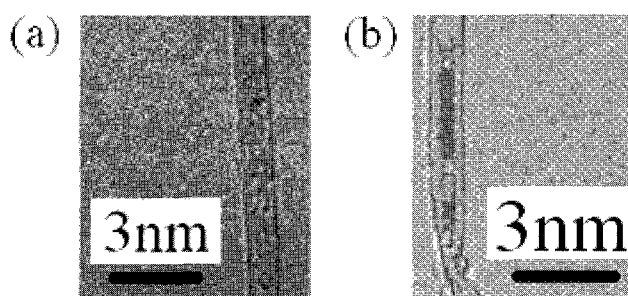


Fig.3 TEM image of (a) $\text{PdCl}_2@$ SWNTs and (b) $\text{Pd}@$ SWNTs

[1] A. Javey et al., *Nano Lett.*, 5, 345 (2005).

[2] L. J. Li et al., *Nat. Mater.*, 4, 481 (2005).

Corresponding Author Hisanori Shinohara

E-mail nori@nano.chem.nagoya-u.ac.jp, **Tel:** (+81) 52-789-2482, **Fax:** (+81) 52-789-1169

Energetics of Ice Nanotubes inside Carbon Nanotubes

○Takahiro Kurita,¹ Susumu Okada,^{1,2,3} and Atsushi Oshiyama^{1,2,3}¹*Graduate School of Pure and Applied Sciences, University of Tsukuba,
Tennodai, Tsukuba 305-8571, Japan*²*Center for Computational Sciences, University of Tsukuba,
Tennodai, Tsukuba 305-8577, Japan*³*CREST, Japan Science and Technology Agency,
4-1-8 Honcho, Kawaguchi, Saitama 332-0012, Japan*

Water is familiar and indispensable to human beings and a lot of works have been performed to clarify its properties. In particular, more than ten polymorphs have been identified in its solid form (ice) and a new polymorph is still quested.

Recent X-ray diffraction measurements have found that liquid phase water inside carbon nanotubes (CNTs) is transformed to several solid phases at around room temperature.¹ It is argued that stable structures have the shape of polygonal ice nanotubes (ice NTs) which is originally proposed by molecular dynamics simulations.² This structure draws attention as a new polymorph of ice.

We have performed total-energy electronic-structure calculations based on density functional theory to discuss energetics of ice NTs and its encapsulation by CNTs. We have found that ice NTs themselves have about 500 meV cohesive energies which are about 70% of corresponding value of the most stable bulk ice Ih, and thus ice NT is a new family of ice polymorphs. On the other hand, energy gain upon encapsulation inside CNT is about 10 meV per water molecule. For electronic structures, we have found that band structures of ice NT encapsulated in CNT is a simple superposition of those of the constituents. These features reflect weak interaction between water molecule and CNT and therefore we conclude that CNT acts as a template to forge ice NT.

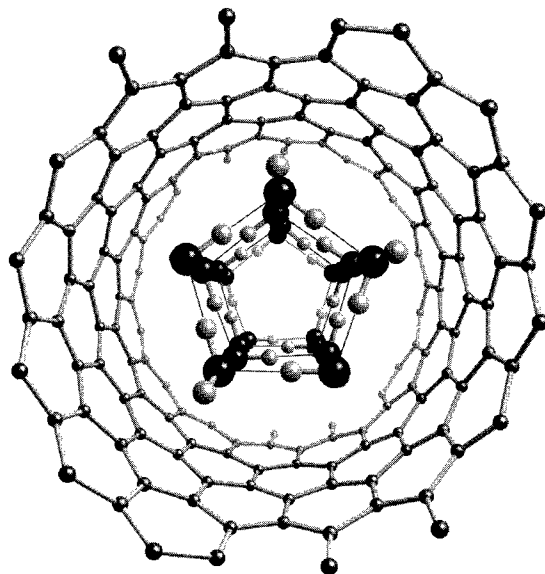


Figure 1: Atomic structure of ice nanotube encapsulated in carbon nanotube.

[1] Y. Maniwa et al., Chem. Phys. Lett. **401**, 534 (2005).

[2] K. Koga et al., Nature, **412**, 802 (2001).

Corresponding Author: Takahiro Kurita

E-mail: kurita@comas.frsc.tsukuba.ac.jp

Tel: +81-29-853-5600 (ext. 8233) / Fax: +81-29-853-5924

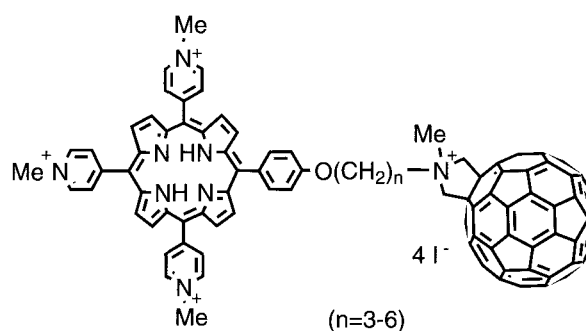
Synthesis of water-soluble cationic porphyrin-C₆₀ hybrids toward efficient photo cleavage of DNA

○Takahiro Yoshida, Takashi Hirota, and Kensuke Okuda

Faculty of Pharmaceutical Sciences, Okayama University, Okayama 700-8530, Japan

Like bleomycin, the compounds which have affinity to nucleic acids and cleave them has been great interest for anticancer drugs. From the point of this view, fullerene and cationic porphyrin are both interesting components which have two functions. Suitably water-solubilized C₆₀ derivatives are well known to cleave DNA under photo irradiation by the generation of active oxygen species. It has also been shown that some cationic C₆₀ derivatives bind to DNA. *Meso*-tetrakis(*N*-methylpyridinium-4-yl)porphyrin (TMPyP) has also been shown that photochemical cleavable activity of DNA and binding to DNA such as intercalation. Such compounds have potential as anticancer drugs for photodynamic therapy. We anticipated that these components may have better affinity to DNA and higher efficiency as photochemical nuclease activity once they are distributed suitably by covalent linkage. We report here the synthesis of such porphyrin-C₆₀ hybrids, *i.e.*, C₆₀ having positively charged porphyrins with various lengths of alkyl linkage toward efficient photo cleavage of DNA.

Synthetic procedures were as follows. 5-[4-[(ethylcarbonyl)oxy]phenyl]-10,15,20-tris(4-pyridyl)porphyrin¹ are hydrolyzed using alkaline, then alkylated by various *N*-alkyl glycine derivatives. After deprotection, they were subjected to 1,3-dipolar cycloaddition to C₆₀ and paraformaldehyde. Finally excess MeI gave water-soluble porphyrin-C₆₀ hybrid compounds which have various lengths of alkyl linkage (Figure).



Now we are estimating their potency on photonuclease activity using plasmid DNA and also investigating their reaction mechanism.

(1) Christiane Casasa, Bernadette Saint-Jalmes, Christophe Loup, C. Jefferey Lacey, and Bernard Meunier, *J. Org. Chem.*, **1993**, *58*, 2913-2917.

Corresponding Author: Kensuke Okuda

E-mail: okuda@pharm.okayama-u.ac.jp

Tel & Fax: +81-86-251-7932

Synthesis of Thiolated [60]Fullerene Derivative *via* Nitrofullerene Intermediate and Its Application to Thin Film Formation on Au

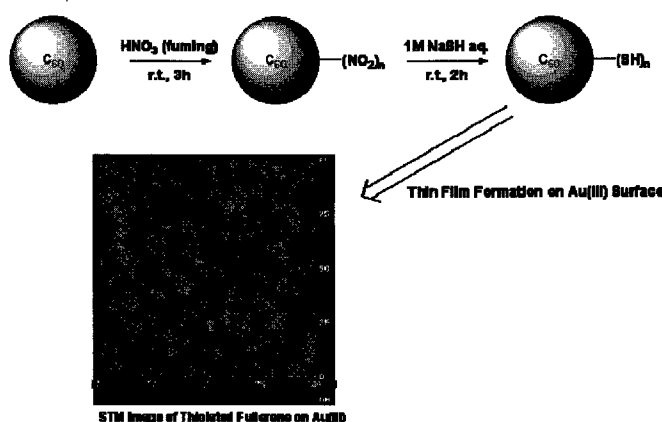
○Masaru Sekido¹, Hirokazu Fukidiome², Masamichi Yoshimura²,
Kazuyuki Ueda², Masatomi Ohno¹

¹*Department of Advanced Science and Technology, Toyota Technological Institute*

²*Nano High-Tech. Research Center, Toyota Technological Institute*

2-12-1 Hisakata, Tempaku, Nagoya 468-8511, Japan

The effective methods for the surface modification of fullerene have been developed using nitrofullerene intermediate¹⁾ in our group: briefly nitrofullerene intermediate was prepared by the reaction of C₆₀ with HNO₃ (fuming) at room temperature and the nitro groups on this intermediate were further substituted by nucleophilic reaction to give OH, NH₂, and SH introduced fullerene derivatives. Typically the mixture of nitrofullerene and 1M NaSH (aq.) was stirred at room temperature for 2 h to give a dark brown solution. After adjusting pH at 3 by adding 1N HCl thiolated fullerene was collected on a 0.1μm pore filter membrane and washed with water to give brown powder. The obtained thiolated fullerene was then dissolved in water to give brown aqueous solution.



By dropping the aqueous solution of thiolated fullerene on Au and dried in air, a well-ordered thin film of thiolated fullerene was observed on the surface of Au by AFM. Because of its well-ordered structure and electrical conductivity of fullerene thiolated fullerene may be applied for molecular devices.

References: V. Anantharaj, J. Bhonsle, T. Canteenwala, and L. Y. Chiang, *J. Chem. Soc., Perkin Trans. 1*, 1999, 31-36.

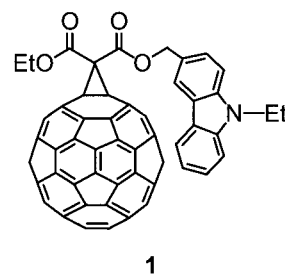
Corresponding Author: Masaru Sekido, sekido@toyota-ti.ac.jp, tel:052-802-1841, fax:052-809-1721

Synthesis and Photophysical Properties of [60]Fullerene Adducts Carrying Oligocarbazole Moieties (2)

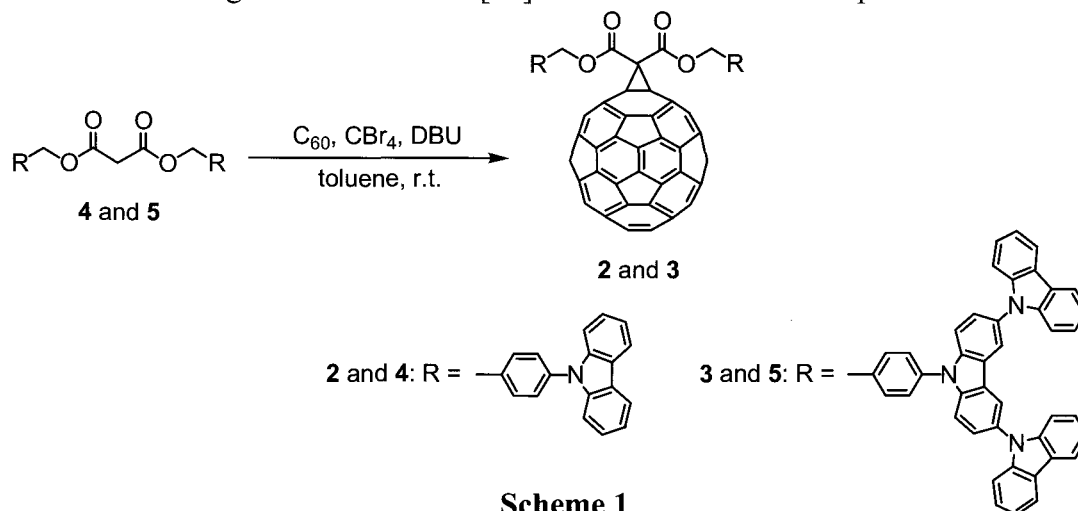
○Takashi Konno, Yosuke Nakamura, Satoru Watanabe, Masato Suzuki, and Jun Nishimura

Department of Nano-Material Systems, Graduate School of Engineering, Gunma University

[60]Fullerene–donor dyads linked by covalent bondings have attracted much interest from the aspects of charge-separated states arising from the intramolecular photoinduced electron transfer. Especially, porphyrins and related compounds have been extensively utilized among a variety of donor moieties. In contrast, there have been only a few examples of carbazole-linked fullerene adducts, although carbazole is a good electron donor known as a component of photoconductive poly(*N*-vinylcarbazole) (PVCz). Quite recently, we have successfully prepared [60]fullerene adduct **1** bearing a carbazole residue by using Bingel reaction. Unexpectedly, the photoinduced electron transfer via the excited states of [60]fullerene was not evidently detected in adduct **1**. Aiming at the construction of further new fullerene-donor dyad systems, the introduction of two carbazole moieties or oligocarbazole moieties onto the [60]fullerene surface was examined. We have designed two [60]fullerene adducts **2** and **3** bearing two carbazole or oligocarbazole moieties attached to the cyclopropane ring symmetrically. The trimeric carbazole moieties in **3** have larger π -conjugated system and more electron-donating ability than the single carbazole systems in **2**.



Both **2** and **3** were prepared by the Bingel reactions using **4** and **5**, respectively (Scheme 1). The fluorescence spectra of **2** and **3** were measured in benzene or benzonitrile at 430-nm excitation. In benzene, the spectra of **2** and **3** were similar to those of [60]fullerene monoadducts without a carbazole moiety; the fluorescence of [60]fullerene moiety for **2** and **3** is not quenched in benzene. In benzonitrile, however, the fluorescence of **3** was extremely quenched, although **2** showed almost the same emission as that in benzene. The quenching in **3** indicates that the intramolecular electron transfer from the carbazole moiety to the fullerene moiety via $^1C_{60}^*$ takes place. More detailed photophysical investigation and the synthesis of other oligocarbazole-linked [60]fullerene adducts will be presented.



Scheme 1

*Corresponding author: Yosuke Nakamura

E-mail: nakamura@chem.gunma-u.ac.jp Tel: +81-277-30-1312 Fax: +81-277-30-1314

Two New Metalloporphyrin Dimers: Molecular Scaffold for C₆₀ and C₇₀

○Sumanta Bhattacharya^a, Kazuyuki Tominaga^b, Takahide Kimura^a, Hidemitsu Uno^b and Naoki Komatsu^a

^aDepartment of Chemistry, Shiga University of Medical Science, Seta, Otsu 520-2192, Japan

^bIntegrated Center for Sciences (INCS), Ehime University, Matsuyama, 790-8577, Japan

Supramolecular chemistry involving porphyrins and fullerenes crossed each other to give rise to an interdisciplinary field in which the imagination of chemists has facilitated the design and construction of unprecedented fullerene-based supramolecular architectures. Thus, tailoring of porphyrin with judiciously chosen functionalities plays an important role in controlling/modifying the electronic structure. Implicit in this picture is that the interactions ought to be effective and selective. In continuation of our efforts to investigate the fullerene-containing host-guest ensembles [1], we have introduced a new metalloporphyrin dimer, M₂-1 (Fig. 1), as a designed host molecule in the present work.

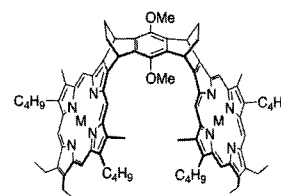


Fig. 1. Structures of M₂-1 (M = Zn or Ni)

The values of binding constants of M₂-1 to the C₆₀ (K_{C60}) and C₇₀ (K_{C70}) have been determined in toluene by optical absorption and fluorescence spectroscopic methods. Appearance of isosbestic and isoemissive points in UV-Vis and fluorescence spectroscopic investigations, respectively, followed by Jobs plot of continuous variation establishes the 1:1 stoichiometry between fullerenes and M₂-1. Large K values in the magnitude of $\sim 2.9 \times 10^4$ and $\sim 1.9 \times 10^5 \text{ dm}^3 \text{ mol}^{-1}$ were obtained for the 1:1 complexes of Zn₂-1 with C₆₀ and C₇₀, respectively, which results selectivity (K_{C70}/K_{C60}) of ~ 6.5 . However, introduction of Ni metal in place of Zn in 1 dramatically changes the magnitude of K for fullerene/Ni₂-1 complexes. K of C₆₀/ and C₇₀/Ni₂-1 complexes are $\sim 1.7 \times 10^4$ and $\sim 2.6 \times 10^4 \text{ dm}^3 \text{ mol}^{-1}$, respectively. The remarkable decrease in K_{C70} was caused by just changing the metal, which can be explained by difference in their complex structures. A comprehensive theoretical calculation reveals that C₇₀ complexes with Zn₂-1 and Ni₂-1 favor side-on and end-on orientations, respectively. From above foregoing discussions it can be concluded that while dispersive forces associated with π - π interactions play an important role in forming side-on C₇₀/Zn₂-1 complex, electrostatic interaction is the key factor behind the formation of stable end-on C₇₀/Ni₂-1 complex.

Acknowledgements:

This work was supported by Grant-In-Aid (No 17-05389 and 17350022) from Ministry of Education, Culture, Sports, Science and Technology, Japan.

References:

[1] S. Bhattacharya, T. Shimawaki, X. Peng, A. Ashokkumar, S. Aonuma, T. Kimura, N. Komatsu, *Chem. Phys. Lett.* **430**, 435 (2006).

Corresponding Author: Sumanta Bhattacharya

TEL: +81-77-548-2102; FAX: +81-77-548-2405; Email: sumanta@belle.shiga-med.ac.jp

2P-30

Polymerization during mechanochemical oxidation under oxygen atmosphere.

○Hiroto Watanabe¹, Yuichi Ishiyama¹, Yusuke Tajima², and Mamoru Senna¹.

¹ Faculty of Science and Technology, Keio University, 3-14-1 Hiyoshi Kohoku-ku,
Yokohama-shi Kanagawa-ken 223-8522, Japan

² Nano-Integration Materials Research Unit, RIKEN, Wako, 315-0198

As we recently demonstrated oxidation of C₆₀ via a mechanical stressing under oxygen atmosphere [1], we observed formation of the fullerene oxide C₆₀O_n, containing both epoxy and carbonyl types of oxygen, with the average value of n up to 12. We also found that ¹O₂ plays a decisive role as an activated species and is generated through energy transfer from mechanically excited fullerene during mechanical stressing. We postulated that, epoxy groups were formed between ¹O₂ and excited state of fullerene (C₆₀*), while carbonyl groups between ¹O₂ and ground state of C₆₀. However, if the lifetime of the C₆₀* is shorter than the lifetime of ¹O₂ in air, yields of the pure epoxide were extremely low under the present reaction conditions. We therefore presumed polymerization of the epoxide during mechanical stressing. As we milled pure C₆₀O epoxide in Ar atmosphere under the same milling condition, most of the milled product lost their solubility in toluene. As shown in Figure 1, HPLC analysis of supernatant toluene of milled powder revealed the co-existence of poly epoxydized fullerene (C₆₀O_n, 2<n<4) and unsubstituted fullerene (C₆₀). Formation of C₆₀ is a clear evidence of reversible polymerization between epoxy ring and C=C double bonds of bare fullerene cage via mechanical stressing. The same polymerization also took place during mechanochemical oxidation in O₂ atmosphere, seriously reducing the yields of pure epoxides. Beside its adverse effects against the selective oxidation via mechanical stressing, the reversible feature of the polymerization can be utilized as a new strategy for the production of fullerene poly epoxide, which would not be obtained from any other types of oxidation process.

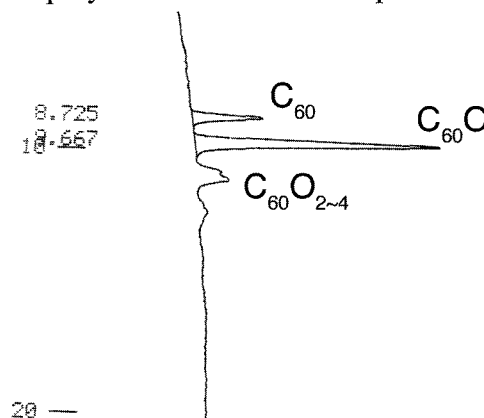


Figure 1. HPLC analysis of supernatant

Reference: [1] Hiroto Watanabe, Yuichi Ishiyama, Mamoru Senna, Abstract of the 31st Fullerene-Nanotubes General Symposium, 2006, p. 65.

Corresponding Author Tel.: +81-045-566-1569; **e-mail:** senna@applc.keio.ac.jp

Extraordinarily Large Association Constants of Azulenes with Fullerenes

○Naoki Komatsu, Sumanta Bhattacharya, A. F. M. Mustafizur Rahman, Takahide Kimura

Department of Chemistry, Shiga University of Medical Science, Seta, Otsu 520-2192, Japan

Fullerene-based supramolecular complexes are of great importance in not only separation of fullerenes, but also construction of photosynthetic systems and photonic devices. For the stability of the complexes in solution, host molecules with concave shape have been designed such as calixarene, resorcarene, cyclodextrin and carbon nanoring. However, it was recognized that concave-convex interaction is not always necessary for stable complexation in 1997 when the remarkably close approach between curved π -surface of fullerene and flat π -surface of porphyrin was found. However, such a nonclassical strong π - π interaction in a solution phase has been known only in the fullerene-porphyrin complexes so far. Here, we describe another example of the strong flat- π /curved- π interaction between fullerene and azulene having much smaller π -conjugate system than porphyrin.

The association constants are summarized in Table 1. Azulenes showed large association constants and almost no selectivity to C_{60} and C_{70} . As compared with designed host molecules so far, the association constants of azulenes are comparable to or larger than bridged calixarenes, azacalixpyridines, cyclotrimeratrylenes, and di- and tetraporphyrins. However, they are smaller than carbon nanorings, cyclic diporphyrins and hexaporphyrins. Among the flat π -conjugated molecules, azulenes exhibited the largest association constants. Their association constants for C_{60} are more than 10 times larger than those of the tetrahexylporphyrins (run 3). Naphthalene, structural isomer of azulene, and other alternately conjugated aromatics were reported to show much less binding constants towards fullerenes (run 4). Such remarkable difference is probably due to their difference in physical properties, especially electron-donating character of azulenes, which are originated from the difference in their conjugation systems, alternate and nonalternate conjugation.

Table 1. Association Constants of π -conjugated flat molecules with C_{60} ($K_{C60} / \text{dm}^3 \cdot \text{mol}^{-1}$) and C_{70} ($K_{C70} / \text{dm}^3 \cdot \text{mol}^{-1}$) in toluene at 298 °C and their ratio (K_{C70} / K_{C60}).

Run	Flat Molecule	K_{C60}	K_{C70}	K_{C70} / K_{C60}
1	Azulene	9.1×10^4	8.2×10^4	0.91
2	1,3-Dichloroazulene	6.9×10^4	7.4×10^4	1.1
3	Tetrahexylporphyrin	2.6×10^3	1.7×10^4	6.8
4	Naphthalene	0.67	11	16

A part of this work was supported by Industrial Technology Research Grant Program in 2005 from New Energy and Industrial Technology Development Organization (NEDO) of Japan.

Corresponding Author: Naoki Komatsu

TEL: +81-77-548-2102, FAX: +81-77-548-2405, E-mail: nkomatsu@belle.shiga-med.ac.jp

**Polymer Chain Length Effects on Temperature-Responsive
Phase Transition Behaviors of [60]Fullerene End-Bonded
Poly(*N*-isopropylacrylamide)**

○Atsushi Tamura, Katsumi Uchida and Hirofumi Yajima

*Department of Applied Chemistry, Faculty of Science, Tokyo University of Science,
12-1 Ichigaya Funagawar-machi, Shinjuku-ku, Tokyo 162-0826, Japan*

Biological activity of [60]fullerene, such as antioxidant activity, antitumor effect and enzyme inhibition have attracted much attention for a promising material utility in the biomedical field. In order to overcome the insolubility of C₆₀ and fabricate a new biomaterial, we have synthesized novel water-soluble C₆₀ end-bonded poly(*N*-isopropylacrylamide) (PIPAAm-C₆₀)^[1].

PIPAAm-C₆₀ is soluble in aqueous media below its lower critical solution temperature (LCST). Above the LCST, the dehydration of polymer chain occurred and PIPAAm-C₆₀ made insoluble in aqueous media, as shown in Figure 1. Moreover, the PIPAAm-C₆₀ formed micelle-like structure in aqueous media below the LCST, induced by the self-assembly of hydrophobic C₆₀ molecules.

In this study, to investigate the polymer chain length effects on aggregation behavior and temperature-responsive phase transition behavior, PIPAAm-C₆₀s with various polymer chain length were synthesized by using atom transfer radical polymerization (ATRP) technique. Gel permeation chromatography (GPC) and dynamic laser light scattering (DLS) measurements revealed that unimers and aggregations of PIPAAm-C₆₀ coexisted in aqueous media. Differences in PIPAAm chain length affect the ratio and the size of unimers and aggregations. Consequently, it is implied that the increase in the molecular weight of the PIPAAm tethered-chain prevent the PIPAAm-C₆₀ from transforming into micellar aggregations.

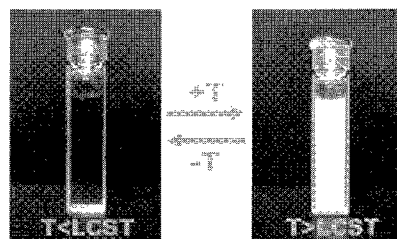


Figure 1. Temperature-induced reversible phase transition behavior of PIPAAm-C₆₀ in aqueous media.

Reference: [1] A. Tamura, K. Uchida, H. Yajima, *Chem. Lett.* **2006**, 35, 282.

Corresponding Author: Hirofumi Yajima

E-mail: yajima@rs.kagu.tus.ac.jp

Tel: +81-3-3260-4272 (ex.5770)

Fax: +81-3-5261-4631

Physicochemical property of water-soluble fullerene-chitosan conjugate

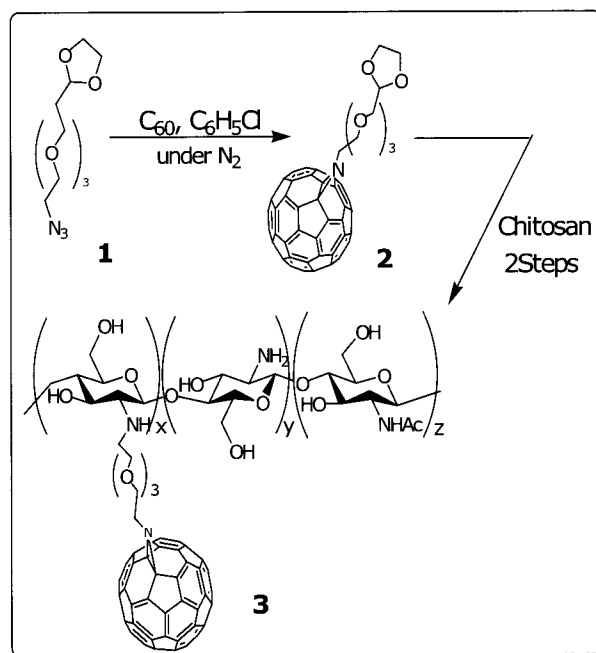
○Yoshifumi Mishima¹, Katsumasa Nemoto¹, Hitoshi Sashiwa², Katsumi Uchida¹, and Hirofumi Yajima¹

¹Department of Applied Chemistry, Tokyo University of Science, Tokyo 162-0826, Japan

²National Institute of Advanced Industrial Science and Technology, Osaka 563-8577, Japan

Fullerene has been known to be an antioxidant agent against excess reactive oxygen species such as superoxide anion and hydroxyl radical, which caused various disease and process of aging. Accordingly, water-soluble fullerene derivatives have recently attracted a great deal of attention as functional biomaterials with unique biological activities such as antioxidants, neuroprotective properties, enzyme inhibition, and DNA cleavage. Chitosan, a natural cationic polymer prepared by N-deacetylation of chitin, is interesting material owing to the unique properties such as biodegradability, non-toxicity, immuno stimulating effect, antimicrobial effect, and cholesterol-reducing effect^{1, 2}. Thus, we have investigated about a novel material to possess the unique properties of fullerene and chitosan. In this study, the conjugates of fullerene and chitosan were synthesized and then to scrutinize the physicochemical properties of the conjugates in aqueous solution were analyzed UV-vis spectroscopy, and DLS measurements. Their scavenging activities were estimated by ESR measurement.

The conjugate of fullerene and chitosan was synthesized according to the previously reported method³, and confirmed by ¹H-NMR measurements. The result from UV-vis absorption showed that the solubility of fullerene in water was increased by the addition of chitosan (17mg/mL). Further, DLS measurement revealed that the conjugate is self-assembled. The result indicates that the conjugate forms a micelle-like structure composed of inner core of fullerene and outer shell of chitosan. With regard to a considerable bioability of the conjugate, it was found that the 50% inhibitory concentration (IC₅₀) for hydroxyl radical scavenging is less half-concentration than that of chitosan. At present, the study of the relationship between their physicochemical properties and scavenging activities is in progress.



- References** [1] R. Xing et al. *Bioorg. Med. Chem.* 13 (2005) 1387-1392
 [2] R. Xing et al. *Bioorg. Med. Chem.* 13 (2005) 1573-1577
 [3] K.Nemoto et al., Abstracts of the 30th Fullerene-Nanotubes General Symposium, 3P-3 (2006)

Corresponding Author: Hirofumi Yajima

E-mail: yajima@rs.kagu.tus.ac.jp

Tel: +81-3-3260-4272 ext.5760 **Fax:** +81-3-5261-4631

2P-34

Abundance of C₆₀ revisited

Yusuke Ueno and Susumu Saito

Department of Physics, Tokyo Institute of Technology, Meguro-ku, Tokyo 152-8551, Japan

Although many interesting properties of C₆₀ have been revealed since a macroscopic production of C₆₀ fullerene [1], the microscopic formation process of C₆₀ has not been clarified yet. Therefore, the mystery, why C₆₀ clusters are by far most abundant in carbon clusters, still remains unsolved. We address these issues using transferable tight-binding model as well as the density-functional theory.

We first study the reactions between carbon clusters using the molecular dynamics combined with the transferable tight-binding model parametrized by Omata *et al* [2]. We find that C₁₀ is the first stable ring cluster at elevated temperature, in good accord with experimental mass spectra. Interestingly, reaction between these *sp*-hybridized C₁₀ rings gives rise to the *sp*²-network planar C₂₀ cluster. Reaction between C₂₀ clusters is found to give the closed-cage C₄₀ fullerene. Therefore, we can expect that C₄₀, C₅₀, C₆₀, C₇₀ etc. might be abundant fullerene clusters.

Next, in order to clarify the speciality of C₆₀ among these fullerenes, we study the reactivities of D_{5h} C₅₀, I_h C₆₀ and D_{5h} C₇₀ using the local-density-approximation in the framework of the density-functional theory. If C₆₀ is less reactive than C₅₀ and C₇₀, it explains why C₆₀ is more abundant than other fullerenes including C₇₀ [3]. To quantify the reactivity of each fullerene, we calculate the total energies of the system consisting of a fullerene and a carbon atom as a function of the distance between the fullerene surface and the C atom. It is found that some of C₇₀ sites actually have larger reaction energies than that of C₆₀, confirming that C₇₀ is more reactive than C₆₀ although it is energetically more stable than C₆₀.

References:

- [1] W. Kratschmer, L. D. Lamb, K. Fostiropoulos and D. R. Huffman, *Nature* **347** (1990) 354.
- [2] Y. Omata, Y. Yamagami, K. Tadano, T. Miyake and S. Saito, *Physica E* **29** (2005) 454
- [3] H. W. Kroto, J. R. Heath, S. C. O'Brien, R. F. Curl and R. E. Smalley, *Nature* **318** (1985) 162

Email: ueno@stat.phys.titech.ac.jp **Tel:** 03-5734-2387

Synthesis and Characterization of Carbene Derivatives of $\text{La}_2@C_{80}$

○ Chika Someya,¹ Michio Yamada,¹ Takatsugu Wakahara,¹ Takahiro Tsuchiya,¹
Yutaka Maeda,² Takeshi Akasaka,¹ Naomi Mizorogi,³ and Shigeru Nagase³

¹ Center for Tsukuba Advanced Research Alliance, University of Tsukuba, Tsukuba, Ibaraki
305-8577, Japan

² Department of Chemistry, Tokyo Gakugei University, Koganei, Tokyo 184-8501, Japan

³ Institute for Molecular Science, Okazaki, Aichi 444-8585, Japan

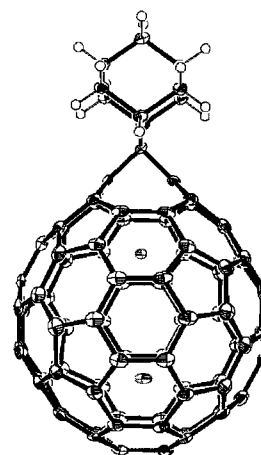
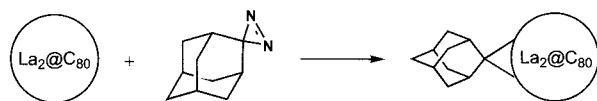
Endohedral metallofullerenes have received extensive attention on the past two decades only to their fascinating structures and electronic properties. It is expected that chemical functionalization of these materials offer a means to modify their chemical and physical properties.

Up to now, we had some reports of functionalization of endohedral metallofullerenes. Among these, we have succeeded the selective derivatization of $\text{La}@C_{82}\text{Ad}$ (Ad = adamantylidene) accomplished by the reaction of $\text{La}@C_{82}$ with adamantanediazirine. [1] Such a carbene addition could be effective method for functionalizing other metallofullerenes.

Meanwhile, $\text{La}_2@C_{80}$ has much attention for the three-dimensional random motion of the encapsulated two La atoms. [2] Recently, we have reported the characterization of the silylated and Prato adducts of $\text{La}_2@C_{80}$. [3] It is revealed that the motion of the encapsulated atoms is controllable by chemical derivatization of the carbon cage.

Herein, we report the syntheses and characterizations of carbene derivatives of $\text{La}_2@C_{80}$. We found that two La atoms are fixed at longitudinal position in the carbene derivative, unlike the silylated and Prato adducts of $\text{La}_2@C_{80}$. It is noted that the motion of La atoms is controllable by the addition positions and modes.

Scheme



ORTEP drawing of $\text{La}_2@C_{80}\text{Ad}$

References : [1] Maeda, Y. et al. *J. Am. Chem. Soc.* **2004**, *126*, 6858. [2] (a) Akasaka, T. et al. *Angew. Chem., Int. Ed. Engl.* **1997**, *36*, 1643. (b) Kobayashi, K. et al. *Chem. Phys. Lett.* **2003**, *374*, 562. [3] (a) Yamada, M. et al. *J. Am. Chem. Soc.* **2005**, *127*, 14571. (b) Yamada, M. et al. *J. Am. Chem. Soc.* **2006**, *128*, 1402.

Corresponding Author: Takeshi Akasaka
TEL & FAX: +81-29-853-6409, E-mail: akasaka@tara.tsukuba.ac.jp

Magnetic Properties of Solvent-Free $M@C_{82}(I)$ ($M = Y, La, Lu$) Metallofullerene Solids

○Takao Akachi¹, Yasuhiro Ito¹, Hitomi Takahashi², Hisashi Umemoto¹, Takashi Inoue³,
Shunji Bando², Wataru Fujita¹, Kunio Awaga¹, Ryo Kitaura¹, Toshiki Sugai¹,
and Hisanori Shinohara^{1,4,5}.

¹Department of Chemistry, Nagoya University, Nagoya 464-8602, Japan

²Department of Materials Science and Engineering, Meijo University, Nagoya 468-8502,
Japan

³Toyota Central R&D Laboratories, Inc., Nagakute, Aichi, 480-1192, Japan

⁴Institute for Advanced Research, Nagoya University, Nagoya 464-8602, Japan

⁵CREST, Japan Science and Technology Corporation, c/o Department of Chemistry, Nagoya
University, Nagoya 464-8602, Japan

Magnetic properties of several metallofullerenes have been reported during the past decade [1]. Phase transitions have been observed for microcrystals of $La@C_{82}$ [2,3], $Ce@C_{82}$ [2], and $Sc@C_{82}$ [4] at 120-150 K. Recently, we reported magnetic properties of solvent-free $Y@C_{82}(I)$ microcrystals [5], whose temperature dependence is similar to those of $La@C_{82}$ and $Sc@C_{82}$. $M@C_{82}(I)$ ($M = Y, La, Lu$) has a similar charge state of $M^{3+}@C_{82}^{3-}$ [1,6]. Since La^{3+} , Y^{3+} , Lu^{3+} ions have either no f-electrons or closed f-orbital, we might expect interesting magnetic properties peculiar to these unique electronic structures. Here, we report magnetic properties of solvent-free $M@C_{82}(I)$ ($M = Y, La, Lu$) microcrystals.

$M@C_{82}(I)$ ($M=Y, La, Lu$) were separated and purified from arc processed soot by the multi-step HPLC method [1]. Powder samples of $M@C_{82}(I)$ were heated at 300 °C under 10^{-6} Torr for 24 hours. These samples were put in a quartz cell for magnetic measurements. Magnetic susceptibility of these samples was measured by a superconducting quantum interference device (SQUID, a Quantum Design MPMS-XL7). Applied magnetic field was 1000 Oe and the temperature was lowered to 2 K from 300 K. We also performed electron spin resonance (ESR, a JEOL JES-FA200) on a $Lu@C_{82}(I)$ powder in the temperature range between 4 and 280 K.

Fig. 1 shows temperature dependence of magnetic susceptibility of $Lu@C_{82}(I)$. A broad featureless dependence in the temperature of 40-300 K suggests that present sample of powdered $Lu@C_{82}(I)$ does not have phase transition unlike the $Y@C_{82}(I)$ and $La@C_{82}(I)$ cases.

Furthermore, weak ESR signals were observed for $Lu@C_{82}(I)$ powder at 4 and 20 K, but disappeared above 100 K. The broadening and disappearance of the ESR signals at the higher temperatures are probably related to a large nuclear quadrupole moment of Lu atom (quadrupole moment = 5.7 barns).

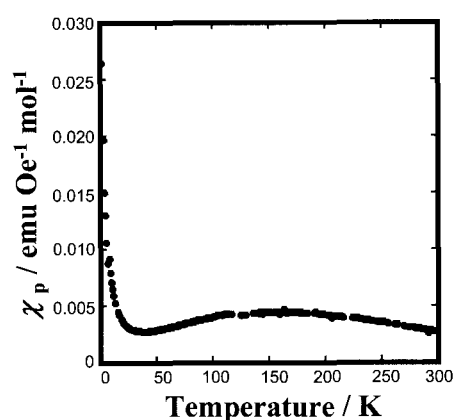


Fig.1: Temperature dependence of magnetic susceptibility (χ_p) of solvent-free $Lu@C_{82}(I)$ microcrystals.

[1] H. Shinohara, *Rep. Prog. Phys.* **63**, 843 (2000).

[2] C. J. Nuttall *et al.*, *Phys. Rev. B* **62**, 8592 (2000).

[3] T. Watanuki *et al.*, *Molecular Crystals and Liquid Crystals* **340**, 639 (2000).

[4] Y. Ito *et al.*, submitted to *Chem Phys Chem.* : Y. Ito *et al.*. Abstract of The 22th Fullerene General Symposium, January 10, 2002, Okazaki, Japan.

[5] T. Akachi *et al.*. Abstract of The 29th Fullerene-Nanotube General Symposium, July 25, 2005, Kyoto, Japan.

[6] C. Knapp *et al.*, *Appl. Phys. A* **66**, 249 (1998).

Corresponding Author Hisanori Shinohara

E-mail nori@nano.chem.nagoya-u.ac.jp **Tel:** (+81) 52-789-2482, **Fax:** (+81) 52-789-1169

Element Specific Magnetization Measurements of ErY-Metallofullerenes by Soft X-ray Magnetic Circular Dichroism

Haruya Okimoto¹, Ryo Kitaura¹, Yutaka Kitamura¹, Yasuhiro Ito¹,
 Daisuke Ogawa¹, Takao Akachi¹, Naoki Imazu¹, Toshiki Sugai¹,
 Tomohito Matsushita², Takayuki Muro², Hitoshi Osawa², Tetsuya Nakamura² and
 Hisanori Shinohara^{1,3}

¹Department of Chemistry and Institute for Advanced Research,
 Nagoya University, Nagoya 464-8602, Japan

²Japan Synchrotron Radiation Research Institute, Hyogo 679-5198, Japan

³CREST, Japan Science and Technology Corporation, c/o Department of Chemistry,
 Nagoya University, Nagoya 464-8602, Japan

Endohedral Metallofullerenes are expected to show novel magnetic properties due to encapsulated metal atoms. Especially hetero-di-metallofullerenes (which includes two different kind of metal atoms in fullerenes) are particularly interesting. Recently isolation of HoTm@C₈₂, ScYLaN@C₈₀ was reported[1,2]. Kodama *et al.* reported a study on carbon-metal interaction of di-heteo-mMetallofullerenes by ¹³C-NMR[3]. However, magnetic properties of solid state hetero-di-metallofullerenes have not been reported. Soft X-ray magnetic circular dichroism (SXMCD) is an extremely sensitive and element specific method to obtain detailed information on surface magnetization. SXMCD can be used to obtain magnetization of each metal in fullerenes separately from a diamagnetic fullerene cage and the other metal according to an element specificity of SXMCD. Here, we report the element specific magnetic property of hetero-di-metallofullerene(ErYC₂@C₈₂) which should be compare with that of Er₂C₂@C₈₂ for understanding intramolecular magnetic interaction.

SXMCD measurements have been performed on BL25SU in SPring-8. ErY binary metallofullerenes were coated on a Cu sample plate, which was baked at ~400K in a load-lock chamber under a pressure of 1×10^{-5} Pa. The sample was cooled down to 9 K by using a Liq.He continuous flow-type cryostat equipped with a Liq. N₂ radiation shield. X-ray absorption and the MCD spectra were obtained by the total electron yield method. Er₂O₃ was used as a reference for determination of magnetic susceptibility.

Figure 1 shows $1/\chi - T$ plots of ErYC₂@C₈₂ and Er₂C₂@C₈₂ at a magnetic field up to 2 T. The results indicate that intra-molecular magnetic interactions of these di-metallofullerenes are relatively weak and that magnetic moment of metal atom in fullerene is mainly governed by a crystal field effect due to the negatively-charged fullerene cage.

References: [1] K. Kikuchi *et al.*, *Chem. Phys. Lett.*, **319**, 472 (2000).

[2] N. Chen *et al.*, *J. Phys. Chem B*, **110**, 13322 (2006).

[3] T. Kodama *et al.*, *Proceedings of Bunshi Kozo Toronkai*, 2P089, 2006.

Corresponding Author: Hisanori Shinohara

TEL: +81-52-789-2482, FAX: +81-52-789-1169, E-mail: noris@cc.nagoya-u.ac.jp

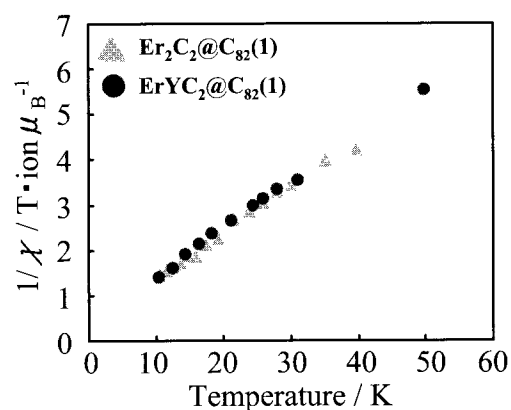


Fig1. $1/\chi - T$ plot of Er₂C₂@C₈₂ (I) and ErYC₂@C₈₂ (I)

Development of Pulsed Ion Valve for High-resolution Ion Mobility Measurement

○ ○ T. Sugai¹, H. Shinohara^{1,2,3}

¹*Department of Chemistry (RCMS), Nagoya University*

²*Institute for Advanced Research, Nagoya University*

³*CREST, Japan Science and Technology Agency*

Mobility measurements on various fullerenes have clarified novel structures and phenomena such as carbide structures and fullerene formation processes[1,2]. These achievements are accomplished by the high sensitivity and the high measurement speed of the method. However, the mobility or structural resolution and mass limitation prevent us to apply this method to go more advanced measurements on fullerene isomer identification and on nanotube production processes. This limitation comes from continuous detection system consisting of a quadrupole mass filter and an aperture with differential pumping. To exceed the limitation, we are developing pulsed ion valve (PIV), which is the key device to connect a high-pressure drift cell (DC) to a high-vacuum time of flight mass spectrometer (TOF). Here we present the observation of ions passing through the valve.

The measurement system consists of a continuous ion source, PIV, and TOF with differential pumping system using a 1200 l/s diffusion pump. With ion source in air, we have succeeded to observe ions passing through the PIV (Fig 1). When the ion source is turned off these peaks disappear. We are now developing a new setup utilizing this PIV for the mobility measurements, where the ion source is replaced with the pulsed ion source using an ionization laser. The mobility is measured by observing the time difference between the ionization laser and the opening time of PIV. We have checked the PIV works at more than 5 atm, which enables us to separate a C₈₀ spherical I_h isomer and an elongated D_{5d} isomer. With this PIV, we are planning to explore new structures of fullerenes and to observe production processes of nanotubes.

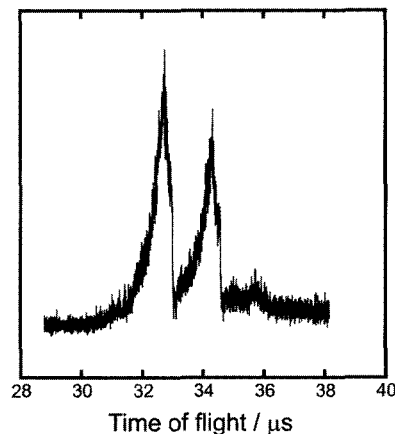


Fig. 1 Observed ions with PIV

References:

[1] T. Sugai *et al.*, *J. Am. Chem. Soc.* **123**, 6427 (2001).

[2] von Helden *et al.*, *J. Chem. Phys.* **95**, 3835 (1991).

e-mail: sugai@nano.chem.nagoya-u.ac.jp tel: +81-52-789-2477 fax: +81-52-789-1169

Variation of Electronic Properties in Gd@C₈₂ Metallofullerene Induced by Polyhydroxylation

Jun Tang^{1,2, §}, Gengmei Xing¹, Yuliang Zhao^{1,*}, Long Jing¹, Xingfa Gao¹,
Ryotaro Kumashiro², Katsumi Tanigaki^{2,*}

¹ Lab for Bio-Environmental Health Sciences of Nanoscale Materials, Institute of High Energy Physics, The Chinese Academy of Sciences, Beijing 100049, China.

² Department of Physics, Graduate School of Science, Tohoku University, Sendai 980-8578, Japan

Novel features of metal atom encapsulated in fullerene cages have attracted significant attention due to the completely different properties from those of the common compounds. However, how the electronic properties of encaged metal atom change when outer fullerene cage is chemically modified is also an important but still an unknown question. In this case, we synthesized and purified the Gd@C₈₂ and Gd@C₈₂(OH)_x with increasing number of hydroxyls and studied electronic interactions between the inner metal atom and the outer carbon cage of fullerene derivatives using synchrotron radiation x-ray photoemission spectroscopic techniques.

Fig. 1 shows the Gd valence band photoemission spectra for Gd@C₈₂ and Gd@C₈₂(OH)_x. In Gd@C₈₂ 31.4 eV energy level is not observed but it emerges in Gd@C₈₂(OH)₁₂. Surprisingly, this photoemission signal vanishes in Gd@C₈₂(OH)₂₀ and appears again in Gd@C₈₂(OH)₂₆. The energy level periodically appears or disappears with changing the number of OH groups on the fullerene cage surface. The results indicate that polyhydroxylation of metallofullerenes can be a new way for creating desired materials with novel electronic, optical, or magnetic functions.

In this meeting, we will discuss how the outer polyhydroxylation of C₈₂ cage modulate the electronic properties of the encaged Gd atom in more detail.

[1] Tang J.; Xing G.M.; Zhao Y. L.; Jing L.; Gao X. F.; Cheng Y.; Yuan H.; Zhao, F.; Chen, Z.; Meng, H.; Qian H. J.; Su R. Ibrahim K. *Advanced Materials*. 2006, 18, 1458.

*Corresponding Author: zhaoyuliang@ihep.ac.cn; tanigaki@sspns.phys.tohoku.ac.jp.

§ Present address: Department of Physics, Graduate School of Science, Tohoku University, Sendai 980-8578, Japan.

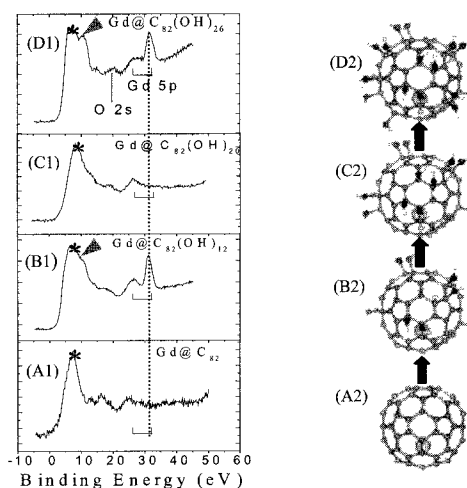


Figure 1. The valence band PES of Gd@C₈₂ (A1), Gd@C₈₂(OH)₁₂ (B1), Gd@C₈₂(OH)₂₀ (C1), Gd@C₈₂(OH)₂₆ (D1) with the incident photon energy 140.0eV. A2-D2 show schematic draws for the hydroxyl additions. Photon energy is 140.0 eV.

3P-1

Growth of Carbon nanotubes on Si substrates using alcohol gas source in a high vacuum

○Kenji Tanioku¹, Tomoyuki Shiraiwa¹, Takahiro Maruyama^{1,2}, Shigeya Naritsuka^{1,2}

¹ Dept. of Materials Science & Engineering, Meijo Univ., 1-501 Shiogamaguchi, Tempaku,
Nagoya 468-8502

² Meijo Univ. 21st CENTURY COE program "Nano Factory", 1-501 Shiogamaguchi, Tempaku,
Nagoya 468-8502

Because of their extremely small size and unique electronic properties, carbon nanotubes (CNTs) have been expected for application in various fields. However, the growth mechanism of CNT has not been evident yet. Although *in situ* observation by scanning electron microscopy (SEM) or electron diffraction is effective to clarify the growth mechanism, growth pressure is not low enough to enable use of an electron beam during CNT growth at present [1]. In this study, to achieve CNT growth in a high vacuum, growth of CNT was performed under low pressure using alcohol gas source.

Firstly, SiO₂(100nm)/Si substrates were introduced into a ultra-high vacuum (UHV) chamber equipped with UHV-STM, followed by deposition of Co catalyst of 0.6nm in thickness by electron beam (EB) evaporation. To prevent oxidation of the catalyst, 1×10^{-3} Pa of H₂ gas was flowed into the chamber during an increase of substrate temperature before CNT growth. The growth temperature was set from 500°C to 700°C. Then, ethanol was jetted onto the substrate surface for 5 hours to grow CNTs. The pressure was kept at 1×10^{-3} Pa during the growth. The grown CNTs were characterized by SEM and Raman spectroscopy.

Figure 1 shows an SEM image of CNTs grown at 500°C. Web-like CNTs were observed on all over the surface. Figure 2 shows their Raman spectra. The diameter of CNTs was estimated to be about 0.9nm to 1.1nm by the Raman shift of RBM peaks. As the growth temperature increased, the diameter became large. The G/D ratio was estimated to be about 16, from Fig. 2 (b). From these results, we concluded that CNTs with a good crystalline were obtained even in a high vacuum.

[1]T. Shiokawa, B. Zhang, M. Suzuki and K. Ishibashi, Jpn.J.Appl.Phys. 45 (2006) 23.

Corresponding Author: Takahiro Maruyama

TEL: +81-52-838-2386, FAX: +81-52-832-1172, E-mail: takamaru@ccmfs.meijo-u.ac.jp

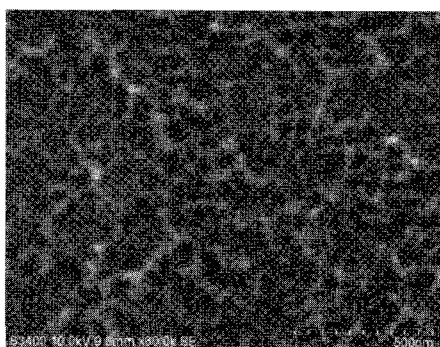


Fig.1 SEM image of CNTs grown at 500°C and 1×10^{-3} Pa.

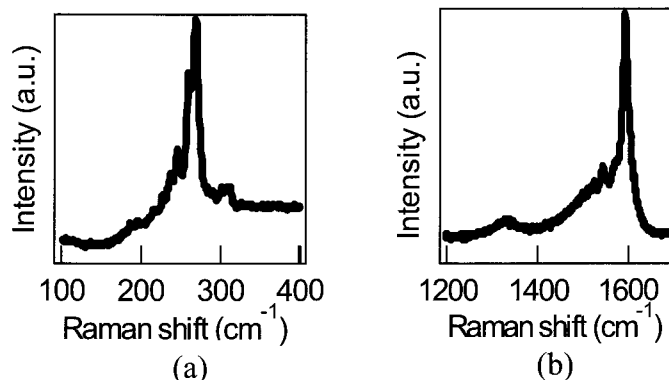


Fig. 2 Raman spectra of (a) RBM and (b) high frequency region of CNTs grown at 500°C and 1×10^{-3} Pa.

3P-2

Study of Carbon Source Gas Separation for Fabrication of Carbon Nanotubes

○Takeshi Hikata¹, Kazuhiko Hayashi¹, Ken-ichi Sato¹, Tomoyuki Mizukoshi², Yoshiaki Sakurai², Itsuo Ishigami², Takaaki Aoki³, Toshio Seki³, and Jiro Matsuo³

¹Sumitomo Electric Industries, Ltd., Osaka 554-0024, Japan

²Technology Research Institute of Osaka Prefecture, Osaka 594-1157, Japan

³Faculty of Engineering Quantum Science and Engineering Center, Kyoto University, Kyoto 606-8501, Japan

Carbon nanotubes have been expected as the excellent electric wires with high strength and light weight. However, there are two main problems for the quality in the fabrication process of CNT. The first problem is that it is difficult to obtain long length because the growth rate of carbon nanotube (CNT) decreases with reacting time by covering of unnecessary harmful carbon formed on a nano-sized metal particle catalyst. The second is that the carbon nanotubes have much defect through influence of carbon source gas in CVD process. Therefore, we proposed the novel techniques with the separation of carbon source gas supply and CNT growth as the solved method at the previous report [1]. It was indicated in the experiments that the graphite without defect generated on Fe surface in Ar gas by carbon through the Fe foil where carbon source gas was provided on the other side of the Fe foil. It is required to control the carbon source supply and the unnecessary carbon removal on carbon source supply side of Fe for continuous growth.

For continuous growth, we consider possibility for two methods of simultaneous and alternate treatments for carbon supply and removal on the catalyst. The simultaneous treatment is composed of the carbon supply as chemical reaction with carbon source gas and the physical removal of carbon by etching of such Ar ion. The alternate treatment is composed of the supply and removal of carbon on the catalyst.

We attempted the alternate treatment by using pure Fe foil with thickness of 20~50 μm . Both sides of the Fe foil were separated by stainless gaskets with coated Ag. The carbon source gas was provided on one side of Fe foil and Ar gas was provided on the reverse side. On the side of carbon source supply, CO gas was provided as the carbon supply gas for 1 hour and then, CO₂ gas was provided as the carbon removal gas for 5 minutes at 850 °C. The generated carbon was removed and Fe surface was oxidized on the carbon source supply side of the Fe foil. On the reverse side of the Fe foil, the graphite was generated with thickness of a few μm through heat treatment, and then the generated graphite dissolved into Fe. It is indicated that the graphite on the Fe foil was resolved into Fe by decrease of carbon concentration in Fe by oxidization gas. Therefore, it was considered that the Fe shape was required to form as the filament structure with high aspect ratio for size of the exposed Fe on carbon source supply side and the thickness such as Fig.1 for prevent of graphite solution by drop of the carbon concentration.

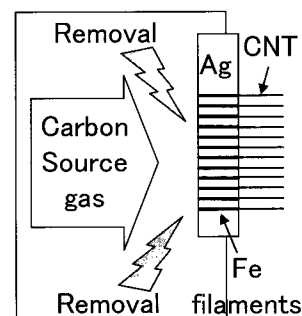


Fig.1 Concept for the alternative treatment method.

Corresponding Author: Takeshi Hikata /E-mail: hikata-takeshi@sei.co.jp

TEL: +81-6-6466-5790, FAX: +81-6-6466-6583

[1] T.Hikata et al., The 31st Fullerene-Nanotubes General Symposium, 2P-24(2006).

Effect of metallicity on the diameter distribution of single walled carbon nanotubes synthesized by catalytic ACCVD

Krishnendu BHATTACHARYYA ○, Yoshiyuki SUDA, Yosuke SAKAI, Hirotake SUGAWARA, Atsushi OKITA, Takeshi SAITO, Atsushi OZEKI, Masayuki MAEKAWA and Junichi TAKAYAMA

*Graduate School of Information Science and Technology, Hokkaido University,
North 14, West 9, Sapporo 060-0814, Japan*

Abstract:

Remarkable electrical, thermal and mechanical properties make single walled carbon nanotubes (SWNTs) the most prospective material for the next generation electronics and various other applications. Controlled synthesis, in terms of SWNT-diameter, metallicity, length, alignment etc, is the fundamental requirement to achieve such potential applicability successfully. However, achieving the desired control via external synthesis-parameters is still in its early phase. Recently, bulk estimation of relative abundance of various SWNTs from photoluminescence spectroscopy [1] opens a new pathway to further study and analyze the growth mechanism. We report experimental results on the chirality distribution of SWNT samples grown under various growth conditions. The results point towards the existence of different diameter distribution in the as-grown SWNT samples, depending on metallicity.

References:

[1] Y. Oyama, R. Saito, K Sato, J. Jiang, Ge. G. Samsonidze, A. Gruneis, Y. Miyauchi, S. Maruyama, A Jorio, G. Dresselhaus, M. S. Dresselhaus: **Photoluminescence intensity of single-wall carbon nanotubes**, *Carbon* **44** (2006) 873 – 879

Corresponding Author: Yoshiyuki Suda

E-mail: suda@ist.hokudai.ac.jp

Tel&Fax: +81-11-706-6482 / +81-11-706-7890

3P-4

Production of SWNTs by AC arc discharge in H₂-Ar-CH₄ mixture gas

○M. Shibata, X. Zhao, S. Inoue and Y. Ando

21st COE Program “Nano Factory”, Department of Materials Science & Engineering,
Meijo University, Tenpaku-ku, Nagoya 468-8502, Japan

Single-wall carbon nanotubes (SWNTs) have been produced by DC arc discharge evaporation of carbon anode containing 1at% Fe catalyst in H₂-Ar mixture gas¹⁾. However, more than 50% of evaporated anode becomes cathode deposit, and the production yield of SWNTs (the ratio of obtained SWNTs amount to the evaporated anode amount) is only 5%. In the present study, we used AC arc discharge instead of DC arc discharge to prevent cathode deposit formation, and added 1% CH₄ gas also into H₂-Ar mixture gas to increase the carbon atoms in arc plasma.

Figure 1 shows the production yield of SWNTs and the obtained SWNTs amount, when two carbon electrodes containing 1at% Fe were evaporated by AC arc discharge in 39%H₂-60%Ar-1%CH₄ mixture gas for 3 min. It can be seen that the maximum production yield of SWNTs is 25% at the current of 75A, which is factor of five larger than that of DC arc discharge. Figure 2 shows the evaporation amount of spurious anode and cathode under different AC arc currents as the cleaning control was set at 50. It is clear that both electrodes have been evaporated, and no deposit can be formed. There are some Fe catalytic nanoparticles coexisting with SWNTs, but EDX and TGA analyses indicate that the percentage of Fe element decreases from ~ 10 to less than 5 at%. Therefore, the as-grown SWNTs can be easily purified by a simple method, heat treatment at 420°C in air and then rinsing with hydrochloric acid.

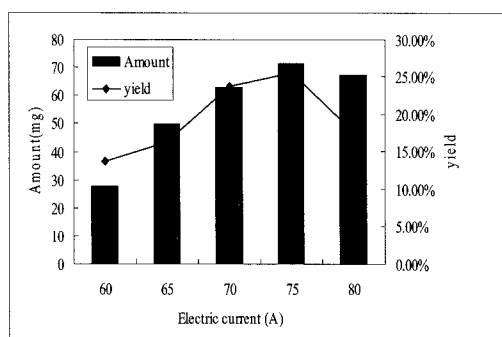


Fig. 1 Amount and yield of SWNTs

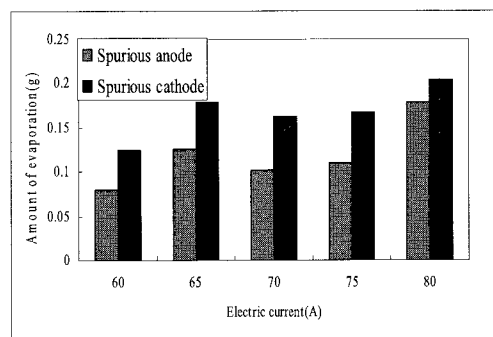


Fig. 2 Amount of evaporation

Reference

- 1) X. Zhao et al., *Chem. Phys. Lett.*, **373** (2003) 266.

The effect of SiO₂ thickness on the growth of SWNTs

○Toshiya Murakami¹, Takahiro Tokuda¹, Yuki Hasebe¹, Kengo Higashi¹, Kenji Kisoda², Koji Nishio¹, Toshiyuki Isshiki¹, and Hiroshi Harima¹

¹*Department of Electronics and Information Science, Kyoto Institute of Technology,
Matsugasaki Sakyo-ku Kyoto 606-8585, Japan*

²*Faculty of Education, Wakayama University, Sakaedani Wakayama-shi 640-8510, Japan*

Improvement of preparation of metallic catalysts is an important factor for efficient and chirality-controlled growth of single-walled carbon nanotubes (SWNTs). We have researched the effect of Fe-Co bimetallic catalysts on Si/SiO₂ substrates for their efficient growth by chemical vapor deposition (CVD). [1] In addition to a choice of catalysts, selecting substrates is also a critical parameter to improve efficiency of their growth. Here we report the dependence of SiO₂ thickness on the yield of SWNTs.

SWNTs were grown on Si substrates with various SiO₂ thicknesses by CVD. The Co catalysts were loaded on substrates by spin coating of ethanol solutions of Co acetate with fixed cobalt concentration of 0.01wt%. The relative intensity of the G band plotted against the SiO₂ thickness is shown in Fig.1. The yield of SWNTs is proportional to the G band intensity. The intensity maximum was located at around 70 nm. That is, the appropriate SiO₂ thickness for the SWNTs growth is about 70 nm. The less efficient production on thin SiO₂ was explained that catalyst activity of Co went out because of reacting with the silicon substrate. [2] The decline of the SWNTs yield for thicker SiO₂ has not been discussed before. Several possibilities for loss of catalyst activity were considered as follows: (1) Growth temperature on thick SiO₂ is decreased because of faster thermal relaxation than that of thin one, (2) Number of active catalysts decreased due to diffusion of catalyst particles into SiO₂ film deeply, (3) Inactive cobalt silicate is formed by reaction of Co with SiO₂. We checked (1) by analyzing Raman spectra and found temperature difference of a few ten degrees between 0 and 130 nm of SiO₂ thickness. Checking the other possibilities using high-resolution TEM is under way.

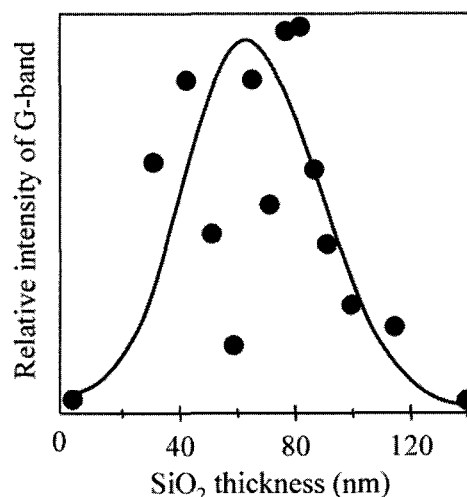


Figure 1
Relative intensity of the G band in Raman spectra of SWNT plotted against the SiO₂ thickness.

[1] T. Murakami, *et. al.*, J. Appl. Phys. **100**, 094303, (2006)

[2] Y. Homma, *et. al.*, J. Phys Chem **107**, 12161, (2003)

Corresponding Author: Toshiya Murakami

E-mail: dj990101@djedu.kit.ac.jp

3P-6

Recovery of carbon nanotubes dispersed with amphiphilic oligopeptides in water

○Atsushi Yamamoto¹, Shin-ya Masuhara¹, Yoshihiro Furukawa², Ryosaku Kawabata², Kishio Hidaka³, Masao Kamahori⁴, and Shin Ono¹

¹Graduate School of Science and Engineering, University of Toyama, Gofuku 3190, Toyama 930-8555, Japan

²Hitachi High-Technologies Co., 1-24-14 Nishi shimbashi, Tokyo 105-8717, Japan

³Materials Research Laboratory, Hitachi Ltd, Hitachi-shi, Ibaraki 319-1292, Japan

⁴Central Research Laboratory, Hitachi Ltd, Kokubunji-shi, Tokyo 185-8601, Japan

For purification of carbon nanotubes (CNTs), we have designed some amphiphilic oligopeptides which can disperse CNTs in water. Among them, Pep-2 (Fig.1) consisting of three Gly and two Phe as the hydrophilic and hydrophobic residues, respectively, was prepared and demonstrated to effectively disperse CNTs in water by means of UV-vis absorption spectroscopy and TEM. In this study, we examined some methods to recover CNTs from their dispersed aqueous solutions of our designed amphiphilic oligopeptides, especially Pep-2.

To prepare the CNT-dispersed aqueous solutions, CNTs were added to the aqueous solutions of our designed amphiphilic oligopeptides and ultrasonication followed. Then the obtained black suspensions were centrifuged and decanted to remove the insoluble materials. The supernatants were used for the recovery experiments.

Addition of methanol was firstly examined. Upon addition of methanol to the CNTs-dispersed supernatant using Pep-2, CNTs came out in the solution and could be collected by centrifugation. The UV-vis spectra of the upper aqueous solution showed that almost of CNTs in the supernatant were recovered from the CNTs-dispersed supernatant. The effect of other organic solvents on the recovery of CNTs was also evaluated.

Secondly, alkali treatment of the CNTs-dispersed supernatants was effective on the recovery of CNTs. Addition of sodium hydroxide solution to the CNTs-dispersed supernatant resulted in the formation of CNTs-precipitates. This formation of the precipitates should be attributed to the hydrolysis of the C-terminal Bzl ester and the generated carboxy group. The other method to recover CNTs using an enzyme was also examined and the effectiveness will be discussed.

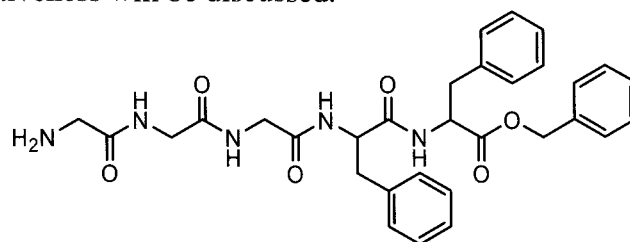


Fig. 1. Structure of amphiphilic oligopeptide Pep-2.

Corresponding Author: Shin Ono

E-mail: shinono@eng.u-toyama.ac.jp

Tel&Fax: +81-76-445-6845

Separation of Metallic and Semiconducting Single-Walled Carbon Nanotubes by Electric Field

○Yoshikazu Wakizaka¹, Ken-ichi Nakayama^{2,3}, Satoshi Tanaka³, Yoshiaki Sakurai⁴,
Yasuo Kanematsu¹, Masaaki Yokoyama^{1,2}

¹Center for Advanced Science and Innovation, Osaka University, 2-1 Yamadaoka, Suita, Osaka 565-0871, Japan ²Department of Polymer Science and Engineering, Yamagata University, 4-3-16 Jyonan, Yonezawa, Yamagata 992-8510, Japan ³Department of Material and Life Science, Osaka University, 2-1 Yamadaoka, Suita, Osaka 565-0871, Japan ⁴Technology Research Institute of Osaka Prefecture, 2-7-1 Ayumino, Izumi, Osaka 594-1157, Japan

Single-walled carbon nanotubes (SWNTs) have lots of potential applications for materials of electrical or optical devices. High purity metallic-SWNTs (m-SWNTs) or semiconducting-SWNTs (s-SWNTs) are needed to make such devices which educed their intrinsic performance but they cannot be selectively grown by a present synthesis method. Recently, some researchers have been separated them by AC dielectrophoresis [1], anion exchange chromatography of DNA wrapped SWNTs [2], centrifugation in a THF solution of amine [3] and selective oxidation of s-SWNTs by H₂O₂ [4].

We reported here a new separation method which has potential for large scale separation. At the first step, the electrophoretic behavior of micelled SWNTs in the microchip was observed by *in situ* measurements of Raman spectra. From the time development of the spectra, it was found that electrophoretic velocity was different between m-SWNTs and s-SWNTs.

At the next step, we tried separating and extracting each type of SWNTs using a handmade electrophoretic bath. Applying DC 100 V for 18 hours, the sample solution was separated to 6 fractions. From the Raman spectra (Figure 1), fraction no.1 (near the anode) and no.6 (near the cathode) were revealed to include high purity m-SWNTs and s-SWNTs, respectively.

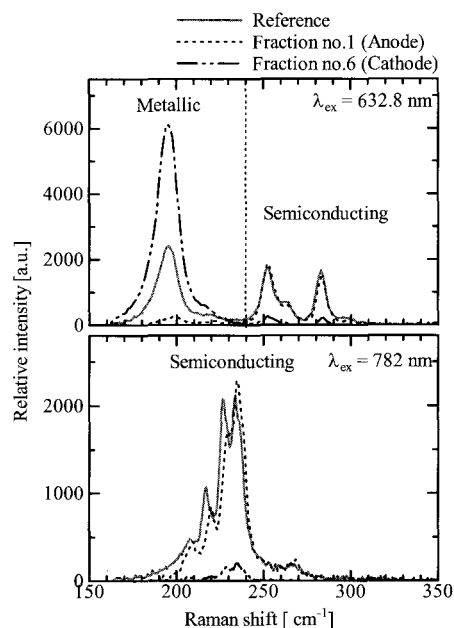


Figure 1. Raman spectra of separated SWNTs

References: [1] R. Krupke *et al.*, *Science* **301**, 344 (2003), [2] M. Zheng *et al.*, *Science* **302**, 1545 (2003), [3] Y. Maeda *et al.*, *J. Am. Chem. Soc.* **127**, 10287 (2005), [4] Y. Miyata *et al.*, *J. Phys. Chem. B.* **110**, 25 (2006)

Corresponding Author: Yoshikazu Wakizaka (E-mail: y-wakizaka@casi.osaka-u.ac.jp, Tel: +81-6-6879-7755, Fax: +81-6-6879-7878)

Synthesis of vertical-aligned carbon nanotubes on SiO₂/Si substrate by microwave plasma chemical vapor deposition using CH₄/H₂ gasses

○T. Naitou¹, A. Watanabe¹, Y. Hayashi¹, T. Tokunaga², K. Kaneko²

¹Nagoya Institute of Technology, Gokiso, Showa, Nagoya, 466-8555, Japan

²University of Kyushu, 744 Motooka, Nishi, Fukuoka 819-0395, Japan

Carbon based nanofibers (CNFs), nanotubes (CNTs) or nanowires are of great interest as a building block for the next generation of electronics or a number of applications because of their outstanding electrical, thermal, and mechanical properties.

In the current study, we synthesized the CNTs on pre-deposited Fe catalyst metal on SiO₂/Si substrate by a microwave plasma-enhanced chemical vapor deposition method using a 2.45GHz, 100W microwave power supply. During deposition the H₂ gas was adjusted to achieve various CH₄ concentrations at a total pressure of 20 Torr.

Figures 1 and 2 show the Raman spectra of CNTs synthesized at CH₄ concentrations of 10% and 33%, and the SEM image the CNTs synthesized at CH₄ concentration of 10%, respectively. The Raman intensity ratio (I_G/I_D) increases with decreasing in the CH₄ concentration. We also found that the two zone-holdings at around 1550 cm⁻¹. Although the two zone-holdings disappeared, the CNTs become well-aligned and uniform in size with increase in CH₄ concentration.

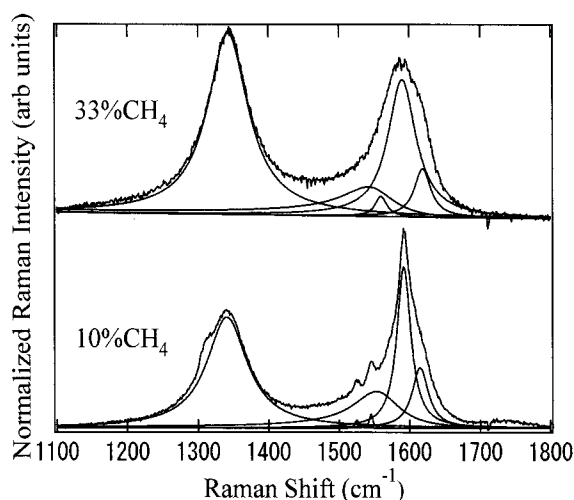


Fig. 1. Raman spectra of CNTs synthesized at CH₄ concentrations of 10% and 33%.

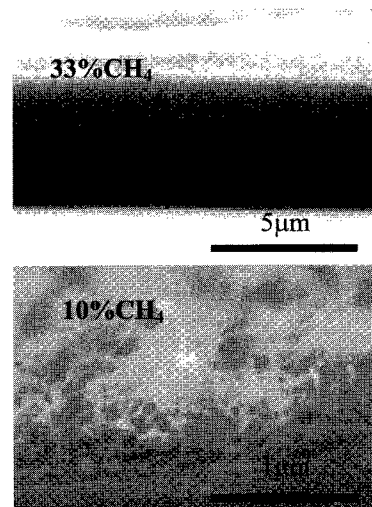


Fig. 2. SEM images of CNTs synthesized at CH₄ concentrations of 10% and 33%.

Corresponding Author : Tsunahiko Naitou, E-mail : murat55jp@yahoo.co.jp, Tel&Fax : 052-735-5104

Size control of catalytic nanoparticles by thermal treatment toward diameter control of single-walled carbon nanotubes

○Akira Yamazaki^{1,3}, Goo-Hwan Jeong*^{1,2}, Satoru Suzuki^{1,2}, Hideyuki Yoshimura³,
Yoshihiro Kobayashi^{1,2}

¹ NTT Basic Research Laboratories, NTT Corporation, Japan

² JST/CREST, Japan

³ Department of Physics, Meiji University, Japan

*Present address: Department of Physics, Göteborg University, Sweden

Diameter control of single-walled carbon nanotubes (SWNTs) is a crucial issue in maximizing the practical potential of SWNTs. Recently, wet catalysts, such as metal-incorporated ferritins, have been widely used for the diameter control due to their predetermined size [1]. In this paper, we report size control of catalytic Co nanoparticles, obtained from Co-filled apoferritin [2], by thermal annealing with the aim of diameter-controlled growth of SWNTs. Sizes of nanoparticles and SWNTs grown by methane-CVD were evaluated from atomic force microscope images. We found that Co nanoparticle size gradually decreased from 2.4 nm to 1.2 nm through repetitive annealing at 1000 °C in Ar ambient as shown in Fig. 1. Results of X-ray photoelectron spectroscopy and secondary ion mass spectroscopy indicate that the decrease of the nanoparticle sizes is caused by thermal evaporation of the particles. By utilizing this phenomenon for the SWNT growth, we found that thinner SWNTs with a narrower diameter distribution grew as the nanoparticles became smaller. Our results show that thermal treatment provides a simple and straightforward technique to prepare catalysts having a desired size and uniformity toward diameter-controlled SWNT growth.

References:

- [1] G. -H. Jeong et al., JAP **98** (2005) 124311
[2] G. -H. Jeong et al., JACS **127** (2005) 8238

Corresponding Author: A. Yamazaki

E-mail: a.yama@will.brl.ntt.co.jp
Tel&Fax: 046-240-4070/4718

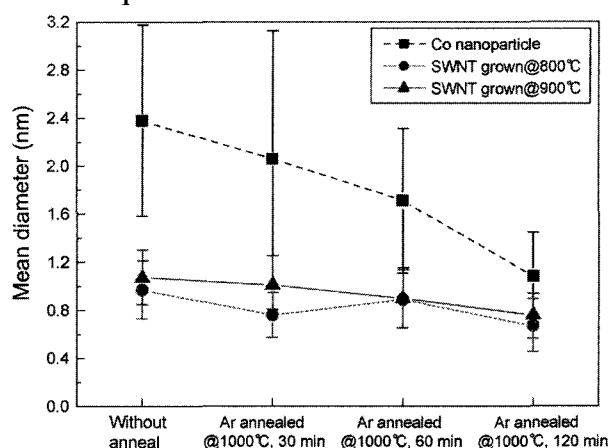


Fig. 1: Changes of Co nanoparticle size by thermal annealing and the SWNT diameters grown from the resultant particles.

Production, Purification and Characterization of Double-Wall Carbon Nanotubes Synthesized by Hydrogen Arc Discharge

○ Naoki Imazu¹, Masahiro Shiraishi¹, Naoki Kishi¹, Ryo Kitaura¹, Toshiki Sugai¹, Takeshi Hashimoto², Xinluo Zhao³, Yoshinori Ando³ and Hisanori Shinohara^{1,4,5}

¹Department of Chemistry, Nagoya University, Nagoya 464-8602, Japan

²MEIJO NANO CARBON CO.,LTD.,Japan

³Department of Materials Science & Engineering Meijo University, Nagoya 468-8502, Japan

⁴CREST, Japan Science and Technology Agency, c/o Department of Chemistry, Nagoya University, Nagoya 464-8602, Japan

⁵Institute for Advanced Research, Nagoya University, Nagoya 464-8602, Japan

Double-wall carbon nanotubes (DWNTs) have been widely studied not only for the unique structural and electronic properties but for their possible industrial applications. To characterize such properties of DWNTs in detail, we have to first prepare high quality DWNTs without impurities such as metal particles and amorphous carbons. Arc-discharge with Fe catalyst in a H₂-Ar atmosphere can produce high quality SWNTs. [1] Furthermore, residual Fe can easily be removed because of a small number of graphene sheets around Fe catalyst (Figure1). Furthermore, we have found that the present method can also produce DWNTs in high yield only with a slight experimental modification. Here, we report the production, purification and characterization of the DWNTs so produced.

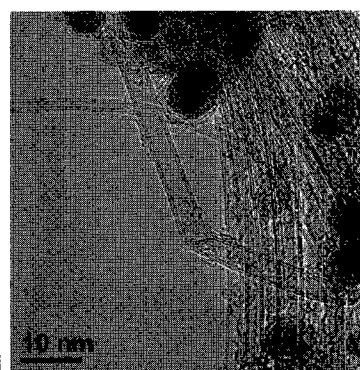


Figure 1. TEM image of as-grown DWNTs

The purification procedure is the following:(i)Air oxidation at 420°C for 30 min, (ii)HCl treatment for 1 day, (iii)Refluxing with H₂O₂ for 3 hours and further HCl treatment for 1 day, and (iv)Heating under 10⁻⁶ torr at 1400°C for 3 days. After the purification, residual weight was about 10 % of the as-grown. Figure2 shows a result of thermogravimetric analysis (TGA) of purified and as-grown DWNTs. After the purification, the on-set temperature shifted to much higher temperature region, which is due to removal of amorphous carbon. Furthermore, residual weights resulting from the presence of Fe particles have reduced from about 65 % to 0.5 %. We will discuss the yield and quality of the present DWNTs in terms of HR-TEM and other characterization.

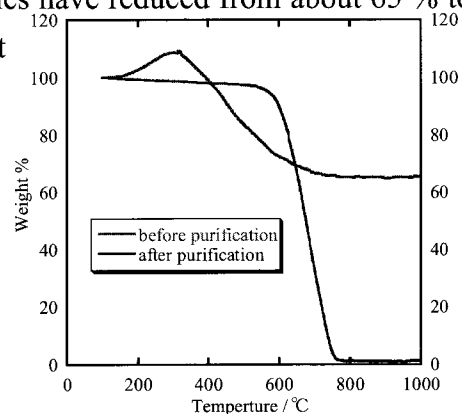


Figure 2. TGA result

References:

- [1] X-L Zhao ,et al, *Chem.Phys.Lett.* **373** 266–271 (2003)

Corresponding Author: Hisanori Shinohara

TEL: +81-52-789-2482, FAX: +81-52-789-1169

E-mail: noris@cc.nagoya-u.ac.jp

3P-11

Cytotoxicological Studies of Carbon Nanotube Particles with Cultured Animal Cells. ~Standardization for in vitro test~

Yuki MORIOKA, Takao SAITO, Michiko KUSUNOKI*,
Motohiro YAMAMOTO^{***}, ○ Katsuya KATO

AMRI, AIST; Anagahora, Shidami, Moriyama-ku, Nagoya, 463-8560, Japan

**JFCC; 2-4-1 Mutsuno, Atsuta-ku, Nagoya, 456-8587 Japan*

***Tokai Carbon Co., Ltd.; 1-2-3 Kitaayama, Minato-ku, 107-8636 Japan*

Abstract: We present here a toxicological assessment of carbon nanotube particles synthesized by the SiC surface decomposition method on mouse osteoblast-like MC3T3-E1 cells in vitro.

Carbon nanotubes (CNT) are becoming increasingly studied, not only for their possible application in the electronic, optics, and mechanical materials, but also in biological application, such as imaging and drug delivery. Because of this, it is imperative to examine the toxicity of these carbon-based nanostructures^{1), 2)}. Here, we examine the cytotoxicology of new carbon nanotube particles in mouse osteoblast-like cell MC3T3-E1 culture. Carbon nanotube particles were prepared according to the previous report³⁾. Briefly, the particles were synthesized by surface decomposition of SiC particles heated to 1700°C and held at this temperature for 1 h in a vacuum. Firstly, the adsorptions of three kinds of proteins (IgG, BSA and cytochrome c) were checked. These materials had high ability for protein adsorption (~30-40 mg/g CNT). Using a traditional cytotoxicity/viability staining assay, we determined that the CNT particles were low toxicity for the cell with a low concentration (0.1 and 0.01 mg CNT/ml medium), but, in higher conc.(0.5 mg/ml), the cell proliferation was reduced a little compared to the hydroxylapatite positive control. The toxicity was also checked using LDH (lactate dehydrogenase) test. As results, in all conc. of CNT particles, the release ratio of LDH from cell were very low, indicating that the particles were reduced the cell activity, but no burst of plasma membrane occurred.

References: 1) F. Tian *et al. Toxicology in Vitro* **20** (2006) 1202-1212. 2) A. Magrez *et al. Nano Lett.*, **2006**; 6 (6); 1121-1125. 3) M. Kusunoki, *et al.*, *Appl. Phys. Lett.*, (1997) **71** 2620 -2622.

Corresponding Author; Katsuya KATO, **E-mail;** katsuya-kato@aist.go.jp

Tel & Fax; TEL: +81-52-736-7295; Fax: +81-52-736-7405

In Situ TEM Study on Field Emission from an Isolated CNT: Field Enhancement Depending on Emitter-Anode Gap

Kensuke Okumura*, Kazuyuki Seko, Kouji Asaka and Yahachi Saito

Department of Quantum Eng., Nagoya University, Nagoya 464-8603, Japan

Carbon nanotubes (CNT) are promising candidates for cold cathode electron field emitters because of their electrical, chemical, mechanical properties and high aspect ratio, which brings about field enhancement on their tips. It is known that field enhancement depends on the distance between a CNT tip and an anode surface [1,2]. In this work, the dependence of the threshold field on the distance between the copper anode and the cathode which is an isolated MWNT attached to tungsten needle was studied by in situ transmission electron microscopy (TEM).

A small bundle of MWNTs was attached to the tip of a tungsten needle by electrophoresis. The CNT emitter and a copper anode were mounted in a special sample holder for TEM (Fig.1). The diameter of this MWNT is about 20nm and the length of the bundle from the W tip is about 8 μm . The distance d between the CNT emitter and the copper anode was varied between 2 μm and 14 μm . The electric voltage was applied until the emission current exceeded 100nA and then it was decreased. The voltage at which the emission current became 100nA was defined as the threshold voltage V_t .

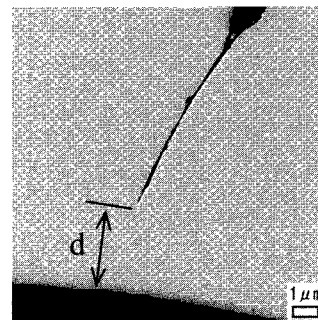


Fig.2

Figure 2 shows that the V_t and the threshold field E_t ($=V_t/d$) against the gap d . The V_t decreases from 99V at $d=14\mu\text{m}$ to 58V at $d=2\mu\text{m}$, while the E_t increases from 7.1V/ μm at $d=14\mu\text{m}$ to 29V/ μm at $d=2\mu\text{m}$. The increase in the E_t at a small d can be explained by the fact that the CNT tip to the anode is approximated to a parallel plate configuration and the geometrical field enhancement decreases.

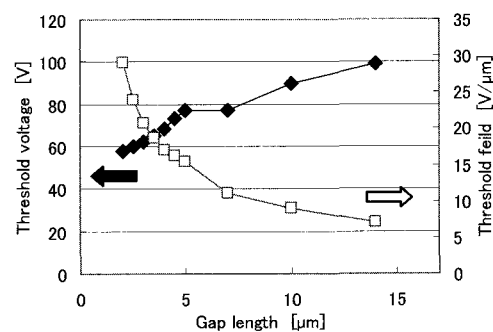


Fig.2

[1] Y.Saito et al., *Mol. Cryst. Liq. Cryst.*, **387**, 79 (2002)

[2] R.C.Smith et al., *Appl. Phys. Lett.* **87**, 103112 (2005)

E-mail: okumura@surf.nuqe.nagoya-u.ac.jp

Tell: 052-789-3714 Fax: 052-789-3703

Field emission microscopy of MWNTs deposited with aluminum

○T.Yamashita, T. Matsukawa, K.Seko, K.Asaka, H. Nakahara, and Y. Saito

Department of Quantum Eng., Nagoya University, Furo-cho, Nagoya 464-8603

Field emission of electrons from a multiwall carbon nanotube (MWNT) with a closed end occurs preferentially from pentagons at the cap when the nanotube surface is clean [1]. It has also been shown that the electron emission is enhanced from the adsorbed molecules when residual gas molecules adsorbed on the surface [2]. In this work, effects of aluminum deposited on the surface of MWNTs were studied by field emission microscopy (FEM).

MWNTs produced by arc discharge were attached to a tungsten hairpin by graphite-bond. Aluminum was deposited onto an apex region of a CNT emitter by using a tungsten filament in the FEM chamber. The amount of aluminum deposited on the CNT cap was changed from ~ 1 nm to ~ 10 nm in terms of mean film thickness. The base pressure of the FEM chamber was $\sim 5 \times 10^{-10}$ Torr.

Figure 1 shows FEM patterns of a clean surface of a CNT and how it changed when aluminum was deposited. Figure 2 represents time-traces of emission current before and after aluminum deposition. The emission current was stabilized considerably over 300 seconds by the aluminum deposition, though the emitter without aluminum showed large fluctuation.

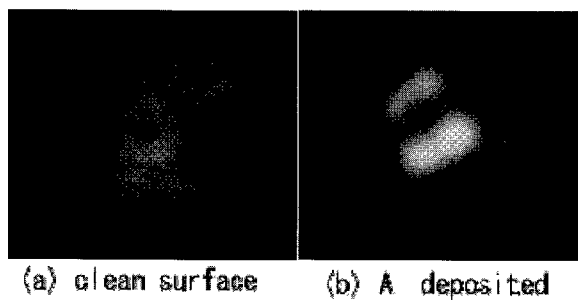


Fig. 1

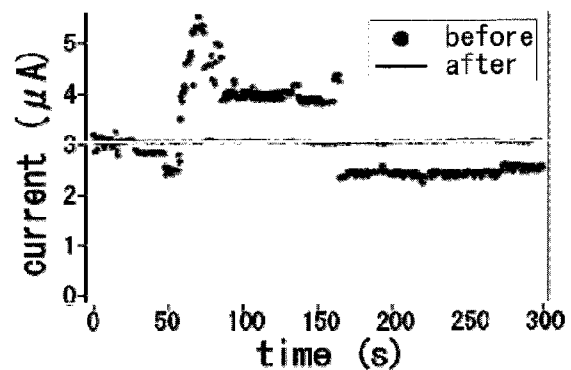


Fig.2

[1] Y. Saito, K. Hata and T. Murata: Jpn. J. Appl. Phys. 39, L271 (2000)

[2] K. Hata, A. Takakura and Y. Saito: Surface Sci. 490, 296-300 (2001)

Corresponding author: Tetsuya Yamashita

E-mail: yamashita@surf.nuqe.nagoya-u.ac.jp

TEL: +81-52-789-3714, FAX: +81-52-789-3703

Reactive Carbon Nanotube Solubilizers

- Individual solubilization and Pulsed Laser Irradiation

○Kaori Narimatsu, Tsuyohiko Fujigaya, Yasuro Niidome and Naotoshi Nakashima

*Department of Applied Chemistry, Graduate School of Engineering,
Kyushu University, Motooka 744, Nishi-ku, Fukuoka 819-0395, Japan*

We report details about carbon nanotube (CNT) solubilizers based on a novel concept, that is, “reactive carbon nanotube solubilizers” that are compounds carrying a reactive moiety for the introduction of the desired functional groups.^{1,2)} In this study, the anthracene moiety-carrying poly(styrene-alt-maleic anhydride) copolymer (**1**, Figure 1) was synthesized by a one-pot synthesis. It was found that the copolymer acts as excellent CNT solubilizers. The vis-near-infrared (IR) spectrum of single-walled carbon nanotubes (SWNTs)/**1** in solution showed characteristic structural spectral features, suggesting the individual dissolution of the SWNTs and the atomic force microscopic image showed a wrapping of SWNTs by **1**. To demonstrate the concept of the “reactive carbon nanotube solubilizer”, a SWNTs/**1** solution was reacted with amino compound, and the introduction of the amide bonding was confirmed.

We examined the effect of near-IR pulsed-laser irradiation onto the SWNTs/**1** solution.²⁾ The near-IR light was absorbed by the SWNTs and converted to heat through photothermal conversion of SWNTs, which did not greatly degrade the polymer-wrapped SWNTs. The local and transient heat via the irradiation resulted in SWNT-flocculation without raising the macroscopic temperature of the solution.

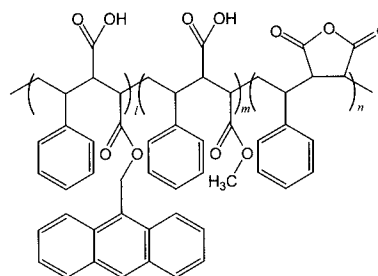


Figure 1. Chemical structure of **1**.

References

- 1) K. Narimatsu, J. Nishioka, H. Murakami, and N. Nakashima, *Chem. Lett.*, **2006**, 35, 892.
- 2) K. Narimatsu, Y. Niidome, and N. Nakashima, *Chem. Phys. Lett.*, **2006**, 429, 488.

Corresponding Author : Naotoshi Nakashima

E-mail : nakashima-tcm@mbox.nc.kyushu-u.ac.jp

Tel&Fax : 092-802-2840

Separation of Semiconducting-Enriched Single-Walled Carbon Nanotubes using a Long Alkyl-Chain Benzenediazonium Compound

○Shouhei Toyoda¹, Yoshifumi Yamaguchi², Masataka Hiwatashi², Yasuhiko Tomonari², Hiroto Murakami², and Naotoshi Nakashima¹

¹*Department of Applied Chemistry, Graduate school of Engineering, Kyushu University, 744 Motoooka, Nishi-ku, Fukuoka 819-0395, Japan,* ²*Department of Science and Technology, Graduate School of Material Science, Nagasaki University, Nagasaki, 852-8521, Japan*

Single-walled carbon nanotubes (SWNTs) contain both metallic and semiconducting SWNTs. Because of this situation, their applications, especially in the fields of nano-electronics in the future, are limited. The separation of the metallic and semiconducting SWNTs is a great challenge in the science and technology of carbon nanotubes. Toward the goal, then separation on the basis of their different physical properties and different chemical selectivity has already been reported, while the efficient bulk separation of the metallic and semiconducting SWNTs is difficult.¹⁻² We designed and synthesized 4-dodecyloxybenzenediazonium tetrafluoroborate (**1**) that preferentially reacts with metallic single-walled carbon nanotubes (SWNTs) by kinetic control.³ We first determined the suitable experimental conditions for the preferential reaction of **1** with individually dissolved SWNTs by monitoring the decrease in absorbance for the metallic SWNT in the range of 400-650 nm in the absorption spectrum of the SWNTs. The reacted SWNTs were thoroughly rinsed with THF to obtain THF-insoluble SWNTs. The Raman spectrum of the THF-insoluble SWNTs showed a strong peak near $\sim 180\text{ cm}^{-1}$ corresponding to a semiconducting breathing band. The metallic breathing bands ($\sim 220\text{ cm}^{-1}$) and Breit-Wigner-Fano (BWF) modes (1520 cm^{-1}) corresponding to the metallic-SWNTs were much weaker than those of the pristine SWNTs. All the results indicate that the THF-insoluble SWNTs are semiconducting-enriched SWNTs.

References:

1. N. Nakashima, *International J. Nanosci.* **2005**, *4*, 119-137
2. H. Murakami, N. Nakashima, *J. Nanosci. Nanotechnol.* **2006**, *6*, 16-27.
3. S. Toyoda, Y. Yamaguchi, M. Hiwatashi, Y. Tomonari, H. Murakami, N. Nakashima, *Chem. Asian J.*, in press.

Corresponding Author : Naotoshi Nakashima

E-mail: nakashima-tcm@mbox.nc.kyushu-u.ac.jp

Tel&Fax : 092-802-2840

Carbon Nanotube-coating on Photografted Polymer Films

○Shinsuke Haraguchi¹, Yoshifumi Yamaguchi², Tsuyohiko Fujigaya¹, Yasuro Niidome¹, and Naotoshi Nakashima¹

¹*Department of Applied Chemistry, Graduate School of Engineering, Kyushu University, 744 Motoooka, Nishi-ku, Fukuoka 819-0395, Japan*

²*Department of Science and Technology, Graduate School of Material Science, Nagasaki University, Nagasaki, 852-8521, Japan*

Carbon nanotubes (CNTs) have received considerable attention by many researchers because of their remarkable electrical, mechanical and thermal properties[1-4]. In this study, we describe coating of polymers (PET, PP, PMMA, etc.) with single-walled carbon nanotubes (SWNTs).

First, a vinyl polymer bearing cationic charge was introduced to the polymer films by photografting. Subsequently, the films were dipped in aqueous solutions of shortened-SWNTs. Figure 1 show a typical photograph of the obtained SWNT-coated polymer film. Figure 2 shows a scanning electron microscopic image of the film, in which we see bundles of the SWNTs. Surface resistivity of the SWNTs-coated films exhibited a drastic decrease compared to those of the original films, indicating the formation of SWNTs networks on the surfaces of the polymer films.

The presented method is very simple and applicable to many polymer films.

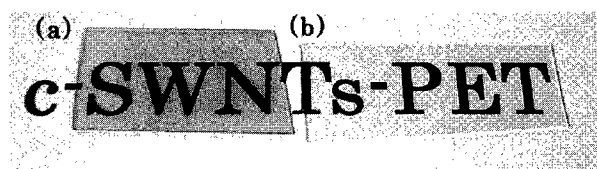


Fig.1. Photograph of (a) SWNTs /PET and (b) virgin-PET film.

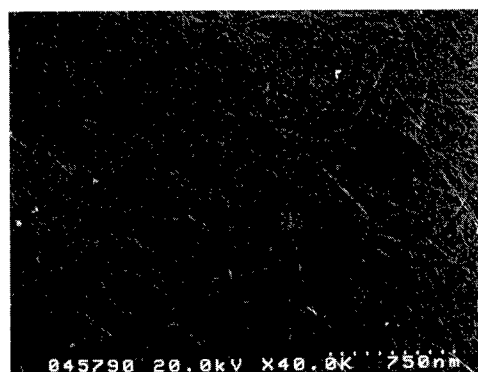


Fig.2. SEM image of a SWNTs/PET.

References

1. *Understanding Carbon Nanotubes: From Basics to Applications* (Eds., A. Loiseau, P. Launois, P. Petit, S. Roche, J.-P. Salvetat), Springer, Berlin, **2006**.
2. *Carbon Nanotubes: Properties and Applications* (Ed., M. J. O'Connell), CRC Press, **2006**.
3. N. Nakashima, A. Fujigaya, H. Murakami, "Soluble Carbon Nanotubes", in "Chemistry of Carbon Nanotubes", eds, V. A. Basiuk, and E. V. Basiuk, American Scientific Publisher, in press.
4. N. Nakashima, *International J. Nanosci.* **2005**, *4*, 119-137

Corresponding Author: Naotoshi Nakashima

E-mail: nakashima-tcm@mbox.nc.kyushu-u.ac.jp

Tel&Fax: +81-92-802-2840

3P-17

Role of van der Waals Interaction during DC Electrodeposition of Carbon Nanotubes

○Takanori Matsumoto and Masahito Sano

*Department of Polymer Science and Engineering, Yamagata University
4-3-16 Jyonan, Yonezawa, Yamagata 992-8510 JAPAN*

Under suitable conditions, carbon nanotubes (CNTs) are electrodeposited efficiently by applying DC electric field to the electrodes immersed in a CNT dispersion in organic solvents. This DC electrodeposition has the following properties.

- (1) CNTs are so strongly adhered to the anode surface that it requires scratching the anode surface to remove the CNT film.
- (2) All CNTs form thin, straight bundles and lie parallel to the anode surface, despite the fact that the dispersion contains many other forms of CNT aggregates.
- (3) A trace amount of water in the dispersing solvents prohibits electrodeposition.
- (4) There is a high possibility that only semiconducting CNTs are deposited.

When CNTs are treated in strong acids, they attain a negative zeta-potential and deposit on the anode surface. The above properties indicate that the electrostatic interaction merely moves CNTs toward the anode surface by electrophoresis and is not responsible for adhesion. We speculate that van der Waals (VDW) interaction plays an important role in adhesion, especially when incoming CNTs are adhered on top of the already deposited CNTs. If VDW interaction is relevant, then the solvent must have a significant effect on the deposition efficiency.

At the last meeting, we reported the results of changing the organic solvents. According to the Lifshitz theory, the Hamaker constant is given by the differences between the static dielectric constant of CNTs and a solvent, together with the dielectric permittivity of these materials at higher frequencies. We have shown that the solvent dependence of the deposition efficiency agrees with the theory if we assume that the contribution of the organic solvents at higher frequencies is much smaller than that of CNTs. Fitting the experimental data with the theory gave the static dielectric constants of CNT to be 3 ~ 6. In order to verify the previous results and to improve accuracy, we have repeated the experiments using other kinds of solvents and different CNT sources,.

Corresponding Author: Masahito Sano

E-mail: mass@yz.yamagata-u.ac.jp, Tel&Fax: +81-(0)238-26-3072

Development of DMFC Stack Cell using Catalytic-Metal-Particles Dispersed Arc-Soot

○ K. Shinohara^a, K. Higashi^a, Y. Izumi^a, M. Yamamoto^a, S. Oke^a, H. Takikawa^a,
N. Aoyagi^b, T. Okawa^b, T. Sakakibara^c, S. Nakamura^c, S. Sugawara^c,
K. Yoshikawa^d, K. Miura^d, S. Itoh^e, and T. Yamaura^e

^a *Department of Electrical and Electronic Engineering,
Toyohashi University of Technology*

^b *Daiken Chemical Co., Ltd*

^c *ENAX, INC.*

^d *Fuji Research Laboratory, Tokai Carbon Co., Ltd.*

^e *Product Development Center, Futaba Corporation*

Carbon nanohorn (CNH), which is a kind of the carbon nano-carbon materials, attracts the attention as an electrode material of Direct Methanol Fuel Cell (DMFC) ⁽¹⁾. On the other hand, it has been indicated that the arc soot, which is also one of nano-carbon materials similar to CNH, prepared at 80 kPa, can support the finer Pt-Ru nano-particles with highly dispersion ⁽²⁾. We have been investigated the single cell DMFC with Pt-Ru and Pt supported arc-soot. In the present study, 6-cell-stacking DMFC, as shown in Fig.1, was examined, This stack cell has good performance on open voltage.

This work was partly supported by the Excellent Research Project of the Research Center for Future Technology, the Research Project of the Venture Business Laboratory, and the Research Project of Research Center for Future Vehicle, Toyohashi University of Technology; the 21st Century COE Program “Intelligent Human Sensing” from the Ministry of Education, Culture, Sports, Science and Technology; and JSPS Core University Program (JSPS-KOSEF in the field of “R&D of Advanced Semiconductor” and JSPS-CAS program in the field of “Plasma and Nuclear Fusion”.

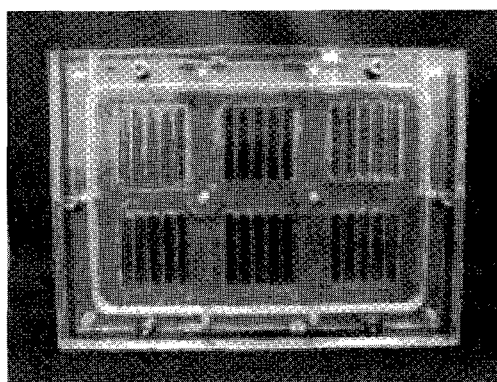


Fig.1 DMFC stack cell

[1] T. Yoshitake, *et al.*: *Physica B.*, **323**, 1627 (2002)

[2] K. Higashi, *et al.*: *Appl. Plasma Sci.*, **13**, 99 (2005)

Corresponding Author: Kenji Shinohara, Hirofumi Takikawa

TEL: +81-532-44-6644, FAX: +81-532-44-6644, E-mail: shinohara@arc.eee.tut.ac.jp

TEL: +81-532-44-6727, FAX: +81-532-44-6727, E-mail: takikawa@eee.tut.ac.jp

Photoinduced Charge-Separation of Chemically Modified Carbon Nanohorns

○Osamu Ito, Atula Sandanayaka, Yasuyuki Araki, Masako Yudasaka, Sumio Iijima, Nikos Tagmatarchis,

IMRA, Tohoku University, NEC, Meijo University, Japan, and Hellenic Inst, Greece

Carbon nanohorns (CNHs) have been extensively studied, due to their unique properties. However, their photo-physical properties dispersed in solutions have not been studied much. Here, we report light induced charge separation processes of chemically modified CNHs dispersed in aqueous solution by employing the steady-state and transient spectroscopic methods.¹⁾ From the fluorescence lifetime measurements of cationic zinc porphyrin (ZnP^{4+}) attached on CNHs (Fig. 1), appreciable shortening of the fluorescence lifetime of ZnP^{4+} was observed by the adsorption on CNHs as shown in Fig. 2, suggesting the photoinduced charge separation via the singlet excited state of ZnP^{4+} . The transient absorption spectra (Fig. 3) show the absorption peaks due to radical cation of ZnP^{4+} in the 450–800 nm regions, which may be broaden by interaction with CNHs and overlapping with triplet state of ZnP^{4+} . In addition, further longer wavelength bands than 800 nm may be attributed to electron trapped in CNHs.

By the steady-light illumination in the presence of electron mediator (methyl viologen dication, MV^{2+}), the accumulation of $\text{MV}^{\bullet+}$ was confirmed by the characteristic 620-nm band in the co-presence of hole transfer reagent (benzyl dihydro-nicotinamide, BNAH) as shown in Fig. 4. This observation indirectly supports the generation of electron-rich species by the photo-excitation of ZnP^{4+} on CNHs; afterward, the electron mediates from CNHs to MV^{2+} , yielding $\text{MV}^{\bullet+}$, whereas the hole on ZnP^{4+} mediates to BNAH, retarding back electron transfer processes. Finally, steady-state concentration of $\text{MV}^{\bullet+}$ can be accumulated as electron pool in aqueous solution.

[1] Pagona, Sandanayaka, Tagmatarchis, Yudasaka, Iijima, Ito, *et al.*, *J. Phys. Chem. B* **2006**, *110*, 20729.

Corresponding Author: Osamu Ito
TEL FAX: +81-22-217-5608, E-mail: ito@tagen.tohoku.ac.jp

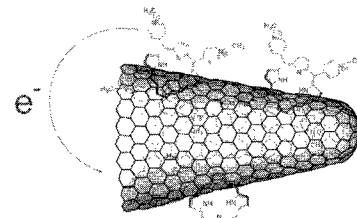


Fig. 1. ZnP^{4+} -CNH hybrids.

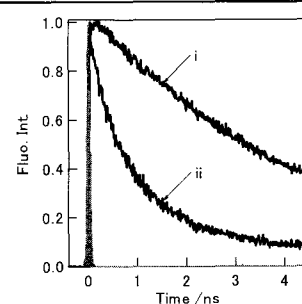


Fig. 2. fluorescence time profiles of (i) ZnP^{4+} and (ii) ZnP^{4+} -CNHs.

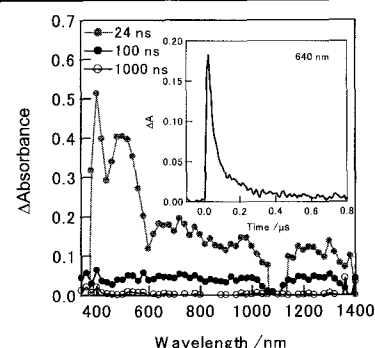


Fig. 3. Transient absorption spectra of ZnP^{4+} -CNHs.

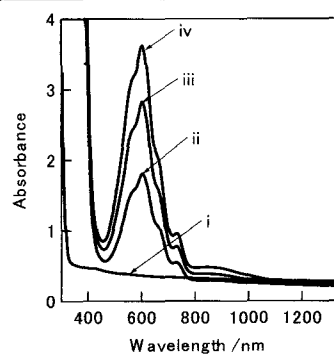


Fig. 4. Accumulation of $\text{MV}^{\bullet+}$ with BNAH; 532 nm light on ZnP^{4+} -CNHs.

Production of single-wall carbon nanohorns with high purity

○ Takeshi Azami^{a,*}, Ryota Yuge^a, Daisuke Kasuya^a, Tsutomu Yoshitake^a, Yoshimi Kubo^a, Masako Yudasaka^a, and Sumio Iijima^{a,b,c}

^a *Fundamental and Environmental Research Laboratories, NEC Corporation
34 Miyukigaoka, Tsukuba, 305-8501, Japan*

^b *JST/SORST, c/o NEC, 34 Miyukigaoka, Tsukuba, Ibaraki 305-8501, Japan*

^c *Meijo University, 1-501 Shiogamaguchi, Tenpaku-ku, Nagoya, 468-8502, Japan*

Since the discovery of single-wall carbon nanohorns (SWNHs) in 1998 [1], we developed a CO₂-laser ablation apparatus for large scale production of SWNHs, and the high production rate of 1 kg/day was achieved [2]. Further investigation revealed that the production of high-purity SWNHs, 95%, was possible, which is shown in this report.

SWNHs were formed by the laser ablation in the reaction chamber and transported into the collection chamber by an argon stream. In the collection chamber, the SWNHs were deposited at the bottom or on the ceiling. We examined the purities of these SWNHs by thermogravimetric analysis (TGA) and transmission electron microscopy (TEM) observation, and found that SWNHs deposited at the bottom had the high purity of >90%, while those at the ceiling, much lower. In order to obtain the larger quantity of SWNH with higher purity at the chamber bottom, we further examined the laser-power densities and laser spot velocities at the target surfaces. The laser power density was controlled by coordinating the laser-spot size. The laser spot velocity was controlled by choosing the target-rotation speed. As a result, the SWNH quantity was maximized at 30 or 45 kW/cm² and 2 to 3 rpm. The graphitic impurities (GGB) [3] increased with the rotation speed as shown in Fig. 1. Thus we concluded that the optimum condition for the production of SWNHs in a large scale with the purity of 95% was 30 kW/cm² of the laser power density and 2 rpm of the target rotation speed.

This work was performed under NEDO's research grant "Manufactured Goods Applying Nanocarbon Project".

[1] S. Iijima, et al., *Chem. Phys. Lett.* **309** (1999) 165., [2] T. Azami, et al., 30th Fullerene-Nanotubes General Symposium (2006), 3p-27., [3] J. Fan, et al., *J. Phys. Chem. B* **109** (2005) 10756.

*Corresponding author: Takeshi Azami

E-mail: azami@frl.cl.nec.co.jp Tel: +81-29-850-2612, Fax: +81-29-856-6137

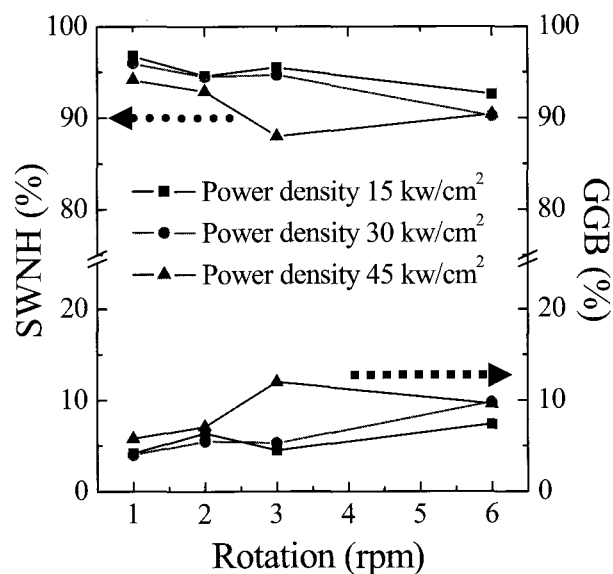


Figure 1. Effect of laser power density and laser velocity on purity of the SWNHs.

Arc-Soot Electrode with Highly Dispersed RuO₂ for Electrochemical Capacitor

OM. Yamamoto¹, K. Higashi¹, K. Shinohara¹, S. Oke¹, H Takikawa¹,
X. J. He², S. Itoh³, T. Yamaura³, K. Miura⁴, K. Yoshikawa⁴

¹Department of Electrical and Electronic Engineering,
Toyohashi University of Technology

²School of Chemistry and Chemical Engineering, Anhui University of Technology

³Product Development Center, Futaba Corporation

⁴Fuji Research Laboratory, Tokai Carbon Co., Ltd.

Electrochemical capacitors using carbon electrode with dispersed RuO₂ nano-particles have been proposed [1], usually called super capacitor. In order to obtain higher performance of the capacitor, the carbon materials, which can support RuO₂ with higher number density and better dispersion, is required [2].

In the present study, the arc-soot (AS), which was prepared by means of arc discharge method from the graphite under particular condition, was examined as a super capacitor. Metallic Ru was supported on AS through a batch reaction based on colloid formation and reduction in ethylene glycol solution. After well kneading the Ru-dispersed AS (Ru-AS), binder (PTFE) and conductive material (KB), the electrode was formed by hot pressing. Then, Ru was oxidized by electrochemical oxidation. The mixture ratio was Ru-AS: PTFE: KB = 8:1:1. The supported quantity of Ru was 10 wt% to 20 wt% against amount of AS.

Figure 1 shows a result of CV curves. Current increases linearly with supported amount of Ru. Capacitances of these capacitors were approximately 58 F/g (Ru, 10 wt.%) and 95 F/g (Ru, 20 wt.%), respectively.

This work was partly supported by the Excellent Research Project of the Research Center for Future Technology, the Research Project of the Venture Business Laboratory, and the Research Project of Research Center for Future Vehicle, Toyohashi

University of Technology; the 21st Century COE Program "Intelligent Human Sensing" from the Ministry of Education, Culture, Sports, Science and Technology; and JSPS Core University Program (JSPS-KOSEF in the field of "R&D of Advanced Semiconductor" and JSPS-CAS program in the field of "Plasma and Nuclear Fusion".

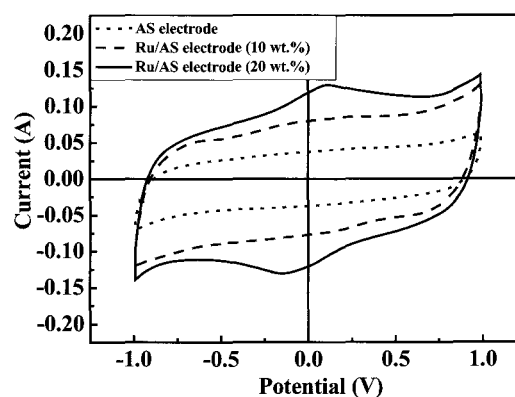


Fig.1. CV curves

[1] T. Nanaumi, *et al.*, *Electrochemistry*, **70**, 681-685 (2002)

[2] J. H. Jang, *et al.*, *J. Power sources*, **123**, 79-85 (2003)

Corresponding Author: Masanobu Yamamoto, Hirofumi Takikawa

TEL: +81-532-44-6644, FAX: +81-532-44-6644, E-mail: yamamoto@arc.eee.tut.ac.jp

TEL: +81-532-44-6727, FAX: +81-532-44-6727, E-mail: takikawa@eee.tut.ac.jp

Magnetism of O₂ adsorbed in SWNH: evaluation of adsorption space

○Hitomi Takahashi, Shunji Bandow, Sumio Iijima

*Department of Materials Science and Engineering, Meijo University,**1-501 Shiogamaguchi, Tenpaku, Nagoya 468-8502, Japan*

Magnetic susceptibilities (χ) of adsorbed O₂ on heat-treated single-wall carbon nanohorns (HT-SWNHs) show anomalous features as compared with those on as-grown SWNHs. In an atmospheric O₂, liquefaction occurs at ~ 90 K, at which the temperature dependence of χ indicates discontinuity, and then the slope of χ decreases due to freezing of rotational freedom of O₂ molecules. Solidification occurs at ~ 50 K (cubic γ -phase), and two kinds of phase transitions take place at ~ 43 (rhombohedral β -phase) and ~ 24 K (monoclinic α -phase), accompanying the magnetic transition. On the other hand, the solidified O₂ in the nano-space (internal site) does not give clear magnetic transition corresponding to γ - β at ~ 40 -50 K; only a gentle slope of χ can be observed between ~ 30 -100 K [1]. For the solidified O₂ on the sidewall of SWNH (external site), clear magnetic transition corresponding to γ - β can be found. By using such a difference in the magnetism, we evaluate the change of the adsorption sites of HT-SWNHs with respect to the heat-treatment temperature.

Figure 1 is a summary of the results of magnetism for adsorbed O₂ on heat-treated SWNHs at various temperatures and corresponding schematics representing the conceptualized images of adsorbed O₂ onto the SWNHs. From the detailed analyses, it was found that the selective adsorption to the "near-hole site" is needed to explain the magnetism observed.

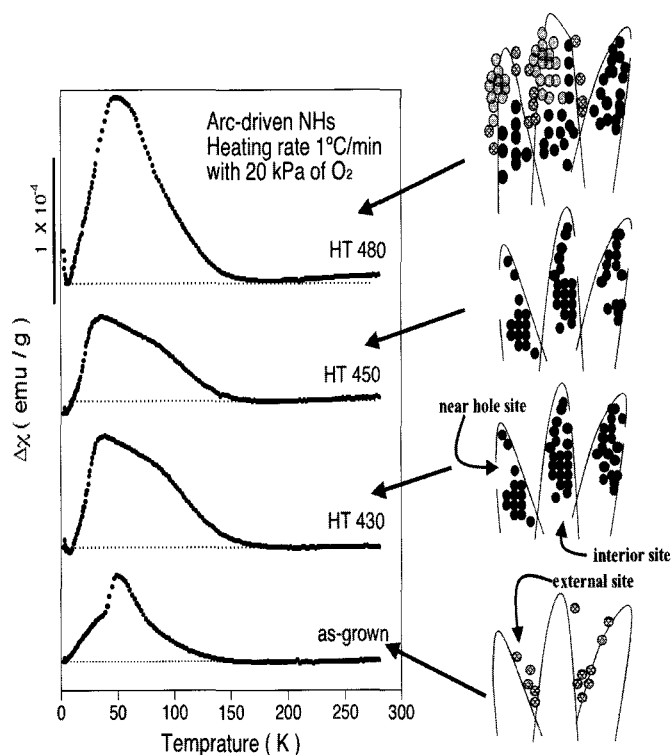


Fig.1 Heating temperature dependence on the magnetism of adsorbed O₂ and corresponding schematics representing the adsorbed O₂.

[1] S.Bandow et al., Chem. Phys. Lett. 401 (2005) 380.

Corresponding: Hitomi Takahashi, E-mail: m0534011@ccmailg.meijo-u.ac.jp, Fax & voice: +81-52-834-4001

Boron nano-particles supported arc-generated nanohorns

○Takayuki Inagaki, Shunji Bandow, Sumio Iijima

*Department of Materials Science and Engineering Meijo University,
1-501 Shiogamaguchi, Tenpaku, Nagoya 468-8502, Japan*

Boron clusters can be applied to the Drug Delivery System, since ^{10}B (natural abundance of ~20 %) nuclei disintegrate with emitting the α -ray when irradiating the low energy neutron. The ranges of the α -particle rays are short enough, and hence they normally stay in a cell. This characteristic is useful for killing the cancer cells without damaging the surrounding normal cells, if the boron clusters are effectively transported to the cancer part. Recently the studies of drug-delivering system using nanohorn aggregates are carried out in the bio-chemistry, in which the medicinal molecules are encased in the interior of nanohorn, and such medicine encased nanohorn-aggregates will be injected to the living body. If the boron clusters can be deposited onto the nanohorns, such a drug-delivering capsules are possibly destroyed by the low energy neutron irradiation and the boron cluster itself will act as medicine due to disintegration. In this study, we try to support the boron nano-particles on the nanohorns simultaneously in the synthesizing process.

Mixed powder of boron and carbon was introduced to 3 mm diameter cylindrical hole drilled at the center of 5 mm diameter carbon rod. Concentrations of boron were changed between 1 and 30 % by weight, and the boron containing carbon rod thus prepared was set at the end of an anode electrode and vaporized by the DC arc discharge with a current of 100 A in an atmospheric pressure of mixture gas environment of Ar and O_2 (5 % of O_2).

From 1 % of boron containing rod, although the production rate of nanohorns was increased as compared with that from pure carbon rod, no remarkable change in the nanohorns themselves was observed. On the other hand, from 3 % of boron containing rod, the carbon nanotubes were easily observed by SEM as indicated in Fig. 1. From 30 % of boron containing rod, we could frequently find the boron related nano-particles that uniformly deposited on the nanohorn-aggregates as shown in Fig. 2. Sizes of these particles are 3-5 nm. Detailed results of analyses of these particles including structural information will be reported.

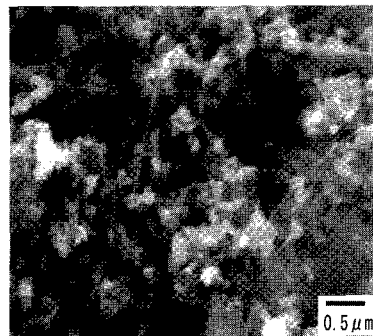


Fig. 1. Scanning electron micrograph of arc soot obtained from 1 % of boron containing rod. Nanotubes can be seen.

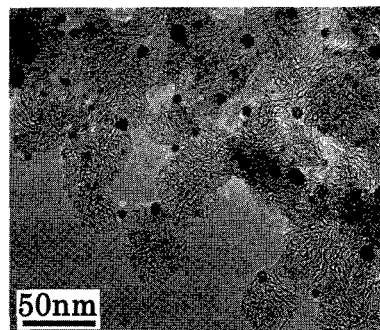


Fig. 2. Transmission electron micrograph of arc soot obtained from 30% of boron containing rod. Boron related nano-particles are deposited on the nanohorns.

Corresponding Author: Takayuki Inagaki, **Email:** m0534004@ccmailg.meijo-u.ac.jp, **Fax & voice** +81-52-834-4001.

High yield production of small diameter carbon nanohorns by means of DC arc discharge and their characterization

○Takayuki Inagaki, Manabu Harada, Shunji Bandow, Sumio Iijima

*Department of Materials Science and Engineering, Meijo University,
1-501 Shiogamaguchi, Tenpaku, Nagoya 468-8502, Japan*

The average size of the aggregates of single-wall carbon nanohorn (SWNH) generated by arc discharge is ca. 50nm, which is approximately a half of the size with that obtained by laser ablation [1]. Although the arc generated SWNHs particles have characteristic of small size, the production yield and purity are somewhat lower than those by laser ablation. In this study, we have succeeded to solve the problem encountered in arc discharge method by improving the arcing chamber. Hence, we introduce here that the optimum condition for producing the SWNHs with high purity, which can be realized by setting the production rate of ~ 240 mg/min at a low arcing energy-density of ~ 5 kW/cm².

First we describe the details of experimental conditions as follows: arcing current and voltage were 200 A and ~ 20 V, respectively, and they were applied between the 10 mm diameter pure carbon rods with a spark gap of ~ 1 mm. Arcing was conducted in a mixture gas of Ar and O₂, where the O₂ concentration was varied from 0 to 30 %. As a result, we found that a condition of 5 % of O₂ effectively produced the SWNHs with high purity of 85 % and a maximum production rate of more than 1 g for 5 min arcing. Figures 1 and 2 indicate, respectively, a typical TEM image and a TG trace taken for SWNHs from 5 % of O₂. From the TG trace, we can find that the purity of SWNHs is about 85 % and 15 % of large graphite balls is included. Details of the experimental results will be discussed in the poster.

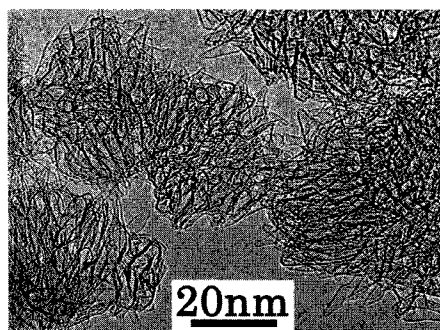


Fig. 1. TEM images of SWNHs produced in 5 % of O₂. SWNH aggregates with the diameter of ~ 30 nm can be found.

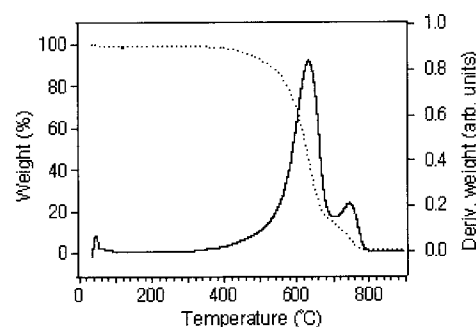


Fig. 2. Thermo-gravimetric analysis of the arc soot produced in 5% of O₂. Two components can be recognized in the derivative curve of weight with respect to T . Low T component is associated with the burning of SWNHs and high T component of large graphite balls.

[1] T. Yamaguchi, S. Bandow, S. Iijima, Chem. Phys. Lett. **389** (2004) 181-185.

Corresponding Author: Takayuki Inagaki,

E-mail: m0534004@ccmailg.meijo-u.ac.jp. **Fax & voice** +81-52-834-4001.

Formation of Nitrogen Atom Endohedral Fullerenes Using a Multipole Mirror-Type Electron Cyclotron Resonance Discharge Plasma

○S. Abe, H. Ishida, S. Nishigaki, T. Kaneko and R. Hatakeyama

Department of Electronic Engineering, Tohoku University, Sendai 980-8579, Japan

The nitrogen atom encapsulated fullerene (N@C₆₀) has characteristic features as novel materials for quantum computer, and has been formed using some plasma methods [1,2]. However, N@C₆₀ formation efficiency is extremely low, and besides the N@C₆₀ formation mechanism has not been clarified in detail.

Therefore, in order to realize the high-efficiency N@C₆₀ formation, we have adopted using an electron cyclotron resonance (ECR) plasma as a nitrogen-ion source [3,4]. The nitrogen ions in the ECR plasma diffuse to a DC-voltage applied copper substrate and are accelerated by an electric field in front of the substrate. Since C₆₀ evaporated by an oven is deposited on the substrate, the nitrogen ions are continuously irradiated to the C₆₀ thin film. The C₆₀ thin film after nitrogen ion irradiation is analyzed by electron spin resonance (ESR), and indicates a very clear hyperfine-split electron paramagnetic resonance spectrum that is considered to originate from N@C₆₀. It is found that the ratio of N@C₆₀ to C₆₀ in the sample depends on the energy of irradiated ions and the optimum condition exists around the ion energy of 20-40 eV. However, the highest ratio of N@C₆₀ to C₆₀ was only 0.01 % at this time.

To increase the ratio of N@C₆₀ to C₆₀, the plasma source is improved to a multipole mirror-type ECR plasma ion source using permanent magnets between the solenoid coils, which can generate a large amount of atomic nitrogen ions N⁺ efficiently due to considerably high temperature electrons under low gas pressures [5]. This magnetic field profile is calculated by MAGNA/FIM to confirm the ECR position which affects confinement of electrons. In this newly developed plasma source, typical values of plasma density and electron temperature are 10¹⁰ cm⁻³ and 30 eV, respectively. Using the multipole mirror-type ECR, much more N⁺ ions are generated due to effective confinement of electrons compared with the conventional ECR ion source, which is confirmed by optical emission spectroscopy. The ratio of N@C₆₀ to C₆₀ is clearly increased with the multipole mirror type ECR ion source.

[1] B. Pietzak, M. Waiblinger, T. A. Murphy, A. Weidinger, M. Höhne, E. Diemel and A. Hirsch, *Chem. Phys. Lett.*, **279**, 259 (1997).

[2] H. Huang, M. Ata and M. Ramm, *Chem. Comm.*, 2076 (2002).

[3] S. Abe, G. Sato, T. Kaneko, T. Hirata, R. Hatakeyama, K. Yokoo, S. Ono, K. Omote and Y. Kasama, Abstracts of the 31st Fullerene-Nanotubes General Symposium, 174 (2006).

[4] S. Abe, G. Sato, T. Kaneko, T. Hirata, R. Hatakeyama, K. Yokoo, S. Ono, K. Omote and Y. Kasama, *Jpn. J. Appl. Phys.*, **45**, 8340 (2006).

[5] G. S. Taki, D. K. Chakraborty, and R. K. Bhandari, *Pramana J. Phys.*, **59**, 775 (2002).

Corresponding Author: Shigeyuki Abe

TEL: +81-22-795-7046, FAX: +81-22-263-9225, E-mail: abe@plasma.ecei.tohoku.ac.jp

Effects of Plasma Parameters on Synthesis of Nitrogen Atom Encapsulated Fullerenes Using an RF Plasma

○S. Nishigaki, S. Abe, T. Kaneko and R. Hatakeyama

Department of Electronic Engineering, Tohoku University, Sendai 980-8579, Japan

A nitrogen atom encapsulated C_{60} ($N@C_{60}$) has favorable properties for quantum computer because the nitrogen atom in C_{60} has no interaction with external environment and its spin relaxation time is relatively long compared to other spin system [1]. Although $N@C_{60}$ has been produced using several plasma methods [2 - 4] so far, the yield of $N@C_{60}$ is extremely low ($N@C_{60}/C_{60} = 10^{-3} - 10^{-2}$ %). Therefore, the purpose of this research is to elucidate a synthesis mechanism of $N@C_{60}$ in order to improve the yield using a radio frequency (RF) discharge which can easily generate a plasma and make its parameters controlled.

An experimental apparatus is schematically shown in Fig. 1. The nitrogen plasma is generated by applying RF power with a frequency of 13.56 MHz to a spiral-shaped RF antenna. The plasma potential ϕ_s and the electron density n_e are controlled by the potential V_g of a grid which is installed at the axial center of the apparatus. The upper side and the lower side of the grid are defined as “plasma production area” and “process area”, respectively. C_{60} is sublimated from an oven (100 mg/hour) and deposited on a water-cooled cylindrical stainless substrate. Nitrogen ions in the plasma are accelerated toward the substrate by a sheath electric field in front of the substrate and are continuously irradiated to C_{60} deposited on the substrate. The irradiated ion energy E_i and ion density can be controlled by varying V_g .

A C_{60} compound including $N@C_{60}$, which is deposited on the substrate, is analyzed by electron spin resonance (ESR) and high performance liquid chromatography (HPLC) to calculate the purity ($N@C_{60}/C_{60}$). It is found that the purity depends on E_i and n_e , and the optimum E_i for synthesis of $N@C_{60}$ is 80 - 140 eV. In this case, the purity of 0.02 - 0.05 % is achieved, which is the highest purity in the results that have ever been reported. However, when E_i is too high, the purity gradually decreases, because the enormous E_i is considered to destroy $N@C_{60}$. When n_e decreases, the purity also decreases due to the lack of the nitrogen ions irradiated to C_{60} .

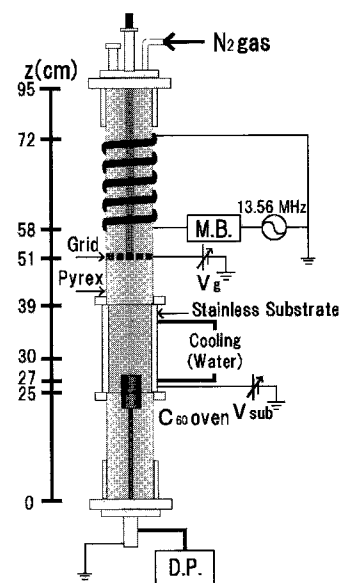


Fig. 1: Schematic of experimental apparatus.

- [1] W. Harneit, *Phys. Rev. A*, **65**, 032322 (2002).
- [2] A. Weidinger, M. Waiblinger, B. Piezak and T. A. Murphy, *Appl. Phys. A*, **66**, 287 (1998).
- [3] M. Ata, H. Huang and T. Akasaka, *J. Phys. Chem. B*, **108**, 4640 (2004).
- [4] S. Abe, G. Sato, T. Kaneko, T. Hirata, R. Hatakeyama, K. Yokoo, S. Ono, K. Omote and Y. Kasama, *Jpn. J. Appl. Phys.*, **45**, 8340 (2006).

Corresponding Author: Shohei Nishigaki

TEL: +81-22-795-7046, FAX: +81-22-263-9225, E-mail: nishigaki@plasma.ecei.tohoku.ac.jp

Ultraviolet Photoelectron Spectroscopy of $\text{Lu}_2@C_{82}(\text{II})$

○Takafumi Miyazaki¹, Masayuki Kato², Konosuke Furukawa², Ryohei Sumii^{3,4}, Hisashi Umemoto⁵, Haruya Okimoto⁵, Toshiki Sugai⁵, Hisanori Shinohara⁵, Shojun Hino¹,

¹ Graduate School of Science & Technology, Ehime University

² Graduate School of Science & Technology, Chiba University

³ Institute for Molecular Science

⁴ Research Center for Materials Science, Nagoya University

⁵ Graduate School of Science, Nagoya University

Ultraviolet photoelectron spectra (UPS) of lutetium atoms encapsulated C_{82} , $C_{2v}\text{-Lu}_2@C_{82}$, will be presented. The UPS were measured at BL8B2 of UVSOR in IMS. The spectra of $C_{2v}\text{-Lu}_2@C_{82}$ are almost identical to those of $\text{Y}_2C_2@C_{82}(\text{II})$ or $\text{Lu}_2C_2@C_{82}(\text{II})$ both of them has C_{2v} symmetry. This finding is another evidence that the electronic structure of atom(s) encapsulated fullerenes is mainly dominated by the cage structure and a principal role of the entrapped atom is to donate electrons to the cage.

The UPS of $C_{2v}\text{-Lu}_2@C_{82}$ are shown in Fig.1. Structures at about 9 and 11 eV are due to Lu4f electrons. Figure 2 shows 40 eV photon excited spectra of $C_{2v}\text{-Lu}_2@C_{82}$ and $\text{Y}_2C_2@C_{82}(\text{II})$. Slight difference between these UPS is in the first band located at around 1.2 eV and the third band located at 2.5 eV. Origin of this difference is not clear and theoretical treatments including encapsulated atoms are required.

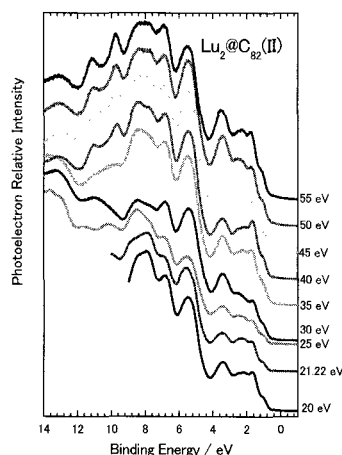


Figure 1 UPS of $C_{2v}\text{-Lu}_2@C_{82}$

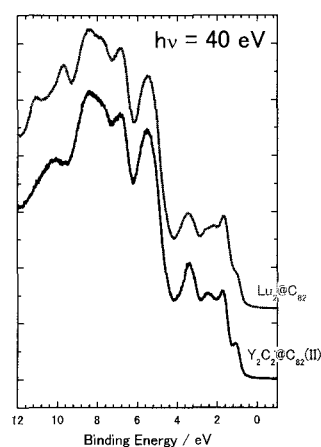


Figure 2 UPS of $C_{2v}\text{-Lu}_2@C_{82}$ & $\text{Y}_2C_2@C_{82}(\text{II})$

Corresponding Author :

S. Hino, E-mail : hino@eng.ehime-u.ac.jp, phone : 089-927-9924

^{13}C NMR Study of $\text{Pr}_2@\text{C}_{80}$

○Manabu Ito¹, Shiho Nagaoka¹, Takeshi Kodama¹, Yoko Miyake¹,
Shinzo Suzuki^{1,2}, Koichi Kikuchi¹, Yohji Achiba¹

¹*Department of Chemistry, Tokyo Metropolitan University, Hachioji, 192-0397, Japan*

²*Department of Physics, Kyoto Sangyo University, Kamigamo-Motoyama,
Kita-ku, Kyoto, 603-8555, Japan*

So far, to clarify a magnetic property of $\text{Ce}^{3+}([\text{Xe}]4f^1)$ in the cage, we have studied the paramagnetic ^{13}C NMR shifts of $\text{Ce}_2@\text{C}_{80}$ and $\text{CeLa}@\text{C}_{80}$ [1,2]. In 1996, $\text{Pr}_2@\text{C}_{80}$ was isolated and its UV-vis-NIR absorption spectrum was measured [3], but till now no magnetic property has been reported. In this study, to elucidate a magnetic property of $\text{Pr}^{3+}([\text{Xe}]4f^2)$ in $\text{Pr}_2@\text{C}_{80}$, we isolated $\text{Pr}_2@\text{C}_{80}$ and measured its ^{13}C NMR spectrum.

Soot containing Pr-metallofullerenes was produced by direct-current (70A) arc discharge of Pr/C composite rods (Pr:C=2:98) under a 500 torr He atmosphere. Pr-metallofullerenes were extracted from the raw soot by refluxing with a TEA/Acetone mixed solvent (1:3) for 6 h. $\text{Pr}_2@\text{C}_{80}$ was isolated by the two-step high performance liquid chromatography method using a PYE column and a Buckyprep-M column. The isolation of $\text{Pr}_2@\text{C}_{80}$ was confirmed by LD-TOF-MS. The UV-vis-NIR absorption spectrum of the isolated $\text{Pr}_2@\text{C}_{80}$ (Fig. 1) is identical to that previously reported [3]. Fig. 2 shows the ^{13}C NMR spectrum of $\text{Pr}_2@\text{C}_{80}$. Only one peak was observed although two peaks whose intensity ratio is 3:1 are expected for the C_{80} cage with I_h symmetry. This may come from line broadening for the missing peak.

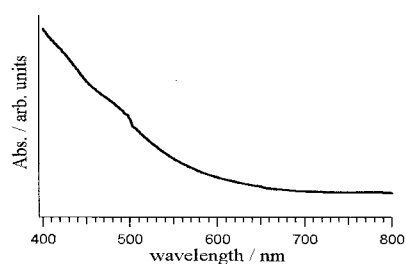


Fig. 1 UV-vis-NIR absorption spectrum of $\text{Pr}_2@\text{C}_{80}$

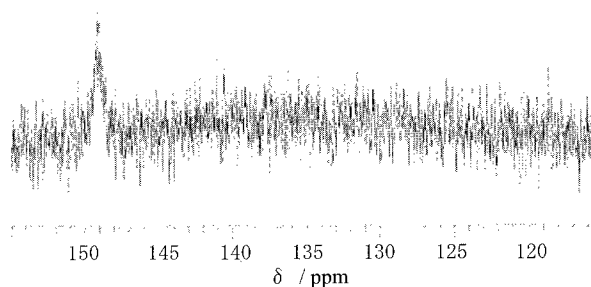


Fig. 2 ^{13}C NMR spectrum of $\text{Pr}_2@\text{C}_{80}$ measured at 125 MHz in CS_2 .

[1] T. Ichikawa et al., The 27th Fullerene-Nanotubes General Symposium, 58 (2004).

[2] T. Komaki et al., The 28th Fullerene-Nanotubes General Symposium, 128 (2005).

[3] J. Ding and S. Yang, *J. Am. Chem. Soc.*, **118**, 11254-11257(1996).

Corresponding Author: Takeshi Kodama

E-mail: kodama-takeshi@c.metro-u.ac.jp

Tel:+81-42-677-2530, Fax:+81-42-677-2525

Fluorescence Properties of Erbium-Metal-Carbide Metallofullerenes: (Er₂C₂)@C_{2n}

○Masahiro Akachi¹, Yasuhiro Ito¹, Ryo Kitaura¹, Toshiki Sugai¹ and Hisanori Shinohara^{1,2,3}

¹*Department of Chemistry, Nagoya University, Nagoya 464-8602, Japan*

²*Institute for Advanced Research, Nagoya University, Nagoya 464-8602, Japan*

³*CREST, Japan Science and Technology Corporation, c/o Department of Chemistry,
Nagoya University, 464-8602, Japan*

Photoluminescence (PL) from erbium metallofullerenes Er₂@C₈₂ has been reported[1,2]. We recently reported [3] that erbium-metal-carbide metallofullerene (Er₂C₂)@C₈₂(III) provides much enhanced fluorescence as compared with the reported Er₂@C₈₂. Obviously, the encapsulated C₂ molecule enhances the fluorescence in (Er₂C₂)@C₈₂(III). Furthermore, the symmetry of C₈₂ cage may also influence the intensity of fluorescence. Cage size may influence the fluorescence intensity because cage-metal interaction should vary depending on the metal-cage distance. Here, we report the PL property of erbium-metal-carbide metallofullerenes with various carbon cages: (Er₂C₂)@C_{2n} (2n=72,74,80,82,84) and discuss the cage size effect to the PL properties.

Figure 1 shows emission spectra of (Er₂C₂)@C_{2n} (2n=72,74,80,84) in CS₂ solution at room temperature, which were measured by a Shimadzu NIR-PL system (CNT-RF). The observed peaks originate in electronic transitions of 4*f* orbital of Er³⁺ (⁴I_{13/2}→⁴I_{15/2}). The spectral features of these spectra are similar to each other, although the fluorescence intensities are very different. The PL intensity of (Er₂C₂)@C₈₂(III) is almost 20 times as strong as (Er₂C₂)@C₈₀. (Er₂C₂)@C₇₄ and (Er₂C₂)@C₇₂ are not fluorescent. We will discuss the fluorescence intensity in terms of the onset of the vis/NIR absorption spectra of these metallofullerenes.

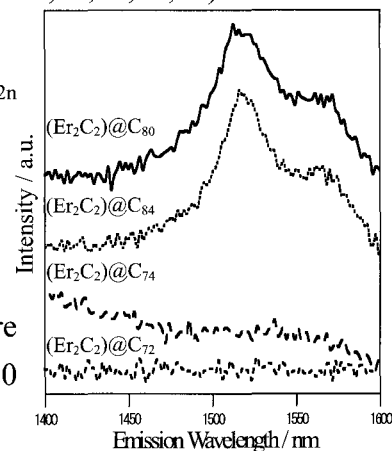


Fig 1 Emission spectra of
(Er₂C₂)@C_{2n} (2n=72,74,80,84)
with an excitation wavelength at 400 nm.

References

- [1] X. Ding *et al.*, *Chem. Phys. Lett.* **269**, 72 (1997).
- [2] R. M. Macfarlane *et al.*, *Phys. Rev. Lett.* **79**, 1397 (1997).
- [3] Ito *et al.*, 31th Fullerene-Nanotubes General Symposium.
- [4] Umemoto *et al.*, 30th Fullerene-Nanotubes General Symposium.

Corresponding Author: Hisanori Shinohara

E-mail: noris@cc.nagoya-u.ac.jp **Tel&Fax:** +81-52-789-2483&1169

Electronic and magnetic properties of acid-adsorbed nanoporous activated carbon fibers

○Hao Sijia, Kazuyuki Takai, and Toshiaki Enoki

*Department of Chemistry, Tokyo Institute of Technology,
Ookayama, Meguro, Tokyo, 152-8551, Japan*

Nanographite featured with open edges has a nonbonding π -electronic state (edge state) of edge origin [1], which causes unconventional electronic and magnetic features [2, 3]. Acid-adsorption effects on the magnetic properties of nanoporous carbon material consisting of nanographite network are investigated by using activated carbon fibers (ACFs) as host material, and nitric acid and hydrochloric acid as guest.

Commercially available pristine ACFs were evacuated at 200°C in a Pyrex glass tube, and then vapor acid purified by freeze-pump-thaw method was introduced. The acid contents of the samples were controlled by the acid concentration and adsorption temperature. No change is observed in the magnetic properties upon adsorption of hydrochloric acid. Figure 1 shows the temperature dependence of the inverse magnetic susceptibility χ_c for HNO₃ adsorbed ACFs (HNO₃-ACFs). The deviation from the linear relation observed in the higher temperature is attributed to the desorption process of HNO₃ accommodated in the nanopores. The temperature

above which the deviation appears is lowered upon the increase in the HNO₃ content. The observed localized spins concentration inversely proportional to the gradient of χ_c^{-1} plots decreases steeply with the increase of the HNO₃ content in the early stage of nitric acid adsorption up to ca. HNO₃/C~0.005. This is caused by the charge transfer interaction with the HNO₃ species facing to the surface of nanographite in the nanopores of ACFs. Above HNO₃/C ~ 0.005, the decrease in the spin concentration becomes moderate and saturated at $\sim 1.0 \times 10^{19} \text{ g}^{-1}$, which is about a quarter of that of the non-adsorbed ACFs. This change in the spin concentration is related to the contribution of the edge-state spins on nanographene, which do not directly face to adsorbed HNO₃ in the nanopores.

[1] Fujita, et al., J. Phys. Soc. Jpn. **66**, 1864 (1997). [2] Shibayama, et al., J. Phys. Soc. Jpn. **69**, 734 (2000). [3] K. Takai, et al., Phys. Rev. B **73**, 035435 (2006).

Corresponding Author: Hao Sijia, E-mail: hao@chem.titech.ac.jp, Tel&Fax: 03-5734-2610

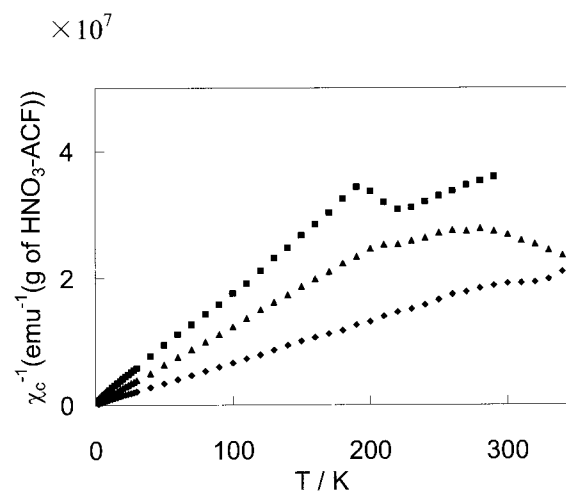


Fig.1 χ_c^{-1} -T plots for HNO₃-ACFs. ◆, ▲, and ■ denote the data for the HNO₃-ACFs with HNO₃/C=0.0014, 0.0024 and 0.204, respectively.

Chemical Control of Nanodiamond Surface Leading to Control of the Water Dispersibility

○Tatsuya Takimoto¹, Naoki Kadota¹, Yoichi Morita², Shuji Aonuma², Takahide Kimura¹ and Naoki Komatsu¹

¹*Department of Chemistry, Shiga University of Medical Science, Seta, Otsu 520-2192, Japan.*

²*Department of Materials Science, Osaka Electro-Communication University, Neyagawa, Osaka 572-8530, Japan.*

It is well-known that strict control of physical properties are required for the fine applications of nanocarbon compounds and that their properties are closely related to their chemical structures. Therefore, chemical control of diamond surface has been extensively investigated; hydrogenation, chlorination, amination, esterification and so on. However, only a few reports referred to the correlation of the surface structure with the physical properties; solubility, hydrophilicity and -phobicity and water repellency. This is probably because the particle size of the diamonds is not small enough and/or the coverage of the functionalities is not enough to affect their physical properties. Herein, we describe control of water dispersibility nanodiamonds (NDs) by the surface functionalization.

The following four kinds of the functionalized NDs, hydrogenated (**1**), hydroxylated (**2**), acetoxylated (**3**) and aminated (**4**), were prepared according to the reported methods. [1-3] The dispersibility of these NDs was determined as follows. ND powder (120 mg) in distilled water (8.0 ml) was bath-sonicated for 1h. After the resulting suspension was centrifuged at 18500 g for 10 min at 20°C, the supernatants (5.0 ml) was separated, evaporated and dried *in vacuo* to give solid. The dispersibility of NDs was determined from the weight.

The dispersibility of the functionalized NDs is summarized in Fig. 1. The dispersibility of **2**, **3** and **4** is found to be ten times larger than that of **1**, indicating clearly that surface functions on NDs remarkably affect their physical properties.

This work was supported by Industrial Technology Research Grant Program in 2005 from New Energy and Industrial Technology Development Organization (NEDO) of Japan.

References:

- [1] Ando, T.; Ishii, M.; Kamo, M.; Sato, Y. *J. Chem. Soc. Faraday Trans.*, **89**, 1783, (1993).
 [2] Ando, T.; Yamamoto, K.; Suehara, S.; Kamo, M.; Sato, Y.; Shimozaki, S.; Nishitani-Gamo, M. *J. Chin. Chem. Soc.*, **42**, 285, (1995).
 [3] Tsubota, T.; Tani, S.; Ida, S.; Nagata, M.; Matsumoto, Y. *Phys. Chem. Chem. Phys.*, **5**, 1474, (2003)

Corresponding Author: Naoki Komatsu

E-mail: nkomatsu@belle.shiga-med.ac.jp

Tel: +81-77-548-2102, **Fax:** +81-77-548-2405

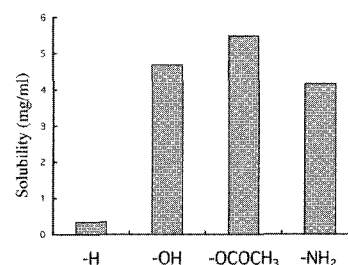


Fig. 1. Dispersibility of functionalized NDs

Encapsulation of La in Spherical Graphitic Shells by Arc Discharge

○Kazunori Yamamoto^a, Takatsugu Wakahara^b, Takeshi Akasaka^b

^a*Nanomaterials Research Group, Quantum Beam Science Directorate,
Japan Atomic Energy Agency, Tokai-mura, Naka-gun, Ibaraki 319-1195, Japan*

^b*Center for Tsukuba Advanced Research Alliance, University of Tsukuba, Ibaraki 305-8577,
Japan*

Abstract:

There has been great interest in the incorporation of foreign materials into fullerene-like multi-shell carbon cage structures such as polyhedral nanocapsules and spherical onions.

Polyhedral nanocapsules filled with LaC₂ crystals were discovered in carbonaceous cathode deposits formed by arc-discharge evaporation and following deposition of La with carbon under an inert gas atmosphere [1, 2]. The transmission electron microscopy (TEM) characterization of the deposits shows that polyhedral graphitic particles generally show a hollow in the center whose shape is given by the outer faceting of the particle.

On the other hand, spherical multi-shell onions filled with metals were formed by irradiation of a composite of graphitic carbon and nano-sized metal crystals at higher temperature alone [3].

In this study spherical multi-shell onions filled with La have been found in the conventional fullerene arc soot of La synthesized at 35 Torr He.

References:

1. R. S. Ruoff, et al., *Science*, **259**, 336(1993).
2. M. Tomita, et al., *Jpn. J. Appl. Phys.*, **32**, L280(1993).
3. F. Banhart, et al, *Chem. Phys.Lett.*, **292**, 554(1998).

Corresponding Author: Kazunori Yamamoto

E-mail: yamamoto.kazunori@jaea.go.jp

Tel&Fax: +81-29-282-6474&+81-29-284-3813.

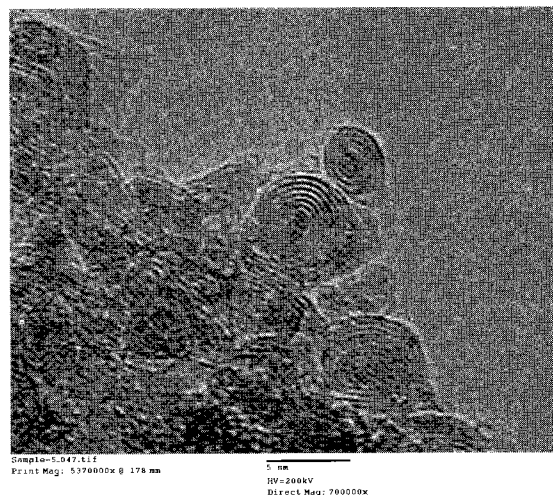


Figure 1. TEM image of onion like structures.

Effect of Annealed Temperature on the Capacitance of Electrochemical Capacitors

*X.J. He¹, M. Yamamoto², K. Higashi², K. Shinohara², S. Oke², H. Takikawa², S. Itoh³, T. Yamaura³, K. Miura⁴, K. Yoshikawa⁴

¹ School of Chemistry and Chemical Engineering, Anhui University of Technology

² Department of Electrical and Electronic Engineering,
Toyohashi University of Technology

³ Product Development Center, Futaba Corporation

⁴ Fuji Research Laboratory, Tokai Carbon Co., Ltd.

Electrochemical capacitors (ECs) are unique energy storage devices that exhibit high power density and long cycle life [1]. Activated carbon (AC) is typically used as the electrode of double layer capacitors. Hydrous ruthenium oxide ($\text{RuO}_2 \cdot \text{H}_2\text{O}$) is among the best candidates for pseudo capacitance materials. Annealed temperature of $\text{RuO}_2 \cdot \text{H}_2\text{O}$ loaded on AC plays an important effect on the capacitance of ECs [2].

In this paper, effect of annealed temperature of $\text{RuO}_2 \cdot \text{H}_2\text{O}$ loaded on AC on the capacitance of ECs is investigated by constant discharge. $\text{RuO}_2 \cdot \text{H}_2\text{O}$ was synthesized by adding AC into ruthenium chloride and ammonium hydrogen carbonate solution under ultrasonic. RuO_2/AC composites were washed 4 times by distilled water and dried at room temperature after separation with a filter paper. The resultant RuO_2/AC composite was annealed at different temperature in air. The annealed RuO_2/AC composite was mixed with binder (PTFE) in the weight ratio of 90:10. The electrode was made by cold pressed at 15 MPa pressure.

Fig. 1 presents effect of annealed temperature on the capacitance of ECs. The results show that specific capacitance of RuO_2/AC electrode passed through a maximum at 150°C when annealed temperature increased from 25 to 280°C . The specific capacitance of ECs reaches $178.2 \text{ F}\cdot\text{g}^{-1}$ (Ru, 20 mol.%).

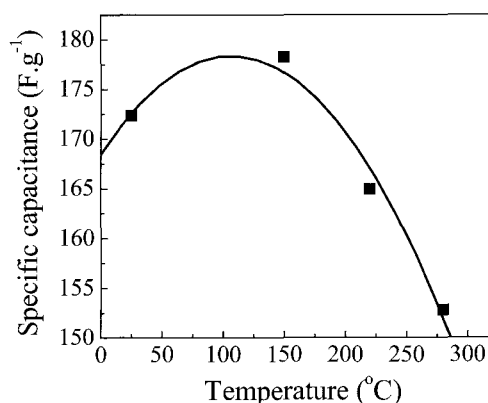


Fig.1. Specific capacitance vs. Temperature

This work was partly supported by the Excellent Research Project of the Research Center for Future Technology, the Research Project of the Venture Business

Laboratory, and the Research Project of Research Center for Future Vehicle, Toyohashi University of Technology; the 21st Century COE Program "Intelligent Human Sensing" from the Ministry of Education, Culture, Sports, Science and Technology; and JSPS Core University Program (JSPS-KOSEF in the field of "R&D of Advanced Semiconductor" and JSPS-CAS program in the field of "Plasma and Nuclear Fusion".

[1] Y. Sato, *et al.*, *Electrochem. Solid-State Lett.*, **3**(3), 113-116 (2000)

[2] J.H. Jang, *et al.*, *J. Electrochem. Soc.*, **153**(2), A321-A328 (2006)

*Corresponding Author: Xiaojun He, Hirofumi Takikawa

TEL: +81-532-44-6644, FAX: +81-532-44-6644, E-mail: xjhe@arc.eee.tut.ac.jp

TEL: +81-532-44-6727, FAX: +81-532-44-6727, E-mail: takikawa@eee.tut.ac.jp

3P-34

Fully-automated CVD system for gram scale production of Super growth SWNTs -A step toward industrial-scale production-

- Don N. Futaba, Tatsunori Namai, Tatsuki Hiraoka, Kenji Hata, Takeo Yamada,
Motoo Yumura and Sumio Iijima

*National Institute of Advanced Industrial Science and Technology (AIST), Tsukuba,
305-8565, Japan*

In addition to scientific innovation, the development of carbon nanotube (CNT) technology (and consequently a CNT-based industry) is reliant upon the availability of CNTs. While commercially available, the current cost for CNTs is greater per weight than gold, which makes them prohibitively expensive for wide-range industrial use. To realize this, not only is an efficient and pure process necessary, scalability plays an essential role. Previously we demonstrated the highly pure and highly efficient synthesis of single-walled carbon nanotubes (water-assisted or “Super-growth” chemical vapor deposition (CVD))¹ which simultaneously addressed problems, such as scalability, purity and cost. Here, we demonstrate the scalability of the Super-growth process with a fully-operational and fully-automated scaled-up CVD system. This batch-style CVD system, designed analogously to semiconductor fabrication processing, operates using a 2” tube furnace, sample cassette storage system with expandable capacity, robotic arm sample manipulation, and utilizes metal foil substrates. The ability to accommodate samples of 48 cm² total area translates to a ~10-fold increase in the yield, and the use of metal foil substrates² results in a 140-fold reduction in cost compared to silicon without limitations in size or shape. This represents one step in the scaling-up process toward industrial-scale SWNT production.

References:

- [1] K. Hata *et al*, *Science*, **306**, 1241 (2004).
[2] T. Hiraoka *et al.*, *J. Am. Chem. Soc.* **128**, 13338 (2006).

Corresponding Author: Don N. Futaba

E-mail: d-futaba@aist.go.jp

Tel&Fax: (029) 861-5080 ext 46763

Mass Production of Carbon Nanotwist and its Field Emission

○Y. Hosokawa^a, R. Sugiura^a, H. Shiki^a, H. Takikawa^a, T. Ina^b, S. Itoh^c, and T. Yamaura^c

^a *Department of Electrical and Electronic Engineering,
Toyohashi University of Technology.*

^b *Fundamental Research Department, Toho Gas Co., Ltd.*

^c *Product Development Center, Futaba Corporation.*

Carbon Nanotwist (CNTw) is a kind of helical carbon nanofiber, without inside diameter, being different from carbon nanocoil (CNC) with a certain inside diameter. CNTw has been prepared on the substrate only in the form of film. In the present, CNTw with high purity was semi-massively produced in powder form by catalytic CVD method with using particularly controlled catalyst. Then the CNTw powder was pasted with non-conductive binder. The pasted CNTw was printed on the conductive glass plate and field electron emission property was examined. The result is shown in Fig. 1. It was found that CNTw-paste printed film has good field emission property and it showed the possibility of the paste for large area FED.

This work was partly supported by the Excellent Research Project of the Research Center for Future Technology, the Research Project of the Venture Business Laboratory, and the Research Project of Research Center for Future Vehicle, Toyohashi University of Technology; the 21st Century COE Program “Intelligent Human Sensing” from the Ministry of Education, Culture, Sports, Science and Technology; and JSPS Core University Program (JSPS-KOSEF in the field of “R&D of Advanced Semiconductor” and JSPS-CAS program in the field of “Plasma and Nuclear Fusion”.

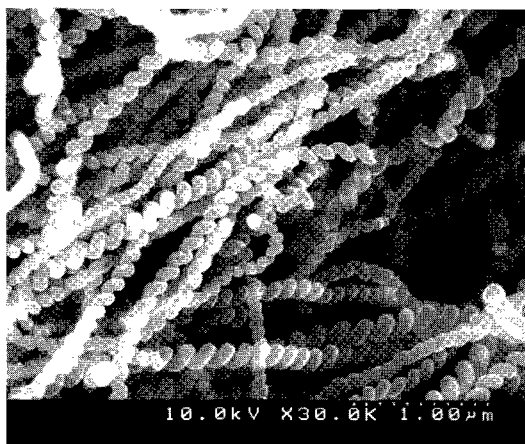


Fig. 1. SEM image of CNTw.

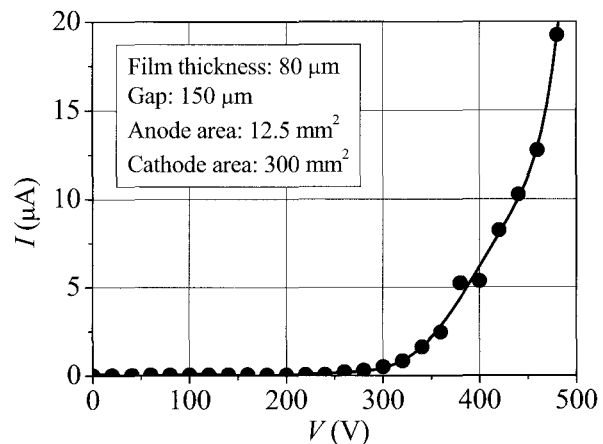


Fig. 2. I - V characteristics

Reference: T. Katsumata, Y. Fujimura, M. Nagayama, H. Tabata, H. Takikawa, Y. Hibi, T. Sakakibara, S. Itoh:
Trans. Mater. Res. Soc. Jpn., **29**, 501 (2004)

Corresponding Author: Yuji Hosokawa, Hirofumi Takikawa

E-mail: hosokawa@arc.eee.tut.ac.jp, Tel & Fax: +81-532-44-6644

E-mail: takikawa@eee.tut.ac.jp, Tel & Fax: +81-532-44-6727

Methodology for Fabricating LB Films of Fullerene

○Yasuhiro F. Miura, Atsushi Yamashita, Issei Matsuoka,
Mitsutaka Urushibata and Michio Sugi

*Graduate School of Engineering, Toin University of Yokohama
1614 Kurogane-cho, Aoba, Yokohama 225-8502, Japan*

Langmuir-Blodgett (LB) films of fullerene (C_{60}) are typically fabricated utilizing chemical modifications or amphiphilic matrices.¹⁾ The chemical modifications and matrices, however, may limit the electrical and optical functions in the ultra-thin systems. In this paper, in order to fabricate C_{60} LB films without introducing chemical modifications and matrices, we propose to employ a modified horizontal lifting method proposed by Ishii²⁾, by which substrates are first immersed in the subphase before spreading the film at the air/water interface, and then the film is lifted up under the floating film of C_{60} .³⁾

A quartz plate, whose surface was hydrophobized with the vapor of 1, 1, 1, 3, 3, 3-hexamethyldisilazane, was set on a Teflon plate hung by stainless steel wires, 0.2 mm in diameter, and immersed in the subphase of pure water in a horizontal position. Then, the floating C_{60} layer was lifted up by raising the substrate with the surface pressure kept at 30 mN/m. The typical raising speed was *ca.* 1 mm/min. The C_{60} film at the air/water interface was also transferred onto the solid support by the conventional horizontal lifting method at the surface pressure of 30 mN/m for comparison.

The absorbance peaks at 216- 266- and 340-nm bands linearly increase with increasing the number of deposition, suggesting the reproducible film deposition. The optical density of the C_{60} LB film increases 3.5 times by the use of the modified horizontal lifting method, suggesting a drastic improvement of the transfer ratio. The atomic force microscopy (AFM) observation has revealed that the substrate surface is well covered by the C_{60} clusters, 0.1-0.4 μm in lateral size, and 30-70 nm in height, without any uncovered areas, while exposure of the bare substrate surface is inevitable by the conventional horizontal lifting method. We have demonstrated that the modified horizontal lifting method has the potential to be a versatile technique for fabricating the C_{60} films without the aid of amphiphilic matrices and/or chemical modifications. We further touch upon the experimental conditions, such as subphase temperature and concentration of the spreading solvent.⁴⁾

Reference

- 1) T. Nakamura H. Tachibana, M. Yumura, M. Matsumoto, R. Azumi, M. Tanaka and Y. Kawabata, *Langmuir*, **8** (1992) 4.
- 2) M. Sugi, *Journal of Molecular Electronics*, **1** (1985) 3.
- 3) Y. F. Miura M. Urushibata, H. Matsuoka, S. Morita and M. Sugi, *Colloids and Surfaces A*, **284-285** (2006) 93.
- 4) A. Yamashita, S. Morita, I. Matsuoka, Y. F. Miura and M. Sugi, *Trans. Mater. Res. Soc. Jpn.*, **31** (2006) 609.

Corresponding Author: Yasuhiro F. Miura

E-mail: yfmiura@cc.toin.ac.jp

Tel & Fax: +81-(0)-45-974-5290

Comparison of evolved gas by some pretreatment methods of CNT

○ Shinji Fukumoto, Toyohito Wada, Yasushi Suzuki

*Analytical Applications Department, SHIMADZU CORPORATION
Kanagawa 259-1304, Japan*

Various evolved gasses have been evaluated by properties of a matter after treatment, reactivity. We evaluated the method to detect change of evolved gas by processing and difference of products, which occurred by using "Pyrolysis GCMS System".

Ordinary to measure weight change with temperature change thermo gravimetric method is used.

On the other hand, EGA (Evolved Gas Analysis)-GCMS is used as one of technique performing qualitative analysis of the gas with weight decrease.

We introduce EGA-GCMS method and application, which we analyzed with this method about SWNT. The refinement of a sample was important in case of analyzing CNT, so we tried to confirm the difference of refinement effect by some pretreatment in EGA-GCMS.

Figure 1 shows a schematic diagram of EGA-GCMS and Figure 2 shows application of the change of evolved gas from CNT.

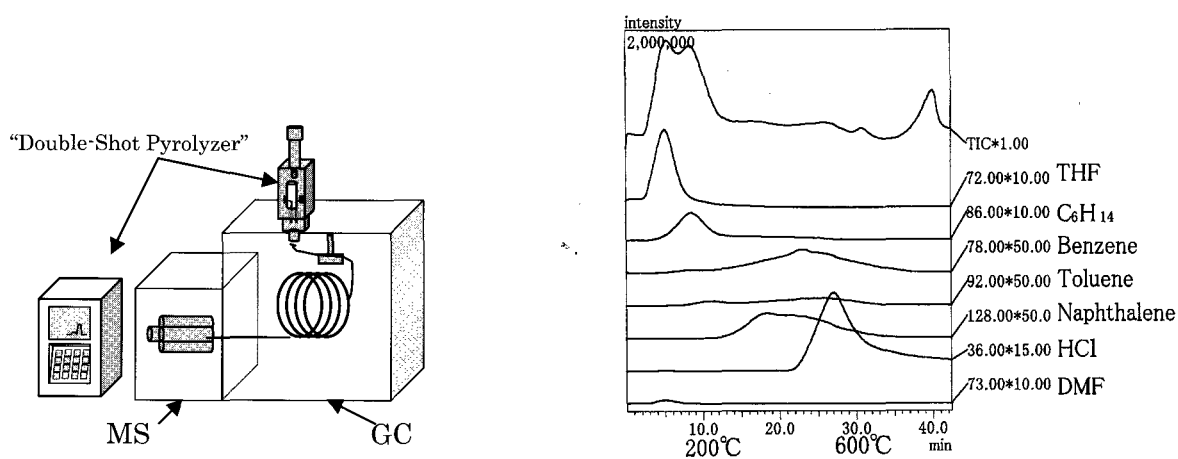


Fig.1 Schematic Diagram of EGA-GCMS

Fig.2 EGA Curves of CNT

References Ohtani.H and Tsuge.S "Polymer Characterization by High-Resolution Pyrolysis-Gas Chromatography" (Hanser Publisher), Munich(1987)

Corresponding Author Shinji Fukumoto **E-mail** fukumoto@shimadzu.co.jp **Tel&Fax** (0463)88-8660/8670

Acknowledgements: We are grateful to Dr. Shinohara and Prof. Nakashima (Kyushu University) for guidance of an offer and analysis of a sample.

An XRD study of multiwalled carbon nanotubes' diameter

○Atsuhiko Kunishige, Tohru Kawamoto, Shoichi Kase, and Yoshiyuki Sumiyama

UBE Scientific Analysis Laboratory, Inc., Kogushi, Ube, Yamaguchi 755-8633, Japan

In application of carbon nanotubes (CNTs), the product performance of electrical conductivity, thermal conductivity and strength has close relation to the tube diameters, length, impurities and defects. At the last symposium, we evaluated length distribution of individually dispersed single-walled CNTs (SWCNTs) by AFM observation and reported the effect of surfactant concentration on the distribution[1].

Reznik et. al.[2] and Maniwa et. al.[3] reported structural properties of multiwalled carbon nanotubes (MWCNTs) by the XRD analysis. Here we report a new evaluation method of MWCNTs about diameters and the distributions, in which we correlates SEM observation results with powder XRD profile analysis.

We used three MWCNT samples of (a), (b) and (c) with different average diameter made in Nanotech Port Co.,Ltd.. Fig.1 shows (002) reflections of these samples, which is indexed on the basis of the hexagonal graphite and fitted to convolutions of Lorentian and Gaussian line shapes.

In Fig.2, we plotted a reciprocal of the full width at half maximum (FWHM) of the (002) peak versus an average outer diameter which was estimated from SEM images such as an inset. We found very good correlation, which can be used for diameter evaluation of MWCNTs. Another correlation with diameter distribution will be discussed.

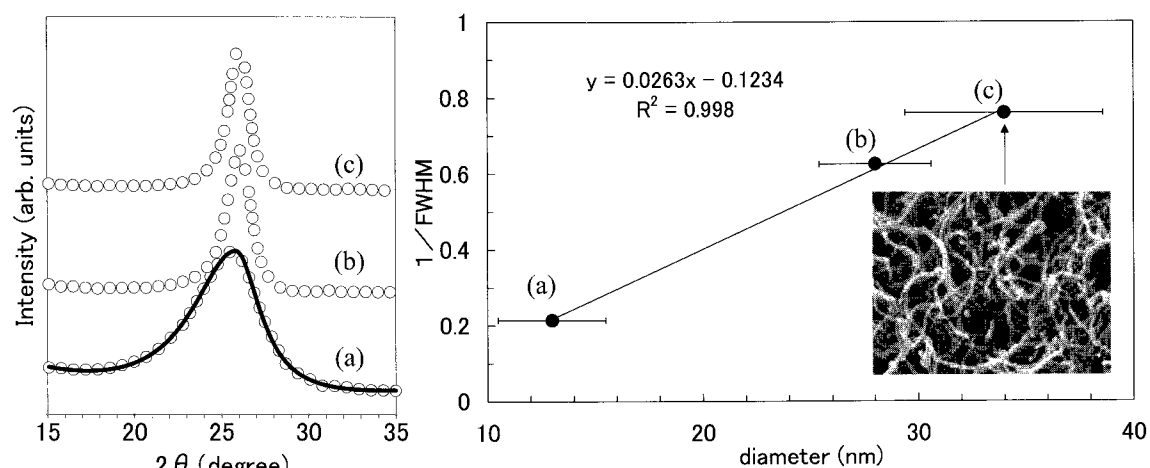


Fig.1. (002) reflections of MWCNT samples.

Fig.2. Relation between diameter and $1/\text{FWHM}$ of MWCNTs' (002) peak. The inset shows a SEM image of the sample (c).

References:[1] H. Nakagawa et. al.: The 31st Fullerene-Nanotubes General Symposium, (2006) 147.

[2] D.Reznik et. al.: Phys.Rev.B **52**,116 (1995) .[3] Y.Maniwa et. al.: Phys.Rev.B **64**,073105 (2001) .

Corresponding Author: Atsuhiko Kunishige

E-mail: atsuhiko.kunishige@ube-ind.co.jp

Tel&Fax: +81-836-31-0987, +81-836-31-0956

発表索引
Author Index

Author Index

～A～

A. F. M. Mustafizur Rahman 2P-31
 Abe Shigeyuki 3P-25, 3P-26
 Abhijit Chatterjee 1-13
 Achiba Y. 2P-17
 Achiba Yohji 2P-8, 3P-28
 Ago Hiroki 1P-17, 1P-18, 3-1
 Aihara Yasutaka 1P-40
 Aikawa Takumi 1P-20
 Ajima Kumiko 1P-25, 2-14
 Akachi Masahiro 3P-29
 Akachi Takao 2P-21, 2P-36, 2P-37
 Akasaka Takeshi 2-1, 2-2, 2-3, 2P-14,
 2P-35, 3P-32
 Akima Nima 2P-1
 Akimaru Hirosuke 2P-7
 Akita Seiji 1-3, 1-12
 Alex Grueneis 1-2
 Ando Hiroaki 1P-4
 Ando Shingo 1P-39
 Ando Yoshinori 3P-10
 Ando Yosinori 3P-4
 Annamalai Karthigeyan 3-8
 Aoki N. 1P-38
 Aoki Nobuyuki 1P-37
 Aoki Takaaki 3P-2
 Aonuma Shuji 3P-31
 Aoyagi Nobuyoshi 3P-18
 Aoyagi Shinobu 2-4, 2P-21
 Arai Fumihito 2P-15
 Araki Yasuyuki 1-11, 2P-5, 3P-19
 Asaka Koji 3P-12, 3P-13
 Atula Sandanayaka 1-11, 3P-19
 Awaga Kunio 2P-36
 Awane Tohru 1P-35
 Awano Yuji 1P-20, 3-3, 3-5
 Azami Takeshi 1P-21, 3P-20

～B～

Bandow Shunji 1P-15, 2P-6, 2P-36,
 3P-22, 3P-23, 3P-24

Bandow Shyunji 1-15

～C～

Catalin Romeo Luculescu 2P-11
 Cherry Ringor 1P-34, 1P-35
 Chien-Chao Chiu 1P-11
 Chih-Chien Chu 1P-33
 Christian Kramberger 1-2

～D～

Deguchi Shigeru 2-12
 Don N. Futaba 1-1, 3P-34

～E～

Ebi Takahiro 2-11
 Enoki Toshiaki 3P-30
 Erik Einarsson 1-2
 Ernst Horn 2-1

～F～

Francis D' Souza 1-11
 Fueno Hiroyuki 1P-7
 Fujigaya Tsuyohiko 1-17, 2P-10, 2P-16,
 3P-14, 3P-16
 Fujita Wataru 2P-36
 Fujiwara Akihiko 1P-33, 2-6
 Fukidiome Hirokazu 2P-27
 Fukuda Toshio 2P-15
 Fukumoto Shinji 3P-37
 Furukawa Konosuke 3P-27
 Furukawa Yoshihiro 3P-6

～G～

G. M. Aminur Rahman 2-1
 Gene Dressselhaus 1P-3
 Gengmei Xing 2P-39
 Goo-Hwan Jeong 1P-12, 3P-9
 Goto Yasutomo 1P-16
 Guishan Zheng 1P-1
 Gunjishima Itaru 3-10
 Guoqing Ning 2P-18

Gustav Amberg	1P-14	～I～	
		Ichida Masao	1P-4
～H～		Ichiki Takahiko	1P-28
Hamada Yoshinobu	2P-20	Iiduka Yuko	2-3
Hao Sijia	3P-30	Iijima Sumio	1-1, 1-15, 1P-15, 1P-21,
Harada Manabu	3P-24		1P-22, 1P-23, 1P-25,
Haraguchi Shinsuke	3P-16		1P-26, 1P-27, 2-14,
Harima Hiroshi	3P-5		2P-2, 2P-6, 2P-13,
Hasebe Yuki	3P-5		3P-19, 3P-20, 3P-22,
Hasegawa Tadashi	2P-14		3P-23, 3P-24, 3P-34
Hashimoto Junichi	1P-8, 1P-9	Ikuta Tatsuya	1P-17
Hashimoto Takeshi	3P-10	Imae Toyoko	1P-33
Hata Kenji	1-1, 2P-7, 3P-34	Imahori Hiroshi	1P-7
Hata Koichi	1P-19	Imamoto Kenta	3-1
Hatakeyama R.	1-6	Imazu Naoki	2P-37, 3P-10
Hatakeyama Rikizo	1-5, 3P-25, 3P-26	Ina T.	3P-35
Hatanaka Masashi	2-8	Inada Koji	2P-5
Hayakawa Masahiro	1P-15	Inagaki Shinji	1P-16
Hayamizu Yuhei	2P-7	Inagaki Takayuki	3P-23, 3P-24
Hayashi Kazuhiko	3P-2	Inoue Sakae	3P-4
Hayashi Terutake	2-9	Inoue Takashi	2P-36, 3-10
Hayashi Y.	3P-8	Ishida Hiroyasu	3P-25
Hayashizaki Yoshihide	2-10	Ishida Masashi	2P-24
Hiasa Ken	1P-19	Ishigami Itsuo	3P-2
Hibino Hiroki	3-9	Ishigami Naoki	1P-17, 3-1
Hidaka Kishio	3P-6	Ishii Tadahiro	2P-11, 2P-12
Higashi K.	3P-33	Ishii Toru	2P-11
Higashi Keisuke	3P-18, 3P-21	Ishijima Akihiko	2P-15
Higashi Kengo	3P-5	Ishiyama Yuichi	2P-30
Hikata Takeshi	3P-2	Isshiki Toshiyuki	3P-5
Hino Shojun	1P-33, 2-6, 3P-27	Ito Manabu	3P-28
Hiraoka Tatsuki	1-1, 3P-34	Ito Osamu	1-11, 2P-5, 3P-19
Hirayama Kouhei	2P-10	Ito Shigeo	3P-18
Hirose Shoji	1P-36	Ito Yasuhiro	2P-23, 2P-36, 2P-37,
Hiroshiba Nobuya	1-5		3P-29
Hirota Takashi	2P-26	Itoh S.	3P-33, 3P-35
Hiwatashi Masataka	3P-15	Itoh Shigeo	3P-21
Homma Yoshikazu	1P-12, 2P-3, 3-9	Itou Kousuke	1-16
Horikoshi Koki	2-12	Iwasa Yoshihiro	2P-1
Hosokawa Y.	3P-35	Iwasaki Takayuki	1P-20, 3-3
Hyakushima Takashi	3-5	Iwase Takayuki	1P-40
		Iwata Nobuyuki	1P-39
		Izumi Yuki	3P-18

～J～		Kikuchi Koichi	3P-28
J. Jiang	1-9, 1P-6	Kikuchi Takashi	2-1
J. S. Park	1-9	Kimura Takahide	2P-29, 2P-31, 3-2, 3P-
Jie Jiang	1P-3		31
Jin Sung Park	1P-3	Kimura Tatsuto	2-15
Jing Fan	1P-22	Kishi Naoki	2P-18, 3P-10
Jing Lu	2P-14	Kishimoto Shigeru	3-7
Jun Tang	2P-39	Kisoda Kenji	3P-5
		Kitajima Tetsuo	1P-36
～K～		Kitamura Yutaka	2P-37
K. Joshi Rakesh	3-4	Kitaura R.	2P-17
Kadota Naoki	3P-31	Kitaura Ryo	1P-16, 2-4, 2P-21,
Kajiwara Kazuo	1P-19		2P-23, 2P-24, 2P-36,
Kako Masahiro	2P-14		2P-37, 3P-10, 3P-29
Kamahori Masao	3P-6	Kobayashi Keita	1P-16, 1P-24
Kanaizuka Katsuhiko	2-7	Kobayashi Tohru	2-10
Kaneko K.	3P-8	Kobayashi Yoshihiro	1P-8, 1P-9, 1P-12,
Kaneko T.	1-6		2P-3, 3-9, 3P-9
Kaneko Toshiro	3P-25, 3P-26	Kobayashi Yoshikazu	1P-7
Kanematsu Yasuo	3P-7	Kodama Takeshi	3P-28
Kanetake Akinori	2P-7	Koga Kenichiro	2P-19, 2P-20, 3S-6
Kase Shoichi	3P-38	Kokai Fumio	1P-24
Kashiwagi Ken	3-6	Kokubo Ken	2-9
Kasuya Daisuke	3P-20	Komatsu Koichi	1P-32
Katagiri Masayuki	3-5	Komatsu Naoki	2P-29, 2P-31, 3-2,
Kataura H.	2P-17		3P-31
Kataura Hiromichi	1-10, 1P-4, 1P-10, 2-13,	Kondo Daiyu	1P-20
	2P-8	Konno Takashi	2P-28
Kato Katsuya	3P-11	Konstantin Iakoubovskii	1-10, 3-8
Kato Koichiro	1-4	Koshino Masanori	2P-22
Kato Masayuki	3P-27	Koshio Akira	1P-24
Kato Toshiyuki	2-10	Koyaizu Reo	1P-39
Kato Yoshiaki	1P-13	Krishnendu Bhattacharyya	3P-3
Kato Yuko	2-4, 2P-21	Kubo Yoshimi	1P-21, 1P-26, 3P-20
Kawabata Akio	1P-20	Kubozono Yoshihiro	1P-33, 2-6
Kawabata Ryosaku	3P-6	Kumai Youko	1P-16
Kawai Jun	2-10	Kumashiro Ryotaro	1-5, 2P-39
Kawai Takazumi	1-14, 1P-10, 1P-22	Kunishige Atsuhiko	1-16, 3P-38
Kawamoto Tohru	3P-38	Kurata Hiroyuki	2-11
Kawarada Hiroshi	1P-20, 3-3	Kurata-Nishimura Mizuki	2-10
Kawasaki Naoko	1P-33, 2-6	Kurita Takahiro	2P-25
Kawase Takeshi	2-11	Kuroda Noritaka	2P-7
Ki Kang Kim	1P-3	Kusunoki Michiko	3P-11

Kuwahara Shota	2P-23, 2P-4	Miyata Yasumitsu	1-10, 1P-4, 1P-10, 2-13
		Miyauchi Yuhei	1P-14, 2P-9
~L~		Miyawaki Jin	1-1, 1P-21, 1P-22
Long Jing	2P-39	Miyazaki Takafumi	3P-27
		Miyazawa Kun'ichi	1P-35
~M~		Miyazawa Kun-ichi	1P-34
Maeda Noriko	2P-12	Miyoshi Takashi	2-9
Maeda Yutaka	2-1, 2-2, 2-3, 2P-14, 2P-35	Mizorogi Naomi	2-1, 2-2, 2-3, 2P-35
Maekawa Masayuki	3P-3	Mizukoshi Tomoyuki	3P-2
Maki Tasuku	1P-20	Mizuno Kenichi	1P-4
Maniwa Yutaka	1P-10, 2P-8	Mizutani Takashi	3-7
Mark H. Ruemmeli	1-2	Mori Sadayuki	1P-32
Maruyama Shigeo	1-2, 1P-14, 2P-9, 2-15	Morioka Yuki	3P-11
Maruyama Takahiro	1P-13, 3P-1	Morita Kouhei	1P-31
Mashino Tadahiko	1P-34, 2-8	Morita Yoichi	3P-31
Mastumoto Takanori	3P-17	Morokuma Keiji	1P-1
Masuhara Shin-ya	3P-6	Motohashi Satoru	1P-40, 2-5
Matsubara Tohoru	1-16	Mukai Sada-atsu	2-12
Matsubayashi Kenji	2-8, 2-9	Murakami Hiroto	3P-15
Matsuda Kazuyuki	2P-8	Murakami Toshiya	3P-5
Matsukawa Tomohiro	3P-13	Murata Katsuyuki	1P-26
Matsumoto Kouzou	2-11	Murata Michihisa	1P-32
Matsumura Sachiko	1P-27	Murata Yasujiro	1P-32
Matsuo Jiro	3P-2	Muro Takayuki	2P-37
Matsuo Keiko	1P-31	~N~	
Matsuo Yukari	2-10	Nagai Moeto	2P-15
Matsuo Yutaka	1P-28, 1P-29, 1P-30, 1P-31, 2-7	Nagano Takayuki	1P-33, 2-6
Matsuoka Issei	3P-36	Nagaoka Shiho	3P-28
Matsushita Tomohiro	2P-37	Nagase Shigeru	2-1, 2-2, 2-3, 2P-14, 2P-35, 2S-3
Matsuura Koji	2P-13	Nagataki Atsuko	1-3
Michael T. H. Liu	2-3	Naitou T.	3P-8
Mildred S. Dresselhaus	1P-3	Nakae Takahiro	1P-30
Minami Nobutsugu	1-10, 3-8	Nakahara Hitoshi	3P-13
Minfang Zhang	2-14	Nakahodo Tsukasa	2-1, 2-2, 2-3
Mishima Yoshifumi	2P-33	Nakajima Koji	2-3
Miura K.	3P-33	Nakamura Eiichi	1P-28, 1P-29, 1P-30, 1P-31, 2-7
Miura Koji	3P-18	Nakamura Shigeo	1P-34, 2-8
Miura Kouji	3P-21	Nakamura Sotaro	3P-18
Miura Yasuhiro F.	3P-36	Nakamura Takamitsu	2-11
Miyake Yoko	3P-28	Nakamura Tetsuya	2-4, 2P-37
Miyamoto Yoshiyuki	1-14, 1P-2, 1P-10		

Nakamura Yosuke	2P-28	Ohashi Hirotaka	1-5
Nakanishi Takashi	1S-2	Ohdo Ryota	1P-17, 3-1
Nakano Satoshi	1-15	Ohno Masatomi	2P-27
Nakashima Naotoshi	1-17, 2P-10, 2P-16, 3P-14, 3P-15, 3P-16	Ohno Yutaka	3-7
Nakayama Atsuko	1-15	Ohshima Satoshi	2P-13
Nakayama Ken-ichi	3P-7	Ohshima Yoshihisa	1P-36
Nakayama Yoshikazu	1-3, 1-12	Ohta Yohei	2-6
Namai Tatsunori	3P-34	Okada Susumu	1-7, 1-8, 2P-25
Nanao Takeshi	1P-29	Okamoto Atsuto	3-10
Naniki Takashi	2-5	Okawa Takashi	3P-18
Narimatsu Kaori	3P-14	Okazaki Toshiya	2-13, 2P-2, 2P-22
Naritsuka Shigeya	1P-13, 3P-1	Oke S.	3P-33
Nemoto Katsumasa	2P-33	Oke Shinichiro	3P-18
Nihei Mizuhisa	1P-20, 3-3, 3-5	Oke Sinichiro	3P-21
Niidome Yasuro	1-17, 2P-16, 3P-14, 3P-16	Okimoto Haruya	2-4, 2P-18, 2P-37, 3P-27
Nikawa Hidefumi	2-1	Okita Atsushi	3P-3
Nikos Tagmatarchis	3P-19	Okubo Shingo	2-13, 2P-22
Nishibori Eiji	2-4, 2P-21	Okuda Kensuke	2P-26
Nishide D.	2P-17	Okumura Kensuke	3P-12
Nishide Daisuke	2P-23, 2P-24	Onari S.	1P-6
Nishigaki Shohei	3P-25, 3P-26	Ono Shin	3P-6
Nishimura Jun	2P-28	Onoe J.	1P-38
Nishimura Suzuka	1P-13	Osawa Hitoshi	2P-37
Nishio Koji	3P-5	Oshima Takumi	2-9
Nishiyama Yoshitaka	2-11	Oshiyama Atsushi	1-7, 2P-25
Noguchi Yuichi	1-17	Osuka Atsuhiro	3-2
Nokariya Ryo	1P-39	Ozeki Atsushi	3P-3
Nosho Yosuke	3-7	~R~	
Nouchi Ryo	2-6	Ryuzaki K.	1P-38
Nozue Tatsuhiro	1P-20	~S~	
Numao Shigenori	1-15, 2P-6	Said Kazaoui	1-10
~O~		Saito Hiroshi	1-18
Ochiai Y.	1P-38	Saito R.	1-9, 1P-6
Ochiai Yuichi	1P-37	Saito Riichiro	1P-3
Oda Tatsuki	1P-5	Saito Susumu	1-4, 2P-34
Ogata Hironori	1P-40, 2-5	Saito Takao	3P-11
Ogawa Daisuke	2P-24, 2P-37	Saito Takeshi	2P-2, 2P-13, 2P-22, 3P-3
Ogawa K.	1P-38	Saito Yahachi	1P-19, 3P-12, 3P-13
Ogawa Kenichi	1P-37	Sakai Tadashi	3-5
Ogino Toshio	1P-8, 1P-9		

Sakai Yosuke	3P-3	Shiraishi Kenji	1-7
Sakakibara Toshihiro	3P-18	Shiraishi Masahiro	2P-18, 2P-23, 3P-10
Sakashita Hirofumi	1P-5	Shiraiwa Tomoyuki	1P-13, 3P-1
Sakata Makoto	2-4, 2P-21	Shirakawa Syogo	2-9
Sako Yuki	1P-33	Shoda Kaoru	1-16
Sakoda Satoru	1P-4	Somada Hiroshi	1-3
Sakuma Naoshi	3-5	Someya Chika	2P-35
Sakurai Masahiro	1-4	Stephan Irle	1P-1, 1S-1
Sakurai Yoshiaki	3P-2, 3P-7	Suda Yoshiyuki	3P-3
Sandanayaka Atula	2P-5	Suenaga Kazu	2P-2, 2P-22
Sano Masahito	1-18, 3P-17	Sugai T.	2P-17
Sasaki K.	1P-6	Sugai Toshiki	1P-16, 2P-4, 2P-18, 2P-23, 2P-24, 2P-36, 2P-37, 2P-38, 3P-10, 3P-27, 3P-29
Sashiwa Hitoshi	2P-33	Sugawara Hirotake	3P-3
Satake Eriko	2-8	Sugawara Syuichi	3P-18
Sato Hideki	1P-19	Sugi Michio	3P-36
Sato K.	1-9	Sugiura R.	3P-35
Sato Ken-ichi	3P-2	Sumanta Bhattacharya	2P-29, 2P-31
Sato Kentaro	1P-3	Sumita Yuzo	3S-5
Sato Shintaro	1P-20, 3-3, 3-5	Sumii Ryohei	3P-27
Sato Yoshinori	2P-14	Sumiyama Yoshiyuki	1-16, 3P-38
Sato Yuta	2P-22	Suzuki Hirotaka	2P-1
Sawaya Shintaro	1-12	Suzuki Mariko	3-5
Seki Toshio	3P-2	Suzuki Masato	2P-28
Sekido Masaru	2P-27	Suzuki Satoru	1P-8, 1P-9, 1P-12, 2P-3, 3-9, 3P-9
Seko Kazuyuki	3P-12, 3P-13	Suzuki Shinzo	2P-8, 3P-28
Senna Mamoru	2P-30	Suzuki Shogo	1P-19
Seto Shihori	1P-40	Suzuki Yasushi	3P-37
Shiba Kiyotaka	1P-27	Sze Yun Set	3-6
Shibata Masafumi	3P-4	~T~	
Shigeta Masahiro	2P-10	Tahara Kazukuni	1P-31
Shiki H.	3P-35	Tajima Yusuke	2P-30
Shimizu Akio	2P-15	Takagi Daisuke	1P-12, 2P-3, 3-9
Shimotani Hidekazu	2P-1	Takaguchi Yutaka	1P-33
Shinagawa Masashi	1P-17	Takahashi Hitomi	2P-36, 3P-22
Shinohara H.	2P-17	Takahashi Koji	1P-17
Shinohara Hisanori	1P-16, 2-4, 2P-4, 2P-18, 2P-21, 2P-23, 2P-24, 2P-36, 2P-37, 2P-38, 3P-10, 3P-27, 3P-29	Takahashi Kyoko	2-8
Shinohara K.	3P-33	Takahashi Teruo	2P-11
Shinohara Kenji	3P-18, 3P-21	Takahashi Yutaka	1P-24
Shiomi Junichiro	1P-14, 2-15		
Shiozawa Hidetsugu	1-2		

Takai Kazuyuki	3P-30	~W~	
Takaiwa Daisuke	2P-19	Wada Toyohito	3P-37
Takamori Hisayoshi	2P-16	Wakabayashi Hideaki	2P-2, 2P-22
Takayama Junichi	3P-3	Wakabayashi T.	2P-17
Takikawa H.	3P-33, 3P-35	Wakahara Takatsugu	2-1, 2-2, 2-3, 2P-14, 2P-35, 3P-32
Takikawa Hirofumi	3P-21, 3P-18		
Takimoto Tatsuya	3P-31	Wakizaka Yoshikazu	3P-7
Tamura Atsushi	2P-32	Watanabe A.	3P-8
Tanabe Fumiyuki	1P-32	Watanabe Hiroto	2P-30
Tanaka Hideki	2P-19, 2P-20	Watanabe Satoru	2P-28
Tanaka Kazuyoshi	1P-7		
Tanaka Satoshi	3P-7	~X~	
Tanaka Y.	1P-6	X.J. He	3P-33
Tanigaki Katsumi	1-5, 2P-39	Xiaobin Peng	3-2
Tanioku Kenji	1P-13, 3P-1	Xiaojun He	3P-21
Tazawa Masaya	2P-3	Xingfa Gao	2P-39
Thomas Pichler	1-2	Xinluo Zhao	3P-4, 3P-10
Tohji Kazuyuki	2P-14	Xu Jianxun	1P-23
Tokuda Takahiro	3P-5		
Tokunaga T.	3P-8	~Y~	
Tominaga Kazuyuki	2P-29	Y. F. Li	1-6
Tomonari Yasuhiko	3P-15	Yajima Hirofumi	2P-11, 2P-12, 2P-32, 2P-33
Toyoda Shouhei	3P-15		
Tsuchiya Takahiro	2-1, 2-2, 2-3, 2P-35	Yamada Michio	2-2, 2P-35
Tsudome Mikiko	2-12	Yamada Takeo	1-1, 3P-34
Tsuji H.	1P-38	Yamagami Yuichiro	1-4
Tsuji Hajime	1P-37	Yamaguchi Yoshifumi	3P-15, 3P-16
Tsuji Masaharu	1P-17, 1P-18, 3-1	Yamamoto Atsushi	3P-6
		Yamamoto Hiroshi	1P-39
~U~		Yamamoto Kazunori	2-1, 3P-32
Uchida Katsumi	2P-11, 2P-12, 2P-32, 2P-33	Yamamoto M.	3P-33
Uchida Kazuyuki	1-7	Yamamoto Masanobu	3P-18, 3P-21
Ueda Kazuyuki	1P-11, 2P-27, 3-4	Yamamoto Motohiro	3P-11
Uehara Naoyasu	3-1	Yamashita Atsushi	3P-36
Ueno Taro	1-10	Yamashita Shinji	3-6
Ueno Yusuke	2P-34	Yamashita Tetsuya	3P-13
Umemoto Hisashi	2P-36, 3P-27	Yamaura T.	3P-33, 3P-35
Umeyama Tomokazu	1P-7	Yamaura Tatsuo	3P-18, 3P-21
Uno Hidemitsu	2P-29	Yamazaki Akira	1P-12, 3P-9
Urushibata Mitsutaka	3P-36	Yamazaki Tomoko	2-12
Usui Shinji	1P-36	Yana Junzo	2S-4
		Yanagi Kazuhiro	1P-10, 2-13
		Yokoi Hiroyuki	2P-7

Yokoyama Daisuke	3-3
Yokoyama Masaaki	3P-7
Yoshida Takahiro	2P-26
Yoshida Tsuyoshi	1P-20, 3-3
Yoshihara Naoki	1P-18
Yoshikawa K.	3P-33
Yoshikawa Kazuo	3P-18, 3P-21
Yoshikawa Yuya	1-3
Yoshimura Hideyuki	1P-12, 3P-9
Yoshimura Masamichi	1P-11, 2P-27, 3-4
Yoshitake Tsutomu	1P-26, 3P-20
Young Hee Lee	1P-3
Yoza Kenji	2-1, 2-2, 2-3
Yuan Lin	1P-14
Yudasaka Masako	1-1, 1P-21, 1P-22, 1P-23, 1P-25, 1P-26, 1P-27, 2-14, 3P-19, 3P-20
Yuge Ryota	1P-22, 1P-26, 3P-20
Yuliang Zhao	2P-39
Yumura Motoo	1-1, 2P-13, 3P-34
~Z~	
Zdenek Slanina	2-1
Zhi Wang	1P-1
Zujin Shi	2P-2

複写される方へ

本会は下記協会に複写に関する権利委託をしていますので、本誌に掲載された著作物を複写したい方は、同協会より許諾を受けて複写して下さい。但し(社)日本複写権センター(同協会より権利を再委託)と包括複写許諾契約を締結されている企業の社員による社内利用目的の複写はその必要はありません。(社外頒布用の複写は許諾が必要です。)

権利委託先：(中法)学術著作権協会

〒107-0052 東京都港区赤坂 9-6-41 乃木坂ビル

TEL : 03-3475-5618

FAX : 03-3475-5619 E-Mail : info@jaacc.jp

なお、著作物の転載・翻訳のような、複写以外の許諾は、学術著作権協会では扱っていませんので、直接発行団体へご連絡ください。

また、アメリカ合衆国において本書を複写したい場合は、次の団体に連絡して下さい。

Copyright Clearance Center, Inc.

222 Rosewood Drive, Danvers, MA 01923 USA

Phone : 1-978-750-8400 FAX : 1-978-646-8600

Notice for Photocopying

If you wish to photocopy any work of this publication, you have to get permission from the following organization to which licensing of copyright clearance is delegated by the copyright owner.

<All users except those in USA>

Japan Academic Association for Copyright Clearance, Inc.(JAACC)

6-41 Akasaka 9-chome, Minato-ku, Tokyo 107-0052 Japan

TEL : 81-3-3475-5618

FAX : 81-3-3475-5619 E-Mail : info@jaacc.jp

<Users in USA>

Copyright Clearance Center, Inc.

222 Rosewood Drive, Danvers, MA 01923 USA

Phone : 1-978-750-8400 FAX : 1-978-646-8600

2007年2月13日発行

第32回フラーレン・ナノチューブ総合シンポジウム
講演要旨集

<フラーレン・ナノチューブ学会>

〒464-8602 愛知県名古屋市千種区不老町

名古屋大学大学院理学研究科 物質理学専攻

篠原研究室内

Tel : 052-789-5948

Fax : 052-789-1169

E-mail : fullerene@nano.chem.nagoya-u.ac.jp

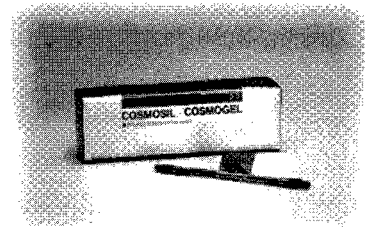
URL : <http://fullerene-jp.org>

印刷 / 製本 名古屋大学消費生活協同組合印刷部



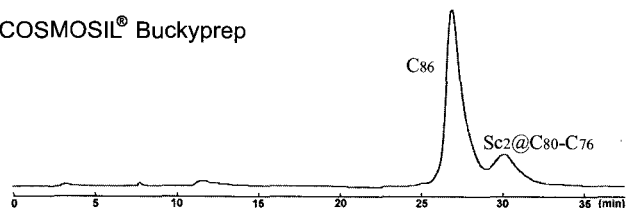
COSMOSIL[®] Buckyprep-M

今まで分離できなかった
金属内包フラーレンが分離可能！！

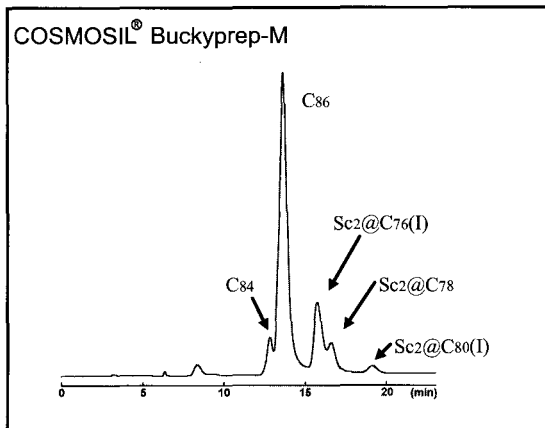


■分析例

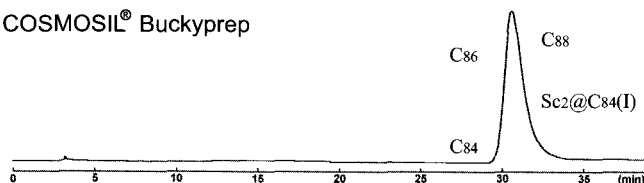
COSMOSIL[®] Buckyprep



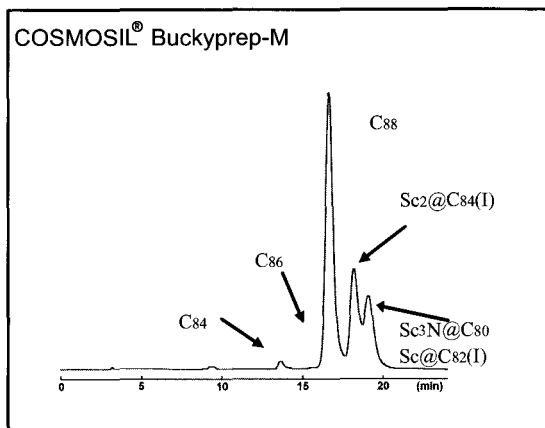
COSMOSIL[®] Buckyprep-M



COSMOSIL[®] Buckyprep



COSMOSIL[®] Buckyprep-M



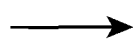
分析条件

カラムサイズ：4.6mm I.D. × 250mm, 移動相：トルエン, 流速：1.0 ml/min, 温度：30°C, 検出：UV312

資料提供：名古屋大学 大学院理学研究科物質理学専攻 篠原 久典教授

■その他COSMOSIL[®] フラーレン関連カラム

フラーレン分離のスタンダードカラム



COSMOSIL[®] Buckyprep

C₆₀, C₇₀等の大量分取に



COSMOSIL[®] PBB

詳しい情報はWeb siteをご覧ください。

ナカライテスク株式会社

〒604-0855 京都市中京区二条通烏丸西入東玉屋町498

価格・納期のご照会 フリーダイヤル 0120-489-552
製品に関するご照会 TEL: 075-211-2703 FAX: 075-211-2673

Web site : <http://www.nacalai.co.jp>

NANORUPTOR[®] —— バイオの技術をナノテクへ

密閉式超音波処理装置

実施例：燃料電池用触媒評価、カーボンナノチューブの分散。

特徴

●密閉処理

溶媒の蒸発・揮散がありません。
コンタミがありません。
ナノリスク対策に対応可能。

●多試料同時処理

最大24試料を同時に処理できます。

●再現性良好

回転機構の採用により均一な超音波照射が可能です。

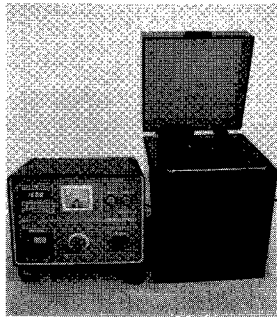
●多彩なラインアップ

汎用機からハイパワー機および連続処理機をご用意しています。

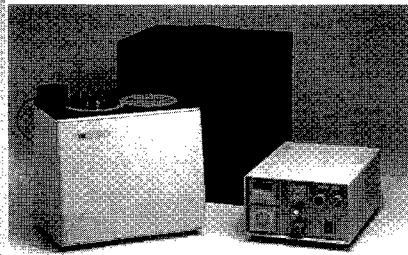


本商品は（独）産業技術総合研究所との共同研究により開発されました。

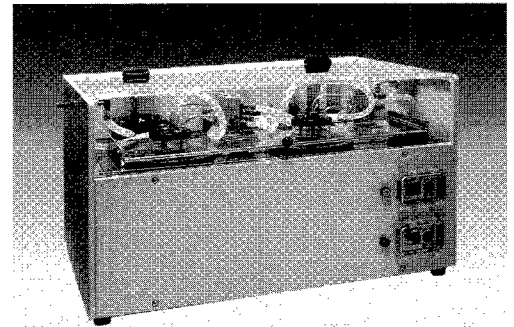
ハイパワー-NANORUPTOR (NR-300)



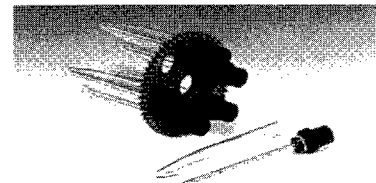
B1ORUPTOR (UCD-250)



B1ORUPTOR (UCW-201)



連続式NANORUPTOR (NR-2028)



密閉容器

用途

精製・分離・混合・分散・反応促進
・触媒評価・各種スクリーニング

20余年培ってきたバイオのナノテクをご利用ください。

デモ機を
ご用意しております。
どうぞお気軽に
お問い合わせ
ください。

お問い合わせ先

販売



コスモ・バイオ株式会社

〒135-0016 東京都江東区東陽2-2-20 東陽駅前ビル
URL: <http://www.cosmobio.co.jp>

TEL (03) 5632-9610 FAX (03) 5632-9619
営業推進部 栗原 mkurihar@cosmobio.co.jp
開発部 笹原 ksasahar@cosmobio.co.jp

製造



東湘電機株式会社

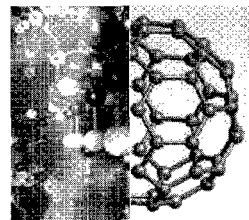
〒232-0027 神奈川県横浜市南区新川町5-29-2 新井ビル2F
TEL (045) 261-8388 FAX (045) 252-8935

技術部長 伊藤
e-mail: k-ito@bioruptor.jp

$$C \times \text{TOYO TANSO} = \infty$$

私たちの炭素の夢は、未来へと無限に広がります。

その優れた特性によって限りない可能性を持つC（カーボン）。
 私たち東洋炭素は、無限に広がるカーボンの応用分野を求めて、
 常に人と環境にやさしくをモットーに、未来技術の創造にチャレ
 ンジしています。金属内包フラーレンやカーボンナノチューブ合
 成用原料の開発など、今、私たちに求められているものは何かを
 常に考え、21世紀に貢献する未来型企业を目指し続けます。



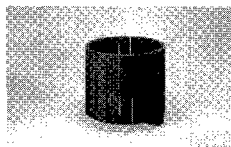
TOYO
 (K) 東洋炭素株式会社

URL <http://www.toyotanso.co.jp/>

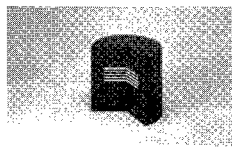
【本社】〒555-0011 大阪市西淀川区竹島5-7-12 TEL 06-6473-7912
 【工場】 詫間事業所・大野原技術開発センター・萩原工場・いわき工場
 【営業所】 東北・つくば・東京・北陸・静岡・名古屋・大阪・広島・四国・九州
 【国内関係会社】 東炭化工株式会社・大和田カーボン工業株式会社

<主な製品>

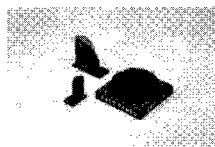
特殊黒鉛製品



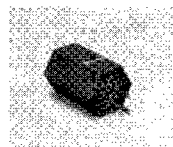
半導体用



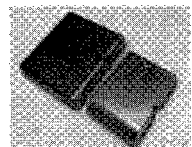
冶金工業用



放電加工用



原子力用



核融合装置用

一般カーボン製品



機械用



電気用

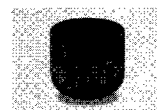
複合材その他製品



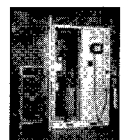
SiCコーティング
製品



黒鉛シート



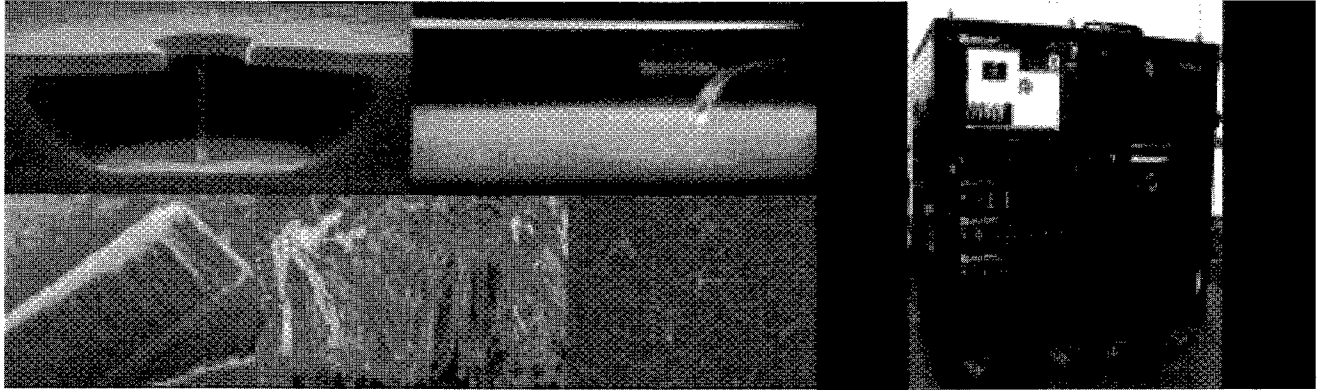
C/Cコンポジット
製品



オンサイト
フッ素発生装置

カーボンナノチューブ成長装置 **BLACK MAGIC**

フィールドエミッションデバイス開発のコアテクノロジー



● 黒盗物語 ●

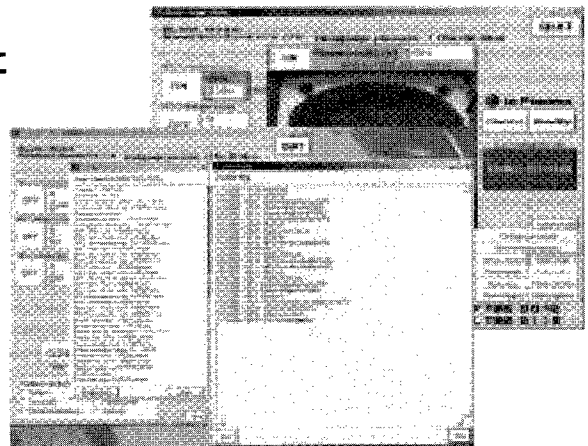
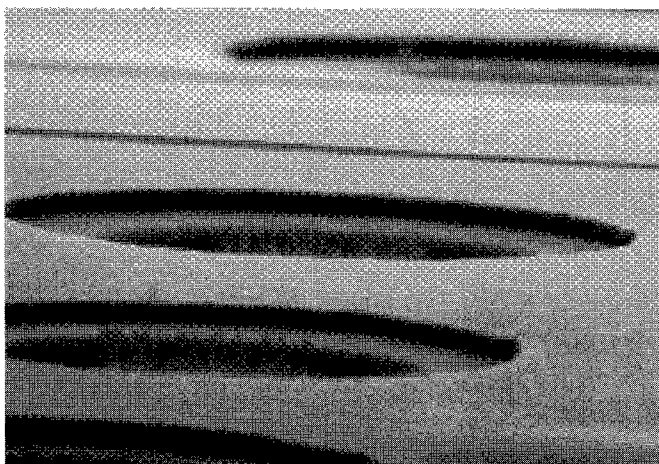
ナノカーボンフラレン、カーボンナノチューブ！
最近では、ただ作りだすだけなら、それは容易であることが判ってきました。
ナノカーボンの圧倒的可能性を認識して、多くの国々で黒盗合戦が始まっているようです。
新素材開発や新技術創生のバネが、この物語に内在しています。
ナノカーボンを掌握し制御することが出来れば、技術革新に勝利します。
しかしながら、これは至難の技です。

CNTs基板成長の最新装置 **"BLACK MAGIC"** をご覧下さい。

NANOINSTRUMENTS Ltd Website: www.nano-inst.com

究極の新世代ディスプレイ

Field Emission Display の開発のために



最新のCNTs成長レシピを
Cambridge Univ.が提供します。

CVD+PECVD カーボンナノチューブ成長装置 by Cambridge University



日本総代理店
アプリオリ 株式会社

TEL: 03-5296-5521
Email: info@apriori.co.jp

FAX: 03-5296-5525
<http://www.apriori.co.jp>

収差補正(Cs)レンズで 世界最高性能の電子顕微鏡

JEM-2100F フィールドエミッション電子顕微鏡

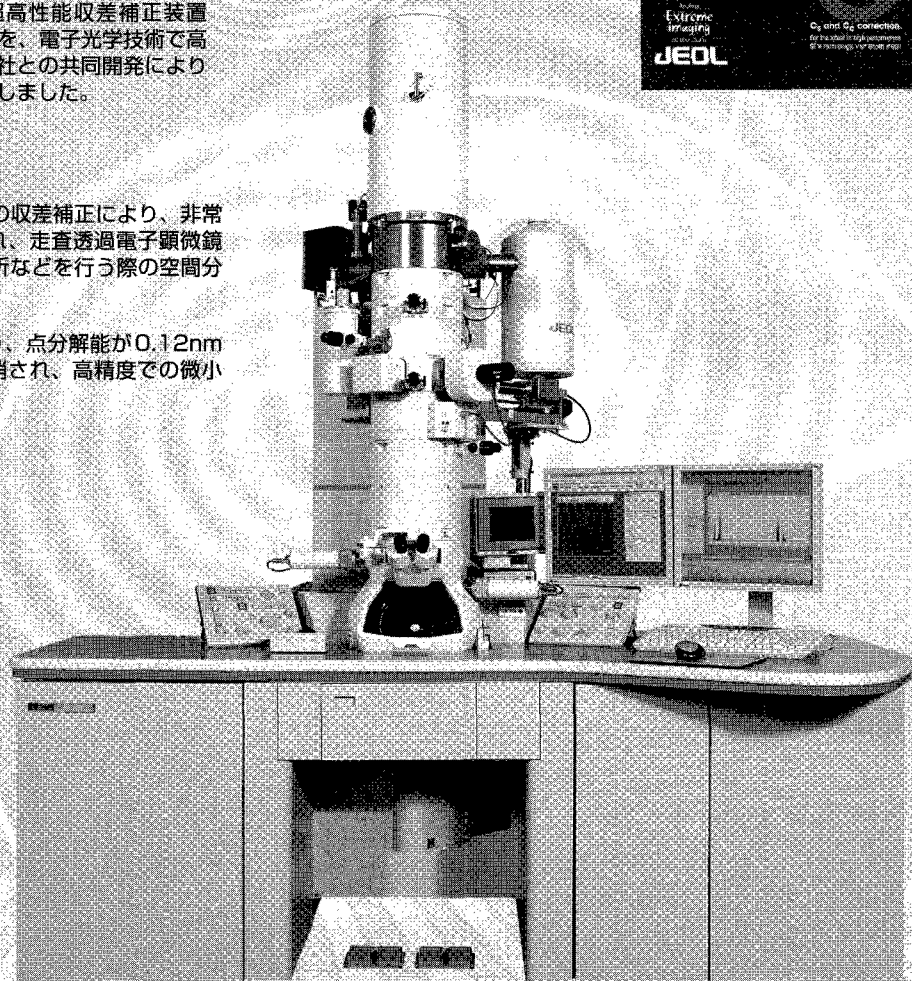
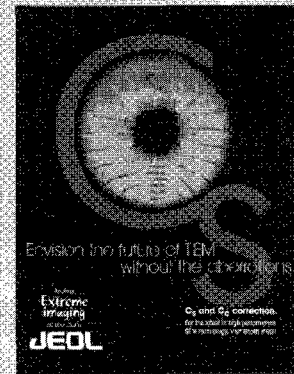
次世代超高性能電子顕微鏡

レンズの球面収差を補正することにより、分解能を飛躍的に向上させた次世代超高性能収差補正装置(球面収差補正形電子レンズ)を、電子光学技術で高い技術を誇るドイツのCEOS社との共同開発により完成させ、最新のTEMに導入しました。

主な特長

照射系(コンデンサ)レンズの収差補正により、非常に細い電子ビームが形成され、走査透過電子顕微鏡(STEM)の分解能や元素分析などを行う際の空間分解能が飛躍的に向上

対物レンズの収差補正により、点分解能が0.12nmまで向上し、フリッジが解消され、高精度での微小結晶界面などの特定が可能



お問い合わせは、電子光学機器営業本部 (EO販促グループ) ☎042 (528) 3353

JEOL
Serving Advanced Technology

日本電子株式会社

<http://www.jeol.co.jp/>

本社・昭島製作所 〒196-8568 東京都昭島市武蔵野3-1-2 ☎(042)543-1111
営業統括本部 〒190-0012 東京都立川市曙町2-8-3 新鈴春ビル3F ☎(042)528-3381
札幌 (011) 726-9660・仙台 (022) 222-3324・筑波 (029) 856-3220・東京 (042) 528-3211・横浜 (045) 474-2181
名古屋 (052) 581-1406・大阪 (06) 6304-3941・広島 (082) 221-2500・高松 (087) 821-8487・福岡 (092) 411-2361



 OZAWA SCIENCE

未来の科学に
率仕する



科学機器・計測システムの技術・情報商社

 **オザワ科学株式会社**

本社 / 〒460-0003 名古屋市中区錦三丁目9番22号
TEL (052) 951-5331 (代) FAX (052) 962-7358
・本社分室・春日井・刈谷・豊田・豊川・浜松・四日市・亀山・岐阜・商品センター

URL <http://www.ozawasc.co.jp>

E-mail welcome@ozawasc.co.jp

CaHC

ライフサイエンスサポート企業へ。

株式会社「カーク」は、『創造と努力』『誠実と感謝』を企業理念とし、
科学・医学・産業の研究・開発の発展に寄与するため
試薬をはじめ、工業薬品、検査薬、分析機器の販売を通して顧客に貢献しています。
特に、バイオサイエンス・ライフサイエンスの分野において、
オンリーワン、ナンバーワンとしての存在を目指しています。

For Customer



株式会社 カーク

〒460-0002 名古屋市中区丸の内 3-8-5
Tel 052-971-6533(代)
<http://www.cahc.co.jp>

愛知東営業所 0564-66-1580
岐阜営業所 058-268-8151
浜松営業所 053-431-6801
三重営業所 059-236-2531

米国・MTR社 フラーレン・ナノチューブ

株式会社マツボー
東京都港区虎ノ門3-8-21
電話 03-5472-1723
FAX 03-5472-1720
email: fulen@matsubo.co.jp

1. フラーレン混合物 (C60:70%, C70:25%, High Fullerene:5%)

2. フラーレンC60

純度 >99%
>99.5%
>99.98%
Sublimed

3. フラーレンC70

純度 >99%
>99%
>99.5%
Sublimed

4. SWナノチューブ(20-40%) クローズドエンド

5. SWナノチューブ(50%-70%) クローズドエンド

6. SWナノチューブ(70~80%)
50~60%がオープンエンド

7. MWナノチューブ(95%) クローズドエンド

8. MWナノチューブ(70~80%)
50~60%がオープンエンド

9. MWナノチューブ(85~90%)
95%以上がオープンエンド

*High Fullerenes 95%

C76

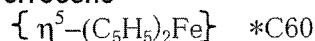
C78

C84>95%

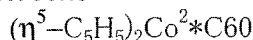
C6099.9%(OH)_n n=22-26

C6099.9%(OH)_n n=22-26

*Bucky Ferrocene-molecular hybrid C60 w/ Ferrocene



*Bucky Cobaltocene-ionic hybrid C60 w/ Cobaltocene



*Complex C60 w/ Pt: (h2-C60)Pt(PPh₃)₂

*Complex C60 w/ Fe: (h2-C60)Fe(Co)₄

*Complex C60 w/ Ni: C60 (h3-C₅H₅)Ni(h5-C₅H₅)₂

*Mixture of isomers C60F36

*20-30%C13enrichedC60=99.0%

*Higher Order Mixed Fullerenes(C76,78,84)

*New Endohedral Metallofullerene Gd@C82

*Halogenated Fullerenes

1.C60Br₂₄

2.C60C16

3.C60Br₈Br₂

4.Mixtures of isomers of C60F36

*水溶性 Amino Acids complexes of C60

(w/Aminocaproic(A) and w/Aminobutyric(B) acids)w/unique solubility in water
(50mg/ml)

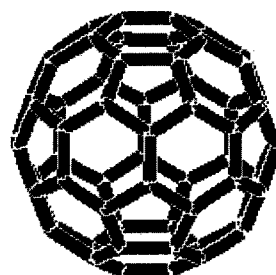
(A)C60(H)NH(CH₂)₅COO⁻NA⁺

(B)C60(H)NH(CH₂)₃COO⁻NA⁺

*PCBM(6,6-Phenyl-C61-Butyl acid-Methylester)

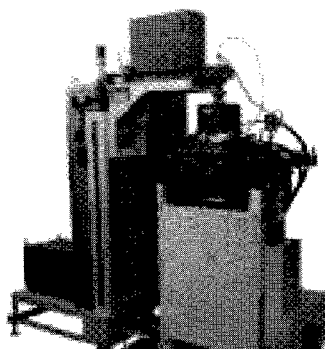
価格表にない種類のフラーレン・ナノチューブを
ご希望の場合はメーカーに問い合わせますので
お申し付け下さい。

*C60, 70の純度はHPLCにより測定されています。



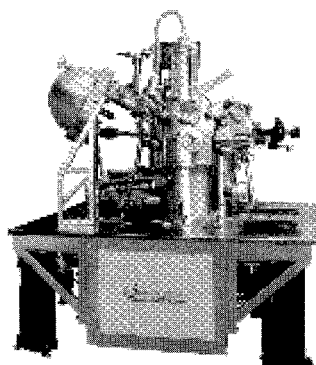
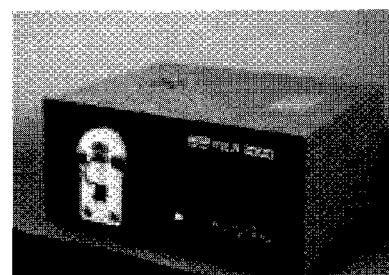
ULVAC

真空のことなら三弘アルバックへ

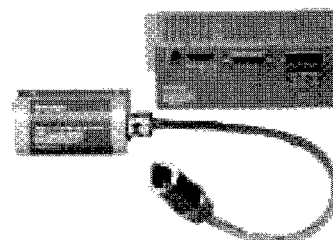


CNT 作成装置
CN-CVD-400

ゴールドイメージ炉
MILA-3000



ナノテクノロジーの分析に
VT-STM/AFM



残留ガスの測定に
MALIN

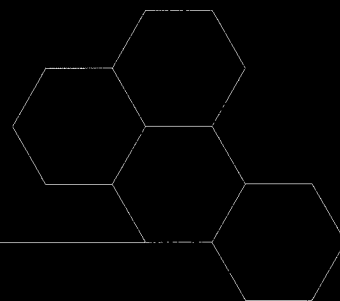
<取扱メーカー>

- 株式会社アルバック (真空ポンプ・真空機器・成膜装置)
- アルバック機工株式会社 (小型真空ポンプ・小型真空排気装置)
- アルバック理工株式会社 (加熱炉・熱分析・熱物性測定)
- アルバック・ファイ株式会社 (表面分析・ナノテクノロジー)
- アルバッククライオ株式会社 (クライオポンプ)
- アルバックテクノ株式会社 (真空機器メンテナンス・表面処理)

真空機器のご用命は・・・ 三弘アルバック株式会社

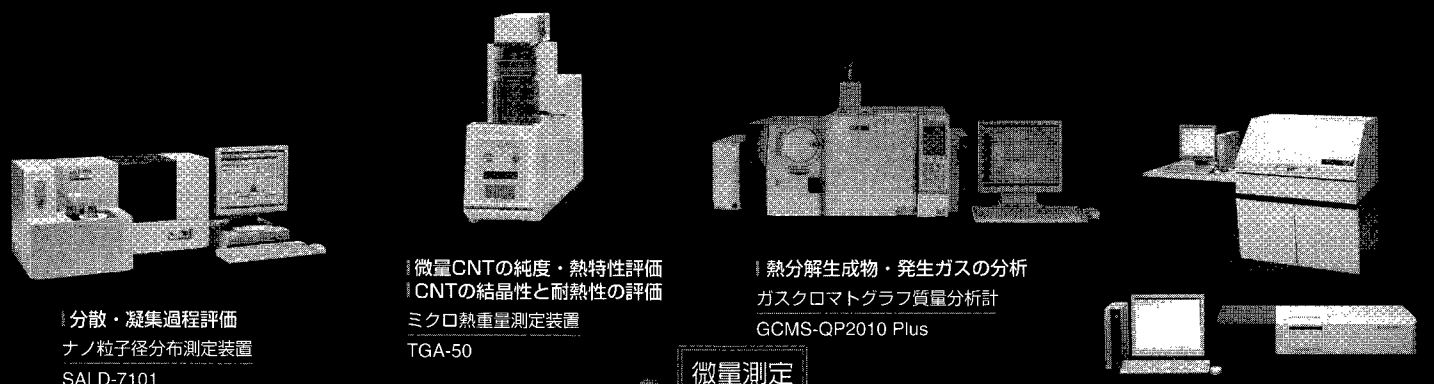
本 社 〒465-0081 愛知県名古屋市名東区高間町5-4-4
TEL (052) 702-6811 FAX (052) 702-6866
三重営業所 〒510-0244 三重県鈴鹿市白子町213-1 白子 SOHO ビル 1F
TEL (0593) 86-4857 FAX (0593) 86-6122
岐阜営業所 〒509-0125 岐阜県各務原市鵜沼南町3-20 川村ビル1-5
TEL (0583) 84-7701 FAX (0583) 70-6968

<http://www.sanko-ulvac.co.jp>



Total Solution Focused Carbon Nanotube

島津は総合分析機器メーカーとして、
 カーボンナノチューブの多面的評価法について、ご提案いたします。



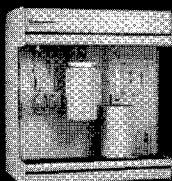
分散・凝集過程評価
 ナノ粒子径分布測定装置
 SALD-7101

微量CNTの純度・熱特性評価
 CNTの結晶性と耐熱性の評価
 ミクロ熱重量測定装置
 TGA-50

熱分解生成物・発生ガスの分析
 ガスクロマトグラフ質量分析計
 GCMS-QP2010 Plus



比表面積と吸着特性
 マイクロメリティクス
 高速比表面積/細孔分布測定装置
 アサップ2020シリーズ

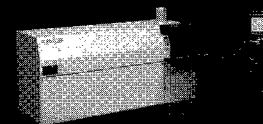


凝集分散

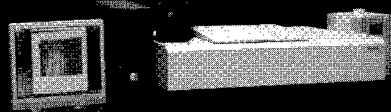
微量測定

純度

CNTの紫外可視近赤外吸収スペクトル測定
 紫外可視近赤外分光光度計 紫外可視近赤外分光光度計
 SolidSpec-3700 UV-3600



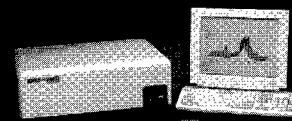
SWNTの近赤外PL3次元分布測定
 近赤外フォトルミネッセンス測定システム
 NIR-PL System



カイラリティ

直径

触媒元素の測定
 ツインシーケンシャル形ICP発光分析装置
 ICPS-8100



*こちらは特注製品となります

直径測定
 精製前後の観察
 CNTとポリマーコンポジット試料の観察
 走査型フローブ顕微鏡
 SPM-9600



観察

直径測定
 結晶性と耐熱性の評価
 ラマン分光光度計
 Holo-Probe モニタリングシステム



あらゆるナノテク材料を観察・測定
 ナノサーチ顕微鏡
 SFT-3500



住友商事のカーボンナノチューブ

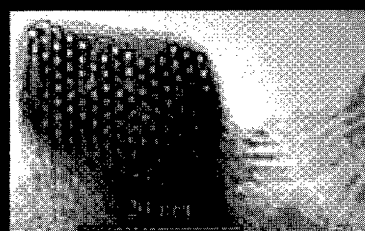
Produced by Carbon Nanotechnologies Inc. (CNI)

◆ 単層カーボンナノチューブ(SWNT)は、グラファイト構造の(グラフェン)シート層で構成されている、直径約1nmの筒状分子です。ナノカーボン材料のなかでも、複数層からなる多層カーボンナノチューブ(MWNT)や、他のカーボン材料に比べて格段に優れた導電性・熱伝導性・構造的特性を有し、幅広い応用が期待されています。住友商事は、CNI社の日本・アジア地域での総代理店として、各種用途に適した製品のご提供に加え、共同開発の推進や事業化支援プロジェクトの実施など、カーボンナノチューブの応用製品開発を総合的に支援しています。

● HiPco® 単層カーボンナノチューブ

直径約1nmの単層カーボンナノチューブです。基礎研究や高機能用途向けに、触媒残留率の異なる下記3製品をご提供しております。

製品名	触媒残留率
HiPco® As Produced (未精製品)	< 35 wt%
HiPco® Purified (精製品)	< 15 wt%
HiPco® Super Pure (超高純度品)	< 5 wt%



* Bucky Plus™(フッ化カーボンナノチューブ)など修飾品も対応可能です。

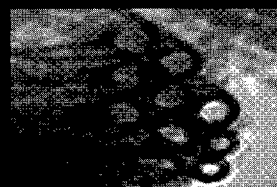
■ 単層カーボンナノチューブ ■

● CNI Xシリーズ

CNI社独自の製法で製造された、用途別産業応用向けカーボンナノチューブです。量産性に優れ、導電性樹脂複合材(EML, ESD, Anti-Static)、フィールドエミッション用途などに、安定した製品供給が可能です。詳細につきましては、下記連絡先までお問合せください。

● 二層カーボンナノチューブ

CNI社独自の製法で製造された、直径約2nmの二層カーボンナノチューブです。



■ 二層カーボンナノチューブ ■

上記製品群を中心に、研究用から量産対応品、また共同開発によるカスタマイズ対応など、用途に応じたカーボンナノチューブの開発を進めています。弊社までお気軽にお問合せ下さい。

本件に関するお問合せ先

住友商事株式会社 電子材部 (担当:小野/青木)

E-mail : nano@em.sumitomocorp.co.jp

TEL : 03-5166-5857 FAX :03-5166-6234

住所 : 〒104-8610 東京都中央区晴海1-8-11

URL : www.sumitomocorp.co.jp/section/joho/nanotube.shtml



JASCO Corporation

高機能、簡単操作がcaつてない 測定環境を実現 多目的な Raman series です。

NRS-3000シリーズは、操作性の向上を実現しました。試料のセットからオートアライメントなどの装置の最適化、測定までをスピーディーに行えます。また、低波数測定ユニットへの切替えもボタンひとつで行えます。測定結果の解析には、データベース機能を用い簡単検索、ジャスコキャンパスを用いた簡単レポート作成機能があります。ラマン分析の可能性を大幅に広げました。



Laser Raman Spectrophotometer

レーザラマン分光光度計

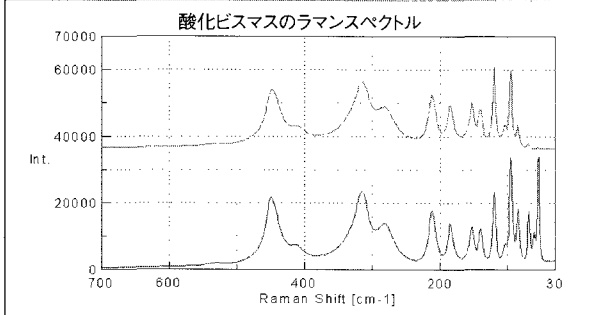
NRS-3000 series

NRS-3100/3200/3300

●特長

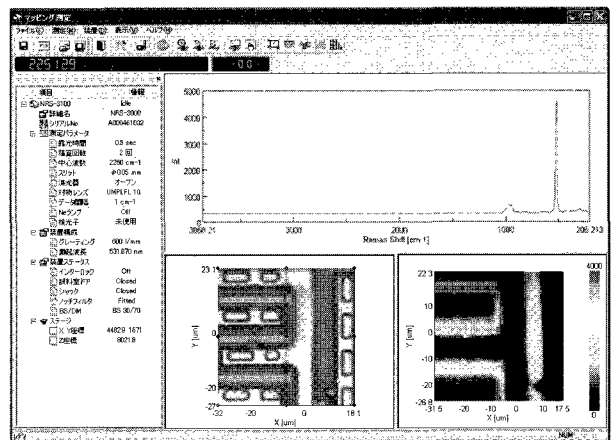
- ▶ ユーザーフレンドリーな操作性を実現
- ▶ ダイレクトドライブ方式のモノクロメータと高性能ノッチフィルタの組合わせにより、高い波数精度・再現性と高感度化を実現
- ▶ グレーティングを最大3枚搭載でき、多様な測定に対応
- ▶ レーザを最大6台まで搭載可能
- ▶ 日本分光独自のSRI機能 (SRI: Spatial Resolution Image) によりPCモニター上で試料像とアパーチャ像およびレーザビームを同時観察
- ▶ コンフォーカル光学系により深さ方向の測定が可能
- ▶ イメージング測定に対応可能
- ▶ オートアライメント機能によりシステムの安定性を追及
- ▶ レーザ放射安全基準Class1の安全性を確保
- ▶ スペクトル検索プログラムおよびデータベースを標準搭載

低波数測定ユニットの測定例



低波数測定ユニットは、無機物などの格子振動低波数域を精度よく測定する場合に有効になります。

●シリコンパターンのマッピング測定例



マッピング測定で機能と操作性が向上しました。画像情報をもとに測定者が画像上でマウスを使って、測定エリアを指定できます。また、測定中のデータを色分け図で表示することで測定結果をリアルタイムで確認することができます。

JASCO は日本分光株式会社の登録商標です。

光と技術で未来を見つめる

日本分光

JASCO 日本分光株式会社

〒192-8537 東京都八王子市石川町2967-5
PHONE 042 (646) 4111 (代表)
FAX 042 (646) 4120 <http://www.jasco.co.jp/>

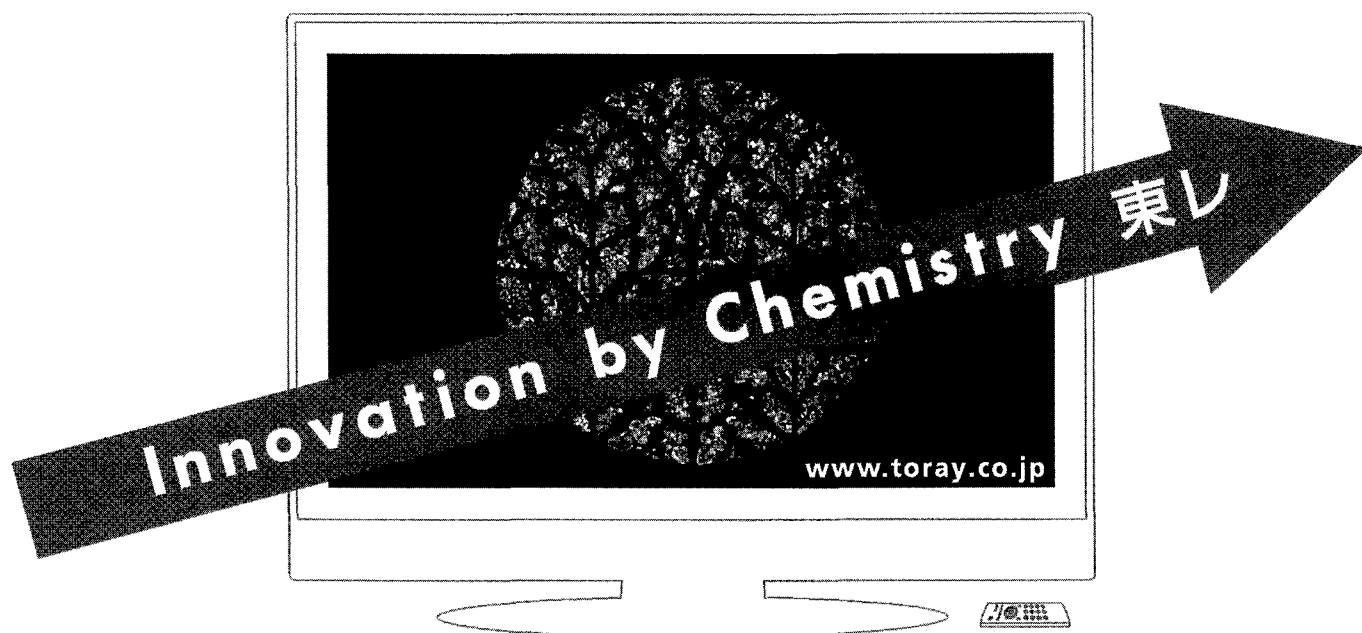
北海道S-C 011(741)5285
日本S-C 022(748)1040
筑波S-C 029(857)5721
東京S-C 03(3294)0341
西東京S-C 042(646)7001

神奈川S-C 045(989)1711
名古屋S-C 052(452)2671
大阪S-C 06(6312)9173
広島S-C 082(238)4011
九州S-C 092(588)1931



ISO14001 ISO9001
JSAE 024 JQA-0777

ディスプレイを美しく見せるのも、私たちの仕事です。



東レの「電子情報材料・機器」は、
テレビ、携帯電話、PCなど、
映像ディスプレイの
高精細化に貢献しています。
先端材料で、新しい価値を創ります。

TORAY
Innovation by Chemistry

週刊 **ナノテク** Nano Tech Weekly

コアテクノロジーからマーケットまで全てをカバー/ナノテクを分かりたい人、ビジネスにしたい人へのベストソリューションを提供/ナノテク国家プロジェクトからナノマテリアル、IT、バイオ、メディスン、エネルギー、MEMSに至るまで徹底取材

雑誌名：週刊ナノテク 予定頁数：16~32頁
発行日：毎週月曜日 体裁：A4変形、中綴じ
発行予定部数：15,000部 年間購読料：5万7,750円(本体5万5,000円)

産業タイムズ社

〒101-0021 東京都千代田区外神田5-5-4 第二日昌ビル
Tel.03-3834-5131 Fax.03-3834-5188
<http://www.semicon-news.co.jp/> <http://www.weeklynano.com>

〒101-0021 東京都千代田区外神田5-5-4
第二日昌ビル
Tel.03-3834-5131(代)/Fax.03-3834-5188

産業タイムズ社の出版案内

詳細カタログ呈

Fax.での注文も承ります。定価は税・送料込み。

2007年
2月末発刊予定

液晶・PDP・ELメーカー計画総覧2007年度版

大画面化する薄型テレビ市場へ
浸透するLCD/PDP
A4変形判・約380頁

好評発売中!

半導体工場ハンドブック2007

史上最高の投資に突入した
次世代ラインの全貌
A4変形判・129頁・定価3,150円(本体3,000円)

好評発売中!

アジア半導体/液晶ハンドブック2006

台湾・韓国・中国・東南アジアの
メーカー別プロフィール・設備投資を一覧
A4変形判・98頁・定価4,200円(本体4,000円)

好評発売中!

プリント回路メーカー総覧2006年度版

グローバル競争時代に勝ち抜く
有力基板メーカーの最新戦略
B5判・306頁・定価16,800円(本体16,000円)

好評発売中!

半導体産業計画総覧2006-2007年度版

過熱するサバイバル競争
勝ち組みの戦略
A4変形判・526頁・定価19,950円(本体19,000円)

好評発売中!

日本半導体/FPDベンチャー年鑑2006

先鋭のベンチャー企業群が
日本のハイテクビジネスを変える
A4変形判・230頁・定価10,500円(本体10,000円)

好評発売中!

半導体産業会社録2006年度版

日本で唯一の半導体産業ダイレクトリ
“最新・大改訂版”
A4変形判・509頁・定価15,750円(本体15,000円)

好評発売中!

中国エレクトロニクス企業総覧2006

中国のFPD・半導体・ITなど
1500社の詳細データを全集録
A4変形判・550頁・定価26,250円(本体25,000円)

好評発売中!

ナノテク産業総覧

ナノテクキーカンパニー700社収録
キーパーソン300人網羅
A4変形判・540頁・定価25,200円(本体24,000円)

㈱東京プログレスシステム

住所:107-0052 東京都港区赤坂 2-17-68-502
電話:03-5570-0457 FAX:03-5570-0462
URL: <http://www.tokyoprogress.co.jp>
Mail: omori@tokyoprogress.co.jp または
eml-omori@wonder.ocn.ne.jp

営業品目

◎ 安定同位体元素

Gas centrifuge: Si, S, V, Cr, Fe, Ni, Zn, Ge, Se, Kr, Mo, Cd, Sn, Te, Xe, W, Os, Pb,
Electro magnetic: Mg, K, Ca, Ti, Cu, Zn, Ga, Rb, Sr, Zr, Ru, Pd, Ag, In, Sb, Ba, La, Ce,
Nd, Sm, Eu, Gd, Dy, Er, Yb, Lu, Hf, Ta, Re, Ir, Pt, Tl
Photo chemical: Hg
Laser: Yb その他、安定同位体ガスなど

◎ ダイヤモンド粉末・その他の超硬材料

1. 爆発ダイヤモンド(DD)-黒鉛に爆薬の爆発による圧力をかけ合成する。粒子は多結晶体で研磨に最適と言われている。
2. 超分散ダイヤモンド(UDD)-爆薬 TNT の分子中の炭素が爆発による高温・高圧下でダイヤモンドに変わったもの。粒径は30~50ナノのクラスターになっている。エレクトロニクス産業での高精度研磨・表面処理・潤滑剤などの用途がある。
3. 静圧合成ダイヤモンド(工業用ダイヤモンド)-黒鉛に約5万気圧・1300℃以上の圧力をかけて合成したダイヤモンドを粉砕したもの。
4. その他研磨用ダイヤモンドペースト・BN・CBN など

◎ 水酸化フラーレン: C60(OH)_n: n=18~24

価格:1グラム 12,000円 3グラム 30,000円

◎ その他 MTR 社のフラーレン誘導体類 :合成はお問合せください。

☆新製品・高純度・新価格 C60/PCBM, 純度99.5%以上

(価格:250mg, ¥93,000- 1gr: ¥180,000- 10gr: ¥1,600,000-)

☆新製品・新価格 C70/PCBM 純度99%以上

(価格:250mg, ¥150,000- 1gr: ¥370,000- 10gr: ¥3,200,000-)

★その他 C60:(C13 置換) ★C60:C70 (C13 置換)★Mixture C60 & C70(C13 置換)

★C60F₃₆, ★C60 F₄₀ ★Higher fullerene mixture C76, C78, C80 & C84

★C60CHCOOH(1.2-methanbofullerenC60)-61-carboxylic acid

★[η⁵(C₅H₅)₂Fe]₂*C60

★Type A: C60HNH(CH₂)₃ COONa & ★Type B: C60HNH(CH₂)₅ COONa

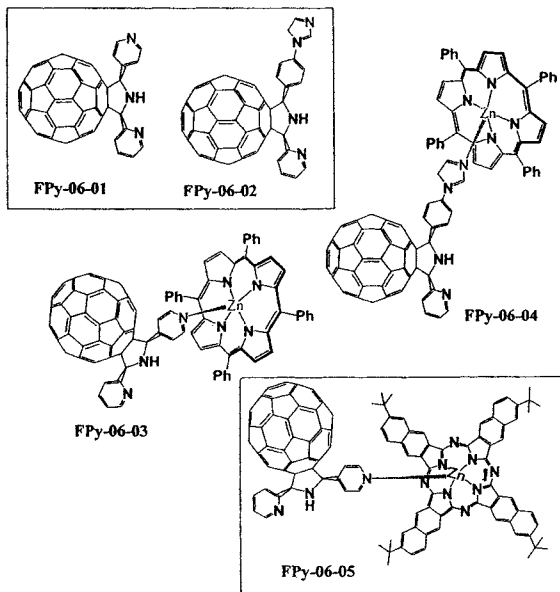
★C60C(COOEt)₂ & ★C60[C(COOEt)₂]₂ ★C60Br₂₄ など

◎その他 別ページ:Chemical structures of Fullerene derivatives 参照

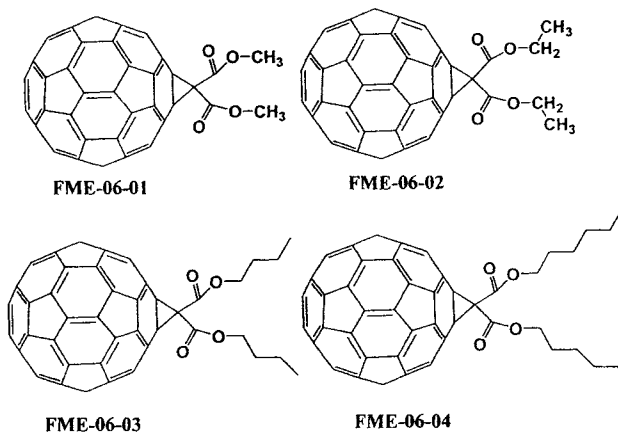
◎翻訳 <英語・ドイツ語・フランス語・ロシア語など>・技術調査 etc.

Chemical structures of Fullerene derivatives

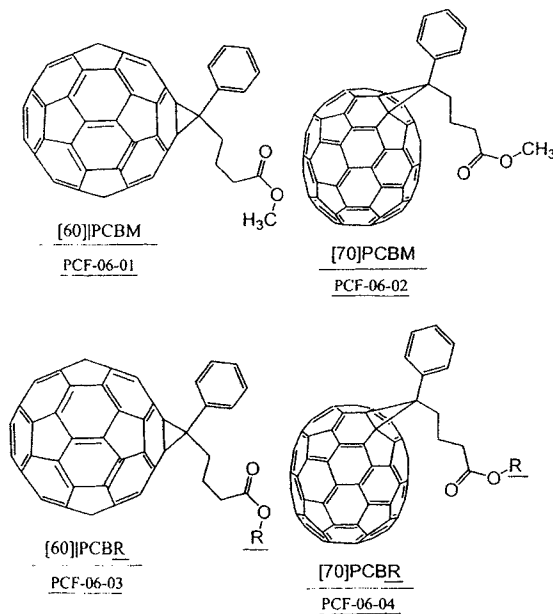
Fullerene derivatives for solar energy conversion
Part I. Photo responsive self-assembled dyads
mimics of natural photosynthetic antenna



Fullerene derivatives for solar energy conversion
Part II. Materials for plastic solar cells:
Fullerene malonic acid esters

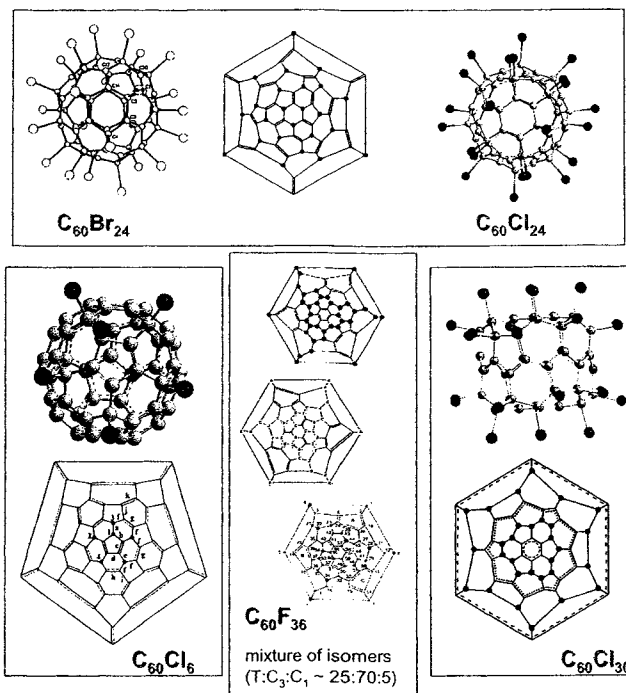


Fullerene derivatives for solar energy conversion
Part III. Materials for plastic solar cells:
PCBM-type Fullerene derivatives



R = -C₂H₅, -C₄H₉-n, -C₆H₁₃-n, C₈H₁₇-n, ...

Halogenated fullerene



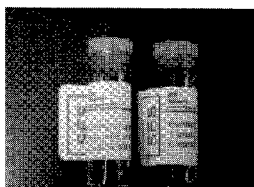
Tokyo Progress System LTD.

ナノテクノロジー・材料プログラム

ナノテク材料

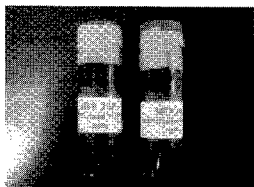
カーボンナノチューブ

多層カーボンナノチューブ (MWNT)、
アーク放電 CLOSED (両端:閉)



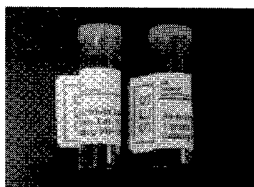
純 度: 40-50%、
チューブ径: 1.2-20ナノメータ
チューブ長: 2-5ミクロン

純 度: 75-85%、
チューブ径: 7-12ナノメータ
チューブ長: 1-10ミクロン



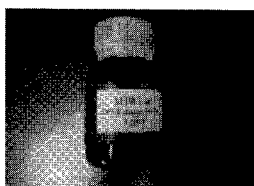
純 度: 95%
チューブ径: 35ナノメータ
チューブ長: 60-100ミクロン

多層カーボンナノチューブ (MWNT)、
アーク放電 OPEN (両端:開)



純 度: 80%
チューブ径: 1.2~20ナノメータ
チューブ長: 2~5ミクロン

単層カーボンナノチューブ (SWNT)、
アーク放電 CLOSED (両端:閉)



純 度: 50-70%
チューブ径: 0.7~1.2ナノメータ
チューブ長: 10~20ミクロン

単層カーボンナノチューブ (SWNT)、
CVD法 OPEN (両端:開)

純 度: 90%
チューブ径: 平均1.14ナノメータ
チューブ長: 0.2~100ミクロン

応用製品群

カーボンナノチューブ応用製品

- カーボンナノチューブ蒸着 (Si, Mo, 石英, ガラス)
- 垂直に整列したカーボンナノチューブ
- 単層カーボンナノチューブ薄膜パターン
- フィールドエミッション用の陰極板
- FED用カーボンナノチューブパターン
- カーボンナノチューブ・ガス放電管

フラーレン

- C76フラーレン 純度95%
- C78フラーレン 純度95%
- C84フラーレン 純度98%
- 水溶性C60フラーレン
- C60CHCOOHフラーレン
- C60H36水素化フラーレン
- C70H36水素化フラーレン
- C60Oオキシライドフラーレン
- C70Oオキシライドフラーレン

ハイブリッドC60シリーズ

- ハイブリッドC60・Pt
- ハイブリッドC60・Fe
- ハイブリッドC60・Ni
- バッキーC60・フェロセン
- バッキーC60・コバルトセン

誘導体フラーレン

- C60-Cholesterol
- C60-estrogen
- Water-solubleC60 (OH) n n=22-26 (anti-HIV)
- Phenyl-and keto-C60carboxylates
- GeneralC60alcohol
- Optically active fullerene-pinene derivatives
- General unsaturatedC60 cyclic ketone
- Saturated C60 ketone

- 20-30%C13エンリッチド99%C60フラーレン
- 85-90%C13エンリッチド98%C70フラーレン
- 金属内包フラーレン (Gd@C82)
- C60フィルム (Si, サファイヤ, 石英, ガラスなど)

次世代ナノテク技術で新時代を築く

株式会社ATR

〒270-0021 千葉県松戸市小金原7丁目9番地4
TEL: 047-394-2112 FAX: 047-394-2100
E-mail: atr@scilab.co.jp

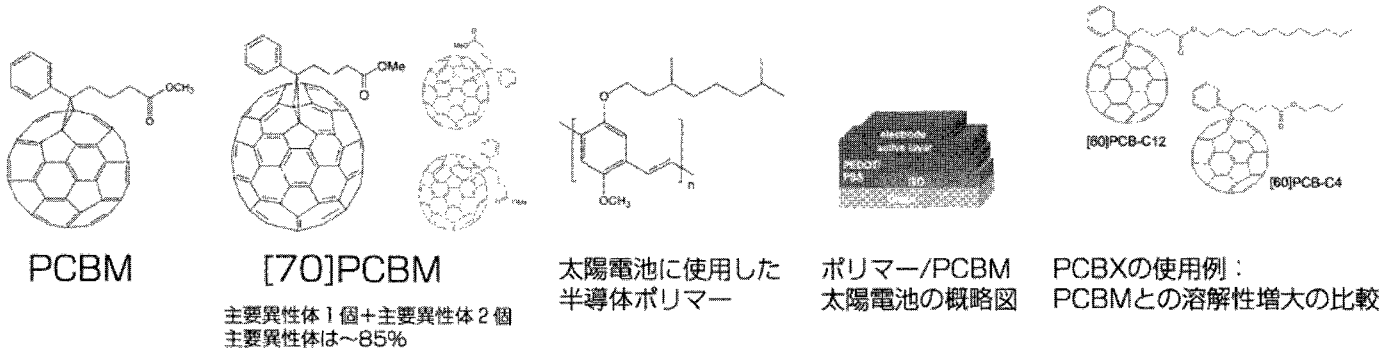
分子エレクトロニクスへの[60]PCBMとPCBMアナログの応用

はじめに

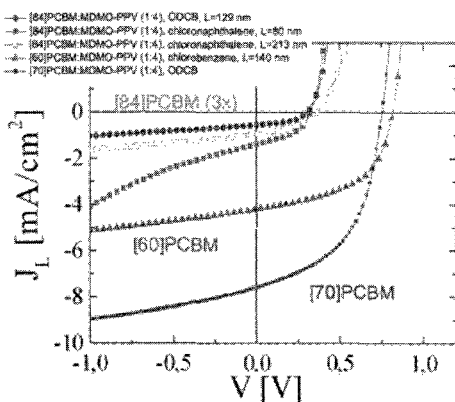
フラーレンを土台とした有機エレクトロニクスは商業的に高い可能性を秘め、業界で脚光を浴びています。例えば、半導体ポリマーに混合すれば、太陽電池、両極性の電解効果トランジスター(FET)、光検知器を低コストで製造できます。

FETには、高品質のフラーレン誘導体が使用されます。

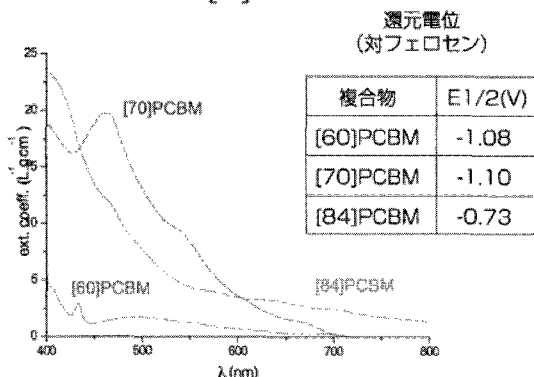
従来、加工可能なC60-誘導体である[60]PCBMが最も多く使用されてきましたが、[60]PCBMのバリエーションや多種のフラーレン誘導体の応用によっても莫大な利益が見込めます。[60]PCBMのバリエーションは実に広く、溶解性、紫外線吸収(バンドギャップ)、安定性、還元電位などフラーレン誘導体の属性は特殊分野にも応用が可能です。以下に、[70]PCBMや[84]PCBMなどのPCBMアナログの特性と一部のPCBXの特性とを比較します。



MDMO-PPV/PCBM太陽電池

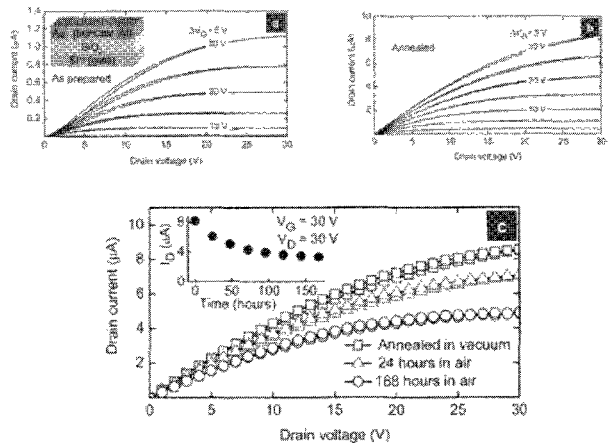


*[70]PCBMの吸光度が[60]PCBMの吸光度を上回ることにより性能が向上：2.5%⇒3%
 *この種のポリマーの太陽電池にとって、[84]PCBMのLUMOは低過ぎ。



UV-Vis absorbance of [60]PCBM, [70]PCBM and [84]PCBM (in toluene)

電解効果トランジスター内部の[84]PCBM



*有機FET内部の[84]PCBMに適したn型半導体
 *これらの[84]PCBM有機FETは空気中で安定。

結論

- ・フラーレンの同調特性(吸光度の増加など)により、太陽電池の効率が向上。
- ・有機FET内部の[84]PCBMは、空気中で著しく安定。
- ・PCBXの使用によりフラーレンの溶解性を変化させると、加工条件は最適化される(活性層用の溶媒の加工条件など)。

次世代ナノテク技術で新時代を築く

株式会社ATR

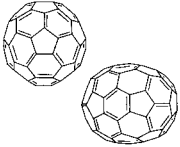
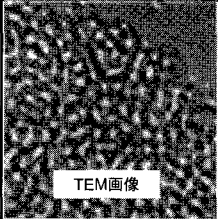
〒270-0021 千葉県松戸市小金原7丁目9番地4
 TEL : 047-394-2112 FAX : 047-394-2100
 E-mail : atr@scilab.co.jp

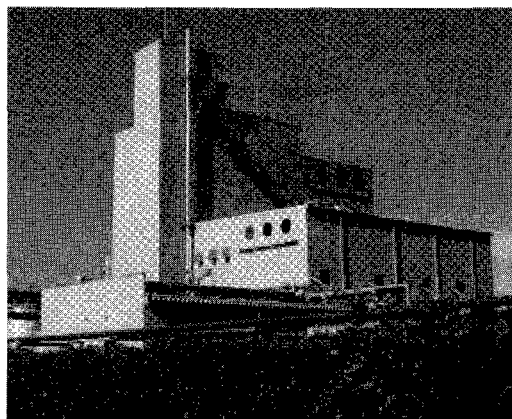
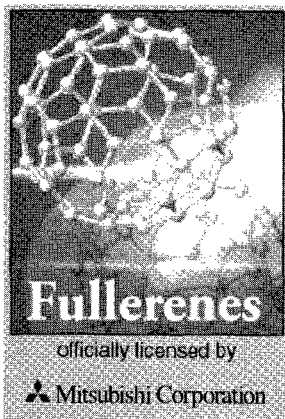
nanom

フラーレン サンプル価格一覧

2007年1月1日現在

銘柄		分子構造	純度 (HPLC面積%:代表値)	販売単価	取扱数量
nanom purple フラーレンC60	ST		>99	3,000円/g	10g以上
				8,000円/g	1g以上
	TL		>99.5	10,000円/g	1g以上
	SU		>99.5/昇華精製品	15,000円/g	1g以上
	SUH	>99.9/昇華精製品	35,000円/g	1g以上	
nanom orange フラーレンC70	ST		>97	40,000円/g	1g以上
	SU		>98/昇華精製品	200,000円/g	0.5g

銘柄		分子構造	平均粒径	販売単価	取扱数量
nanom mix C60:約60% C70:約25% その他:高次フラーレン	ST		数10μm	500円/g	50g以上
				600円/g	10g以上
	ST-F		数μm	700円/g	50g以上
				800円/g	10g以上
nanom black フラーレン類似構造を有する特殊な煤 炭素含有量:96.0%以上	ST	 TEM画像	数10μm	350円/g	100g以上
				60,000円/kg	1kg以上
	ST-F		数μm	550円/g	100g以上
				90,000円/kg	1kg以上



本格量産工場(40Ton/年)

販売単価には消費税は含まれておりません。
別途申し受けます。

御購入金額が25,000円以上(税抜)の場合、
送料は弊社負担と致します。

御購入金額が25,000円未満(税抜)の場合、
一律1,500円(税抜)の諸掛を申し受けます。

フロンティアカーボン株式会社は
三菱商事株式会社から正規に
ライセンスを受け、フラーレン
nanom®を製造販売しています

三菱商事株式会社は日本における
フラーレン物質・製造特許の
専用実施権を保有しております
(特許第2802324号)



Frontier Carbon Corporation

フロンティアカーボン株式会社
〒104-0031 東京都中央区京橋1-8-7
京橋日殖ビル5F TEL:03-5159-6880

フロンティアカーボン株式会社は、フラーレンを
大量製造販売しているオンリーワンカンパニーです

nanom

フラーレン誘導体 サンプル価格一覧

2007年1月1日現在

銘柄	分子構造	溶解度 (wt%)				販売単価	取扱数量
		Toluene	o-Xylene	ODCB	PGMEA		
nanom spectra E100 PCBM (phenyl C61-butyl acid methyl ester)		2.2	3.1	>10	0.05	80,000円/g	1g以上
						130,000円/g	0.5g
nanom spectra E200 PCBNB (phenyl C61-butyl acid n-butyl ester)		>10	>10	>10	0.22	150,000円/g	1g以上
						240,000円/g	0.5g
nanom spectra E210 PCBIB (phenyl C61-butyl acid i-butyl ester)		3.5	5.9	>10	0.07	150,000円/g	1g以上
						240,000円/g	0.5g

銘柄	分子構造	溶解度 (wt%)				販売単価	取扱数量
		PGMEA	乳酸エチル	CHN	MAK		
nanom spectra G100 側鎖部分の長さはカスタマイズ可能です		0.2	0.1	19.9	1.2	100,000円/g	1g以上
						160,000円/g	0.5g

銘柄	分子構造	販売単価	取扱数量
nanom spectra E110 C70PCBM 位置異性体の混合物になります		250,000円/g	0.5g
nanom spectra E910 付加数 n=2-3 の混合物になります		100,000円/g	1g以上
		160,000円/g	0.5g

銘柄	分子構造	組成	販売単価	取扱数量
nanom spectra D100 水酸化フラーレン (n = ca. 10)		C60(OH)n n=約10 (MS)	10,000円/g	1g以上
			12,000円/g	0.5g
nanom spectra B100 酸化フラーレン (n = 1-2 が主成分)		C60(O)1: 約30% C60(O)2: 約25% その他: C60, 三酸化体以上	25,000円/g	1g以上
			30,000円/g	0.5g
nanom spectra A100 水素化フラーレン (n = ca. 30)		C60(H)n n=約30 (MS)	12,000円/g	1g以上
			15,000円/g	0.5g



ハイテクの一步先に、いつも。

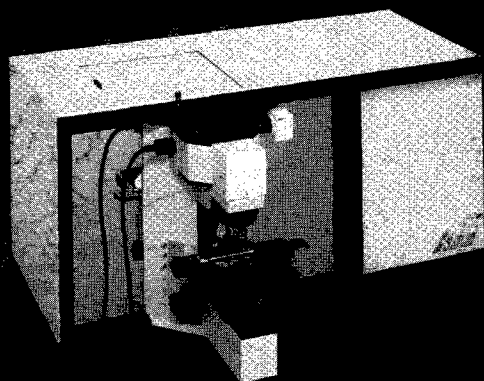
HORIBA

Explore the future

CNTの測定にはデファクトスタンダードの LabRamHR-800が最適

～RBM/フォトルミネッセンスを同一スポットで測定～

顕微レーザーラマン分光測定装置 LabRamシリーズ



- ・244nm～1064nmのレーザによる測定が可能
- ・焦点距離800nmの分光器により高分解能測定を実現

SWCNTの近赤外領域の蛍光測定を 大幅にスピードアップ

～ ナノテクリサーチに ～

近赤外対応蛍光分光測定装置 SPEX NanoLogシリーズ

- ・InGaAsアレイ検出器による高感度測定
- ・高速・高分解能マトリックスマッピング
- ・モジュールユニットだからアプリケーションに
応じた各種NIR検出器の組み合わせも可能



HORIBA JOBIN YVON

株式会社堀場製作所

科学システム営業部 03-3861-8234

本社 〒601-8510 京都市南区吉祥院宮の東町2 TEL(075)313-8121

●仙台(022)308-7890 ●つくば(0298)56-0521 ●東京(03)3861-8231
●横浜(045)451-2091 ●名古屋(052)936-5781 ●大阪(06)6390-8011
●広島(082)288-4433 ●愛媛(0897)34-8143 ●福岡(092)472-5041

製品の詳しい情報は

<http://www.jyhoriba.jp>

<http://www.horiba.co.jp> e-mail:info@horiba.co.jp